



CELLULOSE NITRATE OBJECTS IN COLLECTIONS: HISTORY OF SCIENCE AND TECHNOLOGY HAND IN HAND WITH CONSERVATION OF CULTURAL HERITAGE

Artur Louro Mendonça Neves
Master in Conservation and Restoration

DOCTORATE IN Conservation and Restoration of Cultural Heritage
NOVA University Lisbon
Março, 2023



CELLULOSE NITRATE OBJECTS IN COLLECTIONS: HISTORY OF SCIENCE AND TECHNOLOGY HAND IN HAND WITH CONSERVATION OF CULTURAL HERITAGE

Artur Louro Mendonça Neves

Master in Conservation and Restoration

Adviser: Maria João Seixas de Melo
Full Professor, NOVA University of Lisbon

Co-advisers: Robert Friedel
Emeritus Professor, The University of Maryland

Maria Elvira Callapez
Principal Investigator, University of Lisbon

Examination Committee:

Chair: Maria Paula dos Santos Diogo
Full Professor, NOVA School of Science and Technology,
NOVA University Lisbon

Rapporteurs: Susan Mossman,
Senior Curator of Materials at the Science Museum, London
Marisa Sofia Coutinho Lourenço Pamplona Bartsch,
Head of Department at the Deutsches Museum

Adviser: Maria João Seixas de Melo,
Full Professor, NOVA School of Science and Technology,
NOVA University Lisbon

Members: Ana Maria Martelo Ramos,
Associate Professor, NOVA School of Science and Technology,
NOVA University Lisbon

Maria Paula dos Santos Diogo
Full Professor, NOVA School of Science and Technology,
NOVA University Lisbon

Cellulose nitrate objects in collections: history of science and technology hand in hand with conservation of cultural heritage

Copyright © Artur Louro Mendonça Neves, NOVA School of Science and Technology, NOVA University Lisbon.

The NOVA School of Science and Technology and the NOVA University Lisbon have the right, perpetual and without geographical boundaries, to file and publish this dissertation through printed copies reproduced on paper or on digital form, or by any other means known or that may be invented, and to disseminate through scientific repositories and admit its copying and distribution for non-commercial, educational or research purposes, as long as credit is given to the author and editor.

ACKNOWLEDGMENTS

I start by thanking my supervisor, Professor Maria João Melo, for her invaluable guidance and mentorship throughout this journey of learning and discovery. I am deeply indebted to Professor Robert Friedel for his unwavering support, inspiration and for the unforgettable experience I shared with him in the USA. Additionally, I wish to express my heartfelt appreciation to Professor Maria Elvira Callapez for her contagious enthusiasm that continually fueled this research.

I thank Fundação para a Ciência e Tecnologia for funding this PhD project with a doctoral grant, PD/BD/136678/2018. This acknowledgement is extended to the NOVA School of Science and Technology, NOVA University of Lisbon, Department of Conservation and Restoration and to LAQV/REQUIMTE, as well as to the CORES Doctoral Programme.

I wish to express my profound appreciation to Fulbright Portugal, in partnership with Fundação para a Ciência e Tecnologia, for generously awarding me a 4-month research scholarship, grant PS00326022. This invaluable support facilitated the development of two pivotal chapters within this thesis. Throughout this period, I was privileged and deeply honored to be affiliated with the Department of History at the University of Maryland, College Park, my esteemed Fulbright host institution. Their commitment to providing me with essential resources and guidance, especially Professor Philip Soergel, greatly contributed to the remarkable academic journey I embarked upon. I extend my heartfelt gratitude to Professor Ray Phaneuf for accepting me into his lab within the Department of Materials Science and Engineering. My gratitude knows no bounds, as he generously provided me with access to the indispensable microFTIR equipment that played a pivotal role in shaping the outcomes of this research endeavor.

I am grateful to the Smithsonian Institution and to the National Museum of American History (NMAH), especially Dr. Kristen Frederick-Frost for supporting the analysis of the celluloid objects. It is paramount to underscore that this undertaking unfolded amid the challenges posed by the COVID-19 outbreak, leading to substantial restrictions on external researchers to pursue research inside the Museum's facilities. Despite these serious constraints, Dr. Kristen Frederick-Frost demonstrated unwavering commitment, surmounting obstacles to

enable the realization of this project. Words fall short in conveying the depth of my appreciation for her remarkable efforts. I extend my thanks to the curators Deborah Warner, Rachel Anderson, to the NMAH's Conservation Department staff for the permission to use the laboratory stereomicroscope and other resources, especially conservator Dawn Wallace for the Hirox micrographs; and the NMAH's National Numismatic Collection staff for allowing the use of the portable X-Ray fluorescence spectrometer. I thank Dr. Edward Vicenzi and Dr. Thomas Lam, from the Museum Conservation Institute (MCI), for their extraordinary endeavors in facilitating the analysis of microsamples. Their exceptional dedication became evident when circumstances, stemming from the COVID-19 pandemic, restricted my access to the MCI facilities. Their support and commitment during this challenging time were instrumental in ensuring the progression of this research.

I must also express my gratitude to Professor Matthew Collins for his instrumental role in connecting me with Dr. Dan Kirby. Dr. Kirby's enthusiasm for the billiard ball research and his subsequent pivotal contribution through the ZooMS analysis are deeply appreciated.

My profound appreciation extends to the National Museum of Dentistry in Baltimore, USA, and to Dr. Scott Swank and Patrick Cutter, for their invaluable support in facilitating the analysis of historical dentures. Notably, the analysis of these dentures was not originally envisioned in the initial Fulbright study plan. During the waiting period for analysis permission from the NMAH, due to the COVID-19 pandemic, Professor Robert Friedel and I approached the National Museum of Dentistry with hopes of fostering a productive collaboration. The outcome surpassed expectations, yielding remarkable results that are difficult to acknowledge in mere words.

Back to Portugal, my idea was to extend my Fulbright experience to my home country, working closely with cultural institutions in the analysis of celluloid objects. I was very happy to find the same generosity, support, and enthusiasm in the two institutions from Guimarães whose comb collections are addressed in this thesis: Sociedade Martins Sarmiento, namely to Dr. João Antero Gonçalves Ferreira for authorizing the analysis of the objects and Salomé Duarte for all her support during the investigation carried out at the institution; and Casa da Memória de Guimarães, namely Dr. Catarina Pereira for the authorization, support and shared information about the comb industry in Guimarães. I thank you very much.

Lastly, I am compelled to express my heartfelt gratitude to the SOLEIL synchrotron in France, and specifically to the DISCO beamline under the guidance of Dr. Matthieu Refregiers, as well as to IPANEMA with special acknowledgment of Dr. Mathieu Thoury. Their unwavering support, guidance, and engaging discussions were instrumental in the development of the project pursued in this thesis – the application of Deep UV synchrotron luminescence in the examination of celluloid heritage. I am equally indebted to Dr. Maëva L'Heronde, whose

expertise played a pivotal role in the meticulous preparation of the samples, a crucial component of this research. I extend my gratitude to Dr. Frédéric Jamme for supporting a second project at SOLEIL, which was not addressed in this thesis and hopefully will be published in the future.

I would like to extend my whole-hearted appreciation to my friends and family, whose unwavering support was my anchor throughout this journey. To my mother, father, brother, girlfriend, and grandparents, your love, encouragement, and untiring belief in me were fundamental in propelling me across the finish line. You enriched this endeavor beyond measure.

ABSTRACT

Celluloid is a notoriously challenging material for conservation science due to its fast, dangerous, and complex degradation. The conservation of celluloid heritage continues to be at risk and it is urgent to develop sustainable and efficient preservation strategies. This doctoral project innovatively addresses this challenge by adopting an interdisciplinary approach combining conservation science with the history of science and technology. By focusing on early industrial formulations and using the first products made with celluloid as case studies, billiard balls and dentures, this project contributes to a new understanding of celluloid's materiality, historical significance and conservation needs.

The history of celluloid billiard balls and celluloid dentures has long remained shrouded in mystery. Historians deemed celluloid billiard balls as an impractical failure. This perception was largely due to a lack of understanding of the billiard balls' composition. Using a multi-analytical approach to analyze billiard balls from the National Museum of American History (NMAH, Washington, D.C., EUA), it was found that they were made with a bone-cellulose nitrate composite (75%/25% by wt.), patented by John Wesley Hyatt in 1869. By correlating this material information with written sources, the bone-cellulose nitrate composite was found to be consistently employed in celluloid billiard ball production from the 1870s to the 1950s and played a crucial role in bringing the decline of ivory in billiard balls.

Similarly, celluloid dentures have been considered a product with limited success and likely insignificant after the 1880s. This study aimed at characterizing the early celluloid-vermilion (mercury sulfide, HgS) compositions of denture collections from the NMAH and the National Museum of Dentistry, Baltimore, USA. The results of these analysis, combined with source research, revealed an unexpected finding, namely that celluloid remained a significant material in dental prosthetics production up until the 1940s. These findings offer valuable insights into the evolution of celluloid billiard balls and dentures manufacture and highlight the importance of continued efforts to identify and understand the various formulations of

celluloid, in all its material dimensions, as this knowledge significantly contributes to the conservation of its cultural heritage.

In Portugal, celluloid has entered oblivion since research on early plastics is very scarce. Therefore, a vital objective of this thesis was to contribute to a broader understanding of its historical significance in Portugal. Two comb collections from Casa da Memória de Guimarães and Sociedade Martins Sarmento (Guimarães) were analyzed, revealing the presence of celluloid, horn, cellulose acetate, and polystyrene. The results were used, in conjunction with written and statistical sources, to examine the impact of celluloid on the evolution of the Portuguese comb industry. The case study of Portugal offers a compelling illustration of the interplay between horn and celluloid in the shift from traditional industries to modern plastic manufacturing sectors. It is now of outmost importance to establish preservation strategies for these collections due to their importance in the history of plastics in Portugal.

The experience of analyzing different heritage collection in the USA and Portugal with handheld Raman MIRA DS, demonstrates the efficacy of this technique to characterize celluloid and plastics. The device's portability and versatility facilitated in-situ analysis producing high-quality spectra validated through reference comparison and supplemented by μ FTIR. This thesis strongly advocates for the broader implementation of handheld Raman spectroscopy in studying plastics heritage.

Finally, in response to the need for effective methods to study celluloid degradation, this thesis presents an innovative approach to address this critical research issue. Synchrotron Deep UV multispectral micro luminescence spectroscopy (DUV- μ PL) was employed for the first time to investigate celluloid heritage, taking advantage of its high sensitivity and spatial resolution. This approach proved essential for detecting early degradation markers and characterizing the heterogeneous environments of zinc oxide, which are linked to the manufacturing or degradation history. Overall, this thesis shows the considerable potential of DUV- μ PL for the study of plastics heritage and for the development of innovative methods for its preservation.

Keywords: Celluloid, material culture, degradation, billiard balls, dentures, combs

RESUMO

O celulóide é um dos materiais mais desafiantes para as ciências da conservação devido à sua rápida, perigosa e complexa degradação. Apesar de vários esforços passados, a conservação dos objetos históricos de celulóide continua em risco e é urgente desenvolver estratégias de preservação que sejam eficientes e sustentáveis. Este projeto de doutoramento aborda o desafio da conservação do celulóide de uma forma inovadora, adotando uma abordagem multidisciplinar que combina as ciências da conservação com a história da ciência e tecnologia. Ao focar-se nas formulações industriais primordiais e usando como casos de estudo os primeiros produtos fabricados com celulóide, bolas de bilhar e dentaduras, este projeto contribui para uma nova compreensão da materialidade, significância e conservação do celulóide.

A história das bolas de bilhar e dentaduras de celulóide há muito que permanece envolta em mistério. As bolas de bilhar de celulóide têm sido consideradas pelos historiadores como um fracasso, sobretudo devido à falta de conhecimento sobre a sua composição. Usando uma abordagem multi-analítica para analisar bolas de bilhar de celulóide do National Museum of American History (Museu Nacional da História Americana, Washington, D.C., EUA), foi descoberto que estas eram produzidas com uma mistura de osso moído e nitrato de celulose (75%/25% em peso), processo patenteado por John Wesley Hyatt em 1869. Correlacionando esta informação com fontes históricas, esta tese demonstra que este material compósito foi utilizado na produção de bolas de bilhar de celulóide, de forma consistente, desde 1870 até 1950, e desempenhou um papel crucial na abolição do marfim em bolas de bilhar.

Do mesmo modo, historicamente, as dentaduras de celulóide têm sido consideradas como um produto com sucesso limitado e provavelmente insignificante após 1880. Este estudo teve como objetivo a caracterização das composições de celulóide-vermelhão (sulfureto de mercúrio, HgS) encontradas nas coleções de dentaduras do National Museum of American History e do National Museum of Dentistry (Museu Nacional da Odontologia), Baltimore, EUA. Os resultados desta análise, juntamente com análise de fontes escritas, revelaram uma descoberta inesperada, nomeadamente que as dentaduras de celulóide permaneceram um material

significativo na produção de próteses dentárias até 1940. Estes resultados são fundamentais para uma nova percepção sobre a evolução industrial das bolas de bilhar e dentaduras de celulóide e destacam a importância de estudar as diversas formulações do celulóide, em todas as suas dimensões materiais, uma vez que este conhecimento contribui significativamente para a conservação da sua cultura material.

Em Portugal, existe um risco sério de que o celulóide caia no esquecimento, uma vez que a investigação sobre os chamados pré plásticos é escassa. Por essa razão, esta tese procura também contribuir para uma compreensão mais alargada da significância deste material neste país. Duas coleções de pentes da Casa da Memória de Guimarães e da Sociedade Martins Sarmento (Guimarães) foram analisadas, revelando a presença de celulóide, chifre, acetato de celulose e poliestireno. Os resultados foram utilizados, em conjunto com fontes escritas e estatísticas, para examinar o impacto do celulóide na evolução da indústria portuguesa de pentes. O caso português é ilustrativo da interação entre o chifre e o celulóide na transição de indústrias tradicionais para a indústria moderna dos plásticos. É urgente estabelecer medidas de preservação para estas coleções dada a sua importância na história dos plásticos em Portugal.

A análise de diferentes coleções, tanto nos EUA como em Portugal, com o espectrómetro portátil Raman MIRA DS, demonstrou a eficácia deste equipamento para caracterizar o celulóide e plásticos no geral. A portabilidade e versatilidade do equipamento facilitaram a análise *in-situ*, produzindo espectros de alta qualidade validados por comparação com referências materiais e complementados por μ FTIR. Esta tese recomenda a implementação mais ampla da espectroscopia Raman portátil no estudo dos plásticos históricos.

Finalmente, em resposta à necessidade de métodos eficazes para estudar a degradação do celulóide, esta tese apresenta uma abordagem inovadora: tirando partido da sua alta sensibilidade e resolução espacial, microespectroscopia multiespectral de luminescência UV de sincrotrão (DUV- μ PL) foi usada pela primeira vez para investigar a degradação do celulóide em objetos históricos. Esta abordagem é demonstrada como essencial para detetar marcadores de degradação nas fases iniciais de degradação e caracterizar os ambientes heterogêneos do pigmento óxido de zinco; ambientes esses ligados à história de manufatura e/ou degradação. Esta tese mostra o grande potencial do DUV- μ PL para o estudo dos plásticos em geral.

Palavras Chave: Celulóide, cultura material, degradação, bolas de bilhar, dentaduras, pentes

CONTENTS

SYNOPSIS.....	XXXVII
1 GENERAL INTRODUCTION.....	1
1.1 Cellulose nitrate.....	2
1.2 Parkesine.....	3
1.3 Celluloid	5
1.4 The identification of celluloid.....	13
1.5 The degradation of celluloid objects.....	22
1.6 Photoluminescence for the study of polymer degradation.....	30
1.7 Research aims and methodology	32
1.8 References.....	35
2 THE BEST BILLIARD BALL IN THE NINETEENTH CENTURY: COMPOSITE MATERIALS MADE OF CELLULOID AND BONE AS SUBSTITUTES FOR IVORY BILLIARD BALLS.....	47
2.1 Introduction.....	48
2.2 Results.....	50
2.3 Discussion.....	57
2.4 References.....	61
3 HISTORY AND CONSERVATION OF CELLULOID DENTURES	67
3.1 Introduction.....	68
3.2 Experimental	75
3.3 Results and discussion.....	79
3.4 Conclusions	92
3.5 References.....	94

4	THE MATERIALITY OF THE “BEST PORTUGUESE COMB” EVOLUTION OF THE COMB INDUSTRY IN PORTUGAL, C. 1880-1970.....	101
4.1	Introduction.....	101
4.2	Celluloid and the comb industry of Guimarães.....	103
4.3	Horn, celluloid and plastic.....	108
4.4	Importation of plastic materials from 1923 to 1960	114
4.5	The singularity of the plastics industry in Guimarães	117
4.6	Conclusion.....	121
4.7	References.....	123
5	NOVEL MARKERS TO EARLY DETECT DEGRADATION ON CELLULOSE NITRATE-BASED HERITAGE: AT THE SUBMICROMETER LEVEL USING SYNCHROTRON UV-VISIBLE MULTISPECTRAL LUMINESCENCE	129
5.1	Introduction.....	130
5.2	Results and discussion.....	135
5.3	Conclusions	143
5.4	Methods	144
5.5	Instrumentation	145
5.6	References.....	149
6	CONCLUSIONS	155
6.1	Discussion.....	155
6.2	Future perspectives	159
6.3	References.....	161
	APPENDICES.....	163
	Appendix 1. The best billiard ball in the nineteenth century: composite materials made of celluloid and bone as substitutes for ivory billiard balls.....	165
	Appendix 2. History and Conservation of Celluloid Dentures	203
	Appendix 3. The materiality of the “best Portuguese comb”: Evolution of the comb industry in Portugal, c. 1880-1970.	219
	Appendix 4. Novel markers to early detect degradation on cellulose nitrate-based heritage at the submicrometer level using synchrotron UV-Visible multispectral luminescence. ...	229

LIST OF FIGURES

Chapter 1. General Introduction

Figure 1.1. Left, Christian Friedrich Schönbein (1799-1868) and a bottle of collodion from the London Science Museum collection. Source: Source: Science Museum Group © The Board of Trustees of the Science Museum. Right, the chemical synthesis of cellulose nitrate by Schönbein. Its innovation was in the use of a mixture of nitric acid and sulfuric acid, which produces nitronium ions (NO_2^+) that will react with the cellulose hydroxyl groups to produce nitrate groups.....	2
Figure 1.2. Left, Photograph of Alexander Parkes taken in Vienna in 1875. Right, Circular molded plaque of red Parkesine. Source: Science Museum Group © The Board of Trustees of the Science Museum.	3
Figure 1.3. <i>Left</i> , John Wesley Hyatt (1837-1920). <i>Right</i> , The installations of the Celluloid Manufacturing Company, Newark, New Jersey. Source: Celluloid Corporation Records, 1883-1943. Archives Center, National Museum of American History.	5
Figure 1.4. Left, tortoiseshell comb from the Portuguese national museum Soares dos Reis (19 th century). Right, imitation tortoiseshell celluloid comb from the Smithsonian Collection (1900s) (ID Number 2006.0098.0901).	6
Figure 1.5. Celluloid small memo notebook (left) and folding ruler (right), from the Portuguese Perlov's collection. The handwritten note in the memo book shows how they were used.	7
Figure 1.6. Left , Advertisement for <i>Challenge</i> Cleanable Collars; from The Literary Digest 1919. Hagley ID, Box/folder number, E.I. du Pont de Nemours & Company Advertising Department records (Accession 1803), Manuscripts and Archives Department, Hagley Museum and Library, Wilmington, DE 19807. <i>Right</i> , celluloid <i>challenge</i> cleanable collar from the Hagley Museum and Library, Delaware, USA.	8
Figure 1.7. Left, John Wesley Hyatt 1878 patent drawing on an "Improvement on Piano Keys" (USP 210750). Right, note on Hammacher, Schlemmer & Co ivory and celluloid pianos keys (Music Trade Review, 1908).	9
Figure 1.8. Left, Edison Blue Amberol records. Source: Archeophone Archives. Right, Edison Amberola from the Smithsonian Institution Collection (ID Number ME.310542).	10
Figure 1.9. Left, Patient with tuberculosis of the spine wearing a celluloid orthopedic body jacket [18]. Right, information slide from the 1930s showing the evolution of small pox vaccination processes. Source: Sanofi Pasteur "The Legacy Project".	11

Figure 1.10. First phase of cellulose nitrate degradation, starting with homolytic scission of a nitrate in C2 or C3 and the release of $\bullet\text{NO}_2$. In the second phase, the alkoxy radical promotes chain scission with $\bullet\text{NO}_2$ release and aldehyde formation, detected at 1740 cm^{-1} in IR or converts into a ketone/hydroxyl intermediate by $\bullet\text{H}$ abstractions, for more information see text..... 25

Figure 1.11. a) The excited state hydroperoxide leads to glycosidic bond cleavage with the formation of a gluconolactone. This intermediate is then transformed into an anhydride with the release of $\bullet\text{CH}_2\text{ONO}_2$, which converts into a final product, methyl nitrate, by $\bullet\text{H}$ abstraction. In an alternative pathway, in acidic conditions, the C1 keto intermediate decomposes into oxalic acid or erythronic acid as proposed by Quye et al. b) The keto-enol tautomerism, in the presence of accumulated $\bullet\text{NO}_2$, leads to addition reactions and formation of multi-nitrated rings which will disintegrate the rings. 26

Chapter 2. The best billiard ball in the nineteenth century: composite materials made of celluloid and bone as substitutes for ivory

Figure 2.1. Historical billiard balls studied. A) John Wesley Hyatt and 1868 “original” celluloid billiard ball. National Museum of American History, Smithsonian Institution. B) Billiard balls studied: Hyatt 1868, Crystalate, Bonzoline and Ivorylene. The ivory billiard ball is from the Smithsonian Collection (ID number CL.329507). Bonzoline and Crystalate resemblance with ivory is evident. The interior of the Bonzoline and of the Ivorylene are shown. 49

Figure 2.2. Molecular characterization of 1868 Hyatt billiard. Left, Infrared spectra of a bone particle from the 1868 billiard ball surface (top), of the average of 3 microsamples acquired from the surface (middle), compared with a reference prepared with 70% ground cow bone and 30% pure cellulose nitrate by weight (bottom). Right, infrared spectra of the references used for the development of the calibration curves for formulation quantification..... 51

Figure 2.3. Microscopy of the 1868 Hyatt billiard ball. A) Microscope image of the surface showing its heterogenous granular surface and cracking (Hyrox Digital Microscope). B) Bone particle by 3D light microscopy. C) Bone-celluloid composite sample by 3D light microscopy. D) SEM-EDS false color composite image showing the distribution of phosphorous (represented as blue) and zinc (represented as green). E) Compositional distribution of major components as single element images, where the X-ray intensity is represented in rainbow scale, including carbon (C), oxygen (O), sodium (Na), magnesium (Mg), aluminum (Al), silicon (Si), phosphorous (P), sulfur (S), calcium (Ca) and zinc (Zn), by SEM-EDS..... 52

Figure 2.4. X-Ray fluorescence spectra for 1868 Hyatt, Bonzoline and Crystalate billiard balls and Ivorylene pool ball. The bonzoline and crystalate spectra were collected on white and red balls. On the Ivorylene three different areas were studied: the white region where the ball number is found (blue), the yellow layer (red) and the brown core (black)..... 53

Figure 2.5. Molecular characterization of the Bonzoline and Crystalate billiard balls and Ivorylene pool ball. The average infrared spectra obtained for the bonzoline and crystalate billiard balls (black spectra) are compared with average spectrum obtained for the 1868 Hyatt billiard ball. The μRaman spectrum of white Bonzoline billiard balls, shows a characteristic spectrum of bone (black spectrum). White

crystalate μ Raman spectrum shows additional bands related to cellulose nitrate groups, calcite, camphor, and zinc oxide. Both red bonzoline and crystalate billiard balls show the characteristic bands of synthetic red pigment barium lithol red (PR49:1). The Ivorylene infrared spectra of the brown core (brown spectrum) and yellow layer (orange spectrum), both show the main absorptions of the bone-celluloid composite. The μ Raman spectrum of the Ivorylene yellow layer (orange spectrum) identified bone, chrome yellow and anatase; and of the brown core sample (brown spectrum) phthalocyanine green (PG7) and anatase..... 54

Figure 2.6. Microimaging of the Ivorylene pool ball. A) Location of the samples analyzed: the brown core and the yellow layer. B) Yellow layer sample viewed using 3D visible light microscopy. C) Composite SEM-EDS image showing the distribution of carbon (blue), calcium (green), and silicon (red). D) Backscattered electron image showing sub-micrometer-sized chrome yellow particles, white particles within on a gray matrix made of complex CN: bone: camphor and other additives shown in C). E) Brown core sample under the visible light microscope. The white polygon represents the area imaged. F) Distribution of calcium (Ca) and phosphorous (P) in blue for bone, iron (Fe) in orange, aluminum (Al) and silicon (Si) in red for aluminosilicates, barium (Ba) and sulfate (S) in green for the additive barium sulfate, BaSO₄; by SEM-EDS. 55

Chapter 3. Safeguarding our dentistry heritage: a study of the history and conservation of nineteenth-twentieth century dentures

Figure 3.1. A) Scheme of the steam apparatus patented by the Hyatt brothers in 1874 [28]. B) Sectional view of the celluloid steam apparatus manufactured by the Celluloid Manufacturing Company and sold by S. S. White Dental Manufacturing Company [32], [33]. C) Example of one of these steam machines, collection of the National Museum of American History, catalog number M-08954. D) Scheme of the "dry-heat" apparatus patented by Ferdinand Heindsmann, assignor to S.S. White, in 1875. E) Patent model, NMAH collection, catalog number M-04242. F) "Heindsmann's heater" was manufactured and sold by S. S. White Dental Manufacturing Company in 1876 (Catalogue of dental materials, furniture, instruments, etc., for sale by Samuel S. White, 1876). 72

Figure 3.2. A) Raman spectra of a cellulose nitrate reference, camphor and celluloid (cellulose nitrate + 30% wt camphor). B) Cellulose nitrate and camphor chemical structures. Cellulose nitrate is showed with a degree of substitution 2 (on average, two nitrate groups and one hydroxyl group per monomer). Cellulose nitrate used for celluloid had a degree of substitution of 2.2. C) Raman spectra of vermilion (HgS, mercury sulfide) and zinc oxide (ZnO), also known as zinc white. 79

Figure 3.3. Raman spectra of celluloid (cellulose nitrate + camphor) dentures acquired with handheld Raman, using different acquisition times: JUSTI 24, 14 s acquisition time; MGM-09686 (denture 1 (black) and 2 (blue)), 3.5 s; 2002.99.5780, 6 s; SSW21, 10 s. Vermilion and phthalate peaks are highlighted in red and green, respectively..... 80

Figure 3.4. XRF spectra of celluloid dentures MG.M-09686 (dentures 1 and 2) and vulcanite dentures MG.291116.0046 and MG.291116.0049, normalized to the maximum (corresponding to Zn K α emission line). A higher relative intensity of vulcanite's Hg emission lines is observed. The analysis points are marked in the images of the dentures. 84

Figure 3.5. A) Photographs of dentures JUSTI 21, JUSTI 24 and SSW21, with indication of teeth analyzed with handheld Raman. **B)** Infrared spectra of JUSTI 21 beeswax coating. **C)** Raman spectra acquired from the porcelain teeth of JUSTI 21 (black, 1.2 s, 1 scans) and JUSTI 24 (red, 14 s, 10 scans) and from the human teeth of SSW21 (blue, 7 s, 10 scans). 85

Figure 3.6. Infrared spectra acquired from the dentures identified as vulcanized rubber, by the detection of bands in the CH stretching (3000–2800 cm^{-1}) and bending regions (1450–1375 cm^{-1}). Denture 2002.99.4797 has porcelain gums. Dentures MG.29116.0046 and 0049 were micro sampled in different regions due to color differences, a dark and a light red, which showed spectral variations. . 86

Figure 3.7. A) Dental blank 2002.99.5831 and detail of the inscription where it is possible to read “S.S. White Resovin. Trademarks. Rec. in U.S. Pat. Off. and elsewhere. Made in U.S. of A.”; **B)** XRF spectrum of MG.29116.0061, showing the strong emission of chloride. **C)** Raman of dental blank 2002.99.5831 (black, 4 s, 10 scans) and denture MG.29116.0061 (blue, 3 s, 10 scans). **D)** Infrared spectra of dental blank 2002.99.5831 (black and denture MG.29116.0061 (blue), compared to a reference spectrum of 83% PVC:17%PVAc copolymer (grey)..... 88

Figure 3.8. A) Advertisement of Luxene, Bakelite Corporation, circa 1940 (J. Harry DuBois Collection on the History of Plastics, NMAH.AC.0008). **B)** Photography and detail of the top of the denture 2002.99.5459 where the inscriptions “LUX” and “E” are read. **C)** Raman spectra (785nm, maximum power) of dentures 2002.99.5459 (black, 9s, 10scans), 2002.99.5524 (blue, 3s, 1 scan) and a phenol-formaldehyde Aramith billiard ball (grey, 8s, 1 scan). 90

Figure 3.9. Raman spectra (785nm, maximum power) of JUSTI 23 (black, 10s, 10 scans) and of a PMMA reference (grey, 5s, 1 scan). 91

Chapter 4. For the history of celluloid: Evolution of the comb industry in Portugal, c. 1880-1970

Figure 4.1. Number of comb workshops and factories in Portugal from 1879 to 1916. There is no information between 1891-1895 and 1904-1910 and after 1916. Source: Portuguese statistical yearbooks (INE)..... 104

Figure 4.2. “Costa, Cerdeira and Commandita” celluloid combs and articles factory at the Guimarães Industrial and Agricultural Exhibition in 1923. Source: Photo library of Sociedade Martins Sarmiento. 107

Figure 4.3. Combs from the João Teixeira’s factory, from Casa da Memória collection. Left, horn combs. Right, celluloid combs in imitation of tortoiseshell. 113

Figure 4.4. Dandruff combs made from celluloid (left) and cellulose acetate (right). They were produced by Fábrica de Plásticos Pátria and are from the collection of Sociedade Martins Sarmiento. This factory advertised its combs as “The best Portuguese comb”..... 114

Figure 4.5. Evolution of the importation of plastic materials in Portugal. Source: Foreign trade reports from 1923 to 1954 (INE)..... 115

Figure 4.6. Evolution of the number of plastics factories and the quantity of cellulosic plastic materials produced in Portugal by the districts of Braga, Leiria, Lisbon and Porto. Source: Industrial Statistics from 1955 to 1967 (INE)..... 118

Chapter 5. Novel markers to early detect degradation on cellulose nitrate-based heritage at the submicrometer level using synchrotron UV–VIS multispectral luminescence.

Figure 5.1. Objects from Perlov’s celluloid collection that consists of 300 everyday celluloid objects, donated by Amy Schenkein and Dadie Perlov, American collectors and majority donors of the Smithsonian Institute's celluloid collection. Containing several objects of different types, from razor blades, fans, pins, postcards or advertising items, this collection is significant of the American technological advances in the celluloid industry from the 1890s to the 50s. The objects showed were studied in the framework of this research: a 1901 postcard (A), two undated advertisement pins, hereby called the holy bible pin (B) and the American flag pin (C), and an 1899 calendar (D). 130

Figure 5.2. A) Cinematographic film samples S4, S5, S6, 50509 and DIF 50 500. DIF 50 500 was artificially aged ($\lambda \geq 280$ nm, 40 °C): at 50 hours of irradiation the film was yellowed and fragile; at 100h presented cracking; and at 150h the film lost its integrity. B) Multi-layer structure of a generic cinematographic film. The cellulose nitrate is the thickest layer and it is the support of the image. The image is formed by silver colloids dispersed in a proteinaceous matrix which is adhered to the support by another thin layer, the subbing layer. Finally, the anti-halation layer prevents light to be reflected in the image layer causing a halo effect 131

Figure 5.3. Cellulose nitrate side-chain scission starts with de-nitration, by the homolysis of a nitrate group in C2 or C3 and the release of $\bullet\text{NO}_2$ (inducing a DS decrease). In a second phase, hydroperoxides formed in C1, lead to main chain scission through cleavage of the glycosidic bond, with the formation of a gluconolactone as the primary degradation product. This mechanism, triggered by light, produce excited states that can simulate the natural ageing. 134

Figure 5.4. Irradiation of cellulose nitrate films followed by luminescence. Left, unreacted CN film is characterized by a broad excitation spectrum centred at 320 nm ($\lambda_{em} = 390$ nm), and in the first 20h of irradiation the maximum is shifted to shorter wavelengths (290 nm) and then evolve to a maximum at circa 300 nm at 50h of irradiation, which will continue to shift to longer wavelengths. Right, at 130h of irradiation several oxidized functions are observed described by maxima at 266, 325, 366 and 400 nm ($\lambda_{em}=390, 450$ and 480 nm). This agrees with the yellowing observed in the film. 136

Figure 5.5. A) Microscope images (7.1x magnification) of cellulose nitrate homogeneous thin films (150 μm) used as reference films before (t_0) and after 150h of irradiation. B) POLYPHEME raster scanning map of a 150h aged celluloid reference ($\lambda_{exc} = 330\text{nm}$, 20 μm step, 5s acquisition time), together with the average, representative, emission spectrum. Intensity variations of the probed region between 415 and 425nm are due to the topography of the sample. C) Normalized emission spectra of artificially aged cellulose nitrate (top, $\lambda_{exc} = 290\text{nm}$) and celluloid (bottom, $\lambda_{exc} = 330\text{nm}$) irradiated during 50h, 100h and 150h. 137

Figure 5.6. POLYPHEME raster scanning map (10 mm step, 5s acquisition time, $\lambda_{exc} = 330$ nm) of the cinematographic film DIF 50 500. Three regions of interest were distinguished based on characteristic emission spectra: the proteinaceous image layer, with a band at 412 nm; the support layer with a band at 425 nm and a shoulder at higher wavelengths; and other products at the interfaces, air-support, and support-image, characterized by a band at 538 nm..... 139

Figure 5.7. A) Full-field luminescence imaging by TELEMOS of the American flag celluloid advertisement pin ($\lambda_{exc} = 290$ nm, 40x objective). Emission bandpass filters used: 352-388 nm (blue); 412-438 nm (green); 535-607 nm (red). The white-square marks indicate the POLYPHEME map area. **B)** Spatially registered false-colour RGB image of the emission at excitations of 365 (blue), 385 (green) and 405 nm (red) with emission bandpass filter 514 nm (30 nm FWHM). **C)** Raster scanning map by POLYPHEME ($15 \times 15 \mu\text{m}^2$, 5s, 2 accumulations, $\lambda_{exc} = 290$ nm). Colors were designated as follows: blue for the band edge emission at 385 nm, green for the spectral region between 400-450 nm; red for the region between 510-550 nm. **D)** Average spectra calculated from 10 points for each designated color: strong near band edge emission (blue); contributions of ZnO crystal defect emissions between 400-450 nm (green) and strong green band emission (red). The spectral points used are marked in the POLYPHEME map (C) with squares of the correspondent color. The spectral regions viewed using TELEMOS setup are highlighted, with colours corresponding to the bandpass filters used..... 141

Figure 6.1. A) Ivory ball 1875-1920, NMAH **B)** Bone billiard balls, unknown date, Smithsonian Institution, NMAH **C)** Billiard balls made from Parkesine (c. 1860), Science Museum (UK); **B)** Bonzoline billiard balls acquired during this work (1930s); **C)** Papier-Mache billiard balls from the Billiard Museum Weingartner, Austria, Vienna (undated). **D)** Bakelite billiard balls sold by Hyatts-Burroughs Billiard Ball Co (1910s), Smithsonian Institution, NMAH..... 159

Appendix 1. The best billiard ball in the nineteenth century: composite materials made of celluloid and bone as substitutes for ivory

Figure A1. 1. Scheme of Hyatt's US Patent 259984 of 1882. Fig.1 is the central section of a billiard-ball made according to the invention, where A is the core and B is "a wall or shell adapted to fit over the core-set, the nature and construction of which is sufficiently illustrated in Fig. 2." 168

Figure A1.2. Infrared spectra of a bone micro-particle collected from the 1868 billiard ball (black) and from the ground cow femur bone (blue)..... 169

Figure A1.3. Development of the bone-cellulose nitrate calibration line and quantification of the mixture in the 1868 billiard ball. **A)** Infrared spectra of the ground cow bone femur (blue) and cellulose nitrate references (black) between 1900 and 650 cm^{-1} ; these materials were used for the development of the calibration curve. **B)** Overlay of the infrared spectra of the bovine bone-CN reference mixtures, normalized to the $\nu_s\text{NO}_2$ (1280 cm^{-1}) band (%wt bone/cellulose nitrate): 80/20 (green), 70/ 30 (red), 60/40 (blue), 50/50% (black). **C)** The data shows the average ratio and the standard deviation calculated from 6 infrared spectra collected for each reference (blue). The cellulose nitrate concentrations calculated for 4 spectra of the 1868 billiard ball are showed (average 23%, standard deviation 6%). **D)** Overlay of the infrared spectra used for the quantification of the bone-celluloid mixture in the 1868

billiard ball. The colors correspond to the points in C. The spectra are normalized to the $\nu_s\text{NO}_2$ (1280cm^{-1}) band. Acquired from 4 different microsamples collected from the surface of the object. 170

Figure A1.4. SEM-EDS imaging of a bone particle acquired from the 1868 billiard ball sample. The distribution of phosphorous (P), aluminum (Al) and zinc (Zn) is showed. It is possible to observe the homogenous distribution of phosphate in the bone matrix. At the surface of the bone particle, aluminum (Al) particles were found, related to the presence of aluminosilicates. Furthermore, it was possible to observe a homogenous mass adhered to the sample of the bone particle attributed to presence of zinc (Zn), possibly from the celluloid zinc oxide mixture. 171

Figure A1.5. SEM-EDS and Raman spectrum of the blue particle found in the 1868 hyatt billiard ball sample. The SEM-ED component images show a zoom of the area where the blue particle was found, where it is possible to detect strong emission from sodium (Na), aluminium (Al), silicon (Si) and sulfur (S). The blue particle was analyzed with μ Raman (blue spectrum, 785nm laser, 4.35mW, 20s, 10 cycles) and a strong band was observed at 543cm^{-1} . Another blue particle was found in a different microsample and analyzed with μ Raman (black spectrum, 785nm laser, 4.35mW, 150s, 5 cycles). This sample was compressed providing a better-quality Raman spectrum, with the detection of a strong band at 547cm^{-1} . This band is attributed to the ultramarine blue's symmetric stretching vibration (ν_1) of S^{3-} , as it is possible to compare with a reference Raman spectrum (grey, Casa Ferreira). Other bands were detected at $253\text{-}257\text{cm}^{-1}$ attributed to the bending vibration (ν_2) of S^{3-} and a unattributed shoulder at 583cm^{-1} 172

Figure A1.6. μ Raman spectra of the zinc particles (left) found in a microsample of the 1868 billiard ball imaged with SEM-EDS (right). (633nm laser, 4.25 mW, 120s x 5 acquisition time). False color image of the SEM-EDS electron beam-induced X-ray imaging: phosphorous from hydroxyapatite in blue, zinc from ZnO in green. The region of μ Raman analysis is marked by the white circle. Due to the fluorescence detected it was necessary to reduce the laser power and use longer acquisition times. 173

Figure A1.7. Raman MIRA DS spectra obtained from the in-situ analysis of the 1868 billiard ball. Conditions: 1.20s acquisition time, 10 cycles. It was only possible to identify the most intense bands for each of bone, cellulose nitrate, and camphor. This is due to strong background noise. Since this effect was not observed when analyzing pure bone powder, and laser 785nm this does induce strong bone fluorescence this is probably due to another minor component in the mixture, such as a surface treatment, or due to degradation. Calcite (CaCO_3) was also detected by the observation of the characteristic symmetric stretching of the carbonate ($\nu_s\text{CO}_3^{2-}$) at 1088cm^{-1} . This mineral carbonate does not exist in bone, meaning that it was intentionally admixed, possibly as chalk. 174

Figure A1.8. Peptide Mass Fingerprint MALDI spectra of the 1868 billiard ball. The cattle markers are indicated in the spectra. 175

Figure A1.9. Quantification of the bone-cellulose nitrate and camphor-cellulose nitrate formulation of the bonzoline billiard ball. A) Overlay of the infrared spectra of the four microsamples used for the quantification of bonzoline formulation, 2 from the surface (green) and 2 from the interior (black). The spectra are normalized to the maximum (νPO_4^{2-} ($\sim 1036\text{cm}^{-1}$) band. C) The cellulose nitrate concentration

calculated for the two regions are showed (average 20%, standard deviation 2%). D) The camphor concentrations calculated for the three regions are showed (average 27%, standard deviation 2%)... 176

Figure A1.10. Peptide Mass Fingerprint MALDI spectra of the bonzoline billiard ball. The cattle markers are indicated in the spectra. 177

Figure A1.11. Quantification of the bone-cellulose nitrate and camphor-cellulose nitrate formulation of a white crystalate billiard ball. A) Overlay of the infrared spectra of the four microsamples used for the quantification of crystalate formulation, all acquired for the surface of the ball. The spectra are normalized to the maximum (νPO_4^{2-} ($\sim 1036\text{ cm}^{-1}$) band. C) The cellulose nitrate concentration calculated for the four samples are showed (average 21%, standard deviation 2%). D) The camphor concentrations calculated for the three regions are showed (average 19%, standard deviation 1%)..... 178

Figure A1.12. Handheld Raman Mira DS spectrum of the white bonzoline billiard ball. (785nm, 7s acquisition time, 10 cycles). The bands of cellulose nitrate groups are observed at $861, 1284$ and 1453 cm^{-1} , of camphor at 649 cm^{-1} , hydroxyapatite at 960 cm^{-1} , calcite at 1087 cm^{-1} and zinc oxide at 436 cm^{-1} . 179

Figure A1.13. Development of the camphor-cellulose nitrate calibration line and quantification of the plasticizer concentration in the 1868 billiard ball. A) Overlay of the infrared spectra of the cellulose nitrate-camphor mixtures, normalized to the maximum (1280cm^{-1}) (%wt. camphor/cellulose nitrate): 100% cellulose nitrate (black), 10/90 (blue), 20/80 (red), 35/65% (green). For the calibration curve, it was used the ratio between the carbonyl band of camphor, at 1730 cm^{-1} , and the νNO_2 band of the cellulose nitrate, at 1280 cm^{-1} . B) Calibration curve and respective equation and coefficient of determination (R^2) for the linear fitting of the $\nu\text{C}=\text{O } 1730\text{ cm}^{-1} / \nu\text{NO}_2 1280\text{ cm}^{-1}$ ratio calculated from μFTIR in function of the % w/w of camphor. The data shows the average ratio and the standard deviation calculated from the 3 infrared spectra collected for each reference. The colored points are the quantification of camphor in the 1868 billiard ball based on the analysis of 4 microsamples (average 13%, standard deviation 1%). 180

Figure A1.14. μRaman spectrum of the red bonzoline ball at surface. Conditions: 633nm laser, 4.25 mW, 10s x 5 cycles acquisition time. Compared with a barium lithol red reference. Source: Herbst synthetic pigment database (in red, 633 nm). 181

Figure A1.15. Quantification of the bone-cellulose nitrate and camphor-cellulose nitrate formulation of the ivorylene billiard ball. A) Areas of microsampling: surface (black), interior yellow (red) and brown core (green). B) Overlay of the infrared spectra of the three microsamples used for the quantification of ivorylene formulation. The spectra are normalized to the $\nu_s\text{NO}_2$ (1280cm^{-1}) band. C) The cellulose nitrate concentration calculated for the three regions are showed (average 17%, standard deviation 1%). D) The camphor concentrations calculated for the three regions are showed (average 22%, standard deviation 2%)..... 182

Figure A1.16. Peptide Mass Fingerprint MALDI spectra of the ivorylene pool. The cattle markers are indicated in the spectra. 183

Figure A1.17. μRaman spectrum of the yellow ivorylene. Conditions: 633nm laser, 4.25 mW, 40s x 5 cycles acquisition time. Compared with a chrome yellow deep ($\text{PbCr}_4\text{O.PbO}$) reference. Source: UCL London (in red, 633nm); and with and anatase (TiO_2) reference. Source: Jobin-Yvon database (in blue,

633 nm). In more detail, chrome yellow was detected through its μ Raman spectra by the observation of the chromate symmetric stretching $\nu_1(\text{CrO}_4^{2-})$ at 837 cm^{-1} and the symmetric bending $\nu_4(\text{CrO}_4^{2-})$ at 355 cm^{-1} , (2). Anatase (TiO_2) was identified by the detection of the characteristic strong and sharp band of the E_g mode at 140 cm^{-1} (3). 184

Figure A1.18. Raman MIRA DS spectra obtained from the in-situ Raman MIRA DS analysis of the ivorylene pool ball white number region. The point of analysis is marked with a blue X on the pool ball image. Conditions: 0.5s acquisition time, 10 cycles. It was possible to detect anatase (TiO_2), by the observation of bands at 394 , 512 and 638 cm^{-1} (the strong band at 140 cm^{-1} is not observed due the equipment specificities). Raman MIRA DS was as an excellent tool to identify in-situ, bone, celluloid, chrome yellow and anatase in complex mixture. 185

Figure A1.19. SEM-EDS imaging of a dark particle observed in ivorylene’s brown core sample. A) Microscope visible light image by SEM of the sample showing the location of the particle. B) Magnification showing the particle’s morphology. C) SEM-EDS electron beam induced X-Ray imaging showing the distribution of carbon, lead, iron and aluminum. D) Elemental component images, showing the emission of oxygen (O), aluminum (Al), iron (Fe) and silicon (Si). The dark particle showed significant concentrations of iron (Fe), aluminum (Al) and oxygen (O). Fe/Al oxides have dark toned colors, which correlated with the visual observation of the particle and overall core. These oxides are clay minerals, which indicates to the use of this material in the core of the ball. Around this particle were also found particles of lead (Pb), possibly from chrome yellow, and other unidentified aluminosilicates. In this ivorylene core region, EDS quantification of the concentration of magnesium (Mg) in the bone Ca-P rich phase (correlated to the overall distribution of oxygen) was found to be circa 0.3% mass% (elephant ivory has a higher concentration, around 4 %). 186

Figure A1.20. μ Raman spectrum of the brown ivorylene core. Conditions: 633nm laser, 4.25 mW, 15s x 5 cycles acquisition time. Compared with copper phthalocyanine green G (PG7) reference. Source: UCL London (in brown, 633nm); and with and anatase (TiO_2) reference. Source: Jobin-Yvon database (in blue, 633 nm). 187

Figure A1.21. Photograph of the Bonzoline Billiard Balls set acquired in this work. In the top lid it is possible to read “Superior to ivory, being more durable, more reliable, and not subject to atmospheric influences. In tropical climates Indispensable.” The bonzoline billiard balls started being manufactured in England in 1931 by the Composition Billiard Ball Supply Co., Stratford, London. Before that they were manufactured in the USA by the Albany Billiard Ball Company. 188

Figure A1.22. Yearly humidity variations (monthly averages and standard deviations) in Mumbai, India, and London, UK, in the years of 1944 and 1937, respectively. The annual standard deviation for Mumbai was 6.3% and for London 4.8%, which is demonstrative of the more prominent humidity fluctuations in the former. Data was acquired from Integrated Surface Dataset (Global) available at National Centers for Environmental Information. The stations (Chhatrapati Shivaji International and Purely Oaks) were selected based on their proximity to the city centers, and the years selected were the oldest available. 189

Figure A1.23. Charles Dawson, English billiard champion who defended ivory billiard balls in 1899 but later, in 1904, supported the sales of bonzoline. Right, photo of Charles Dawson taken from the book

he authored in 1904 “Practical Billiards”. Advertisement to the Bonzoline Billiard Balls in 1904, where it is possible to read the supportive statement of the Charles Dawson. 190

Figure A1.24. Henry W. Stevenson, English billiards champion who played with crystalate and bonzoline balls. Left, Henry W. Stevenson in 1916 when he made the first 1000 break with bonzoline billiard balls. Right, 1904 advertisement to the Crystalate billiard ball with the referral to Henry W. Stevenson. 191

Figure A1.25. Page from the Brunswick – Balke – Collender Co. 1885 catalog with the price information for “Hyatt Patent Balls” and ivory balls (source: Brunswick digital library). 192

Figure A1.26. Clippings from the Brunswick – Balke – Collender Co. 1928 catalog with the prices of ivorylene and ivory pool sets (source: Brunswick digital library). 193

Figure A1.27. Photograph of the Bonzoline Billiard Balls set acquired in this work. Weights from left to right: 73.559g, 73.348g, 73.089g. 194

Figure A1.28. Photograph of the NMAH’s ivory billiards balls, dated from 1875-1920 (ID Number CL.329507). The dimensions and weight of left and right billiard balls where measured: 57mm and 174.2g; 54mm and 143.8g, respectively. 195

Appendix 2. Safeguarding our dentistry heritage: a study of the history and conservation of nineteenth-twentieth century dentures

Figure A2.1. Advertisement for Hecolite in the Evening Star, Washington, D.C, Friday, February 8, 1935. 203

Figure A2.2. Advertisement for Alcolite in the Indianapolis Times, March 21, 1933. 204

Figure A2.3. Resovin dental plate from the Smithsonian Collection, ID number MG.260892.295. 205

Figure A2.4. Raman MIRA DS analysis of the swaged gold and celluloid dental plate JUSTI 21 from NMD (left) and of the vulcanized rubber and Vitallium alloy denture MG.291116.0046 from NMAH (right), using the 3mm distance objective set up. 206

Figure A2.5. NMAH’s dentures and micro sampling location. Denture photographs source: Smithsonian Institution. 207

Figure A2.6. Right, celluloid denture inside the X-ray fluorescence spectrometer S1 Titan analysis chamber. The analysis area where the x-ray beam interacted with the object is beneath the denture. The chamber lid was closed for analysis. Left, different view where it is possible to see the X-ray fluorescence spectrometer S1 Titan beneath the analysis chamber. The trigger had to pressed during the analysis; the time corresponding to the acquisition time. 211

Figure A2.7. Handheld Raman spectra of the celluloid dentures’ from NMD and NMAH, namely SSW19 (10s), 2002.99.4796 (7s), 2022.99.5818 (8s), 2022.99.5287 (6s), 92.2.0924 (10), MG.M-09686 dental blank (2.6s) and JUSTI 21 (7s)..... 212

Figure A2.8. Infrared spectra of the celluloid dentures’ microsamples from NMD and NMAH. 213

Figure A2.9. Photographs with a 65MP camera (top) and with a Dinolite USB digital microscope AM2111-0.3MP (bottom) showing the conservation condition of 2002.99.5780. 214

Figure A2.10. Photographs with a 65MP camera (top) and with a Dinolite USB digital microscope AM2111-0.3MP (bottom) showing the conservation condition of 92.2.0924, namely the pitting effect at the celluloid gums.....	214
Figure A2.11. Handheld Raman spectra of the teeth of celluloid dentures SSW19 (2s) and MG.M-09686 denture 1 (3.7s). The tooth analyzed for each denture is identified with a circle.....	215
Figure A2.12. XRF spectrum of NMAH’s vulcanized rubber denture MG.291116.0046 in three different points, marked in the denture’s photograph.....	216
Figure A2.13. Infrared spectrum of a calcium stearate reference, for more details on this reference preparation and characterization please see Otero et al. (2014).	216
Figure A2.14. Infrared spectra of NMD dental plate 2002.99.5496 (probably a <i>Luxene</i> dental plate from the Bakelite Corporation).	217
Figure A2.15. Infrared spectra of NMD dental plate JUSTI 23 identified as PMMA. Bands at 1731 and 1150 cm^{-1} are saturated.	217

Appendix 3. For the history of celluloid: Evolution of the comb industry in Portugal, c. 1880-1970

Figure A3.1. Left, overall view of some of the objects from “Fábrica de Plásticos Pátria” from Casa de Memória de Guimarães. Right, the analysis with Raman MIRA DS of celluloid imitation tortoiseshell combs from João Teixeira’s collection in Casa de Memória de Guimarães.	219
Figure A3.2. Overview of some of the objects from “Fábrica de Pentes Pátria” and their Raman MIRA DS analysis at Sociedade Martins Sarmento, Guimarães.	220
Figure A3.3. Raman MIRA DS spectra of the celluloid tortoiseshell imitation combs from João Teixeira’s collection in Casa da Memória, Guimarães. Identification of celluloid is made by the detection of the strong nitrate bands at 1286 and 861 cm^{-1} and camphor sharp fingerprint band at 651 cm^{-1} . The Raman spectra of the combs are compared with a celluloid reference (in grey, cellulose nitrate + 30% camphor wt.)	221
Figure A3.4. Raman MIRA DS spectra of the horn combs from João Teixeira’s collection in Casa da Memória, Guimarães. Horn is identified by the detection of the $\nu\text{C}=\text{O}$ amide I (1667 cm^{-1}), νCC (1614 cm^{-1}), δCH_2 scissoring (1447 cm^{-1}), δCH_2 deformation (1321 cm^{-1}), δCH_2 wagging (1245 cm^{-1}), νCC aromatic (1005 cm^{-1}), νCCH aromatic (853 cm^{-1}), νCS (641 cm^{-1}), $\nu\text{S-S}$ (508 cm^{-1}) [1]. Oral information obtained by Teresa Costa (2006) from João Teixeira is clear that horn was a preponderant material in comb manufacture [2]......	221
Figure A3.5. Raman MIRA DS spectrum of the orange transparent celluloid comb of the “Fábrica de Plásticos Pátria” collection from Sociedade Martins Sarmento, Guimarães. Celluloid is identified by the detection of strong nitrate bands at 1286 and 854 cm^{-1} and camphor sharp fingerprint band at 649 cm^{-1} . The Raman spectra of the combs are compared with a celluloid reference (in blue, cellulose nitrate + 30% camphor wt.).....	222

Figure A3.6. Raman MIRA DS spectrum of the cellulose acetate tortoiseshell imitation comb of the “Fábrica de Plásticos Pátria” collection from Sociedade Martins Sarmento, Guimarães. Cellulose acetate is primary identified by the stretching band of the carbonyl group at 1728 cm^{-1} , and the methyl (CH_3) deformations at 1453 and 1367 cm^{-1} . The identification of additional bands at 1599 , 1580 , 1040 , 820 and 652 cm^{-1} are due to the presence of a phthalate plasticizer, leading also to the shift of the carbonyl stretching band [3]. The Raman MIRA DS spectrum of a cellulose acetate (degree of substitution 2.4) reference is shown (blue). 223

Figure A3.7. Raman MIRA DS spectrum of an celluloid comb imitating horn with the brand name “Aravil”. The Raman spectra of the combs are compared with a celluloid reference (in blue, cellulose nitrate + 30% camphor wt.)..... 224

Figure A3.8. Raman MIRA DS spectra of two polystyrene combs of “Fábrica de Plásticos Pátria” from the collection of Sociedade Martins Sarmento, Guimarães (black spectrum from the white comb and the yellow from the first yellow comb). The Raman spectrum of polystyrene is well known in the literature and identification can be made by band comparison [4]. 225

Figure A3.9. Celluloid combs from the of “Fábrica de Plásticos Pátria” from the collection of Sociedade Martins Sarmento, Guimarães, where it is possible to see the cracking pattern of extreme celluloid degradation. 226

Appendix 4. Novel markers to early detect degradation on cellulose nitrate-based heritage at the submicrometer level using synchrotron UV–VIS multispectral luminescence.

Figure A4.1. UV-Vis absorption spectra of cellulose nitrate films (ca. $1\mu\text{m}$), irradiated at 20h, 50h, 130 and 225 ($\lambda_{\text{irr}} \geq 280\text{nm}$, 60°C). 229

Figure A4.2. *Cellulose nitrate side-chain scission* starts with de-nitration, by the homolysis of a nitrate group in C2 or C3 and the release of $\bullet\text{NO}_2$. The alkoxy radical formed can be converted into a ketone or hydroxyl group. X^\bullet is defined as any radical which will promote H^\bullet , namely $\bullet\text{NO}_2$ or RO^\bullet , which lead to the formation of nitrous acid (HNO_2) or a hydroxyl group (ROH) respectively. C1H is the most labile hydrogen and thus the most easily abstracted. *Hydroperoxide formation at C1* will occur, in the excited state, by reaction of the produced macroradical with oxygen and further H^\bullet abstraction. This leads to the formation of the hydroperoxide and to the formation of another macroradical R^\bullet in the cellulose nitrate structure. *Cellulose nitrate main chain scission* occurs due to the decomposition of the excited state hydroperoxide, leading to scission of the glycosidic bond and formation of a gluconolactone (detected in the infrared at 1735cm^{-1} - 1740cm^{-1}). *Anhydride formation* will occur in a second step, following light absorption, in which the macroradical produced at C5 will react with oxygen, leading to the formation of a carbonyl at C5 and the release of $\bullet\text{CH}_2\text{ONO}_2$, which converts into a final product, methyl nitrate, by H^\bullet abstraction. This anhydride function if detected in the infrared at 1760cm^{-1} ^{19,26}. For more details on the degradation mechanism of CN, please see p. 144 in ref. 26. 230

Figure A4.3. Emission spectra ($\lambda_{exc} = 290\text{nm}$) of artificially aged references irradiated during 50h, 100h and 150h ($\lambda_{irr} \geq 280\text{nm}$, 60°C), using a spectrofluorometer, in A) cellulose nitrate and B) celluloid (70% cellulose nitrate and 30% camphor w/w)..... 231

Figure A4.4. A) Emission spectra ($\lambda_{exc} = 290\text{nm}$) of artificially aged cellulose nitrate irradiated during 50h, 100h and 150h. B) The ratio $I_{425\text{nm}}/I_{510\text{nm}}$ was plotted over irradiation time and a linear regression was calculated. C) $I_{425\text{nm}}$ and $I_{510\text{nm}}$ were calculated as exemplified for $t_{100\text{h}}$, the intensities were corrected for each spectrum by applying a baseline between 360 nm and 550 nm. D) The degree of substitution of the artificially aged cellulose nitrate references was plotted over the irradiation time. At 150h of irradiation, main chain scission leads to the decrease of the νCOC band (1070 cm^{-1}) which is the reference band used for the DS calculation, resulting in higher DS values. Although this measuring technique shows this limitation for high degradation times, below 100h of irradiation the expected DS decrease was observed. In the future, shorter irradiation time intervals will provide more details on how DS correlates with the emission of cellulose nitrate at early stages of degradation ($< 100\text{h}$). 232

Figure A4.5. POLYPHEME raster scan mapping of cinematographic films S4, S5, S6 and 50509. The maps show the intensity variation of the emission band between 500 and 550 nm. Emission spectra collected at the interfaces (green) and the interior (black) of the cross-sections are shown. 233

Figure A4.6. Normalized emission spectra of DIF 50 500 cellulose nitrate support at t_0 (black line) and 150h of irradiation (red line). The spectra are compared with the emission spectrum of cellulose nitrate artificial aged reference irradiated during 150h (blue line)..... 234

Figure A4.7. Infrared spectra of unaged and aged (150 hours, $\lambda_{irr} \geq 280\text{nm}$, 40°C) cellulose nitrate references and cinematographic film DIF 50 500 samples. Using Bussiere et al (2014) calibration curve for the quantification of camphor ($A_{1730}/A_{1655} = 0.013 \times \%\text{camphor}$, in a rough approximation without considering the degree of substitution), in DIF 50 500 we found 6% camphor w/w..... 235

Figure A4.8. a) Emission spectra of zinc oxide from the American Flag Pin (black line) and of a 150h artificial aged cellulose nitrate reference sample (orange line). The ZnO1 band is the band edge emission of ZnO particles (380-385nm); the ZnO2 band/region is due to the ZnO crystal defect emissions between 400 and 450 nm; the ZnO3 broad band is the green emission from ZnO particles; the CN1 band (422nm) is the band that characterizes cellulose nitrate; the CN2 broad band (with max between 500-520 nm) is the band which intensity correlates with cellulose nitrate degradation. b) Emission spectra of a ZnO1 band with very high intensity obtained from the holy bible pin microsample. c) Emission spectra of a high intensity ZnO2 band in comparison to ZnO1, obtained from the 1899 calendar microsample analysis. d) Emission spectra of a ZnO3 band with very high relative intensity in comparison with ZnO1, obtained from the 1901 postcard analysis..... 236

Figure A4.9. A) Raster scanning map by POLYPHEME ($15 \times 15\ \mu\text{m}^2$, 5s, 2 accumulations, $\lambda_{exc} = 290\text{ nm}$) of the American flag celluloid advertisement pin. Three spectral regions were used to map the emission spatial distribution, shown in B). Colors were designated as follows: blue for the band edge emission at 385 nm, green for the spectral region between 400-450 nm; red for the region between 510-550 nm. B) Average spectra, calculated from the selection of 10 spectra from A), were used as reference component

spectra (loadings) to quantify the emission contributions of these spectral regions for each pixel in a direct classical least squares (DCLS) model. For more details, please see text. As an example of the output given by the model for one pixel, the emission spectrum of the marked pixel (X) in map A) is shown (black spectrum). For this spectrum, the model gave a match of 42.8% for the green loading, 28.9% for the blue loading and 28,5% for the red loading. 237

Figure A4.10. TELEMOS, full-field luminescence imaging of the American flag celluloid advertisement pin ($\lambda_{exc} = 290$ nm, 40x objective). Emission bandpass filters used: 352-388 nm (blue); 412-438 nm (green); 535-607 nm (red). The white-square marks indicate the POLYPHEME map area; POLYPHEME, emission distribution profiles for each reference component spectra used in the direct classical least squares (DCLS) modeling of the spectral array. For more details, please see text. It is interesting to observe that the area marked by the green ellipse on the TELEMOS mapping correlates with the POLYPHEME which shows a higher score of the green loading in comparison to blue loading; *Reference component spectra* used in the model, each one obtained for the average of 10 selected POLYPHEME emission spectra. The brighter the pixel on the distribution profile, the higher the correlation with the reference component spectra. The spectral regions viewed using TELEMOS full-field luminescence imaging setup are highlighted, with colors corresponding to the bandpass filters used. 238

Figure A4.11. A) Raman spectra of a whitish particle in the American flag pin sample (633 nm laser) and references of zinc oxide, cerussite ($PbCO_3$) and celluloid (cellulose nitrate and camphor). B) Raman spectrum in the spectral region between 1000 and 1400 cm^{-1} . Peaks attributed to zinc stearate are emphasized in bold. C) FTIR-ATR spectra of the American flag pin (black) and of a zin stearate reference (blue) 240

Figure A4.12. Infrared spectra of Perlov's celluloid objects analysed. Bands at 2918, 2849 and 1539 cm^{-1} observed in the American flag pin are due to zinc stearate. Using Bussiere et al (2014) calibration curve for the quantification of camphor ($A_{1730}/A_{1655} = 0.013 \times \%camphor$, in a rough approximation without considering the degree of substitution), in the calendar we found 18% w/w camphor, in the American flag pin 20%, in the holy bible pin 16% and in the 1901 postcard 15%. 241

Figure A4.13. A) POLYPHEME raster scan mapping of the 1901 postcard ($3 \times 3 \mu m^2$, 5s, 2 accumulation, $\lambda_{exc} = 290$ nm). Colors are associated to the following spectral regions: blue for the band edge emission at 385 nm, green for the spectral region between 400-450 nm; red for the region between 510-550 nm (these regions are highlighted in B). B) Emission spectra of the pixels marked with a cross in the maps showed in A). C) 1901 postcard sample spatially registered false-colour RGB image of the emission at excitations of 365 (blue), 385 (green) and 405 nm (red) with emission bandpass filter 514 nm (30 nm FWHM) The white rectangle marks the POLYPHEME map area..... 242

Figure A4.14. A) POLYPHEME raster scan mapping of the holy bible pin ($2 \times 2 \mu m^2$, 10s, 1 accumulation, $\lambda_{exc} = 290$ nm). Colors are associated to the following spectral regions: blue for the band edge emission at 385 nm, green for the spectral region between 400-450 nm; red for the region between 510-550 nm (these regions are highlighted in B). B) Emission spectra of the pixels marked with a cross in the maps showed in A). C) Holy bible pin sample spatially registered false-colour RGB image of the emission at

excitations of 365 (blue), 385 (green) and 405 nm (red) with emission bandpass filter 514 nm (30 nm FWHM) The white rectangle marks the POLYPHEME map area..... 243

Figure A4.15. A) POLYPHEME raster scan mapping of the 1899 calendar ($6 \times 6 \mu\text{m}^2$, 2s, 2 accumulations, $\lambda_{\text{exc}} = 290 \text{ nm}$). Colors are associated to the following spectral regions: blue for the band edge emission at 385 nm, green for the spectral region between 400-450 nm; red for the region between 510-550 nm (these regions are highlighted in B). B) Emission spectra of the pixels marked with a cross in the maps showed in A). C) 1899 calendar sample spatially registered false-colour RGB image of the emission at excitations of 365 (blue), 385 (green) and 405 nm (red) with emission bandpass filter 514 nm (30 nm FWHM) The white rectangle marks the POLYPHEME map area..... 244

Figure A4.16. Error map of the DCLS modelling performed to the map of the American flag pin sample. Regions of high error (bright intensity) indicate a bad fit. Essentially, this map shows the resin surrounding the sample, which does not fit well with the reference component spectra used..... 244

Figure A4.17. Emission spectrum of the polyester resin used for embedding the celluloid micro samples. 245

LIST OF TABLES

Chapter 1. General Introduction

Table 1-1. Characterization of celluloid artworks/artefacts in the conservation science literature.....	16
Table 1-2. Possible plasticizers used by celluloid companies for camphor total or partial substitution.	20

Chapter 2. The best billiard ball in the nineteenth century: composite materials made of celluloid and bone as substitutes for ivory

Table 2-1. Formulations of the 1868 Hyatt, <i>Ivorylene</i> pool and <i>Bonzoline</i> and <i>Crystalate</i> billiard balls. Weight proportions of bone (B), and camphor (C) are given in relation to cellulose nitrate (CN) as calculated by the calibration curves by infrared spectroscopy; for details, please see the supporting information.	56
---	----

Chapter 3. Safeguarding our dentistry heritage: a study of the history and conservation of nineteenth-twentieth century dentures

Table 3-1. Characterization of NMAH celluloid dentures (MG.M -09686 set) by handheld Raman, μ FTIR and XRF.	81
Table 3-2. Characterization of NMD celluloid dentures by handheld Raman and μ FTIR.....	82
Table 3-3. Characterization of NMD and NMAH vulcanite dentures by handheld Raman, μ FTIR and XRF.....	87
Table 3-4. Characterization of PVC-PVAc dentures from NMD and NMAH by handheld Raman, μ FTIR and XRF.	89
Table 3-5. Characterization of NMD's phenol-formaldehyde dentures by handheld Raman and μ FTIR	90
Table 3.6. Characterization of NMD's PMMA denture by handheld Raman and μ FTIR	91

Chapter 4. For the history of celluloid: Evolution of the comb industry in Portugal, c. 1880-1970

Table 4-1. Evolution of the number of comb workshops and factories in the districts of Lisbon, Viseu, Porto and Braga, between 1890 and 1916. Data for these districts was only registered for the years described. Source: Portuguese statistical yearbooks (INE). 105

Chapter 5. Novel markers to early detect degradation on cellulose nitrate-based heritage at the submicrometer level using synchrotron UV–VIS multispectral luminescence.

Table 5-1. Description and degree of substitution (DS) of the cinematographic films and celluloid objects studied (Perlov’s celluloid collection). 132

Appendix 1. The best billiard ball in the nineteenth century: composite materials made of celluloid and bone as substitutes for ivory

Table A1.1. Transcriptions of the formulations for the manufacture of billiard balls and imitation ivory patented by John Wesley Hyatt and co-inventors from 1865 to 1915. 196

Appendix 2. Safeguarding our dentistry heritage: a study of the history and conservation of nineteenth-twentieth century dentures

Table A2.1. NMD’s denture and sampling location. The microscope images were collected with a DINO-LITE digital microscope. 208

Appendix 4. Novel markers to early detect degradation on cellulose nitrate-based heritage at the submicrometer level using synchrotron UV–VIS multispectral luminescence.

Table A4.1. μ Raman main results for the celluloid object micro samples analysed. The degree of substitution (DS) was calculated with μ FTIR using the calibration curve described in Nunes et al. (2020). 239

SYMBOLS AND NOTATIONS

λ_{exc}	Excitation wavelength
λ_{em}	Emission wavelength
CN	Cellulose nitrate
DS	Degree of Substitution
NMAH	National Museum of American History
NMD	Samuel D. Harris National Museum of Dentistry
μ XRF	Micro-Energy Dispersive X-ray Fluorescence Spectroscopy
μ FTIR	Micro-Fourier Transform Infrared Spectroscopy
ATR	Attenuated Total Reflection
IRE	Internal Reflection Element
ER	External Reflectance
μ Raman	Micro-Raman Spectroscopy
UV-Vis	Ultraviolet-visible
DUV- μ PL	Deep UV synchrotron micro luminescence spectroscopy
NMR	Nuclear Magnetic Resonance
GC/MS	Gas chromatography/Mass Spectrometry
PMF	Peptide Mass Fingerprint
SEM	Scanning Electron Microscope
EDS	Energy dispersive Spectroscopy
XRD	X-Ray diffractometry
SPME-	Solid Phase Microextraction
FF	Front-Face
PMMA	Poly(methyl methacrylate)
PVC	Poly(vinyl chloride)
PVAc	Poly(vinyl acetate)
INE	Instituto Nacional de Estadística

SYNOPSIS

The complexity of the issues surrounding plastics and the need to preserve them as cultural heritage, pose great challenges to history, chemistry, and society, and it is urgent to develop sustainable strategies for their conservation and exhibition. This thesis addressed this challenge focusing on celluloid and bringing a pioneer approach based on a dialog between conservation science and the history of science and technology. The collaboration between these two fields allowed the selection of relevant case studies and their innovative analysis, resulting in a novel perspective on the historical significance of celluloid. This thesis shows the paramount importance of a full understanding of celluloid's materiality for the conservation and preservation of its cultural heritage.

In simple terms, celluloid is a thermoplastic composed of cellulose nitrate and camphor. The invention of the industrial process that allowed the production of a plastic with this composition is credited to John Wesley Hyatt, who patented celluloid in 1870. This material is acknowledged as the first commercially successful semi synthetic plastic material [1]. Celluloid objects are now physical testimonies of a unique cultural context, collected by public and private institutions around the world. Aiming to improve our understanding of celluloid objects history and conservation needs, this thesis started by looking at the formulations used in the first two types of products manufactured with celluloid: billiard balls and dentures.

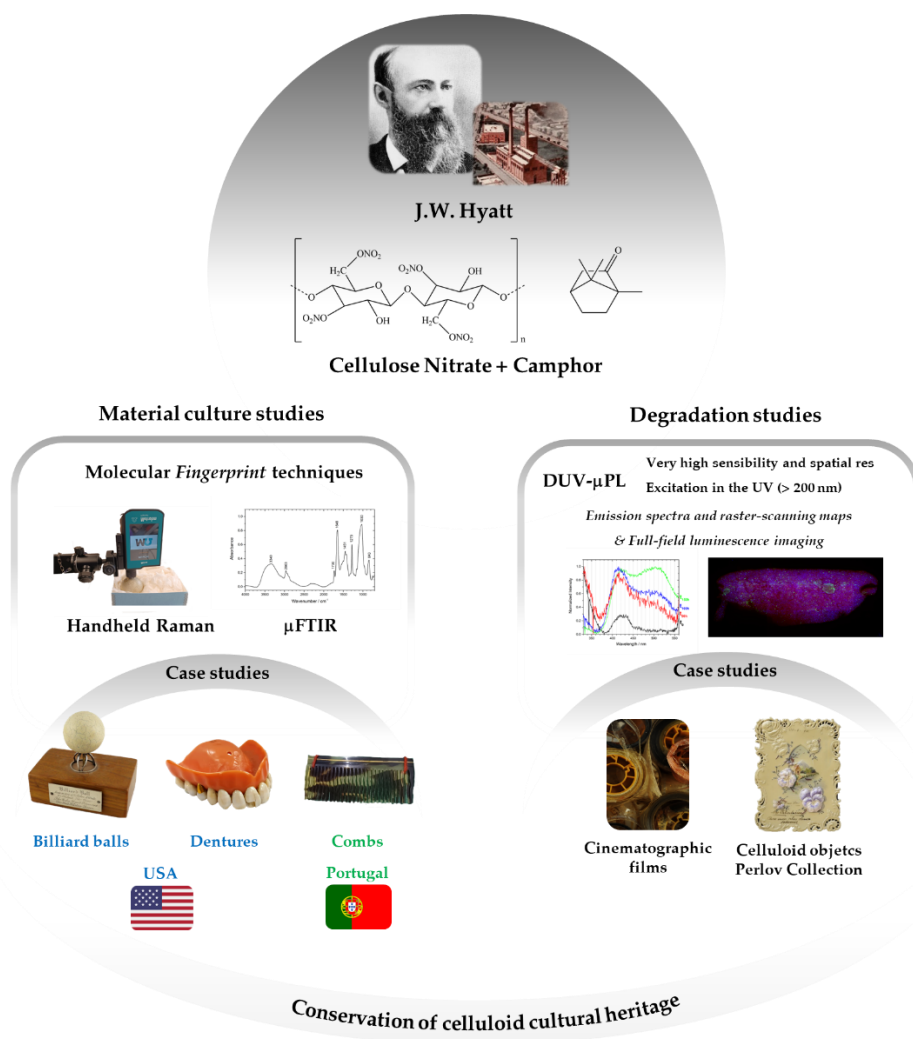
The celluloid billiard balls were a black box. Historians could not ascertain which materials had been used for their manufacture and how; and based on cellulose nitrate properties, celluloid was considered an unsuccessful substitute for ivory, disregarding, however, the possibility of a composite material [1], [2], [3]. To open the box required 1) the characterization of the billiard balls composition and 2) a more careful reading of the written sources on celluloid manufacture and on the billiards world. With this goal, celluloid billiard balls from the Smithsonian Institution's National Museum of American History (NMAH), Washington, D.C., USA, were characterized using a multi-analytical approach. In short, it was discovered that the celluloid billiard balls were made with a ground bone-cellulose nitrate composite (75%/25% by wt.). This composition was successful in the practice of billiards at least until the 1950s and its role in abolishment of ivory billiard balls significant [4]. This work demonstrates how the billiard balls history of development and use can be a remarkable example to explore the dynamics between innovation, sports, environment, and society [5], [6] (**Chapter 2**).

Contrary to the billiard balls, the data on the formulations used for celluloid dentures were consistent: cellulose nitrate, camphor, and vermilion (HgS). However, celluloid success in the denture market was also considered very limited [1]. Thus, it was natural to think that the celluloid dentures had residual expression after the 1880s. For this project, this was

initially considered as an advantage since the analysis of dentures would be informative of early celluloid formulations particularities. With this purpose, the materials of denture collections from NMAH and from the Samuel D. Harris National Museum of Dentistry (NMD, Baltimore, USA) were characterized for the first time. The results were unexpected and showed that the story of celluloid dentures was much more interesting than originally thought; they were significant in the dental prosthetics market from the 1870s to the 1940s (**Chapter 3**).

A vital goal of this project was to contribute for a broader understanding of Portuguese celluloid history. In Portugal, celluloid is entering oblivion, therefore its urgent to bring to light the artefacts that preserve its material memory. Celluloid was introduced in Portugal by the comb industry of Guimarães in 1895 but there was no known physical evidence of celluloid combs [7], [8]. Therefore, the materials of two comb collections from Casa da Memória de Guimarães and Sociedade Martins Sarmento were characterized in-situ. The discovery of combs made of celluloid, horn, cellulose acetate and polystyrene was indicative of the evolution observed in the international panorama for the comb industry: the transition of a traditional industry to the modern plastic industry. A discussion of the evolution of the Portuguese comb industry was made based on the material identification and written/statistical sources. The Portuguese case-study insights on the complex relationship between horn and celluloid, two materials that coexisted in the industrial landscape of Guimarães for decades. The combs collections from Guimarães are distinctive within the context of Portuguese plastics history. As such, it is crucial to promptly establish adequate preservation measures to ensure their safeguarding (**Chapter 4**).

In conservation science, the fundamental analytical methodology is based on spectroscopic techniques, i.e., the use of electromagnetic radiation (input), interaction with matter, and interpretation of the resulting electromagnetic spectrum (output); these techniques can identify the elemental and molecular composition of materials without putting at risk their physical integrity. In this work, the methodology was primarily built on two molecular fingerprint techniques: in-situ handheld Raman spectroscopy complemented with micro Fourier Transform Infrared spectroscopy (μ FTIR) [9]. Handheld Raman MIRA DS was used for the first-time for the characterization of celluloid collections and was demonstrated as an essential tool for the study of plastics in general (validated by the comparison with references and by comparison with μ FTIR).



Scheme 1. Focusing on J. W. Hyatt’s celluloid industry, this thesis addresses the conservation of celluloid cultural heritage with material culture and degradation studies. The combination of culture material studies with material characterization, primarily with Raman and μ FTIR, allowed a new understanding of celluloid significance. The material information gained on case-studies from the USA and Portugal, namely billiard balls, dentures, and combs, is crucial for their conservation. To understand objects degradation, synchrotron deep-UV multispectral luminescence spectroscopy was tested in celluloid cinematographic films and objects from the Perlov’s collection. This technique proved to be a powerful early warning tool and will contribute to innovative preservation methods.

Finally, this project demonstrates Deep UV synchrotron micro luminescence spectroscopy (DUV- μ PL) as a fundamental technique for the study of celluloid heritage, with the potential to be used for the study of plastics in general. The advantage of luminescence spectroscopy over FTIR, is its higher sensibility, meaning that it detects degradation intermediates in lower concentrations (detection limit of 10^{-9} M). This is crucial for heritage studies since degradation must be detected as soon as possible. Using DUV- μ PL for the study of artificial aged cellulose nitrate and celluloid samples revealed the presence of markers that can be used for

the detection of the degradation process at the early stages. Celluloid objects of the Portuguese Perlov celluloid collection were analyzed both in-situ and as microsamples, showing the equipment's versatility. For these objects, the heterogeneous microenvironments of the zinc oxide-based pigment (zinc oxide was extensively used in celluloid as an opacifier and a stabilizer) were mapped with very high resolution. In the future, it will be necessary to understand the zinc-oxide emission variations which are related to the object's history of manufacture and/or degradation [13], [14] (**Chapter 5**).

Overall, the present study underscores the significance of identifying and comprehending the diverse formulations of celluloid, in all its material dimensions, given that this knowledge is crucial for the conservation of its cultural heritage. It is now crucial to assess the stability of the bone-cellulose nitrate composite, of the celluloid-vermillion formulations, the role of camphor (partial) substitutes, such as plasticizers from the phthalate family, or the effect of surface coatings, such as beeswax. It is necessary to create more procedures that allow museums and smaller cultural heritage institutions to identify the materials in their plastic collections, especially if there is high probability of celluloid presence, such as local comb museums. This thesis recommends the creation of a mobile multi-analytical approach, combining handheld Raman spectroscopy, FTIR-ATR, portable X-Ray fluorescence spectroscopy and portable UV-VIS fluorescence spectroscopy for a complete in-situ characterization of celluloid formulations and degradation.

References

- [1] R. Friedel, *Pioneer Plastic: The Making and Selling of Celluloid*. Madison: The University of Wisconsin Press, 1983.
- [2] J. L. Meikle, *American Plastic: A Cultural History*. New Brunswick: Rutgers University Press, 1997.
- [3] M. I. Shamos, *The illustrated encyclopedia of billiards*. New York: Lyons & Burford, 1993.
- [4] R. Levi, *Billiards In The 20th Century*. Manchester: Riso Levi, 1931.
- [5] P. Trabal, "Resistance to technological innovation in Elite sport," *Int Rev Sociol Sport*, vol. 43, no. 3, pp. 313–330, 2008.
- [6] W. E. Bijker, *Of Bicycles, Bakelite and Bulbs: Toward a Theory of Sociotechnical Change*. Massachusetts: MIT Press, 1997.
- [7] M. Miranda, "Fantástico Plástico: Notas sobre o fabrico do brinquedo de plástico no século XX português," *Mínia*, no. 14, pp. 133–150, 2019.
- [8] A. A. das Neves, "As Indústrias Vimeiranas em 1899," *Memórias de Arduca*, 2017.

- [9] Stuart Barbara, *Analytical Techniques in Materials Conservation*. Chichester: John Wiley & Sons, Ltd, 2007.
- [10] M. R. Derrick, D. Stulik, and J. M. Landry, *Infrared Spectroscopy in Conservation Science*. Los Angeles: The Getty Conservation Institute, 1999.
- [11] Y. Shashoua, *Conservation of Plastics: Materials science, degradation and preservation*. Elsevier Ltd, 2008.
- [12] C. Selwitz, *Cellulose nitrate in conservation*. United States of America: J. Paul Getty Trust, 1988.
- [13] M. Thoury et al., "Synchrotron UV-visible multispectral luminescence microimaging of historical samples," *Anal Chem*, vol. 83, no. 5, pp. 1737–1745.
- [14] L. Bertrand, M. Refregiers, B. Berrie, J. Echard, and M. Thoury, "A multiscalar photoluminescence approach to discriminate among semiconducting historical zinc white pigments," *Analyst*, vol. 138, pp. 4463–4469, 2013.

This thesis is based on the following publications:

Chapter 2. The best billiard ball in the nineteenth century: composite materials made of celluloid and bone as substitutes for ivory

Artur Neves, Robert Friedel, Maria João Melo, Maria Elvira Callapez, Edward P. Vicenzi, Thomas Lam, *forthcoming*

Chapter 3. Safeguarding our dentistry heritage: a study of the history and conservation of nineteenth-twentieth century dentures

Artur Neves, Robert Friedel, Maria Elvira Callapez, Scott Swank, *Heritage Science*, 11:142, 2023.
<https://doi.org/10.1186/s40494-023-00989-2>

Chapter 4. For the history of celluloid: evolution of the comb industry in Portugal, 1880-1970

Artur Neves, Maria Elvira Callapez, *Ler História*, 2023, *accepted*

Chapter 5. Novel markers to early detect degradation on cellulose nitrate-based heritage at the submicrometer level using synchrotron UV–VIS multispectral luminescence

Artur Neves, Ana Maria Ramos, Maria Elvira Callapez, Robert Friedel, Matthieu Réfrégiers, Mathieu Thoury, Maria João Melo, *Scientific Reports*, 11(1), 1–13, 2021.
<https://doi.org/10.1038/s41598-021-99058-6>

GENERAL INTRODUCTION

Celluloid objects were collected by several cultural institutions because they played a significant role in a period of profound cultural changes from the 1870s to the 1950s, marked by the transition from natural to synthetic materials. Celluloid, composed of cellulose nitrate and camphor, is one of the perennial conservation and restoration challenges. This is due to its inherently unstable chemistry, which makes it a hazard for itself as for surrounding objects. This thesis seeks to enhance our understanding of the materiality of celluloid objects, providing insight into their biographies and conservation requirements.

This chapter offers a brief overview of the history of celluloid and the objects created from it. Celluloid objects were primarily manufactured to mimic natural materials and coexisted alongside many other semi-synthetic and synthetic plastics, making identification of this material challenging. Identifying materials in collections, particularly celluloid due to its degradation hazards, is the first step for preservation. The methods used to identify celluloid objects were reviewed, focusing on two molecular fingerprint techniques, Fourier Transform Infrared and Raman spectroscopies, which were used in this thesis for the study of celluloid objects' composition and degradation.

To develop new sustainable celluloid conservation and exhibition strategies, it is fundamental to know its degradation mechanisms in detail. In the last 15 years, significant contributions towards this goal were made, which were critically reviewed in this chapter. Photoluminescence spectroscopy has been used for over 50 years to understand polymer degradation mechanisms. This technique is highly sensitive, meaning it can detect degradation products in very low concentrations at the very earliest stages of degradation, which is a crucial feature for heritage preservation. This thesis will demonstrate the value of this technique in the study and conservation of celluloid heritage.

Celluloid is credited as the first commercially successful semi synthetic plastic material. This is because celluloid was not the first attempt to make a solid and pliable mass with cellulose nitrate.

1.1 Cellulose nitrate

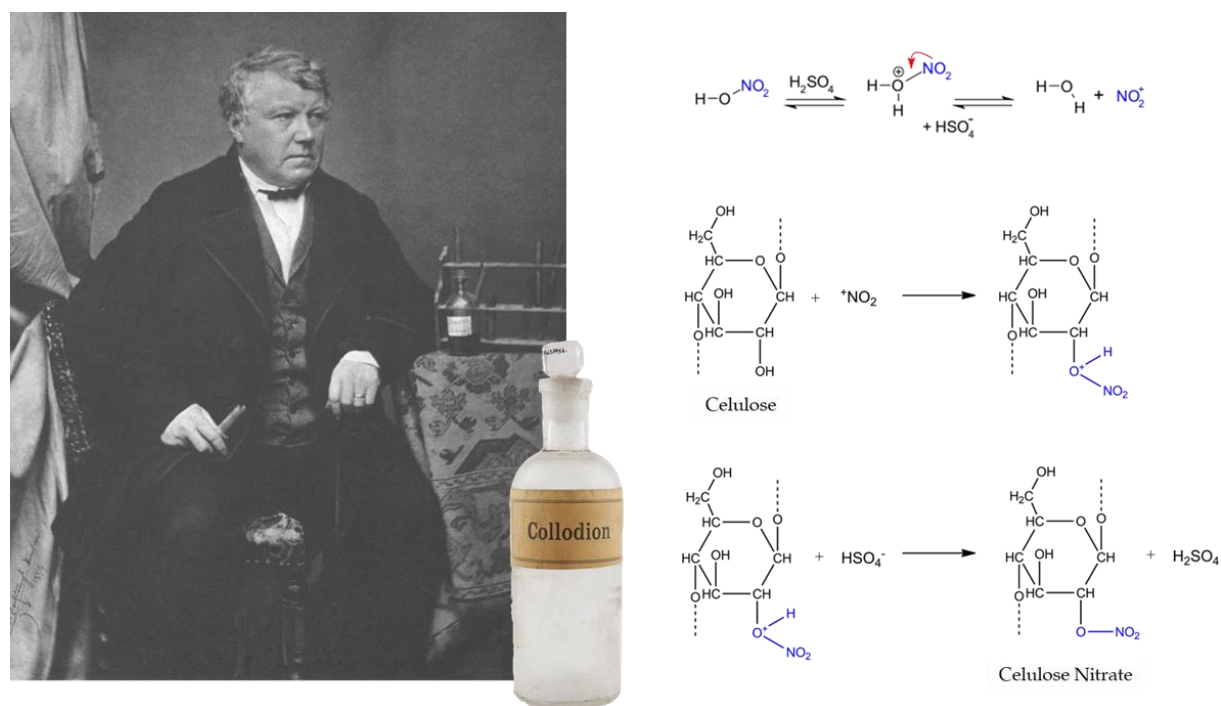


Figure 1.1. Left, Christian Friedrich Schönbein (1799-1868) and a bottle of collodion from the London Science Museum collection. Source: Science Museum Group © The Board of Trustees of the Science Museum. Right, the chemical synthesis of cellulose nitrate by Schönbein. Its innovation was in the use of a mixture of nitric acid and sulfuric acid, which produces nitronium ions (NO₂⁺) that will react with the cellulose hydroxyl groups to produce nitrate groups.

Cellulose nitrate is a polymer composed of d-glucopyranose units linked by glucosidic bonds with a $\beta(1-4)$ conformation. Being a cellulose derivative, the structural differences from cellulose consist of substituting the hydroxyl groups (-OH) by nitrate groups (-ONO₂), **fig 1.1**. In 1833, Henri Braconnot was the first to react concentrated nitric acid with various carbohydrates (potato starch, sawdust, linen and cotton) and to observe the formation of flammable, combustible and explosive substances, which he called xyloidines [1]. In 1846, Christian Friedrich Schönbein (1799-1868) discovered cellulose trinitrate, using an innovative and efficient esterification process consisting of reacting cellulose with a mixture of nitric and sulfuric acids in a proportion of 1:2 or 1:3 v/v [2]. Schönbein's guncotton, which has a nitrogen content higher than 12.3 %, is an explosive material that was used to produce smokeless powder and later cordite. A key characteristic of cellulose nitrate was its solubility in organic solvents. This

led to collodion, a cellulose nitrate solution in a mixture of diethyl ether and ethanol (50/50). This solution led to the development of collodion photography and the first cellulosic plastics [3]–[5].

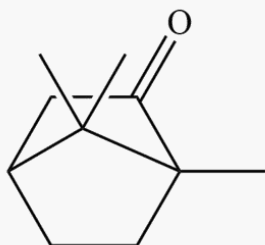
1.2 Parkesine



Figure 1.2. Left, Photograph of Alexander Parkes taken in Vienna in 1875. Right, Circular molded plaque of red Parkesine. Source: Science Museum Group © The Board of Trustees of the Science Museum.

Alexander Parkes (1813-1890) was the first to consciously investigate methods for producing cellulose nitrate plastic, **fig. 1.2**. He wrote, in 1865, that his interest in cellulose nitrate began when he observed the formation of a solid residue after evaporation of the collodion solvent [3]. In an undated note, he wrote that it was in 1852 that he began carrying out the experiments that led to the invention of Parkesine, the precursor of celluloid. Parkesine was exhibited at the International Exhibition in London 1862 and was awarded the bronze medal. According to his 1865 patent, a recipe would consist of 100 parts pyroxylin moistened in naphtha, 10-50 parts nitrobenzene, aniline or camphor and 100 to 200 parts vegetable oil (most likely castor oil) [6]. Parkes founded a company with an initial capital of £10,000 – the Parkesine Company Ltd. This company was unsuccessful and was liquidated in 1868, possibly due to one of these reasons: the use of low-quality raw materials, such as scraps of paper or rags, leading to a product with a “dirty” appearance; the flammability of the material; the use of large proportions of solvents combined with an insufficient drying process, leading to product deformation; failure to conquer specific markets [3], [5], [7], [8].

Camphor (box 1)



Left, Chemical structure of camphor, 1,7,7-Trimethylbicyclo [2.2.1]heptan-2-one (IUPAC), and a picture of refined camphor. **Right**, *Cinnamomum camphora* tree in Serralves Park, Porto, Portugal.

Camphor is a white crystalline solid with a waxy texture and a characteristic strong, fragrant odor. It belongs to the class of organic compounds known as terpenoids. Crude camphor is steam distilled from the camphor tree (*cinnamomum camphora*), which is native to Asia, particularly Japan, Taiwan, and Southeast China. Refined camphor was obtained by sublimation of crude camphor. Before the invention of celluloid, camphor was used for medicinal and religious purposes. In 1932, it was estimated that 80% of camphor was used in the manufacture of celluloid. During celluloid period, the camphor tree was one of the most valuable in the world. There was a ruthless exploration of the forest resources. In 1899, the Japanese government established a monopoly system to control production and prices. This monopoly proved to an unreliable and fluctuating system which led to search for substitutes. Before World War I, synthetic methods were invented in Europe and in the United States of America based on pinenes - one of main constituents of turpentine.

Sources: D. Ponomarev and H. Mettee, "Camphor and its Industrial Synthesis," *Chemical Education Journal*, vol. 18, 2016.; and W. A. Durham, "The Japanese Camphor Monopoly: Its History and Relation to the Future of Japan," *Pac Aff*, vol. 5, p. 797, 1932.

1.3 Celluloid

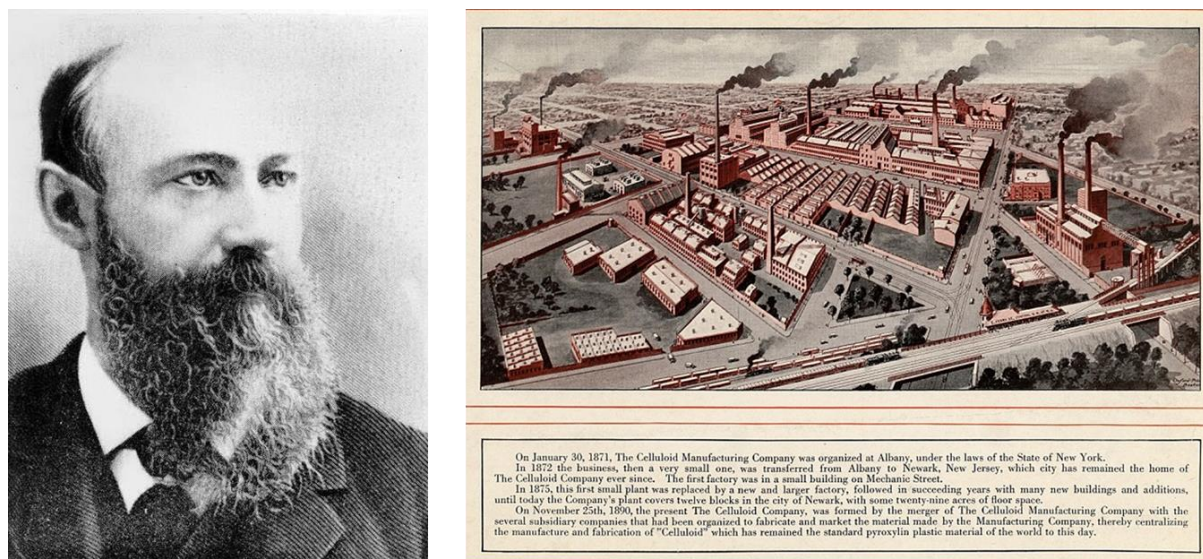


Figure 1.3. *Left*, John Wesley Hyatt (1837-1920). *Right*, The installations of the Celluloid Manufacturing Company, Newark, New Jersey. Source: Celluloid Corporation Records, 1883-1943. Archives Center, National Museum of American History.

In 1863, Phelan and Collender launched a challenge offering \$10,000 (equivalent to \$135,000 today) to the inventor of a billiard ball ivory substitute. The search for a substitute was not a new topic, but the massification of the billiard market, which until then was only upper-class entertainment, created a problem [9]. Friedel (1983) showed that while there was a realistic view that the natural supply was not inexhaustible, what concerned manufacturers were the difficulties in obtaining ivory and transforming it [3].

In collaboration with his brother Isaiah Smith Hyatt, John Wesley Hyatt experimented with well-known plastic formulations of pressed shellac and fillers, such as bone powder, ivory powder or wood pulp. These efforts familiarized him with plastic materials' compression molding processes under pressure and heat. Hyatt continued his experiments and eventually tested with collodion. Due to his previous experience, he found that the collodion contained too much solvent and was unsuitable for manufacturing solid articles. Thus, seeking to "produce a solid solution from mechanical means" Hyatt developed the process that allowed him to establish a new industry. By combining well-ground cellulose nitrate and camphor (50% w/w) and placing the mixture in a mold under heat and pressure with the minimum amount of solvent, he was able to produce a thermoplastic material that retained its shape and surface with effective drying. From this experience emerged the fundamental patent of celluloid - U.S.P. 105,338 (Hyatt and Hyatt 1870). In 1870 the Celluloid trademark was patented by I.S. Hyatt.

Hyatt's Celluloid Manufacturing Company, established in 1871 in Albany, developed an effective business strategy, providing raw celluloid to companies licensed to make consumer goods, **fig. 1.3**. Celluloid was sold as sheets, rods, and tubes to be converted into several products. Although the vast array of applications, the licensed companies were specialized in a narrow range of products, allowing the material to be established in several specific markets [3].

1.3.1 Celluloid objects, from industry to collections

This work focuses on celluloid billiard balls, dentures and combs but it is important to take into consideration the wide range of celluloid products that can be found in heritage collections. Edward C. Worden, the author of the most significant monograph on the nitrocellulose industry, details production processes for collars and cuffs, celluloid stays, brushes, mirrors, and boxes, for playing cards, toys and dolls, celluloid in syringes, celluloid in surgery, piano keys, and for phonograph cylinders, among others [10]. In this thesis, the history of celluloid billiard balls and dentures will be detailed in **chapters 2 and 3**.

1.3.1.1 The imitation of natural materials in everyday and domestic products



Figure 1.4. Left, tortoiseshell comb from the Portuguese national museum Soares dos Reis (19th century). Right, imitation tortoiseshell celluloid comb from the Smithsonian Collection (1900s) (ID Number 2006.0098.0901).

Although celluloid was deemed an inadequate replacement for ivory billiard balls due to its inability to meet the standardized mechanical requirements for billiards, it has been recognized for its exceptional ability to replicate the appearance of costly natural materials with great success. Luxurious every day and domestic objects, such as combs, knives, razor handles, toilet articles, brushes, hand mirrors, umbrella handles, boxes, and furniture, among other fancy articles, were traditionally crafted from expensive natural materials like ivory,

tortoiseshell, and mother-of-pearl. These objects, in which the mechanical properties of the natural materials were less of a concern, were exclusively found in the households of the upper class. Celluloid offered an aesthetically perfect imitation of natural materials with significant economic and technological advantages. This created a new market for lower-income classes since celluloid was considered a desirable material because it was cheap and provided a sense of higher social status [10], **Fig. 1.4**.

1.3.1.2 Ephemeral products



Figure 1.5. Celluloid small memo notebook (left) and folding ruler (right), from the Portuguese Perlov's collection. The handwritten note in the memo book shows how they were used.

Most celluloid objects from the Perlov family collection, donors of more than 1500 celluloid objects to the Smithsonian Institution and 300 to Portugal, are ivory imitations of small articles, such as pocket combs or mirrors, calendars, notebooks or rulers. These objects, called in the 19th century as novelties, were mainly made from celluloid sheets of ivory color, had a modest value, and were typically offered as advertisement souvenirs. Numerous identical copies were produced in large quantities. The production of these novelties can be traced back to the printing industry, which had a long-standing tradition of mass-producing small handbills, cards, prayer sheets, and other ephemeral items. In this case, celluloid was being used as a more resistant alternative to paper, with the fancy appearance of artificial ivory [22]. Many of the celluloid objects of the Perlov's collections of the National Museum of American History (NMAH), Smithsonian Institution, and of Portugal are of these ephemeral typologies, **Fig. 1.5**.

Looking at the celluloid folding ruler, the focus is once again on the properties of celluloid as a cheap, light, flexible, easy to cut and print, and fancy-looking substitute for brass or wood¹.

Celluloid artifacts such as these show the importance of imitation in the innovation process. Celluloid objects were marketed with features of the natural world, thus making them more acceptable to society while gradually introducing new ideas of synthetic plasticity [11], [12].

1.3.1.3 Collars and Cuffs



Figure 1.6. Left, Advertisement for *Challenge Cleanable Collars*; from *The Literary Digest* 1919. Hagley ID, Box/folder number, E.I. du Pont de Nemours & Company Advertising Department records (Accession 1803), Manuscripts and Archives Department, Hagley Museum and Library, Wilmington, DE 19807. Right, celluloid *challenge cleanable collar* from the Hagley Museum and Library, Delaware, USA.

An iconic product made with celluloid were the waterproof detachable collars and cuffs. Detachable linen collars were invented in the early 19th century and were appealing to the growing middle class who had to look presentable and could not afford a clean shirt for each day. Only with the production and commercialization of celluloid sheets was it possible to achieve the technical requirements, such as strength, stiffness, flexibility, color, and product regularity, needed to substitute the linen collars successfully. Also, celluloid was waterproof and easily cleaned with a moist cloth. Rufus Sanborn, Albert Sanborn and Charles Kanouse were the first to use celluloid sheets to manufacture collars and cuffs in 1878 (USP 200939). The manufacturing process was simple: a sheet of muslin or linen was placed between two sheets of

¹ The folding ruler became a popular carpentry accessory after its invention in the mid 19th century.

celluloid. Pressure was applied to unite the three layers, giving celluloid a perfect linen appearance. However, celluloid was always a small fraction of the total collar trade because it was not fashionable. The celluloid collars were undervalued by middle-class critics who associated them with naïve country rustics, the working-class and social “climbers”. Nevertheless, celluloid collars were indeed used by the working-class, railroad workers, police officers, traveling salespeople, waiters or those who lacked access to a professional laundry either financially or geographically, **fig. 1.6.** [5], [13], [14].

1.3.1.4 Piano Keys

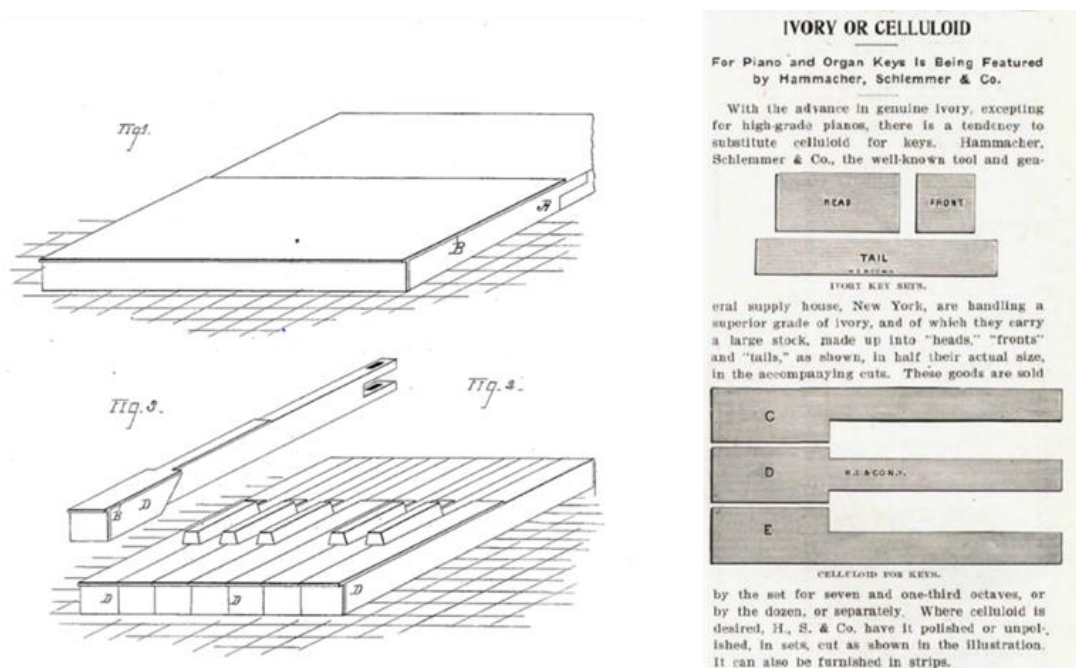


Figure 1.7. Left, John Wesley Hyatt 1878 patent drawing on an “Improvement on Piano Keys” (USP 210750). Right, note on Hammacher, Schlemmer & Co ivory and celluloid pianos keys (Music Trade Review, 1908).

The two most significant products made of ivory in the 19th century were: billiard balls and piano keys. As for the billiard balls, the extent to which celluloid replaced ivory keys remains to be determined. The use of ivory for musical instrument keys was predicated on applying a veneer rather than using solid blocks [15]. In 1878, John Wesley Hyatt devised a method for the manufacture of keyboards from a single sheet of celluloid to avoid the tedious work of cutting and gluing each key separately. This was achieved by coating or placing a sheet of celluloid on top of a keyboard blank, from which the keys were sawed together with the celluloid veneer. This was considered an advantage over ivory, which required the individual cutting of each key prior to assembly. In time, celluloid keys were also sold individually, most probably to be used in key replacements, **fig. 1.7.** The feel of ivory was essential for professional piano players, which shows the importance of the senses in accepting new materials;

the sound of ivory billiards was considered relevant for 19th-century professional billiard ball players. Preliminary studies have shown that celluloid and other ivory substitutes have been used in mechanical pianos, where contact with the keys was unnecessary².

1.3.1.5 Celluloid Phonograph cylinders



Figure 1.8. Left, Edison Blue Amberol records. Source: Archeophone Archives. Right, Edison Amberola from the Smithsonian Institution Collection (ID Number ME.310542).

A comprehensive study of the history of celluloid in music recording technology as still to be performed. E.C. Worden mentions five patents to produce celluloid phonograph cylinders between 1899 to 1910 [10]. In 1906, Jonas Ailsworth, chief chemist for Thomas Edison, fills a patent for a less inflammable “celluloid composition” process, consisting of mixing celluloid with a halogenated fatty acid, giving the example of chlorinated stearic acid (USP 962877, patented in 1910). In 1906, he also filed a patent for a duplicate sound record made with celluloid (USP 953454, patented in 1910). In 1912, Thomas Edison started producing the “Blue Amberol” phonograph cylinders, **fig. 1.8**. They were made of a celluloid coating over a core of plaster of Paris. These records were a significant improvement over the earlier wax cylinders introduced in the 1880s. It was said they were unbreakable and playable for 3000 or more times with no wear. Edison's “Blue Amberol” quickly gained popularity. They were available in various genres, including classical, popular, and folk music. Played at 160 rpm, a Blue Amberol cylinder could produce a recording lasting four minutes or more. These new records were designed to

² Friedel, R., Neves, A., “Saving elephants – understanding the search for substitute ivory”, presented in *Artefacts XXVII: Objects of Science and Technology*, October 16-18, 2022.

be played on the “Amberola” phonograph, which featured a diamond point reproducer, resulting in excellent acoustic quality, **Fig. 1.8**. In 1913, millions of cylinders were used in the USA. The Blue Amberol series represented the lengthiest and most extensive collection of cylinder recordings. The use of phonograph cylinders declined in the late 1920s, and in 1929 Edison ceased production. They were sold in shades of blue/purple, likely with aniline dyes [16].

1.3.1.6 Celluloid in medicine

Celluloid found application in the manufacture of orthopedic body jackets, smallpox vaccine points, vaccine shields, eye bandages, repair cranial defects or used as vials for radium therapy [10], [17]–[19]. While it is conceivable that celluloid has been used for other purposes within the medical field, the full extent of its utilization remains elusive. A brief description is provided for the use of celluloid vaccine points and spine body jackets: the first relates to the topic of ivory substitution, the second to the uses of celluloid in combination with textiles, such as the collars and cuffs.

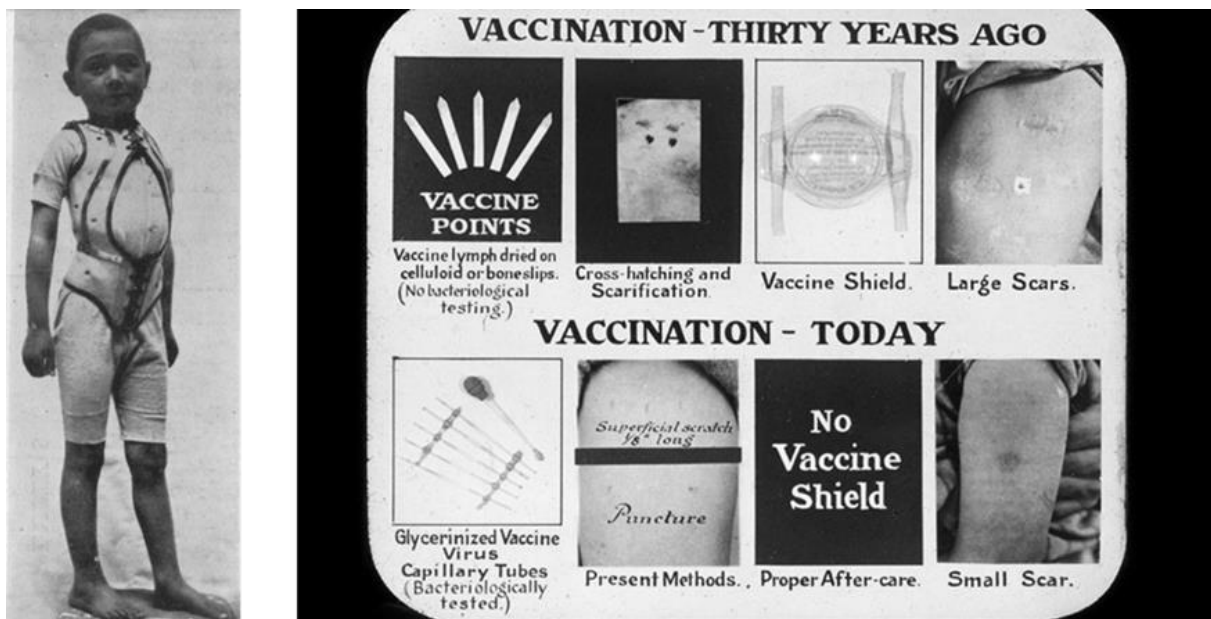


Figure 1.9. Left, Patient with tuberculosis of the spine wearing a celluloid orthopedic body jacket [18]. Right, information slide from the 1930s showing the evolution of small pox vaccination processes. Source: Sanofi Pasteur “The Legacy Project”.

1.3.1.6.1 Smallpox vaccine points

In the 19th century, the main source of smallpox vaccine was humanized lymph. During the early 19th century, Edward Jenner (1749-1823) collected lymph material from the pustule of a person infected with cowpox to develop a vaccine that demonstrated the efficacy of cowpox

in providing immunity to smallpox. Subsequently, Jenner utilized ivory points as a vehicle for the vaccine, which were then utilized to scratch or scrape the skin, thus allowing the vaccine to be administered under the skin [20], [21]. Ivory points were probably relatively expensive to produce, making them less accessible for mass vaccination campaigns. Celluloid was a cheaper material, which could be produced more readily and in larger quantities. The vaccine points were substituted for more sophisticated instruments in the early 20th century, **fig. 1.9**.

1.3.1.6.2 Spine body jackets

In the early 20th century, tuberculosis of the spine was a serious health problem which could cause severe pain, deformity, and even paralysis. At the time, the standard treatment for spinal tuberculosis was to immobilize the affected area using a plaster cast. However, this approach had several drawbacks. The casts were heavy and uncomfortable, and they often had to be removed and replaced as the patient's condition changed. In 1913, Gauvin explained the advantages of celluloid in orthopedic body jackets: they were lightweight, elegant, rigid, yet slightly elastic, possessed a robust structure that remained unaffected by the heat and moisture of the body, retained their shape indefinitely, and were relatively straightforward to fabricate, **fig. 1.9**. A plaster cast was taken of the patient's body, which was subsequently layered with muslin and coated with a celluloid solution until a jacket of suitable strength was achieved. The main problem of celluloid was its inflammability, which ultimately led to its replacement by cellulose acetate [18].

1.3.2 Collecting celluloid

The problems of having a multitude of celluloid objects in a museum collection were pointed out by Coughlin and Seeger (2008) after the acquisition of the Perlov's collection by the Smithsonian Institution (nearly 1500 objects from the 1880s to the 1940s). The authors stated that "from the curatorial perspective, the desirability of acquiring such a large collection was never in question". As celluloid was the first semi-synthetic plastic, "given the importance of plastics in the 20th century this alone gives its significance". For example, the museum collection was enriched by adding items such as campaign buttons related to political history and advertising novelties related to business Americana. However, the curators admitted that the accession of such a large quantity of celluloid objects was intimidating due to the knowledge on the degradation dangers of this material X. But in this case, the curators had the advantage of knowing, empirically, that most of the objects in the Perlov's collection were made of celluloid, which allowed them to prepare accordingly. First, the objects were monitored for off-gassing using acidic vapor indicator strips, primarily using cresol purple. Storage recommendations were established with the primary goal of increasing ventilation. In addition, zeolites

(MicroChamber/Silversafe enclosure paper) were used for the adsorption of the gas emissions, namely nitrogen dioxide. Coughlin and Seeger conceded that the relative humidity of the storage area was difficult to control, ranging from 20% to 65%, far from the ideal 35% to 45% range for celluloid, and that future efforts to have a more stable environment were needed to fully protect the plastic objects [22].

Identification is the fundamental first step to establish proper preservation measures and add crucial information for the object's interpretation and exhibition. This was emphasized in the European Union funded project POPART - the Preservation Of plastic ARTefacts in museum collection (2008-2012): "proper and correct identification of plastic objects requires suitable analytical techniques and needs the support of reference materials" [23]. Museums and smaller cultural institutions that hold plastic objects face the challenge of managing and conserving these high-risk collections. However, proper identification of materials in a collection can be found to be unexplored, incomplete, or inadequate, for example, by misidentification. This can be due to several reasons, like the lack of resources or expertise. Identifying plastics in collections is not straightforward due to the wide variety of materials within the plastic family, consisting of many complex polymers.

1.4 The identification of celluloid

Celluloid was superb at imitating natural materials; therefore, it is very difficult to identify it based on visual means. In addition, its coexistence with cellulose acetate, which shares chemical similarities, and with a plethora of other (semi) synthetic polymers, makes the identification matter a complex endeavor.

The smell of plastics has been used by the conservation community for preliminary plastics identification [24], [25]. The odor of camphor is indicative of celluloid presence. However, when camphor odor is weak or absent, it is necessary to rub the object's surface. From the conservation point-of-view, this is not recommended: it damages the object's surface, increases surface roughness, and induces greater camphor loss, accelerating celluloid degradation. Furthermore, this method may not be reliable due to its empiric nature; it depends on the odor sensibility of the practitioner. It is also an unhealthy method: the evolved gases from celluloid degradation are noxious.

Chemical tests for the identification of cellulose nitrate were devised because of its flammable and chemically unstable nature: diphenylamine, resorcinol, carbazole, aniline acetate and 1-naphthol (Molisch test) [24], [26], [27]. These tests have as a basis the color change observed when the test solution reacts with the sample. Even though these chemical tests can be used as a preliminary step for the characterization of a collection, they present significant

drawbacks: 1) if used directly in the object, it will leave a stain; 2) it is difficult to visually assess the color change when dealing with microsamples collected from the object; 3) the sample cannot be used for further analysis; 4) some of these tests are not celluloid specific meaning that the color change can be misleading.

Recently, a “non-analytical” method for the identification of plastics, in which celluloid is included, was developed – The Plastics Identification Tool (PIT) (<https://plastic-en.tool.cultureelerfgoed.nl/info>). The identification is based on categories: “foam”, “film” (or tapes), “elastomer” (rubbers) and “rigid”, further divided into subcategories. Then, the date is asked, followed by several yes/no questions regarding the properties and degradation of the object. The answers provide a score on the probability of the plastic in hand, which can be improved using a specially developed kit with plastics samples for comparison. This is a similar but improved method of what was already used in some museums, such as the Science Museum of London, for the typological and visual identification of plastics [28]. However, because these methods rely on probabilities, they should only be used for preliminary identification.

With the advances in molecular spectroscopy, namely in the development of portable and handheld devices, it is possible to readily and unequivocally identify the materials found in a heritage collection at the molecular level. Molecular spectroscopy can be performed in situ and used for the qualitative and quantitative characterization of the polymer matrix formulation and degradation. The most used molecular technique in polymer science is Fourier Transform Infrared spectroscopy [29].

1.4.1 Fourier transformed Infrared Spectroscopy

Infrared (IR) spectroscopy measures the interaction of infrared radiation with matter. Because the energy of IR is low, the primary transitions observed in IR spectroscopy are vibrational and rotational. Infrared light (IR) is divided into three spectral regions: the near, mid and far IR. In FTIR, mid IR light ($4000\text{--}400\text{ cm}^{-1}$; $\sim 2.5\text{--}25\text{ }\mu\text{m}$) is generated by a light source and directed to an interferometer. The Michelson interferometers are the most used in FTIR equipment. They work by splitting the beam of light into two separate paths, recombining them, and observing the resulting interference pattern. This interference pattern provides information about the phase difference between the two paths, which is used to accurately determine the frequency of the absorbed vibrations. Without an interferometer, obtaining the precise frequency information needed for accurate infrared spectroscopy would not be possible. After the interferogram reaches the detector, the infrared spectrum is calculated by a computer using a Fourier transform algorithm. The output, the infrared spectrum of the sample, is a plot of the sample’s absorbance as a function of the wavenumber ($1/\lambda$) showing the absorption bands of each molecular vibration [27], [29]–[31].

Because the molecular vibrations are unique to the molecular structure, FTIR is a very powerful tool for material characterization, known as a fingerprint technique. Vibrational frequencies can be divided into two categories: group frequencies and fingerprint frequencies. The group frequencies are ascribed to a specific functional group; the fingerprint frequencies are unique to the molecule as a whole. This means that in a complex mixture, FTIR can unequivocally discriminate between different compounds [32].

There are two requirements for the absorption of IR light by a sample: 1) the frequency of the light must be equal to the frequency of vibration; 2) the vibration must change the dipole moment of the molecule. A large change in the dipole moment will produce intense bands; therefore, highly polar groups, such as the nitrate groups of cellulose nitrate, will produce intense absorption bands in the IR spectrum. Large concentrations of functional groups will also create intense absorption bands since IR spectroscopy obeys to the Lambert-Beer law, i.e., there is a linear relationship between absorbance and concentration:

$$A = \epsilon bc$$

where A is the absorbance; ϵ is the molar absorptivity, b the sample pathlength, and c the concentration.

Therefore, infrared spectroscopy can be used as a quantitative method. For example, the *absorbance ratio* method can be used to calculate the proportion of two compounds in a mixture. In this method, reference samples are prepared by mixing the previously identified compounds in variable concentrations. Then, a calibration curve is obtained by plotting two absorption bands of interest (absorbance ratio) versus the concentration ratio. Then, it is possible to determine the concentration in the “real” sample by applying the calibration curve [30]. Being a quantitative technique, FTIR is also a fundamental technique in studying polymer degradation kinetics [33].

Transmission FTIR is the traditional method and is based on the absorption of infrared radiation as it passes through the sample to the detector. Sirkis [6] pioneered the use of transmission FTIR to study celluloid objects, namely for identifying cellulose nitrate and camphor, **table 1.1**. In 1989, Shearer used micro FTIR to analyze celluloid hand mirrors and a cylindrical box of the Vestry House Museum [34]. In 1993, Derrick et al. studied Antoine Pevsner and Naum Gabo sculptures using micro FTIR. They presented their work at the conference Saving the Twentieth Century organized by the Canadian Conservation Institute in 1991. This conference laid the foundations of the discipline of plastics conservation [35].

Micro FTIR consists of an FTIR spectrophotometer coupled to a microscope with an optical system adapted for infrared radiation. For transmission micro FTIR analysis, it is necessary to collect microsamples (<500 μ m) from the objects under a microscope using appropriate

micro tools. When performed by an expert, this sampling technique leaves invisible traces to the naked eye and depth profiling studies can be pursued. To ensure that the sample has a certain degree of transparency towards the IR light, the sample is compressed between two micro-compression diamond cells (the diamond presents absorption bands between 2500 and 1800 cm^{-1} removed during background acquisition). Micro FTIR are equipped with Mercury-Cadmium-Telluride detectors, cryogenically cooled to liquid nitrogen temperature, which are of fast response and highly sensitive, allowing to detect compounds and degradation products as low as parts-per-billion (ppb) [31]. Finally, the microsample can be retrieved for further experiments, namely complementary μ Raman spectroscopy.

Attenuated total reflectance (ATR) is the most common FTIR method used in heritage studies. Transmission FTIR requires expensive and stationary equipment and expert sample preparation. Portable ATR-FTIR are small, easy to transport, have considerably lower costs and allow recording high-quality infrared spectra in less than 1 min. This promoted its extended use in museums, galleries, archives, and conservation labs [38]. ATR-FTIR is a superficial analysis (0.3 μm - 5 μm), dependent on the intimate contact of the sample's surface with a transparent material with a high refractive index called the internal reflection element (IRE). Because most of the organic materials have a refractive index of 1.5, the refractive index of the IRE must be higher than 2.4 so that all the light is reflected to the IRE after reaching the non-absorbing boundary of the sample. IRE is commonly made of zinc selenide (ZnSe), germanium (Ge) or diamond. At the point of reflection, an exponentially decaying wave – known as the evanescent wave – penetrates the sample. This wave will be attenuated by the absorption of the sample, which will result in observing the characteristic infrared spectrum. The following equation gives the penetration depth of the evanescent wave:

$$d_p = \frac{\lambda}{2\pi n_1 \sqrt{(\sin^2 \theta - \left(\frac{n_2}{n_1}\right)^2)}}$$

where d_p is the penetration depth, λ is the wavelength of the radiation in air, θ the angle of incidence of light at the surface, n_1 the refractive index of the IRE and n_2 the sample's refractive index. This equation shows that d_p increases with the wavelength (λ); therefore, higher absorbances will be observed at decreasing wavenumbers ($1/\lambda$). To obtain a spectrum without this “ATR effect” and increase its resemblance with a transmission IR spectrum, “ATR corrections” can be applied. However, they are not recommended since they deform the spectrum and the result is never identical to transmission [29], [37].

Table 1-1. Characterization of celluloid artworks/artefacts in the conservation science literature.

Objects analyzed	Analytical techniques	Te-	Characterization	Reference
Nail Buffer	FTIR		Cellulose nitrate	Sirkis (1982)

		Camphor	
Hand mirrors and a cylindrical box from the Vestry House Museum	μ FTIR	Cellulose nitrate Camphor	Shearer (1989)
Antoine Pevsner's Torso (1924 to 1926)	μ FTIR SEM-EDS XRD	Cellulose Nitrate Camphor <i>Identification of nitrate/sulphate salts</i>	Derrick et al. (1993)
Tortoiseshell tray, yellow comb, and parts of a jewelry object	FTIR	Cellulose nitrate Camphor	Hamrang (1994)
18 objects donated by The National Museums of Scotland, Science Museum in London, the Musee d'Oyonnax in France, the British Museum and the Museum of London, such as combs, boxes, fans and others	μ FTIR IC	Cellulose nitrate Camphor (100%) <i>Although it was not possible to identify them, the author suggested that some objects also had phthalate plasticizers</i>	Stewart (1997)
10 ivory imitation fans and 1 <i>Zéphyr</i> ventilator fan. One of the ivory imitation fans is dated from 1885. From Palais Galliera, Paris	FT-Raman	Cellulose trinitrate Camphor (all objects) DMP or DBP (3 faux ivory fans) <i>Camphor partial replacement</i>	Paris and Coupry (2005)
Naum Gabo's Construction in Space: Two Cones (1927), Philadelphia Museum of Art	Py-GCMS	Camphor glycerol triacetate phthalic acid esters tri-phenylphosphate.	Sutherland et al. (2012)
Comb, from Palais Galliera, Paris (1910)	SPME-GC/MS	Cellulose nitrate Camphor	Lattuati-Derieux et al. (2012)
Window from Douglas World Cruiser (1924) and Aviator Goggles (1914-1918), from the Smithsonian Institution, Washington, D.C.	FT-Raman	Cellulose nitrate Camphor	Madden et al. (2014)
Orange ruler and degraded ruler from the SamCo collection; "Head of the Pitchfork Lady" by Don aum 1964, The Art Institute of Chicago collection	ER-FTIR	Cellulose nitrate <i>Additional unidentified bands</i>	Saviello et al. (2016)
László Moholy-Nagy plastic substrates from paintings T1 (1926) and T2 (1930), Solomon R. Guggenheim Museum	ATR-FTIR Py-GC/MS	Cellulose nitrate TPP or TCP DEP or DMP diethyl diphenyl urea glycerol triacetate (minor) <i>camphor total replacement</i>	Salvant et al. (2016)
5 cosmetic boxes and purses from the National Museum of Costumes and Fashion, Portugal	μ FTIR ATR-FTIR NMR Py-GCMS	Cellulose nitrate Camphor (all objects) DEP and DMP (all objects) Acetanilide (1 object) <i>Camphor partial replacement</i>	Pereira et al. (2016)
Imitation Ivory reference bought on Ebay; and an ivory imitation Vanity Box (1940s)	ATR-FTIR ER-FTIR	Cellulose nitrate	Bell et al. (2019)
Antoine Pevsner, Head of a Woman. (1923), Hirshhorn Museum; Two mirrors and one toothbrush, from GCI Plastics Reference collection; ruler and one ivory imitation reference from SAMCO reference collection; 15 hair combs from the Harald Szeemann archival collection, early 20 th century (21 objects total)	GC/MS IC	Cellulose Nitrate Camphor (100%) TPP (1 object, ~5%) DEP (2 objects, ~10%) Acetanilide (4 objects, ~20%) <i>Camphor partial replacement</i>	Mazurek et al. (2019)

ATR-FTIR has been successfully applied in the study of celluloid, both for the identification of cellulose nitrate and camphor, **table 1.1**. It is important to highlight the work by Saviello et al. (2016) using External Reflectance (ER) – FTIR. One of the drawbacks of ATR is that it requires intimate contact between the sample and the IRE, meaning that a compression force

needs to be applied to the objects/sample being analyzed. This should be avoided since damage can occur, especially in degraded/brittle materials, which is frequent when dealing with celluloid. External reflectance offers a portable contactless analysis, thus very promising for heritage conservation research. However, reflectance IR spectra are still difficult to interpret because it is a young field of study. Kramers Kronig Transform (KKK) has been applied to the ER spectra to obtain a spectral correspondence with the transmission profile. Saviello et al. (2016) successfully identified celluloid; however, the authors experienced difficulties understanding the additives' signals [38].

1.4.2 Raman Spectroscopy

Raman spectroscopy is a complementary technique to infrared spectroscopy. Both are vibrational techniques and the vibrational transitions observed have the same frequencies. Although the intensity of the bands can differ because the physical mechanisms in action are different: IR is an absorption process, Raman is a scattering effect. In Raman spectroscopy, the sample is irradiated with a laser, i.e., an intense monochromatic light. The main feature observed from this interaction is the Rayleigh scattering, which has the same frequency as the laser (ν_0). The Raman lines are the weak additional features of the scattered light, which have frequencies equal to the difference between the Rayleigh line and the vibrational energy spacings ($\nu_{\text{raman}} = \nu_0 - \nu_{\text{vib}}$). This is due to the inelastic scattering of photons by molecules. From here, we can calculate the frequency of vibration [32].

The intensity of the IR absorption is determined by the change of the dipole moment during the vibration:

$$I \propto \left(\frac{\partial \mu}{\partial Q}\right)^2$$

where μ is the electrical dipole moment and Q is the normal coordinate, ie, the mathematical description of the vibration. Polar bonds, where atoms have different electronegativities, show intense stretching absorptions, such as O-H, C-O, or C=O. On the other hand, if the atoms share similar electronegativities, the absorption bands will be weak, for example C-H or homonuclear bonds, such as C=C.

The change in the polarizability determines the intensity of the Raman lines during a vibration:

$$I \propto \left(\frac{\partial \alpha}{\partial Q}\right)^2$$

where α is the polarizability and Q is the normal coordinate. Polarizability is “the ease of distortion of the electron cloud of a molecular entity by an electric field” [39]. The polarizability is large when there is a dense electron cloud. Therefore, multiple bonds, such as C=C, C=O, C=N, or bonds with heavy metals, will show intense Raman bands [32].

Raman spectroscopy has the major advantage of offering simplicity of measurement: this technique can be used directly on the object without contact or preparation. However, it was not applied as often in polymer science as infrared spectroscopy because of fluorescence noise. Raman bands are weak compared to incident radiation. Therefore, if the sample absorbs in the spectral region of the laser, namely lasers with visible wavelengths, such as 532 and 633 nm, fluorescence emission will create background noise and hide the Raman bands [29], [40].

The development of equipment with near-infrared (NIR) lasers, such as 785 nm and 1064 nm, but more specifically NIR- excited Fourier Transform Raman Spectroscopy (FT-Raman), significantly diminished the problem of fluorescence and increased the importance of this technique in polymer characterization. This was first shown for celluloid objects with the work of Paris & Coupry [41] that established FT-Raman spectroscopy (Nd: YAG laser with excitation at 1064 nm) as a powerful in situ technique to characterize celluloid and its plasticizers, namely camphor, through a sharp peak at 650 cm^{-1} , **table 1.1**. Also using FT-Raman (Nd: YVO4 laser with excitation at 1064 nm), Madden et al. [42] successfully characterized celluloid aviation artifacts. More recently, Neves et al. [43] using a confocal μ Raman (He-Ne laser with an excitation at 633 nm) showed that this technique could characterize the formulation and degradation in celluloid cinematographic films.

Nowadays, one of the key advantages of Raman spectroscopy is that it offers a wide range of mobile options. Divided into portable, handheld and palm size, in situ Raman has become a fundamental technique in studying paintings, manuscripts, sculptures or glass objects [44], [45]. However, in situ Raman studies of (semi) synthetic polymers in heritage are scarce. Klisińska-Kopacz et al. [46] used a portable DeltaNu Raman spectrometer equipped with a 785nm diode laser (120 mW) to characterize PVC cast sculptures of the National Museum of Krakov. Boyden et al. [47] used a portable B&W Tek iRaman Plus spectrometer equipped with a 785 nm diode laser (200mW) and a fiber optic probe for the study of the Plastics Artifacts Collection at Syracuse University Libraries, identifying cellulose acetate, polystyrene and poly(methyl methacrylate). The most frequently used laser wavelength in mobile Raman equipment is 785 nm (diode laser) because it balances Raman intensity and fluorescence suppression. Notwithstanding, longer wavelength laser options are available if better suited for analyzing specific historical artifacts [44].

1.4.3 Identification of camphor substitutes

Although camphor was considered the best cellulose nitrate plasticizer, several alternatives were tested. Sachs and Byron [48] summarized the reasons for camphor substitution: 1) camphor's odor was considered unpleasant; 2) camphor high melting point (175°C), meaning that great care was required to exercise the dangerous temperatures necessary to combine it with cellulose nitrate; 3) the price fluctuations imposed by the Japanese monopoly over the supply of natural camphor.

Table 1-2. Possible plasticizers used by celluloid companies for camphor total or partial substitution.

Compound	Company	References
naphthyl acetate; methyl naphthyl ketone	Zuhl & Eisemaan	Bersch (1904)
Acetochlor; sebacic acid derivates	Goldsmith and British Xylonite Co. Ltd.	Main (1913) [42], [45], Janeiro (1951) [46]
naphthalene	Société Générale pour la Fabrication de Matières Plastics	
Triphenyl, tricresyl and trinaphthyl phosphates	Celluloid Corporation. Celanese Chemical Company. Zuhl & Eisemaan; Rheinisch-Westfälischen SprengstoffFabriken	Bersch (1904) Sachs (1921) [19], [41], Caprio (1943) [45], [47], Reilly (1991) [48] Salvant (2016)
Dehydroacetic acid	Union Carbide	Reilly (1991) [19]
Fructose; Lactose; Sucrose	Rhenische Gummi and Zelluloid Fabrik	Worden (1911) [8]
Aromatic sulfonic acid derivatives. Phthalic acid esters	Farbwerke (Meister, Lucius & Bruning)	Bersch (1904) Main (1913) [45], [46]
aromatic amine acetyl derivatives	Deutsche Zelluloid Fabrik	

John Henry Stevens, the chief chemist of the Celluloid Manufacturing Company, experimented with several compounds in the 1880s and 1890s, ranging from oil of caraway seed, hyssop, sage, tansy, cloves, winter green, chamomile, or cinnamon. Finally, in 1894, he patented acetanilide as a true substitute for camphor: acetanilide had a melting temperature of 112°C and was odorless [49]. The technical literature on celluloid manufacture mentions the use of acetanilide in different terms: Worden (1911) detailed that acetanilide was used

primarily in Germany to replace camphor partially and that it was the most valuable odorless substitute; Masselon, Roberts and Cilliard (1912) stated that acetanilide was used to a large extent in second rate quality products; Stokes and Weber (1917) mentioned that camphor was occasionally replaced by acetanilide and called it the odorless celluloid; Sachs and Byron (1921) talked about the use of ethyl acetanilide in the United States but with unsatisfactory results; Rio de Janeiro (1951) vaguely mentioned that many firms used acetanilide, the most widely used substitute used in colored applications [8], [48], [50]–[52].

A review of the technical literature allowed to identify other camphor plasticizers possibly used at an industrial scale for celluloid manufacture, **table 1.2**. Triphenyl and tricresyl phosphates (TPP and TCP) were very successful in the USA, with the tradename Lindol sold by the Celanese Corporation. First patented by Zuhl and Eisemaan in 1902, these two substances were claimed to be cheaper and make celluloid less flammable, odorless, and resistant to external influences. Also, they had a lower melting point than celluloid (49.9°C for triphenyl phosphate). TPP became the most common plasticizer for cellulose acetate. According to Selwitz (1988), phthalic acid esters started to be used in the 1920s. After 1933, di(2-ethylhexyl) phthalate became the most used because of its low price. These phthalate plasticizers substituted camphor with success in the production of cellulose nitrate lacquers and adhesives [53], [54].

The review of the technical literature was combined with a review of the plasticizers identified in heritage studies, **table 1.1**. In all instances, camphor was only partially replaced by other plasticizers, except for the case of Trolit, manufactured by the Rheinisch-Westfälischen SprengstoffFabriken, Troisdorf, Germany, in the 1920s. The characterization by Salvant et al. [58] of Trolit showed the additional identification of diethyl diphenyl urea. According to Miles [59], this compound was known as Centralite and was the only camphor substitute extensively used in the explosives industry. It received this name because it was first used by a factory called Centralstelle in Berlin.

For the identification of camphor, FTIR is well established by the detection of the CH, CH₃ and carbonyl stretching bands. However, FTIR is not well suited for identifying phthalates since the characteristic bands of these compounds are generally masked by the stronger absorptions of cellulose nitrate and camphor, as first noted by Stewart (1997).

Paris & Coupry [41] showed that Raman spectroscopy is powerful in identifying phthalic acid esters, detecting peaks at circa 1040 cm⁻¹ due to the ortho phthalate planar ring bending and between 1650 and 1550 cm⁻¹ due to the phenyl ring bending [60]–[62]. This was further demonstrated by Madden et al. [42] and Neves et al. [43]; this last work on the analysis of cellulose nitrate cinematographic films in which camphor and a phthalate plasticizer were detected. Although Paris & Coupry and Madden et al. did not detect triphenyl phosphate on

celluloid objects, they showed that this technique could identify this compound based on a strong peak at 1007 cm^{-1} attributed to the bending of the benzene rings.

The identification of triphenyl/tricresyl phosphates and acetanilide has been successful by Pyrolysis Gas Chromatography/Mass Spectrometry (Py-GC/MS). However, due to the destructive nature of this technique, Pereira et al. (2016) successfully tested a novel approach using $^1\text{H NMR}$ to analyze surface exudates (through dissolution in 99.96% deuterated methanol).

1.5 The degradation of celluloid objects

The work of Linda Sirkis in 1982 was pioneering in the study of the degradation of celluloid objects [8]. She described the three main degradation pathways: thermal, photochemical, and hydrolytic by the action of water. The early signs of celluloid degradation were noticeable by the darkening and embrittlement of packing materials, which reacted with the nitric acid released by the polymer. In extreme cases, the celluloid objects showed a crazing pattern leading to total fragmentation. Furthermore, she observed a loss of camphor between 25 to 40% from celluloid objects using Gas Chromatography and noted that camphor impurities accelerated degradation. On the photochemical mechanisms, she stated that they were still unknown. However, using Fourier Transformed Infrared Spectroscopy (FTIR), she suggested that camphor could have an essential role in celluloid photodegradation because of the differences observed in the infrared spectrum of camphor extracted from a degraded plastic compared to the pure material.

In 1988, Rankin, Pullen, and Heuman emphasized the complexity and dangers of celluloid degradation in museum collections [63], [64]. They described the degradation of the early constructivist sculptures of Antoine Pevsner and Naum Gabo; for example, Pevsner's *The Dancer* (1927-29) had yellowed and no longer showed the desired effect of transparency; Gabo's *Construction in Space: Two Cones* (1927) was utterly fragmented. The degradation examples of Naum Gabo sculptures were dramatic and urged the development of efficient preservation strategies for celluloid, cellulose acetate, and plastics in general. It was also in this year that Selwitz wrote the first comprehensive work for the conservation community on the thermal, photochemical, and hydrolytic degradation of cellulose nitrate.

In the 1990s, Derrick, Stulik and Ordonez (1993) studied three Naum Gabo sculptures from The Museum of Modern Art (MoMA) collection [65]. Using FTIR, they observed that samples with different degrees of degradation showed different spectral profiles. Samples collected from the surface showed lower concentrations of camphor than those collected at 2mm depth. The decrease of the carbonyl absorption band at 1730 cm^{-1} confirmed camphor loss at the surface. By FTIR and XRD, the identification of nitrate and sulfate salts showed the

reactivity of the acids formed in celluloid degradation, nitric acid and sulfuric acid, and the danger of contact with metals. In addition, differences between the degradation of transparent and opaque pieces were observed. Also in this decade, Julie Reilly (1991) published an excellent review on the chemistry and preservation of celluloid objects, placing pertinent questions on the inherent sources of celluloid degradation, such as impure camphor or the sulfate content [26]. Another similar work was that of Megan. E. Springate (1997), alerting for the conservation of celluloid objects found in archaeological assemblages [66].

Although this object-driven research was crucial to understanding the physical consequences of celluloid chemical degradation, it proved extremely difficult to devise stabilization procedures [25], [65]. In 1991, Jacques Lemaire changed the paradigm by introducing the concept of the “mechanistic approach” to the conservation community; the complete understanding of the complex mechanisms that lead to chemical evolution is the prerequisite to devising efficient and sustainable conservation strategies [67].

In the 1970s, Jacques Lemaire and his group from the Chemistry Department of Clermont-Ferrand University, Paris, France, initiated fundamental research about polymer degradation by applying this approach. The polymer is considered a chemical reactor, continuously fed with energy, leading to the formation of degradation intermediates in very low concentrations. This results in a cascade of reactions, namely chain-scission and/or reticulation, that modify the physical properties of the polymer. To understand these mechanisms and predict the polymer lifetimes, it is necessary to identify the intermediates at the molecular scale using sensitive molecular techniques, such as FTIR and Raman, in artificially accelerated conditions. Because the reactive intermediates absorb light in defined UV-VIS regions, it is possible to simulate natural aging in photochemical artificial accelerated conditions. Each formulation is characterized by a specific acceleration factor [68].

The research groups of Jacques Lemaire and Norman S. Allen showed that light is the main factor in polymer degradation [68], [69]. Hydroperoxides (COOH) are one of the first and principal reactive intermediates. The production of these groups in the polymer structure is possible because, in the ground state, atmospheric molecular oxygen (O_2) has two unpaired electrons, i.e, it exists in a triplet state and has a biradical behavior. Molecular oxygen will react with the radicals in the polymer matrix, induce hydrogen abstractions and produce hydroperoxides. Hydroperoxides absorb sunlight ($\lambda \geq 300$ nm) and will suffer the homolytic or heterolytic cleavage of the weak oxygen-oxygen bond, leading to the formation of carbonyl groups. The carbonyls will also absorb light inducing Norrish reaction types I and II, producing more reactive intermediates to feed the reactor. In the limit, the polymer matrix collapses.

1.5.1 Cellulose nitrate degradation mechanisms

Due to cellulose nitrate's thermal sensitivity, the study of its thermal decomposition has been pursued ever since its manufacture. The focus on this matter resulted from the severe risk of storing cellulose nitrate explosives. The first important works were published between 1900 and 1912, namely the investigation by Will, a German chemist from Berlin. Although the light sensitive nature of the polymer was already known by 1867, as Frederick Augustus Abel observed that guncotton became acid when irradiated, since explosives were not exposed to light, this subject only gained importance with the increasing application of lacquer finishes in the industry from 1920 onwards [59]. Finally, almost one century passed, Thérias et al. [70] demonstrated that the mechanism of photochemical degradation is identical to thermal, with the oxidation rate being faster. This was a significant breakthrough as it is now possible to relate the thermal and photochemical investigations undertaken over the years. Furthermore, degradation studies can now undergo photooxidative accelerated aging of cellulose nitrate, providing higher reaction rates and, thus faster experimental data acquisition. Based on a critical revision of the works published in the literature [70]–[84], an integrated degradation mechanism is described by three main phases depicted in **Fig. 1.10** and **1.11**.

It is established that the first phase of cellulose nitrate degradation is characterized by the homolytic cleavage of the RO-NO₂ bond in C3, C2 or C6 (kC3: kC2: kC6 = 6: 3.6: 1), forming an alkoxy radical (RO•) and releasing a •NO₂ radical [54], [70]–[74], [78]–[80], [83]–[86]. Recently, Lai (2019) proposed the transformation of the •NO₂ radical by •H abstraction into HNO₂ as an intramolecular heterolytic cleavage, or intramolecular elimination of HNO₂. The free energy of reaction, reaction enthalpies and activation barriers were measured for both the homolytic and heterolytic reactions: the homolytic reaction is endothermic but has a low activation energy, resulting in a faster rate compared to the exothermic heterolytic scission, which has a higher activation energy. The •NO₂ can also react with water to form the pair HNO₂/HNO₃, both strong oxidizing acids [81], [87].

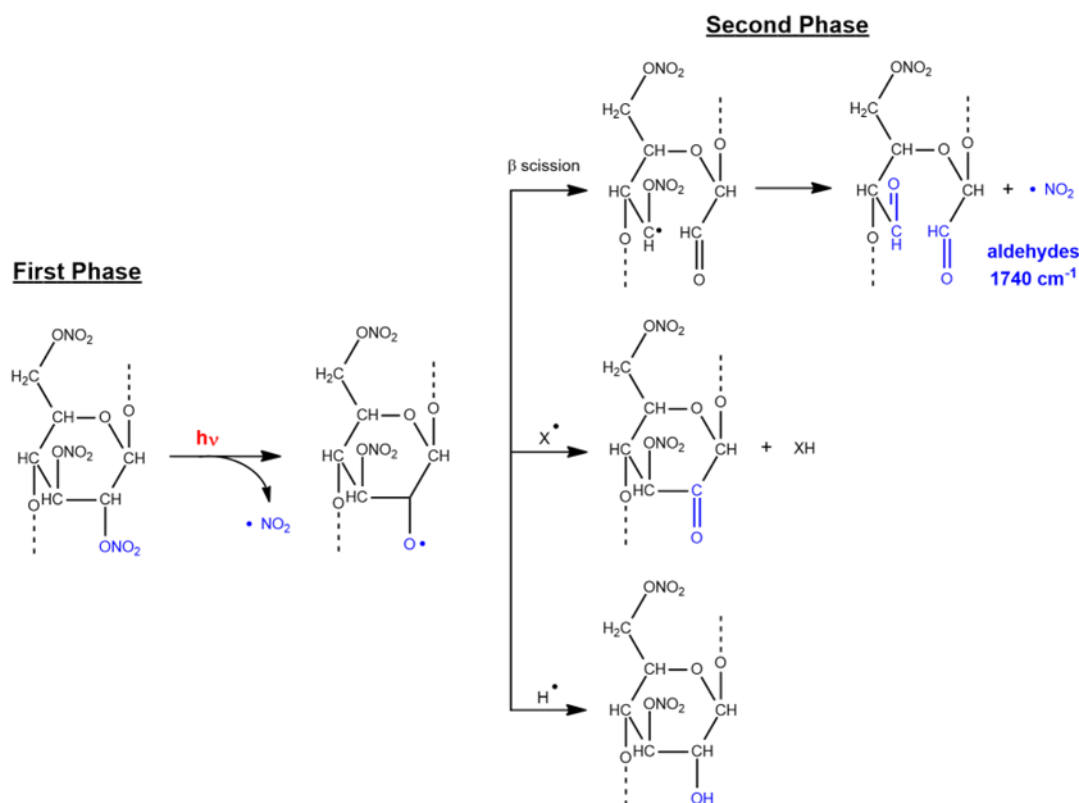


Figure 1.10. First phase of cellulose nitrate degradation, starting with homolytic scission of a nitrate in C2 or C3 and the release of $\bullet\text{NO}_2$. In the second phase, the alkoxy radical promotes chain scission with $\bullet\text{NO}_2$ release and aldehyde formation, detected at 1740 cm^{-1} in IR or converts into a ketone/hydroxyl intermediate by $\bullet\text{H}$ abstractions, for more information see text.

The second phase, characterized by the behavior of the alkoxy radicals formed in this first phase of the degradation, has had different interpretations: Wolfrom et al. [71], Rychly et al. [72] and Chai et al. [77] proposed that the alkoxy radical leads to the cleavage of the C2-C3 bond, inducing the release of another NO_2 radical and the formation of two aldehyde functions in the structure. Jutier et al. [78] identified the formation of a band at 1740 cm^{-1} , by infrared spectroscopy, which they attributed to the formation of these species; more recently, Thérias et al. [70] and Berthumeyrie et al. [73] proposed that the alkoxy radical may form a ketone group, by abstraction of a hydrogen in the α -position by another reactive specie, or a hydroxyl group, by attachment of a hydrogen, the ratio of which depending on the availability of protons in the environment [74]. Hydrogen abstraction plays thus a fundamental role in the degradation of cellulose nitrate. The most labile hydrogen is located at the α -carbon of the ether, in this case the carbon in the C1 position [73], [88]. In the presence of light and oxygen, the formation of a macroradical at this position will promote the formation of hydroperoxides, a key intermediate for the third phase.

Third Phase

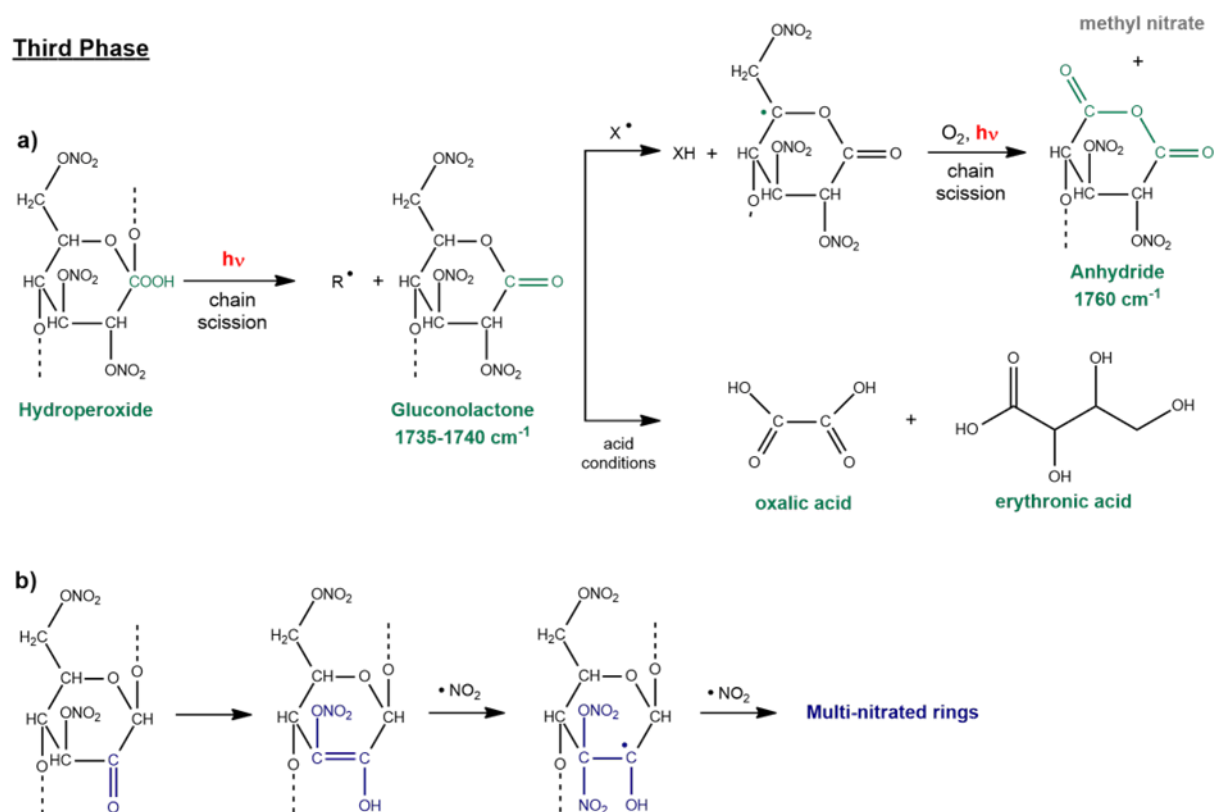


Figure 1.11. a) The excited state hydroperoxide leads to glycosidic bond cleavage with the formation of a gluconolactone. This intermediate is then transformed into an anhydride with the release of $\bullet\text{CH}_2\text{ONO}_2$, which converts into a final product, methyl nitrate, by $\bullet\text{H}$ abstraction. In an alternative pathway, in acidic conditions, the C1 keto intermediate decomposes into oxalic acid or erythronic acid as proposed by Quye et al. b) The keto-enol tautomerism, in the presence of accumulated $\bullet\text{NO}_2$, leads to addition reactions and formation of multi-nitrated rings which will disintegrate the rings.

Hydroperoxides photodecomposition will promote a continuous cleavage of the glycosidic linkages and formation of carbonyl intermediates - the gluconolactones, identified at 1735-40 cm^{-1} in the infrared spectrum. After formation of this intermediate, hydrogen abstraction at the C5 position, in the presence of light and oxygen, leads to the formation of an anhydride, identified at 1760 cm^{-1} , and release of $\bullet\text{CH}_2\text{ONO}_2$, which converts into methyl nitrate, the major volatile in the photodegradation [73]. The continuous photooxidation of these products leads to the total loss of the polymer through the emission of high quantity of volatiles with low molecular weight. Note that Berthumeyrie et al. [73] irradiated cellulose nitrate films in the absence of oxygen observing the formation of the band at 1740 cm^{-1} and loss of the acetal groups. This proves $\bullet\text{NO}_2$ photochemical reactivity, which can be likened to the

hydroperoxide through a photochemically induced cleavage of the nitrite RO-NO bond with release of NO. This had also been observed by Clark and Stephenson [82] and they proposed the formation of oximes by a mechanism similar to the Barton reaction. On the other hand, in the presence of O₂, this oxime intermediate was not produced, meaning that, in competition, molecular oxygen reacts more readily with the macroradicals available. Previously, Tranchant (1962) had already observed that the volatile NO₂ is only present in open-air experiments [79].

Thermal or photochemical degradation of cellulose nitrate are indissociable from its hydrolytic degradation. The polarity of the film and its affinity for water increases with degradation, having Neves et al. [89] identified nitric acid by μ Raman in cellulose nitrate films irradiated at $\lambda > 280$ nm. On this subject, the early works of Allen et al. [74], [90], [91] on the degradation of cellulose nitrate-based cinematographic films are of outmost importance. In practical archival collections, they established that moisture is a critical criterion in film degradation. They concluded that denitration, to form oxides of nitrogen that react with moisture to form HNO₂ and HNO₃ acids, is the primary mechanism that induces chemical changes in the polymer substrate of the films. However, they also added another mechanism based on the formation of highly unstable multi-nitrated rings. As the ketones formed in C2 or C3 exist in equilibrium with an unsaturated enolic isomer, in an enclosed environment such as a film can, the accumulation of nitrite radicals can lead to addition reactions and finally to ring disintegration [74]. Lai (2019) showed that in acid hydrolysis, the favorable protonation site is the nitrate bridging oxygen leading to denitration by releasing NO²⁺, which produces HNO₃ by reacting with hydroxyl anions (OH⁻). Protonation also occurs at the glycosidic bond oxygen, resulting in chain-scission [83].

In artificial aging experiments (70°C and 75%; 55%; 12% relative humidity) of samples prepared according to industrial manufacturing formulations, Quye et al. [75] suggest the formation of oxalic acid and erythronic acid from an intermediate with a ketone group at the C1 position, likely the gluconolactone proposed by Berthumeyrie (2014). The works of Quye et al. (2011), based on the pioneering Ph.D. thesis of Stewart in 1997, proved that manufacturing formulations and processes impact celluloid stability over time. Sulfate ions (above 5 mg per gram of cellulose nitrate) resulting from inadequate washing during manufacture significantly increase the degradation rate [75], [92], [93]. Using a simple swab test with extraction by ion chromatography, she observed that the most degraded natural and artificial aged celluloid artifacts showed higher concentrations of oxalate and sulfate ions. Celluloid objects with higher zinc concentrations were in better condition, proving zinc oxide's empirically long-

known stabilizer action. To assess the degradation extent of cellulose nitrate degradation, these authors used IR band ratios.

Elsasser et al. (2021) and Lozano et al. (2023) performed their artificial aging experiments under 70°C and 75% relative humidity (RH). Lozano proposed, with FTIR-ATR, using absorbance ratios of the nitrate and carbonyl groups versus the acetal structure, that the degradation rate in 3D celluloid objects is higher at the core than at the surface [94], [95]. This agrees with Shashoua's (2008) general degradation proposal for celluloid: 1) water diffuses into the cracks formed at the surface and is adsorbed in the bulk; 2) reacts with the evolved nitrogen oxides and forms nitric acid; 3) initiation of chain-scission reactions at the bulk leading to extreme cracking [24].

On the emission of volatiles, Curran et al. (2018) and Elsasser et al. (2021) identified the emission of furfural from celluloid objects in museum collections, using Solid-phase microextraction gas chromatography/mass spectrometry (SPME-GC/MS) and double shot-gas chromatography/mass spectrometry, respectively [95], [96]. This compound was proposed as a degradation marker for celluloid. Curran et al. (2018) used linear discriminant analysis (LDA) to classify celluloid degradation based on the measured furfural, camphene and 3-carene/ β -terpinene and obtained an accuracy after validation of 83%.

1.5.2 The effect of camphor and other plasticizers

According to the IUPAC terminology for bio-related polymers and applications, a plasticizer is a compound that acts "as a molecularly dispersed substance that decreases the glass-transition temperature (T_g) at which the amorphous phase of a polymer is converted between glassy and rubbery states" [97]. Therefore, the loss of plasticizer by migration or volatilization leads to the increase of the T_g and to polymer embrittlement [24], [98]. Because of its low sublimation temperature, camphor is considered a volatile plasticizer (20°C). Thérias et al. (2011) studied the degradation of celluloid films (70% cellulose nitrate 30% camphor %wt, 60-80 μm) under accelerated aging conditions ($\lambda > 300\text{nm}$, 60°C). The decrease of camphor's carbonyl infrared absorption at 1730cm^{-1} indicated the loss of this plasticizer due to evaporation. Applying an infrared calibration curve to quantify camphor ($A_{1730\text{ cm}^{-1}}/A_{1655\text{ cm}^{-1}} = 0.013 \times \%\text{camphor}$), they measured the loss: after 100h at 60°C, the concentration decreased to 10% wt; after 100h at 100°C to 0% wt. The kinetics of photooxidation of cellulose nitrate versus celluloid was measured by following the evolution of an infrared band at 1766 cm^{-1} attributed to the formation of degradation intermediates. Celluloid degradation rate was faster [85]. Bussiere et al. (2014) correlated the chemical evolution with the physical alterations observed at the macroscale,

showing that the loss of camphor leads to the increase of the polymer micro-hardness (Vickers) [85]. Ultimately, camphor loss and cellulose nitrate chain-scission result in the typical crack pattern observed in celluloid artifacts.

Performing Proton nuclear magnetic resonance (^1H NMR), the Wisconsin Nitrate Film Project (2015) proposed that the reaction of camphor with nitric acid (HNO_3) leads to the formation of camphoric acid, decreasing the amount of the effective plasticizer and accelerating cellulose nitrate degradation [99].

Mazurek et al. (2019), in a work inserted in the Preservation of Plastics Project at the Getty Conservation Institute (GCI), developed an innovative method for studying celluloid objects in museum collections by quantifying the degree of substitution (DS) with ion chromatography (IC) and the degree of polymerization (DP) with size exclusion chromatography (SEC) [100]. Objects in good condition showed higher values of DP and DS than the degraded ones. Furthermore, these results correlated with the conservation condition assessment made with Image Permanence Institute (IPI) Ad-Strips³. Camphor was identified by gas chromatography/mass spectrometry (GC-MS) in all objects (21 in total) in significant amounts (quantification was not performed). With IC, it was possible to identify sulfate and oxalate ions, which correlates with Quye et al. [75], [92], plus nitrites (NO^2^-) and nitrates (NO^3^-).

Kavda et al. (2021) and Elsasser et al. (2021) using Gel Permeation Chromatography (GPC) for the quantification of the average molecular weight (M_w) and for camphor concentration, observed that camphor concentration is reduced by 50% since the early stages of degradation but stabilizes after reaching a plateau around 13.5–17.7 %wt [95], [101]. This agreed with the observation made by Selwitz (1988) that after 30 to 40 years the camphor amount in celluloid remains at a constant 15 %wt [54]. Elsasser et al. (2021) placed questions on the celluloid degradation heterogeneity, showing differences in chain-scission (measured through M_w) and camphor loss across the same celluloid samples.

Waentig (2008) mentioned that the rate of crack formation is slower on celluloid plasticized with dibutyl phthalate (DBP) than in celluloid plasticized with camphor⁴ [25]. Because of its low melting point (-35°C), DBP in excess or weakly bound to the polymer will migrate to the surface, sweat out and form a sticky film [24], [98]. Selwitz (1988) noted that the use of heavier plasticizers than dioctyl and dibutyl phthalates, such as tridecyl phthalate, would improve the stability of 50-year-old cellulose nitrate sheets used by Walt Disney.

Recently, it was found that in cellulose acetate historical films that include plasticizers, namely triphenyl phosphate or diethyl phthalate, degrade 2.5x and 3x times faster than the

³ In 1995, the IPI developed an important “easy-to-use” and economic tool, the AD-strips, which correlate the film condition with the released amount of acetic acid in the air in parts per million.

⁴ However, it is not clear if this author refers to a celluloid totally or partially plasticized by DBP.

pure polymer, respectively [102], [103]. The acceleration by triphenyl phosphate has been attributed to the hydrolysis and the formation of a strong acid - diphenyl phosphate [104], [105]. However, to the author's knowledge, a systematic study on the effect of camphor substitutes (partial or total) in cellulose nitrate aging has still not been performed.

1.6 Photoluminescence for the study of polymer degradation

Luminescence is the "spontaneous emission of radiation from an electronically or vibrationally excited species not in thermal equilibrium with its environment" [39]. Photoluminescence is the de-excitation process, i.e., emission of photons, that occurs due to direct photoexcitation, i.e., absorption of a photon, by an inorganic, organic or organometallic compound. Photoluminescence can be divided into two processes: fluorescence and phosphorescence. Fluorescence occurs when the spin multiplicity is retained, whereas phosphorescence involves the change in spin multiplicity, usually from singlet to triplet states. The spin conversion occurs through a non-radiative process called intersystem crossing. According to Hund's rule, the triplet state energy is lower than the singlet state of the same configuration. Therefore, phosphorescence emission is observed at longer wavelengths (lower energies) than fluorescence emission [106].

The solid-state luminescent properties of polymers have been extensively studied since the 1970s. The emission of polymers originates either from their structural chromophores, from additives or impurities produced during manufacture/degradation. The main advantage of photoluminescence is its sensitivity, being very powerful in detecting and quantifying trace amounts of oxidation products. The detection limit for fluorescence spectroscopy is typically in the nanomolar (nM) to picomolar (pM) range, while the detection limit for infrared spectroscopy is typically in the micromolar (μM) to millimolar (mM) range. This is because the amount of energy involved in electronic transitions is much higher than that involved in molecular vibrations. This is of major interest in degradation studies since the reactive intermediates exist in very low concentrations. In heritage studies, this is crucial, as degradation should be detected as soon as possible. Furthermore, luminescence spectroscopy is a highly versatile technique that follows several photophysical and photochemical processes such as fluorescence quenching, energy transfer or formation of excimers and exciplexes, processes that might occur in the complex degradation mechanisms that cause the collapse of the polymer matrix [107]–[109].

However, for polymers, photoluminescence does not provide the molecular structure information of vibrational spectroscopy techniques, namely FTIR and Raman. The energetic difference between the electronic transitions and their vibronic progressions is low, meaning

structural information in the emission spectra will be absent or unresolved [109]. Therefore, it is necessary to complement luminescence spectroscopy with vibrational spectroscopy, such as FTIR or Raman, or with other structural techniques, such as Nuclear Magnetic Resonance spectroscopy (NMR), to identify the polymer chromophores.

UV-Vis steady-state fluorescence spectroscopy detects the wavelength-dependent intensity of the fluorescence emitted by molecules upon excitation with constant UV-Vis illumination. High-pressure Xenon arc lamps are generally used as the excitation source due to their photon emission in a wide range of wavelengths (250 nm to the infrared). A monochromator separates the light from the xenon lamp into various wavelengths. The excitation wavelength's accuracy depends on the monochromator's bandwidth [108]. There are two modes of collection: right-angle and front-face (FF). FF is used for solid-stated measurements, i.e., of polymer thin films. With this technique, the incident excitation beam is focused on the front surface of the samples. The fluorescence emission is acquired from the same region at an angle that minimizes reflected and scattered light. A photomultiplier detects the sample emission through a monochromator [106].

UV-Vis steady-state fluorescence spectroscopy provides the polymer's fluorescence emission and excitation spectra. The emission spectrum is obtained by exciting the sample with light of any wavelength that is absorbed by the polymer. The excitation spectrum is obtained by recording the variation in the intensity of the emission spectrum as function of the excitation wavelength, which should match the absorption spectrum of the chromophore. If the wavelength maximum of the emission spectrum varies with the excitation wavelength, there is more than one chromophore in the polymer matrix. During polymer degradation, several UV-Vis absorbing intermediates are formed; therefore, it is necessary to examine a wide range of excitation wavelengths to achieve a complete characterization [107].

It is also possible to acquire the phosphorescence emission and excitation spectra. Phosphorescence emission is valuable for characterizing polymers, such as cellulose acetate. However, because of the long phosphorescence lifetimes (up to seconds), the measurements must be carried out under low temperatures (liquid nitrogen -196°C) and/or in the absence of molecular oxygen (O_2), to avoid phosphorescence quenching, which is a drawback in heritage studies [109].

UV-Vis steady-state fluorescence spectroscopy can be used *in situ* using fiber optics and by the analysis of microsamples using a microscope (microspectrofluorimetry). Fluorescence spectroscopy with fiber-optics and microspectrofluorimetry have been used extensively in cultural heritage to study artwork pigments and dyes. Fiber optics allow the analysis of objects with spatial resolutions in the order of the millimeters; however, physical phenomena leading to emission spectrum distortion are common. Microspectrofluorimetry, due to its very high

spatial resolution and confocal microscopy, allows the XYZ spatially resolved (limit of 0.5 μm depth) analysis of valuable artwork microsamples [106], [110]–[112]. However, conventional microscopes have glass-based optical systems that do not allow the excitation of samples in the UV region, which is a disadvantage for studying polymers due to the presence of UV-absorbing chromophores. In this case, it is necessary to use UV-grade microscopes composed of quartz-based optical systems, which have a higher cost.

Overall, research on the characterization of cellulose nitrate using photoluminescence is scarce. McNally and Vanselow (1930) observed cellulose nitrate fluorescence emission with excitation wavelengths under 330 nm [113]. Plitt and Toner (1961) showed that for cellulose derivatives, using an excitation wavelength in the UV range (280–310 nm), the emission maxima was circa 450nm [114]. Hon and Gui (1986) observed the formation of a band with a maximum at 290nm during cellulose nitrate degradation, which they attributed to carbonyl functions by correlation with FTIR. They used first derivative UV-VIS absorbance spectroscopy, which can be compared with the excitation spectrum [76]. Using luminescence spectroscopy to study photooxidation in polyolefins and polyamides, Norman Allen discovered that α - β unsaturated carbonyls are significant intermediates in polymer degradation. These carbonyls were observed in the emission spectra with a band centered at 290nm [115], [116].

In cultural heritage synthetic polymer studies, to note the pioneer works by Toja et al. (2011) and Comelli et al. (2014) in which FTIR, fluorescence spectroscopy and fluorescence lifetime imaging spectroscopy were used to analyze cellulose acetate, poly (vinyl acetate) (PVAc) and acrylonitrile-butadiene-styrene (ABS) from Italian design lamps of the Triennale Design Museum collection. The interpretation of the fluorescence data proved to be challenging due to the difficulty in attributing the emission evolution to specific molecular changes. However, they showed the potential of fluorescence spectroscopy/imaging as an in-situ sensitive method for assessing the surface heterogeneity of plastics in collections.

1.7 Research aims and methodology

This work is divided in two parts: 1) the study of three different types of celluloid objects, billiard balls, dentures and combs, using a multi analytical approach, primary focused on the application of in-situ handheld Raman spectroscopy and micro infrared spectroscopy (**chapters 2-4**); 2) the pioneer use of conventional UV-Vis steady-state fluorescence spectroscopy and synchrotron UV-VIS multispectral luminescence spectroscopy for the study of cellulose nitrate heritage degradation (**chapter 5**).

Chapter 2 is about John Wesley Hyatt's invention of celluloid as a substitute for ivory billiard balls. Even though Hyatt established a factory to manufacture billiard balls in the 1870s

– the Albany Billiard Ball Company - celluloid has been widely regarded as an impractical failure. This view was supported by the lack of clarity about the composition invented by Hyatt for the billiard balls, some suggesting it was just a cellulose nitrate coating on a composite ball (of unknown composition), others that it was made of a shellac composite. In 1983, Robert Friedel asked “to what extent was celluloid actually developed and sold as a substitute for ivory?” After 40 years, by finally determining the compositions analytically and carefully looking at the written record, this work contributes to a new understanding of the crucial role of celluloid in substituting ivory in billiard balls.

The case studies were two billiard balls from the Smithsonian Institution’s National Museum of American History (NMAH): the “original” Hyatt celluloid billiard ball invented in 1868; and an “ivorylene” pool ball, which was sold by from the 1930s-50s. During the research, it was found that “Bonzoline” billiard balls were sold from Albany Billiard Ball Company after the 1880s, and later in England after the 1930s. A set of three balls was purchased for analysis. Their composition was determined using a multi-analytical approach combining in situ handheld Raman MIRA DS and X-Ray fluorescence (XRF) spectrometers and with the analysis of microsamples using micro-Fourier Transform Infrared Spectroscopy (μ FTIR), micro-Raman spectroscopy (μ Raman), Scanning Electron Microscopy - Energy Dispersive X-ray spectroscopy (SEM-EDS) and Zooarcheology by Mass Spectrometry (ZooMS, peptide mass fingerprint).

In **chapter 3**, 21 dentures from the Dr. Samuel D. Harris National Museum of Dentistry (NMD) and Smithsonian Institution’s National Museum of American History (NMAH) were characterized using handheld Raman MIRA DS, μ FTIR and portable XRF. Hyatt readily developed celluloid dentures because he understood that his material properties could compete with vulcanite in the denture market. Contrary to vulcanite, celluloid was easily colored to resemble human gums. Furthermore, its thermoplastic properties allow it to be sold as pre-made forms to dentists who could use them to mold the patient’s mouth with the proper apparatus. For two years, from 1870 to 1872, dental blanks (the pre-made form) were the primary celluloid product manufactured by the Albany Dental Plate Company, Albany, New York. This experience was significant in defining Hyatt’s business strategy for the Celluloid Manufacturing Company in 1872, by distributing celluloid in pre-made forms, sheets, rods, and tubes, to smaller licensed companies to produce celluloid final products. However, similarly to the celluloid billiard balls, the extent to which celluloid dentures were used by society was unclear. Celluloid dentures have been overlooked based on the observation of their lack of success in creating an alternative to vulcanite. The main reasons were the higher price, the dimensional instability and the unpleasant camphor taste. This last problem was one of the most substantial research topics of John Henry Stevens, the chief chemist of the Celluloid

Manufacturing Company, who patented several tasteful and fragrant candidates for camphor substitution. Therefore, was camphor replaced in celluloid dentures at some point in time? Biocompatibility was also crucial in denture development and marketing: to produce red celluloid (and red vulcanite), toxic vermilion (HgS) pigment was used. However, celluloid was soluble in several solvents and easily colored with different coloring agents. Thus, was vermilion eventually replaced in celluloid dentures? Ultimately because historical dentures lack characterization studies, it was complicated to understand the physical differences between vulcanite, celluloid, or other plastic dentures, which creates identification, interpretation, and conservation problems in medicine/dentistry collections. The historical background and characterization of the 21 dentures in chapter 3 shed light on all these questions.

In **chapter 4**, based on the experience gained in the USA using handheld Raman MIRA DS, Portuguese combs from the Casa da Memória of Guimarães and Sociedade Martins Sarmiento, both significant cultural institutions of the city of Guimarães, were characterized to identify celluloid. In Portugal, studies on the use of celluloid are very scarce. The most relevant contributions are the ones by António Amaro da Neves [117] and Manuel Miranda [118], who found that the first factory to employ celluloid in Portugal was a comb factory of Guimarães called “Fábrica de Pentes a Vapor da Madroa” in 1895. However, there were no records of physical evidence, i.e., celluloid combs in this city, or anywhere else in Portugal. Robert Friedel's research focused on two major comb production centers in the 19th century - Leominster (USA) and Oyonnax (France) - to illustrate how the incorporation of celluloid had a profound impact on the economic and technological landscape of these cities [3]. What was the impact of celluloid in Guimarães and how did it relate to the international scene? This chapter contributes, through historical and statistical sources, supported by Raman MIRA DS evidence, to a broader understanding of the introduction and impact of this early plastic in Portugal.

In **chapter 5**, conventional UV-Vis steady-state fluorescence spectroscopy and synchrotron UV-VIS multispectral luminescence spectroscopy were used to detect and characterize luminescent intermediates generated in the early stages of the degradation of cellulose nitrate. These techniques were selected due to their very high sensitivity, a crucial parameter for heritage degradation studies since detecting the degradation intermediates at the earliest stages is necessary. The idea was to develop fluorescence spectroscopy as an early warning tool. Prior studies performed with conventional UV-Vis steady-state fluorescence showed that it was possible to correlate different stages of CN degradation with luminescent intermediates that display specific excitation and emission spectra [119]. CN thin films were irradiated at $\lambda \geq 280\text{nm}$ and species absorbing at 290 nm were formed in the first stage of degradation. At more advanced stages, the appearance of more bands, at 266, 325, 366 and 400 nm, were observed.

However, it was not possible to study historical samples with this analytical setup due to their intrinsic heterogeneous nature. It was necessary to increase the spatial resolution, but the conventional microscope available could not excite the samples in the UV. The confocal fluorescence microscope of the DISCO beamline, SOLEIL synchrotron, was built to excite in the UV region, and with its extended wavelength range (180-600 nm), was tested based on its potential to detect these CN early UV absorbing intermediates in valuable heritage microsamples, namely from cinematographic films from OEAW and DFF and celluloid objects from the Portuguese Perlov collection. Its sensibility of 10^{-9} M is a crucial parameter to establish this technique in plastic heritage studies and for the incorporation of deep UV (DUV) microscopes in conservation laboratories [120], [121].

1.8 References

- [1] H. Braconnot, "De la Transformation de plusieurs substances végétales en un principe nouveau," *Annales de Chimie et de Physique*, vol. 60, pp. 290–294, 1833.
- [2] C. F. Schonbein, "Improvement in preparation of cotton-wool and other substances as substitutes for gunpowder," 4874, 1846
- [3] R. Friedel, *Pioneer Plastic: The Making and Selling of Celluloid*. Madison: The University of Wisconsin Press, 1983.
- [4] R. B. Seymour and G. B. Kauffman, "The rise and fall of celluloid," *J Chem Educ*, vol. 69, no. 4, p. 311, 1992, doi: 10.1021/ed069p311.
- [5] V. E. Yarsley, W. Flavell, P. S. Adamson, and N. G. Perkins, *Cellulosic Plastics*. London: The Plastics Institute, 1964.
- [6] L. S. Sirkis, "The History, Deterioration and Conservation of Cellulose Nitrate and Other Early Plastic Objects," University of London, 1982. [Online]. Available: <http://ir.obihiro.ac.jp/dspace/handle/10322/3933>
- [7] S. T. I. Mossman, "Parkesine and Celluloid," in *The Development of Plastics*, S. T. I. Mossman and P. J. T. Morris, Eds. The Royal Society of Chemistry, 1994, pp. 10–25.
- [8] E. C. Worden, *The Nitrocellulose Industry, Volume II*. London: Constable and Company Ltd., 1911.
- [9] J. E. Boyd, "Celluloid: The Eternal Substitute," *Distillations: using stories from science's the past to understand our world*, 2011. <https://www.sciencehistory.org/distillations/celluloid-the-eternal-substitute> (accessed Sep. 12, 2019).
- [10] V. C. Westmont, "Faux materials and aspirational identity : Celluloid combs and working class dreams in the Pennsylvania anthracite region," *Journal of Material Culture*, vol. 25, no. 1, pp. 93–107, 2019.

- [11] O. Madden, "Balancing Ingenuity and Responsibility in the Age of Plastics," in *The Age of Plastic: Ingenuity and Responsibility*, O. Madden, A. E. Charola, K. C. Cobb, P. T. DePriest, and R. J. Koestler, Eds. Washington D.C.: Smithsonian Institution Scholarly Press, 2017, pp. 1–17.
- [12] R. Friedel, "Is It Real? Imitation and Originality in Plastics," in *The Age of Plastic: Ingenuity and Responsibility*, O. Madden, A. E. Charola, K. C. Cobb, P. T. DePriest, and R. J. Koestler, Eds. Washington D.C.: Smithsonian Institution Scholarly Press, 2017, pp. 51–60.
- [13] R. Friedel, "A white collar with a message," *O say can you see? Stories from the Museum*, 2018. <https://americanhistory.si.edu/blog/white-collar-message> (accessed Aug. 03, 2022).
- [14] J. L. Meikle, *American Plastic: A Cultural History*. New Brunswick: Rutgers University Press, 1997.
- [15] D. H. Shayt, "Elephant under Glass: The Piano Key Bleach House of Deep River, Connecticut," *The Journal of the Society for Industrial Archeology*, vol. 19, no. 1, pp. 37–59, 1993.
- [16] Frank Hoffmann, *Encyclopedia of Recorded Sound*, 2nd edition. New York: Routledge, 2005.
- [17] C. Higgens, "A Note on the Use of Celluloid in Plastic Surgery.," *The Lancet*, vol. 188, no. 4858, pp. 643–644, Oct. 1916.
- [18] H. J. Gauvain, "The use of celluloid in the treatment of tuberculous disease of the spine" *Br Med J*, vol. 1, no. 2736, p. 1200, Jun. 1913.
- [19] K. W. Ney, "The repair of cranial defects with celluloid," *The American Journal of Surgery*, vol. 44, no. 2, pp. 394–399, May 1939.
- [20] D. Baxby, "Smallpox vaccination techniques; from knives and forks to needles and pins," *Vaccine*, vol. 20, no. 16, pp. 2140–2149, May 2002.
- [21] K. Brig, "Stabilising Lymph: British East and Central Africa, 'Tropical' Climates, and the Search for Effective Smallpox Vaccine Lymph, 1890s–1903," *Journal of Imperial and Commonwealth History*, vol. 50, no. 5, pp. 890–914, 2022.
- [22] M. Coughlin and A. M. Seeger, "You collected what? The risk and rewards of acquiring cellulose nitrate ," in *Plastics: Looking at the future and learning from the past* , B. Keneghan and L. Egan, Eds. London: Archetype Publications Ltd. , 2008, pp. 119–124.
- [23] A. Lagana and B. Keneghan, "Which plastics are in my collection? The need for a plastic reference sample collection (SamCo).," in *Preservation of Plastic Artefacts in Museum Collections*, B. Lavédrine, A. Fournier, and G. Martin, Eds. Paris: Comite des travaux historiques et scientifiques, 2012, pp. 37–42.
- [24] Y. Shashoua, *Conservation of Plastics: Materials science, degradation and preservation*. Elsevier Ltd, 2008.

- [25] F. Waentig, *Plastics in Art: A study from the conservation point of view*. Petersberg: Michael Imhof Verlag GmbH & Co., 2008.
- [26] J. A. Reilly, "Celluloid Objects: Their Chemistry and Preservation," *Journal of the American Institute for Conservation*, vol. 30, no. 2, p. 145, 1991.
- [27] B. Stuart, *Analytical Techniques in Materials Conservation*. Chichester: John Wiley & Sons, Ltd, 2007.
- [28] F. Coles, "Challenge of materials? A new approach to collecting modern materials at the Science Museum, London," in *Plastics: Looking at the Future and Learning from the Past*, B. Keneghan and L. Egan, Eds. London: Archetype Publications Ltd. , 2008, pp. 125–131.
- [29] J. M. Chalmers and N. J. Everall, "Qualitative and quantitative analysis of plastics, polymers, and rubbers by vibrational spectroscopy," in *Vibrational Spectroscopy of Polymers: Principles and Practice*, N. J. Everall, J. M. Chalmers, and P. R. Griffiths, Eds. Chichester: John Wiley and Sons, Ltd. , 2007, pp. 1–68.
- [30] M. R. Derrick, D. Stulik, and J. M. Landry, *Infrared Spectroscopy in Conservation Science*. Los Angeles: The Getty Conservation Institute, 1999.
- [31] P. R. Griffiths and J. A. Haseeth, *Fourier Transform Infrared Spectrometry*. New Jersey: John Wiley & Sons, Inc., 2007.
- [32] D. W. Mayo, F. A. Miller, and R. W. Hannah, *Course notes on the interpretation of infrared and Raman spectra*. New Jersey: John Wiley & Sons, Ltd., 2004.
- [33] Jan. F. Rabek, *Polymer Photodegradation: Mechanisms and experimental methods*. Springer Science+Business Media Dordrecht, 1995,
- [34] G. L. Shearer, "An Evaluation of Fourier Transform Infrared Spectroscopy for the Characterization of Organic Compounds in Art and Archaeology," Ph. D. , Faculty of Science of University College London, London, 1989.
- [35] Susan Mossman, "Saving plastics for posterity," *Nature*, vol. 455, p. 288, 2008.
- [36] J. Bell, P. Nel, and B. Stuart, "Noninvasive identification of polymers in cultural heritage collections: evaluation, optimization and application of portable FTIR (ATR and external reflectance) spectroscopy to three dimensional polymer based objects," *Herit Sci*, vol. 7, pp. 1–18, 2019.
- [37] S. Prati, G. Sciutto, I. Bonacini, and R. Mazzeo, "New Frontiers in Application of FTIR Microscopy for Characterization of Cultural Heritage Materials," *Topics in Current Chemistry*, vol. 374, no. 3. Springer Verlag, Jun. 01, 2016.
- [38] D. Saviello, L. Toniolo, S. Goidanich, and F. Casadio, "Non-invasive identification of plastic materials in museum collections with portable FTIR reflectance spectroscopy: Reference database and practical applications," *Microchemical Journal*, vol. 124, pp. 868–877, 2016.

- [39] A. D. McNaught and A. Wilkinson, Eds., IUPAC. Compendium of Chemical Terminology (the "Gold Book"), 2nd edition. Oxford: Blackwell Scientific Publications, 2019.
- [40] F. J. Boerio and S. Wirasate, "Measurements of the chemical characteristics of polymers and rubbers by vibrational spectroscopy," in *Vibrational Spectroscopy of Polymers: Principles and Practice*, N. J. Everall, J. M. Chalmers, and P. R. Griffiths, Eds. Chichester: John Wiley and Sons, Ltd., 2007, pp. 69–112.
- [41] C. Paris and C. Coupry, "Fourier transform Raman spectroscopic study of the first cellulose-based artificial materials in heritage," *Journal of Raman Spectroscopy*, vol. 36, no. 1, pp. 77–82, 2005.
- [42] O. Madden, K. C. Cobb, and A. M. Spencer, "Raman spectroscopic characterization of laminated glass and transparent sheet plastics to amplify a history of early aviation 'glass,'" *Journal of Raman Spectroscopy*, vol. 45, no. 11–12, pp. 1215–1224, 2014.
- [43] A. Neves, E. M. Angelin, É. Roldão, and M. J. Melo, "New insights into the degradation mechanism of cellulose nitrate in cinematographic films by Raman microscopy," *Journal of Raman Spectroscopy*, vol. 50, no. 2, pp. 202–212, 2019.
- [44] A. Rousaki and P. Vandenabeele, "In situ Raman spectroscopy for cultural heritage studies," *Journal of Raman Spectroscopy*, vol. 52, no. 12. John Wiley and Sons Ltd, pp. 2178–2189, Dec. 01, 2021.
- [45] F. Pozzi, E. Basso, A. Rizzo, A. Cesaratto, and T. J. Tague, "Evaluation and optimization of the potential of a handheld Raman spectrometer: in situ, noninvasive materials characterization in artworks," *Journal of Raman Spectroscopy*, vol. 50, no. 6, pp. 861–872, 2019.
- [46] A. Kilsinska-Kopacz et al., "Raman spectroscopy as a powerful technique for the identification of polymers used in cast sculptures from museum collections," *Journal of Raman Spectroscopy*, pp. 1–9, 2018.
- [47] M. N. Boyden, E. M. Kleist, C. K. Asztalos, and T. M. Korter, "Determination of the polymer composition of mid-twentieth century purses by Raman spectroscopy," *Herit Sci*, vol. 10, no. 1, 2022.
- [48] A. P. Sachs and O. Byron, "Camphor substitutes in the manufacture of celluloid," *Ind Eng Chem*, vol. 13, no. 10, pp. 893–901, Oct. 1921.
- [49] J. H. Stevens, "Manufacture of Solid Compounds of Pyroxylin," 517987, 1894
- [50] Masselon, Roberts, and Cilliard, *Celluloid: Its Manufacture, Applications and Substitutes*. London: Charles Griffin and Co., Ltd, 1912.
- [51] H. N. Stokes and H. C. P. Weber, "Effects of heat on celluloid and similar materials," *Technologic Papers of the Bureau of Standards*, no. 98, 1917.
- [52] A. R. de Janeiro, *Indústrias Plásticas: Celulóide, Galalite, Vidro Plástico e Baquelite*. Lisboa: Livraria Bertrand, 1950.

- [53] Y. Shashoua, S. M. Bradley, and V. D. Daniels, "Degradation of Cellulose Nitrate Adhesive," *Studies in Conservation*, vol. 37, no. 2, pp. 113–119, 1992.
- [54] C. Selwitz, *Cellulose nitrate in conservation*. United States of America: J. Paul Getty Trust, 1988.
- [55] J. Bersch, *Cellulose, cellulose products, and artificial rubber, comprising the preparation of cellulose from wood and straw; manufacture of parchment; methods of obtaining sugar and alcohol, and oxalic acid; production of viscose and viscoïd, nitro-celluloses, and cellulose esters, artificial silk, celluloid, rubber substitutes, oil-rubber, and factis*. Philadelphia: H.C. Baird & co, 1904.
- [56] W. Main, *Le celluloid et ses succédanés*. Paris: Gauthier-Villars & Masson et Cie, 1913.
- [57] A. F. Caprio, "Plastics' Parade," *Scientific American*, vol. 169, no. 4, pp. 163–165, 1943.
- [58] J. Salvant, K. Sutherland, J. Barten, C. Stringari, F. Casadio, and M. Walton, "Two László Moholy-Nagy Paintings on Trolit : Insights into the condition of early cellulose nitrate plastic," *e-Preservation Science*, vol. 13, pp. 15–22, 2016.
- [59] F. D. Miles, *Cellulose Nitrate: The physical chemistry of nitrocellulose, its formation and use*. London: Oliver and Boyd, 1955.
- [60] J. Moskowitz, K. Carlos, L. Lindahl-Ackerman, K. L. Reese, T. Begley, and B. J. Yakes, "Portable Raman Spectroscopy for Screening of Phthalate Plasticizers in Food Contact Production Line Tubing and Bottle Cap Gaskets," *ACS Food Science and Technology*, 2022, doi: 10.1021/acsfoodscitech.2c00059.
- [61] T. Nørbygaard and R. W. Berg, "Analysis of Phthalate Ester Content in Poly (vinyl chloride) Plastics by Means of Fourier Transform Raman Spectroscopy," *Appl Spectrosc*, vol. 58, no. 4, pp. 3–6, 2004.
- [62] R. A. Nyquist, "Raman Group Frequency Correlations: Phthalate Esters," *Appl Spectrosc*, vol. 26, no. 1, pp. 81–85, 2005.
- [63] E. Rankin, "A Betrayal of Material: Problems of Conservation in the Constructivist Sculpture of Naum Gabo and Antoine Pevsner," *Leonardo*, vol. 21, no. 3, p. 285, 1988.
- [64] D. Pullen and J. Heuman, "Cellulose Acetate Deterioration in the Sculptures of Naum Gabo," in *Preprints of Contributions to the Modern Organic Materials Meeting*, 1988, pp. 57–66.
- [65] M. Derrick and D. Stulik, "Deterioration of Cellulose Nitrate Sculptures Made by Gabo and Pevsner," in *Proceedings of a Conference Symposium – Saving the Twentieth Century*, Sept. 15-20, 1991, 1993.
- [66] M. E. Springate, "Cellulose Nitrate Plastic (Celluloid) in Archaeological Assemblages: Identification and Care," *Northeast Hist Archaeology*, vol. 26, no. 1, pp. 63–72, 1997.

- [67] Jacques Lemaire, "Prediction of the Long-Term Behaviour of Synthetic Polymeric Materials from Artificial Ageing Experiments," in *Proceedings of Symposium '91 - Saving the Twentieth Century*, 1991, pp. 123–133.
- [68] J. Lemaire, J.-L. Gardette, J. Lacoste, P. Delprat, and D. Vaillant, "Mechanisms of Photooxidation of Polyolefins: Prediction of Lifetime in Weathering Conditions," in *Polymer Durability*, 1996, pp. 577–598.
- [69] N. S. Allen and M. Edge, *Fundamentals of Polymer Degradation and Stabilization*. London: Elsevier Applied Science, 1992.
- [70] S. Thérias et al., "Degradation of celluloid in art works: a study of the degradation mechanisms," *Actes du colloque Sciences des matériaux du patrimoine culturel*, vol. 2, pp. 68–73, 2012.
- [71] M. L. Wolfrom et al., "The Controlled Thermal Decomposition of Cellulose Nitrate I," *J Am Chem Soc*, vol. 77, pp. 6573–6579, 1955.
- [72] J. Rychly, A. Lattuati-Derieux, L. Matisova-Rychla, K. Csomorova, I. Janigova, and B. Lavedrine, "Degradation of aged nitrocellulose investigated by thermal analysis and chemiluminescence," *J Therm Anal Calorim*, vol. 107, no. 3, pp. 1267–1276, 2012.
- [73] S. Berthumeyrie, S. Collin, P. O. Bussiere, and S. Therias, "Photooxidation of cellulose nitrate: New insights into degradation mechanisms," *J Hazard Mater*, vol. 272, no. 2, pp. 137–147, 2014.
- [74] M. Edge, N. S. Allen, M. Hayes, P. N. K. Riley, C. v. Horie, and J. Luc-Gardette, "Mechanisms of deterioration in cellulose nitrate base archival cinematograph film," *Eur Polym J*, vol. 26, no. 6, pp. 623–630, 1990.
- [75] A. Quye, D. Littlejohn, R. A. Pethrick, and R. A. Stewart, "Investigation of inherent degradation in cellulose nitrate museum artefacts," *Polym Degrad Stab*, vol. 96, no. 7, pp. 1369–1376, 2011.
- [76] D. N. S. Hon and T. L. Gui, "Photodegradation of cellulose nitrate," *Polymer Photochemistry*, vol. 7, no. 4, pp. 299–310, 1986.
- [77] H. Chai, Q. Duan, H. Cao, M. Li, and J. Sun, "Effects of nitrogen content on pyrolysis behavior of nitrocellulose," *Fuel*, vol. 264, p. 116853, 2020.
- [78] J. -J Jutier, Y. Harrison, S. Premont, and R. E. Prud'homme, "A nonisothermal fourier transform infrared degradation study of nitrocelluloses derived from wood and cotton," *J Appl Polym Sci*, vol. 33, no. 4, pp. 1359–1375, 1987.
- [79] L. DAUERMAN and Y. A. TAJIMA, "Thermal decomposition and combustion of nitrocellulose.," *AIAA Journal*, vol. 6, no. 8, pp. 1468–1473, 1968.

- [80] T. B. Brill and P. E. Gongwer, "Thermal decomposition of energetic materials 69. Analysis of the kinetics of nitrocellulose at 50°C-500°C," *Propellants, Explosives, Pyrotechnics*, vol. 22, no. 1, pp. 38–44, 1997.
- [81] A. Hamrang, "Degradation and stabilization of cellulose based plastics & artifacts," Faculty of Science and Engineering, The Manchester Metropolitan University, 1994.
- [82] D. T. Clark and P. J. Stephenson, "An ESCA study of the surface chemistry of cellulose nitrates and double based propellants, with particular reference to their degradation in ultra-violet light," *Polym Degrad Stab*, vol. 4, pp. 185–193, 1982.
- [83] A. J. Lai, "Determining the dominant degradation mechanisms in Nitrocellulose," Doctor of Philosophy, University College London, 2019.
- [84] M. Moniruzzaman, J. M. Bellerby, and M. A. Bohn, "Activation energies for the decomposition of nitrate ester groups at the anhydroglucopyranose ring positions C2, C3 and C6 of nitrocellulose using the nitration of a dye as probe," *Polym Degrad Stab*, vol. 102, no. 1, pp. 49–58, 2014.
- [85] P. O. Bussiere, J. L. Gardette, and S. Therias, "Photodegradation of celluloid used in museum artifacts," *Polym Degrad Stab*, vol. 107, pp. 246–254, 2014..
- [86] G. B. Manelis, G. M. Nazin, Yu. I. Rubtsov, and V. A. Strunin, *Thermal Decomposition and Combustion of Explosives and Propellants*. New York: Taylor & Francis, 2003.
- [87] P. W. Atkins and L. Jones, *Chemistry: Molecules, Matter and Change*, 3rd edition. New York: W H Freeman & Co, 1997.
- [88] D. Fromageot, N. Pichon, O. Peyron, and J. Lemaire, "Thermal yellowing sensitised by pre-photo-oxidation of non-deacidified paper," *Polym Degrad Stab*, vol. 91, no. 2, pp. 347–357, 2006.
- [89] A. Neves, E. M. Angelin, É. Roldão, and M. J. Melo, "New insights into the degradation mechanism of cellulose nitrate in cinematographic films by Raman microscopy," *Journal of Raman Spectroscopy*, vol. 50, pp. 202–212, 2018.
- [90] N. S. Allen, M. Edge, J. H. Appleyard, T. S. Jewitt, and C. V. Rorie, "The Degradation and Stabilization of Historic Cellulose Acetate/Nitrate Base Motion-picture Film," *The Journal of Photographic Science*, vol. 36, no. 3, pp. 103–106, 1988.
- [91] N. S. Allen, M. Edge, D. Francis, C. V. Horie, T. H. Appleyard, and T. S. Jewitt, "The Nature of the Degradation of Archival Cellulose-Ester Base Motion-Picture Film: the Case for Stabilization," *The Journal of Photographic Science*, vol. 36, no. 2, pp. 34–39, 1988.
- [92] A. Quye, D. Littlejohn, R. A. Pethrick, and R. A. Stewart, "Accelerated ageing to study the degradation of cellulose nitrate museum artefacts," *Polym Degrad Stab*, vol. 96, no. 10, pp. 1934–1939, 2011.

- [93] R. A. Stewart, "Analytical Studies of the Degradation of Cellulose Nitrate Artefacts," Doctor of Philosophy, University of Strathclyd, 1997.
- [94] M. Valente Chavez Lozano, C. Elsässer, E. M. Angelin, and M. Pamplona, "Shedding Light on Degradation Gradients in Celluloid: An ATR-FTIR Study of Artificially and Naturally Aged Specimens," *Polymers (Basel)*, vol. 15, p. 522, 2023.
- [95] C. Elsässer, A. Micheluz, M. Pamplona, S. Kavda, and P. Montag, "Selection of thermal, spectroscopic, spectrometric, and chromatographic methods for characterizing historical celluloid," *J Appl Polym Sci*, vol. 138, no. 21, 2021.
- [96] K. Curran, M. Underhill, J. Grau-Bové, T. Fearn, L. T. Gibson, and M. Strlič, "Classifying Degraded Modern Polymeric Museum Artefacts by Their Smell," *Angewandte Chemie - International Edition*, vol. 57, no. 25, pp. 7336–7340, 2018.
- [97] M. Vert et al., "Terminology for biorelated polymers and applications (IUPAC recommendations 2012)," *Pure and Applied Chemistry*, vol. 84, no. 2, pp. 377–410, 2012.
- [98] R. King, J. Grau-Bové, and K. Curran, "Plasticiser loss in heritage collections: its prevalence, cause, effect, and methods for analysis," *Heritage Science*, vol. 8, 2020.
- [99] V. Kepley, M. Mahanthappa, H. Heckman, K. Mullen, and A. McQueen, "Investigation of Cellulose Nitrate Motion Picture Film Chemical Decomposition and Associated Fire Risk," 2015.
- [100] J. Mazurek, A. Laganà, V. Dion, S. Etyemez, C. Carta, and M. R. Schilling, "Investigation of cellulose nitrate and cellulose acetate plastics in museum collections using ion chromatography and size exclusion chromatography," *J Cult Herit*, vol. 35, pp. 263–270, 2019.
- [101] S. Kavda, A. Micheluz, C. Elsässer, and M. Pamplona, "Development of a gel permeation chromatography method for analysing cellulose nitrate in museums," *J Sep Sci*, vol. 44, no. 9, pp. 1795–1804, May 2021.
- [102] A. al Mohtar, S. Nunes, J. Silva, A. M. Ramos, J. Lopes, and M. L. Pinto, "First-Principles Model to Evaluate Quantitatively the Long-Life Behavior of Cellulose Acetate Polymers," *ACS Omega*, vol. 6, pp. 8028–8037, 2021.
- [103] A. al Mohtar et al., "Decision making based on hybrid modeling approach applied to cellulose acetate based historical films conservation Fourier Transform Infrared spectroscopy," *Sci Rep*, pp. 1–13, 2021.
- [104] M. T. Giachet et al., "Assessment of the composition and condition of animation cels made from cellulose acetate," *Polym Degrad Stab*, vol. 107, pp. 223–230, 2014.
- [105] D. Littlejohn, R. A. Pethrick, A. Quye, and J. M. Ballany, "Investigation of the degradation of cellulose acetate museum artefacts," *Polym Degrad Stab*, vol. 98, no. 1, pp. 416–424, 2013.

- [106] B. Valeur and M. N. Berberan-Santos, *Molecular Fluorescence: Principles and Applications*, 2nd edition. Weinheim: Wiley-VCH Verlag & Co. KGaA, 2012.
- [107] N. S. Allen, J. Homer, and J. F. McKellar, "The use of luminescence spectroscopy in aiding the identification of commercial polymers," *Analyst*, vol. 101, p. 260, 1976.
- [108] H. Itagaki, "Fluorescence Spectroscopy," in *Experimental Methods in Polymer Science: Modern Methods in Polymer Research and Technology*, T. Tanaka, Ed. San Diego: Academic Press, 2000, pp. 155–260.
- [109] G. Graeme, "Characterization of solid polymers by luminescence techniques," *Pure and Applied Chemistry*, vol. 57, pp. 945–954, 1985.
- [110] M. J. Melo and A. Claro, "Bright light: Microspectrofluorimetry for the characterization of lake pigments and dyes in works of art," *Acc Chem Res*, vol. 43, no. 6, pp. 857–866, 2010.
- [111] A. Claro et al., "The use of microspectrofluorimetry for the characterization of lake pigments," *Talanta*, vol. 74, no. 4, pp. 922–929, 2008.
- [112] P. Nabais, M. J. Melo, J. A. Lopes, T. Vitorino, A. Neves, and R. Castro, "Microspectrofluorimetry and chemometrics for the identification of medieval lake pigments," *Herit Sci*, vol. 6, no. 1, pp. 1–11, 2018.
- [113] J. G. McNally and W. Vanselow, "Measurements of the fluorescence of cellulose acetate, cellulose nitrate and gelatine in ultraviolet light," *J. Am. Chem. Soc.*, vol. 52, no. 10, pp. 3846–3856, 1930.
- [114] K. F. Plitt and S. D. Toner, "A study of the fluorescence of cellulosic polymers," *J Appl Polym Sci*, vol. 5, no. 17, pp. 534–538, 1961.
- [115] N. S. Allen, "Light absorbing species in polyolefins: A fluorescence/derivative UV spectroscopy study," *Polym Degrad Stab*, vol. 6, no. 4, pp. 193–200, 1984.
- [116] N. S. Allen, J. F. McKellar, and D. Wilson, "Luminescence and degradation of nylon polymers: part I: photo-oxidation processes involving phosphorescent species," *Journal of Photochemistry*, vol. 6, pp. 337–348, 1976.
- [117] A. A. das Neves, "As Indústrias Vimaranenses em 1899," *Memórias de Araduca*, 2017. <http://araduca.blogspot.com/2017/11/as-industrias-vimaranenses-em-1899-1.html> (accessed Sep. 12, 2019).
- [118] M. Miranda, "Fantástico Plástico: Notas sobre o fabrico do brinquedo de plástico no século XX português," *Mínia*, no. 14, pp. 133–150, 2019.
- [119] A. Neves, "Um sistema de alerta precoce para a conservação de património em nitrato de celulose: fluoróforos como marcadores de degradação," *MSc Thesis, FCT NOVA*, 2017.
- [120] M. Thoury et al., "Synchrotron UV-visible multispectral luminescence microimaging of historical samples," *Anal Chem*, vol. 83, no. 5, pp. 1737–1745, 2011.

[121] F. Jamme et al., "Synchrotron UV Fluorescence Microscopy Uncovers New Probes in Cells and Tissues," *Microscopy and Microanalysis*, vol. 16, pp. 507–514, 2010.

This is a forthcoming manuscript:

Neves, A., Friedel, R., Melo, M.J, Callapez, M.E., Vicenzi, E.P, Lam, T.

The best billiard ball in the nineteenth century: composite materials made of celluloid and bone as substitutes for ivory

THE BEST BILLIARD BALL IN THE NINETEENTH CENTURY: COMPOSITE MATERIALS MADE OF CELLULOID AND BONE AS SUBSTITUTES FOR IVORY

Abstract

The demystification of how 19th-century novel, designed materials became significant elements of modern technological, economic, and cultural life requires a complete understanding of the material dimensions of historical artifacts. The objects frequently described as the earliest manufactured plastic products – the billiard balls made by John Wesley Hyatt and his associates from the late 1860s—are examined closely for the first time and found to be more complex and functionally more successful than had been described. Analytical techniques, namely optical microscopy, scanning electron microscope (SEM) – energy dispersive X-Ray spectroscopy (EDS), X-Ray fluorescence (XRF), micro-fourier transformed infrared (microFTIR) and handheld/micro-Raman spectroscopies, were used to reveal the complex composition of the Smithsonian Institution’s “original” 1868 celluloid billiard ball. Comparisons with billiard and pool balls commercialized from the 1880s to the 1960s showed an unexpected consistency in material formulations. All specimens were made of an unprecedented composite material made with a mixture of cellulose nitrate, camphor, and ground bone; the source of the bone was identified as cattle by peptide mass fingerprint (ZooMS). Patent specifications and contemporary journal descriptions explained how and when these formulations emerged. Combining technical analyses of compositions with careful reading of the historical record and contemporary descriptions reveals the key elements of the first successful efforts to substitute materials to assist the survival of endangered animals.

Significance

Previous discussions of the earliest efforts to substitute novel materials for scarce or endangered natural materials have overlooked the complexity and success of these efforts. The 155-year-old billiard ball invented by John Wesley Hyatt turns out to be a pioneering example of one of the most significant types of materials in the 20th century and beyond – reinforced polymer composites. A multi-analytical approach incorporating spectroscopic techniques and peptide mass fingerprinting revealed the development and persistence of a composite made of bone, cellulose nitrate, and camphor, hereby called reinforced celluloid. The success of this material in providing a useful and popular alternative to elephant ivory has not been sufficiently appreciated.

2.1 Introduction

Previous discussions of the origins and early development of plastics have overlooked the importance of carefully formulated composite materials. A more careful, analytically informed investigation of early plastic artifacts reveals more complex and interesting materials, important precedents for the emergence of designed and engineered materials in the 20th century. An appreciation of the complexity of these materials and the care with which they were designed for specific purposes has important implications for both their historical interpretation and the challenges they pose for conservation. Billiard balls have long been understood to have inspired the first development of important commercial plastics, but their carefully designed composition has not been understood. The first systematic effort to analyze this composition and to understand their development over time corrects long-held misconceptions about the early plastics and their entry into commerce and culture.

Billiards depended fundamentally on the mechanical behavior of the colliding balls, which by the 19th century were almost invariably made from elephant ivory. Due to the growing demand, ivory billiard ball suppliers were under considerable pressure, leading to calls for ivory replacements in the late 1860s. In 1864, Phelan & Collender, one of the largest manufacturers of billiard suppliers at that time, published a \$10,000 reward challenge for an ivory billiard ball substitute [1]. This call spurred the efforts of a young Albany, New York printer, John Wesley Hyatt (1837-1920) [2–4].

In the collections of the National Museum of American History (NMAH) in Washington, DC, one can find a single billiard ball, with its own wooden pedestal, and a plaque reading: “Made in 1868 of Cellulose Nitrate, Celluloid, The Year John Wesley Hyatt Discovered This First Plastics Resin” (**Fig. 2.1A**). This billiard ball looms large in the mythology of synthetic chemistry and materials innovation. However, as billiard balls, celluloid has been dismissed

as an impractical failure. Due to apocryphal stories, it is even common to think that celluloid billiard balls exploded upon contact, a myth promoted by Hyatt himself in his acceptance speech for the Perkin Gold medal in 1914 [5]. Billiard balls have been seen only as a misstep in Hyatt’s development of the first practical artificial plastic, celluloid, a mixture of cellulose nitrate and camphor, which succeeded in just about any other application [2, 3, 6–10].

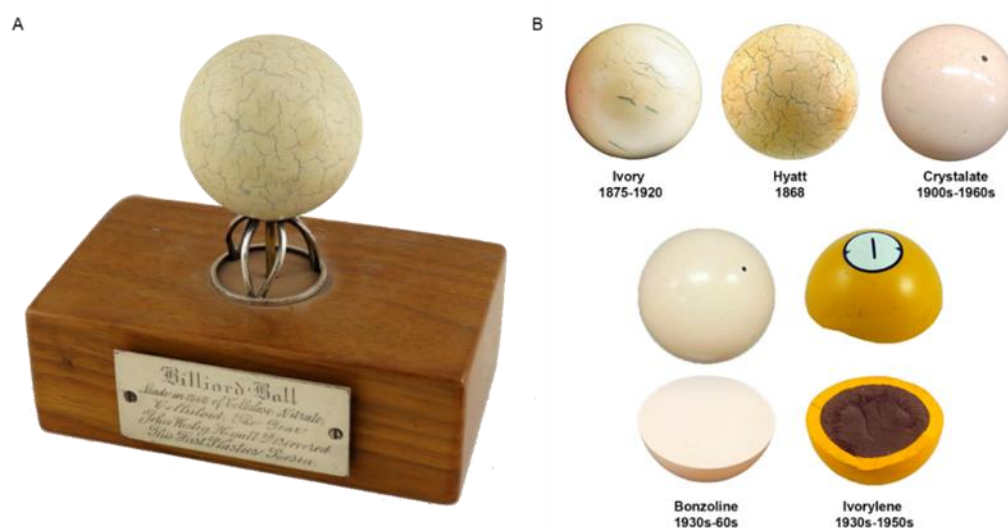


Figure 2.1. Historical billiard balls studied. A) John Wesley Hyatt and 1868 “original” celluloid billiard ball. National Museum of American History, Smithsonian Institution. B) Billiard balls studied: Hyatt 1868, Crystalate, Bonzoline and Ivorylene. The ivory billiard ball is from the Smithsonian Collection (ID number CL.329507). Bonzoline and Crystalate resemblance with ivory is evident. The interior of the Bonzoline and of the Ivorylene are shown.

The history of the Hyatt’s billiard balls is much more interesting, but revealing their larger significance for the history of science and technology required attention to what these billiard balls were made of. To understand the materials and methods used in the manufacture of Hyatt’s 1868 billiard ball, we used a multi-analytical approach consisting of in situ handheld Raman and X-Ray fluorescence (XRF) spectroscopy, completed with the analysis of microsamples utilizing a set of complementary methods, including micro-Fourier Transform Infrared Spectroscopy (μ FTIR), micro-Raman spectroscopy (μ Raman), Scanning Electron Microscopy with Energy Dispersive X-ray spectrometry (SEM-EDS), and Zooarcheology by Mass Spectrometry (ZooMs, peptide mass fingerprint).

To investigate the success of Hyatt’s 1868 innovation as a replacement for ivory, a comparison with other billiard balls of the late 19th and early 20th centuries was necessary. Popular guides on the practice of billiards frequently referenced the use of “composition” billiard balls, such as “Bonzoline” and “Crystalate”, which were acquired, and their composition determined (**Fig. 2.1B**) [11–16]. Bonzoline was introduced by J.W. Hyatt’s Albany Billiard Ball

Company, New York, in the 1880s. Crystalate was invented by George Burt, a former Albany Billiard Ball Co. worker, who established the Crystalate Manufacturing Company in Kent, England, to produce this material in 1900 [17].

The analysis of NMAH's yellow pool ball sold under the name "Ivorylene" from the 1930s-1950s, by Brunswick-Balke-Collender (B-B-C), the former Phelan & Collender, allowed a broader understanding of Hyatt's invention impacts in cue sports (**Fig. 2.1B**). This ball presented a yellow shell and a brown core. In 1882, Hyatt devised a method to create a billiard ball with a core-shell construction with interior and exterior segments made from different materials (U.S. Patent 259984) (**Fig. A1.1**). According to the patent description, a core or interior part of "inexpensive material" lowered the overall costs. While the traditional game, carom billiards, was played with three balls, pool was played with 16 balls (snooker with 22) and, therefore, the economic implications were significant.

Hyatt's first response to the Phelan & Collender 1864 challenge was a process patented in 1865 (USP 50359) that described a combination of pressed shellac with bone or ivory dust (Table S1). Then, on April 6th, 1869 (USP 88633 and 88634), he patented two different processes: 1) related to the invention of a composite material involving the use of a filler, such as paper and leather chips, and an adhesive gum, where shellac is mentioned, and 2) the dipping of a composition ball (probably made with the shellac composite) in a solution of collodion, i.e., a cellulose nitrate solution in diethyl ether and acetone. Finally, on May 4th, 1869 (USP 89582), Hyatt patented a process for manufacturing imitation ivory by mixing ivory or bone dust with cellulose nitrate in a proportion of 75/25% by weight. The experimental data obtained in this study evidence this last patent as the pioneer method for developing an unprecedented bone-celluloid (cellulose nitrate and camphor) composite, which would successfully compete with elephant ivory billiard balls.

2.2 Results

2.2.1 Hyatt's 1868 billiard ball

Hyatt's 1868 billiard ball showed an overall granular heterogeneous surface. With visible light microscopy, μ FTIR and SEM-EDS it was disclosed that this billiard ball is composed of bone particles of several sizes on a celluloid matrix (**Figs 2 and 3**). The 1868 billiard ball proportions of bone (B) to cellulose nitrate (CN) were quantified with μ FTIR: 77% B to 23% CN ($\pm 6\%$ SD), which correlates with the formulation of USP 89582, 1869 and with the date of the billiard ball (**Table 1, Figs. A1.2 and A1.3**). In more detail, with SEM-EDS it was possible to assess the heterogeneity of the mixture at the microscale: the phosphate regions show the variable

dimensions of the bone particles (50 μm to sub-micrometer values); the detection of micro and nanoparticles of aluminosilicate materials adds to the complexity of the mixture (**Fig. 3 and A1.4**). This was confirmed by the detection of ultramarine blue ($\text{Na}_{8-10}\text{Al}_6\text{Si}_6\text{O}_{24}\text{S}_{2-4}$) particles by μRaman , used in low quantities likely to enhance the whiteness of the billiard ball (**Fig. A1.5**) [18]. With X-Ray fluorescence spectroscopy, it was possible to identify zinc and calcium as the main components (**Fig. 4**). Zinc is associated with the white pigment zinc oxide (ZnO), identified with μRaman by detecting its strong E_2 vibration (Zn-O bending) at 436 cm^{-1} , and calcium to calcite (CaCO_3) by the CO_3^{2-} vibration at 1087 cm^{-1} (**Figs. 5, A1.6 and A1.7**) [19, 20].

Peptide mass fingerprint (ZoomS) was used to identify the animal origin of the bone particles. By comparison with MALDI marker ions from known references, it was found that the collagen from Hyatt's 1868 billiard ball is from cattle, indicating that the material used was probably bone-dust, a byproduct of the cattle industry (**Fig. A1.8**).

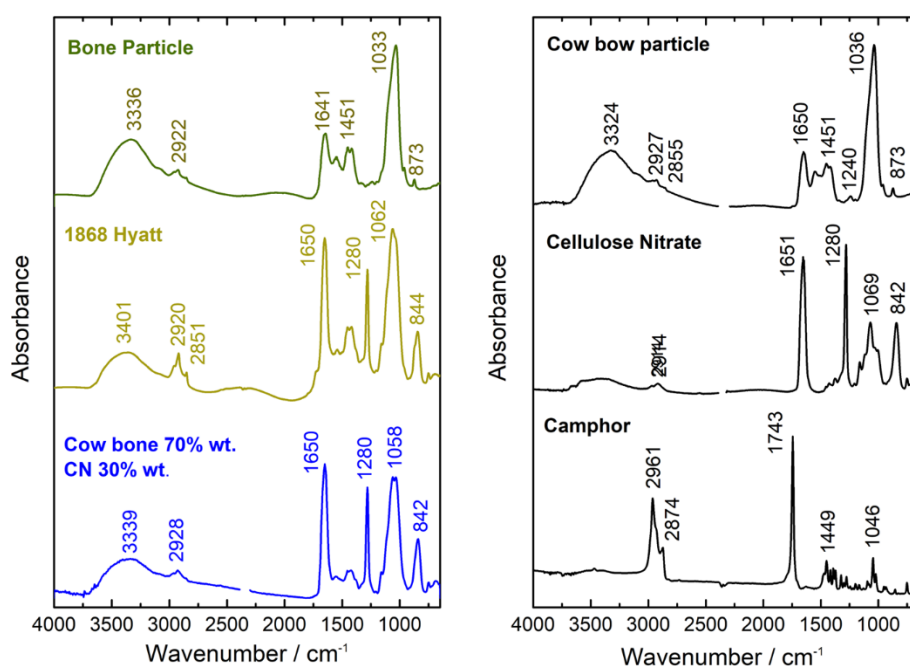


Figure 2.2. Molecular characterization of 1868 Hyatt billiard. Left, Infrared spectra of a bone particle from the 1868 billiard ball surface (top), of the average of 3 microsamples acquired from the surface (middle), compared with a reference prepared with 70% ground cow bone and 30% pure cellulose nitrate by weight (bottom). Right, infrared spectra of the references used for the development of the calibration curves for formulation quantification.

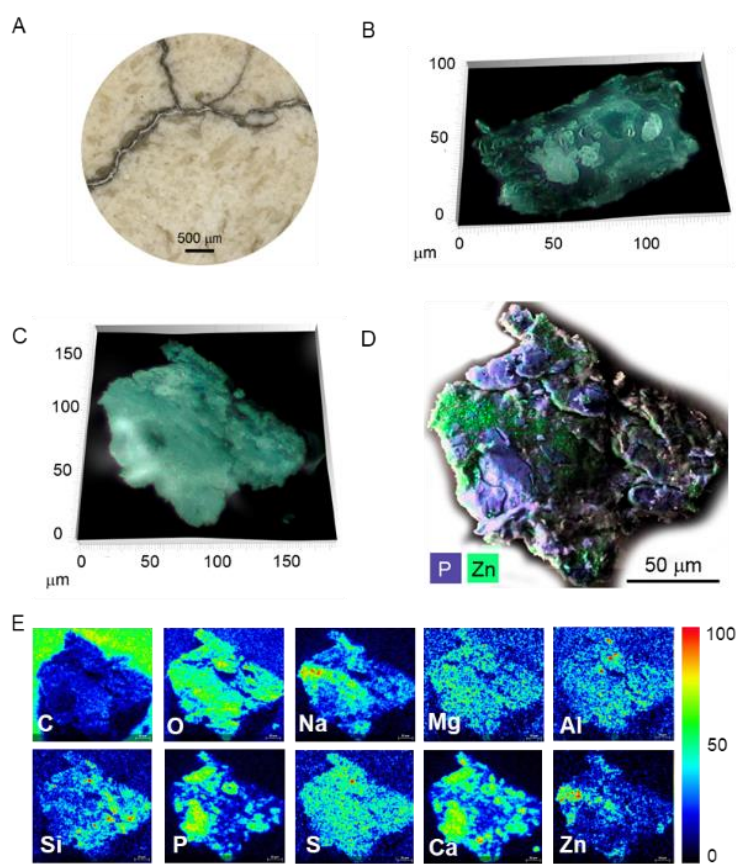


Figure 2.3. Microscopy of the 1868 Hyatt billiard ball. A) Microscope image of the surface showing its heterogenous granular surface and cracking (Hyrox Digital Microscope). B) Bone particle by 3D light microscopy. C) Bone-celluloid composite sample by 3D light microscopy. D) SEM-EDS false color composite image showing the distribution of phosphorous (represented as blue) and zinc (represented as green). E) Compositional distribution of major components as single element images, where the X-ray intensity is represented in rainbow scale, including carbon (C), oxygen (O), sodium (Na), magnesium (Mg), aluminum (Al), silicon (Si), phosphorous (P), sulfur (S), calcium (Ca) and zinc (Zn), by SEM-EDS.

2.2.2 Bonzoline (1930s) and Crystalate (1900-1960s)

The characterization of white bonzoline and crystalate billiard ball showed consistency to the composition found in the Hyatt 1868 billiard ball (**Fig. 5**). For bonzoline, with μ FTIR the proportion of bone to CN was quantified as 80/20% by weight ($\pm 2\%$ SD) and the origin of the bone was confirmed to be cattle by ZooMS (**Table 1, Figs. A1.9 and A.10**). For crystalate, the proportion of bone to CN was quantified as 79/21% by weight ($\pm 3\%$ SD) (**Table 1, Fig. A1.11**). The XRF spectra of the two materials was similar, showing the intense emission lines of zinc and calcium (**Fig. 4**). This correlated with the μ Raman spectra, which showed the presence of zinc oxide (ZnO), by the observation of the Zn-O bending vibration at 436 cm^{-1} , and calcite (CaCO_3) by the CO_3^{2-} vibration at 1087 cm^{-1} (**Fig. 5 and A1.12**).

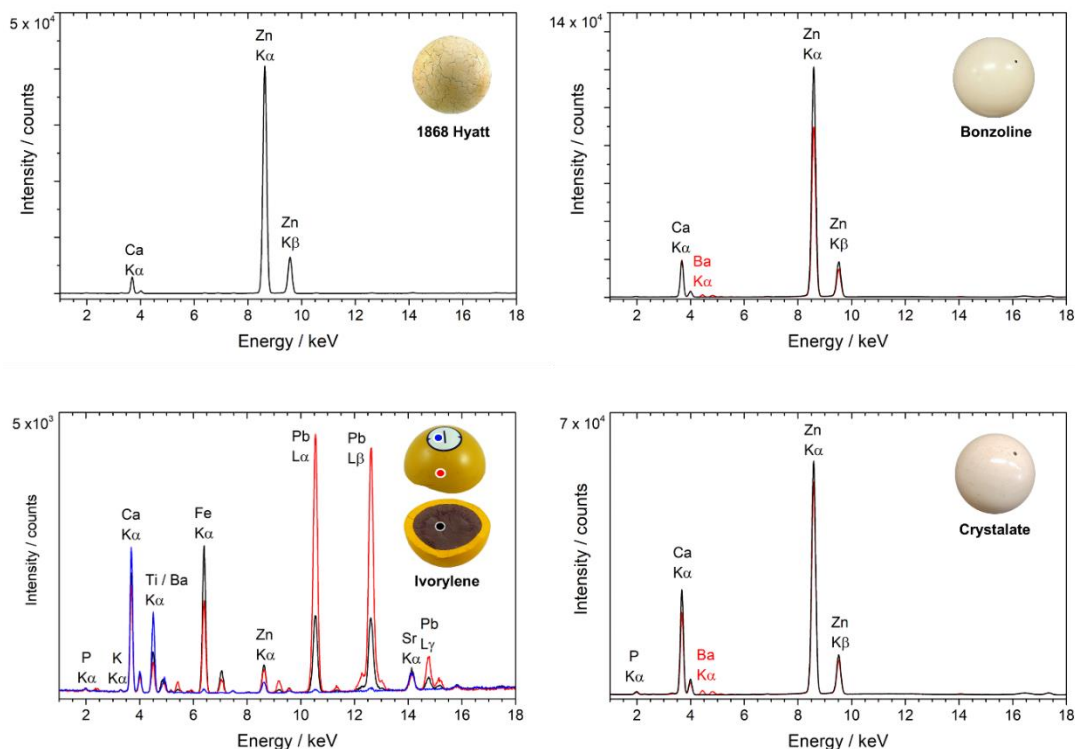


Figure 2.4. X-Ray fluorescence spectra for 1868 Hyatt, Bonzoline and Crystalate billiard balls and Ivorylene pool ball. The bonzoline and crystalate spectra were collected on white and red balls. On the Ivorylene three different areas were studied: the white region where the ball number is found (blue), the yellow layer (red) and the brown core (black).

Bonzoline, crystalate and Hyatt's 1868 billiard balls showed different concentrations of camphor. The patent for the bone-CN composite of May 4th, 1869 (89582) did not mention camphor (**Table A1.1**). Hyatt patented camphor (C) as a plasticizer for CN in 1870 (USP 105338), the fundamental patent for celluloid, in a proportion of 33% C to 77% CN. The ratio by weight of camphor to CN was quantified with μ FTIR for the three billiard balls (**Table 1**): Hyatt's 1868 billiard ball has a proportion of 13% C to 87% CN ($\pm 1\%$ SD, surface) (**Fig. A1.13**); Bonzoline 25%-29% C to 75%-71% CN (lower concentrations at the surface compared to the interior) (**Fig. A1.9**); and crystalate a proportion of 19% C to 81% CN ($\pm 1\%$ SD, surface) (**Fig. A1.11**). The lower concentration of camphor in the Hyatt's 1868 billiard ball can be related to degradation, i.e., volatilization of camphor or due to a higher amount used in bonzoline/crystalate [21].

Remarkably, the same synthetic pigment was identified for the red bonzoline and crystalate balls: a β -naphthol red, possibly the pigment lake PR49:1 (lithol red having Ba^{2+} as metal ion pair), part of a family that includes some of the most stable synthetic reds [22]. The presence of barium confirmed with XRF (**Fig. 4**). PR49:1 was identified with μ Raman by the vibration bands at 1615, 1599, 1455, 1480, 1461, 1447, 1422, 1411, 1344, 1253, 1229, 1212, 1202, 1094,

717 and 525 cm^{-1} , which correlated with a reference spectrum and with literature reference values (**Fig. 5 and A1.14**) [23].

We measured the densities of two NMAH's ivory billiard balls (1.73 and 1.80 g/cm^3), the Hyatt's 1868 billiard ball (1.93 g/cm^3), bonzoline (1.92 g/cm^3) and crystalate (1.97 g/cm^3). We also measured the microVickers hardness of a white bonzoline ball and obtained an average value of 22 HV (± 3 , 10 measurements). This value falls between the Vickers hardness values given by Vollrath et al. [24] for bone (30 HV) and celluloid (12 HV), which correlates with the chemical characterization of the bone-celluloid composite.

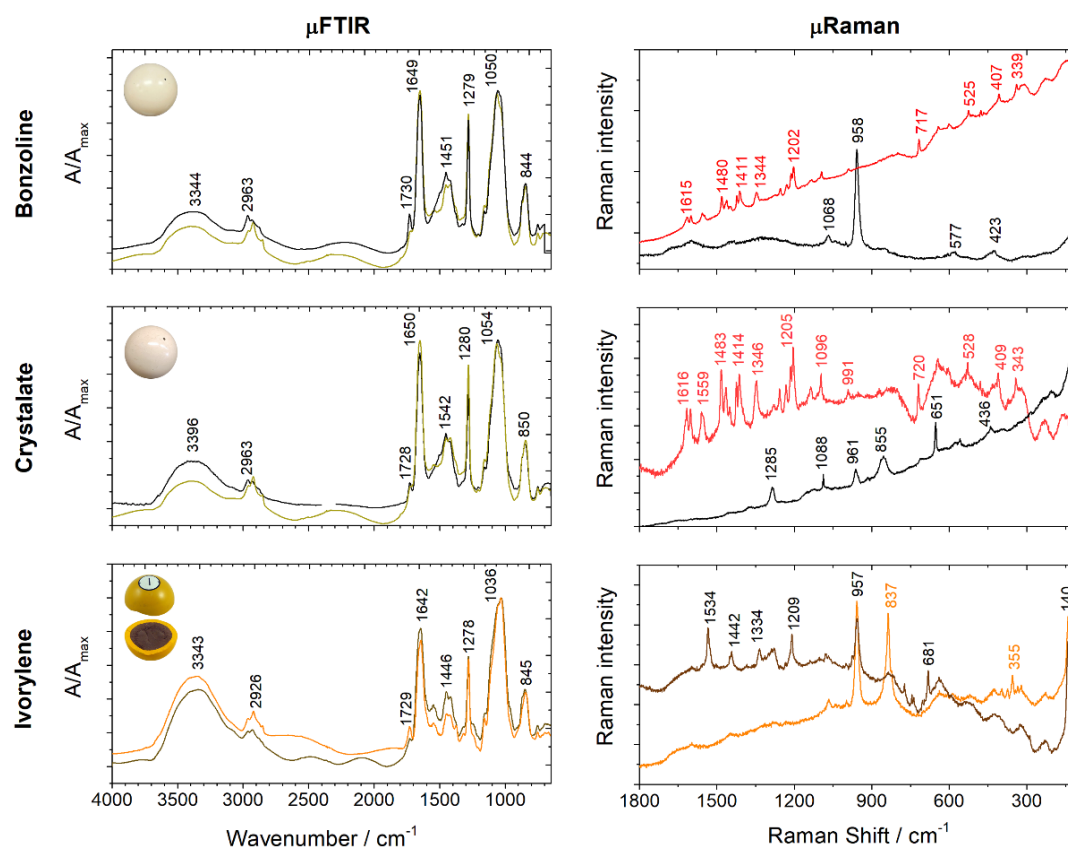


Figure 2.5. Molecular characterization of the Bonzoline and Crystalate billiard balls and Ivorylene pool ball. The average infrared spectra obtained for the bonzoline and crystalate billiard balls (black spectra) are compared with average spectrum obtained for the 1868 Hyatt billiard ball. The μ Raman spectrum of white Bonzoline billiard balls, shows a characteristic spectrum of bone (black spectrum). White crystalate μ Raman spectrum shows additional bands related to cellulose nitrate groups, calcite, camphor, and zinc oxide. Both red bonzoline and crystalate billiard balls show the characteristic bands of synthetic red pigment barium lithol red (PR49:1). The Ivorylene infrared spectra of the brown core (brown spectrum) and yellow layer (orange spectrum), both show the main absorptions of the bone-celluloid composite. The μ Raman spectrum of the Ivorylene yellow layer (orange spectrum) identified bone, chrome yellow and anatase; and of the brown core sample (brown spectrum) phthalocyanine green (PG7) and anatase.

2.2.3 Ivorylene pool ball

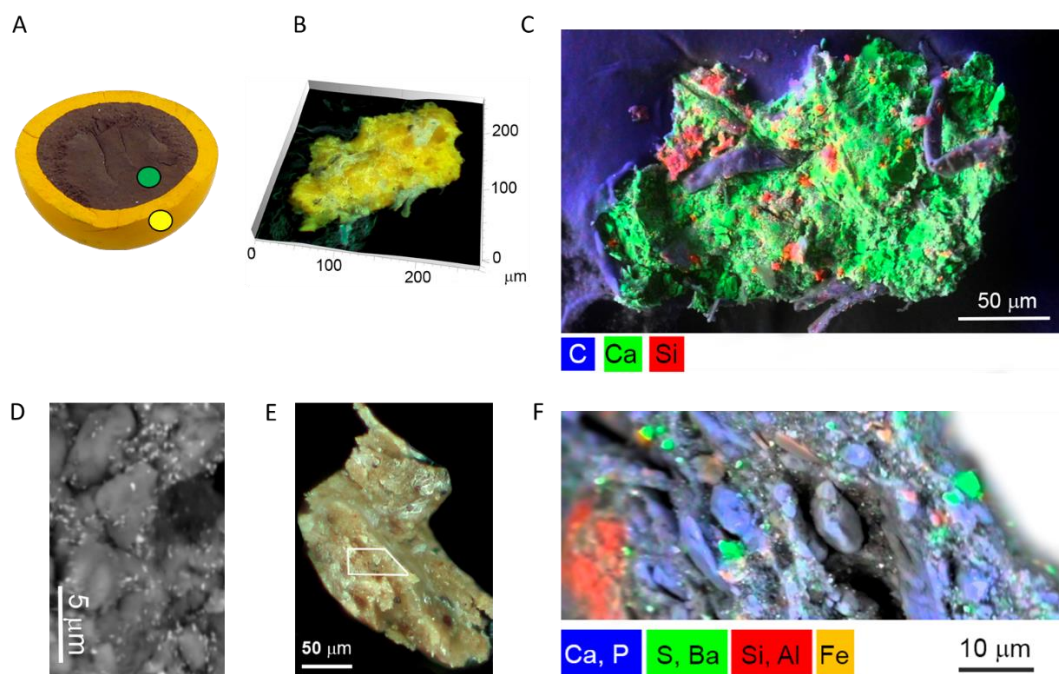


Figure 2.6. Microimaging of the Ivorylene pool ball. A) Location of the samples analyzed: the brown core and the yellow layer. B) Yellow layer sample viewed using 3D visible light microscopy. C) Composite SEM-EDS image showing the distribution of carbon (blue), calcium (green), and silicon (red). D) Backscattered electron image showing sub-micrometer-sized chrome yellow particles, white particles within on a gray matrix made of complex CN: bone: camphor and other additives shown in C). E) Brown core sample under the visible light microscope. The white polygon represents the area imaged. F) Distribution of calcium (Ca) and phosphorous (P) in blue for bone, iron (Fe) in orange, aluminum (Al) and silicon (Si) in red for aluminosilicates, barium (Ba) and sulfate (S) in green for the additive barium sulfate, BaSO_4 ; by SEM-EDS.

Remarkably, both the yellow shell and the brown core of the ivorylene pool ball are made of the bone-celluloid composite, with the overall weight proportions of 83% bone to 17% CN, by μFTIR (Fig. 5 and A1.15). By ZooMS, the bone origin was again identified as cattle (Fig. A1.16). In agreement with XRF data, which displays intense X-Ray emission lines of lead and chromium, the coloring agents of the yellow exterior section were identified by Raman spectroscopy as chrome yellow (lead chromate, PbCrO_4) and anatase (TiO_2) (Figs. 4 and 5 and A1.17 and A1.18); SEM-EDS imaging of a yellow micro-sample showed an overall distribution of calcium and phosphorous from bone, silicate particles, and a type of organic fiber in which anatase was identified (Fig. 6). The fibers are likely cotton based on carbon and oxygen X-ray intensities. Hyatt's pre-1870 patents mention using paper in the filler for billiard balls (Table S1). Thus, it is possible that titanium white was not used as a pigment but was present due to the paper used in the filler [25]. Electron imaging revealed the mean diameter of the lead

chromate particles was 204 nm ± 36 nm (n=10), a value that is consistent with lead chromates' intense pigmentation and opacity (**Fig. 6**) [26].

Table 2-1. Formulations of the 1868 Hyatt, *Ivorylene* pool and *Bonzoline* and *Crystalate* billiard balls. Weight proportions of bone (B), and camphor (C) are given in relation to cellulose nitrate (CN) as calculated by the calibration curves by infrared spectroscopy; for details, please see the supporting information.

	1868 Hyatt	<i>Ivorylene</i> (1930s-50s) Shell	<i>Ivorylene</i> (1930s-50s) Core	<i>Bonzoline</i> (1930s-60s)	Crystalate (1900-60s)	USP 89582 1869	USP 105338 1870
% B to CN	77% (±6)	83% (±1)		80% (±2%)	79% (±2%)	75%	-
% C to %CN	13% (±1)	25% (±2%)		surface 25% (±0.7) interior: 29% (±0.2)	19% (±1%)	-	33%
%B:	74.8% B:	79.6% B:		75.9% B:	76.0% B	-	-
%CN:	22.3% CN:	16.3% CN:		19.0% CN:	20.2% CN		
%C*	2.9% C	4.1% C		5.1% C	3.8% C		
Other additives	Aluminosilicates Calcium carbonate		Aluminosilicates Barium sulfate		Calcium carbonate	-	-
Main colorants**	Zinc oxide (Direct/American Process 1850s) [37] Ultramarine blue (1828) [38]	Chrome yellow PbCrO ₄ (1835) [39] Anatase, TiO ₂ (1926) [40]	Phthalocyanine green G (1938) [41] Anatase, TiO ₂ (1926)		Zinc oxide (1850s) <i>b</i> -naphthol red PR49:1 (1920s) [22]	-	-

* The total is expressed as a percentage of each ingredient. Using patents USP 89582 (1869) and 105338 (1870), we can hypothesize the following percentages as an industrial formulation used by Hyatt: 69.3% bone: 23.1% celluloid nitrate: 7.6% camphor.

**For the dates of introduction in the USA market of the synthetic pigments please see references

In the brown core, it was possible to observe a higher intensity of iron (Fe) X-Ray emission lines (**Fig. 4**). This agreed with the detection by SEM-EDS of Fe aluminosilicates and other Si-Al-Mg-K- rich particles dispersed in the bone-celluloid matrix, which indicates the presence of clay minerals that correlate with the brownish color of the core (**Fig. 6 and A1.19**) (27). Other coloring agents found in the core were anatase (TiO₂), phthalocyanine green G (PG7) and the filler barium sulfate (BaSO₄) (**Fig. 5 and A1.20**). XRF also detected lead (Pb) and indicated the presence of chrome yellow, but copper (Cu), an essential component of phthalocyanine green G, was not detected by XRF (**Fig. 4**). These findings agree with the economic claims of patent USP 259984 (1882): in 1931 the price of chrome yellow was 15 cents per pound while clay and barite (BaSO₄) were sold at circa 1 cent per pound [28, 29]. It is also important to consider that a complete set of 16 pool balls has eight colors. Although pigments are usually present in small amounts, different pigments have different densities. For example, chrome yellow has a

density of $\sim 6.3 \text{ g/cm}^3$, anatase $\sim 3.9 \text{ g/cm}^3$, and barite $\sim 4.5 \text{ g/cm}^3$. As a result, constructing a set of pool balls with an identical core diameter would mitigate the weight differences imparted by the differing materials in the exterior shell. However, explaining the presence of PG7 in a core meant to be unseen is hard.

2.3 Discussion

Hyatt's billiard balls were a successful alternative to ivory and were used for almost 90 years. They were consistently made from a composite material of ground bone, cellulose nitrate, and camphor. As such, they represent a premier example of a reinforced polymer composite, one of the most widespread materials in science and technology today. Historically, celluloid was disregarded as a successful billiard ball because we have focused almost exclusively on the development of polymers and their uses in unalloyed forms. The enormous creativity of Hyatt and his co-workers in reinforcing the celluloid matrix with ground bone and producing a ball from this material was no small thing. This composite met the extraordinary challenge of ivory's supply chain and demanding properties.

The problem of the global ivory trade and its impact on the African elephant population is still a critical issue in wildlife conservation [30]. Modern materials scientists have referred to ivory as a "model bio-composite." To save elephants, ongoing research for ivory-inspired synthesis has been undertaken. One approach to developing synthetic ivory involves the combination of organic and mineral components in bio-inspired ratios [24]. The early 75/25% wt. bone-cellulose nitrate ratio developed by Hyatt in 1868 is noteworthy, given its significant role in abolishing ivory in a highly demanding market. As the effort for ivory replication continues, the challenges remaining and those successfully met are worth noting.

The persistence of Hyatt's composite was crucial in creating a modern idea that artificial materials overachieve the natural world and allow athletes to break records. After Hyatt's invention, many billiard players believed ivory was better than the artificial alternative. The dynamics involved in material choices were complex and depended on interrelated factors. A leading factor was the billiards tradition, which englobed problems of prejudice and performance. In 1899, John Roberts Jr. (1847-1919) played a game against Charles Dawson (1866-1921), where these two famous British champions argued about the type of balls to use, bonzoline or ivory. Dawson wanted ivory due to its social status and because he was not adapted to bonzoline [11]. Early 20th century sources on cue sports discussed the mechanical impacts of playing with these different materials since the "composition" billiard balls were heavier [12, 13, 31]. As shown in this work, the densities of ivory billiard balls varied from 1.73 to 1.80 g/cm^3 . On the other hand, Hyatt's 1868 and the bonzoline billiard balls showed remarkably

consistent densities, 1.92-93 g/cm³. In addition, on each three-ball set made of bonzoline and crystalate, the densities varied below 0.1 g/cm³. Historical records mention professional players' improved performances using composition billiard balls due to their consistent properties, such as Roberts Jr., Henry W. Stevenson (1874-1944) or Willie Smith (1886-1982) [10, 11, 13].

Geography and chemical stability also played a crucial role: bonzoline was marketed as superior to ivory in tropical climates (**Fig. A1.21**), and players were advised on the adverse effects of weather on ivory billiard balls [3, 32, 33]. Ivory is highly susceptible to fluctuations in relative humidity, leading to deformation and cracking [34]. J. Roberts Jr. played in India regularly, where he probably started using bonzoline [10]. Comparing the yearly variations in relative humidity between Mumbai, a tropical climate where Roberts had a billiard table business, and London, a temperate climate, the former exhibits more prominent fluctuations (**Fig. A1.22**).

Lastly, the choice was influenced by entrepreneurial and sports competition. It was a common practice by manufacturers to contract famous players to bring their products to notice and prestige (**Figs. A1.23 and A1.24**) [16]. In 1904, Charles Dawson was advertising the Bonzoline Manufacturing Company, London. In the same year, H. W. Stevenson was promoting the competitor, the crystalate balls manufactured by Endolithic Manufacturing Co., London. Selection based on sports competition is exemplified by Walter Lindrum (1898-1960), an Australian billiards prodigy playing with "composition" billiard balls, who was invited to play in Great Britain as British professionals continued to use ivory partly because they felt confident in beating the colonial challengers with this natural material [10].

The material choice by amateur players was straightforward; it depended on function and economics. The composition billiard balls performed well and were cheaper. In 1885, B-B-C sold a set of 4 standard-size Hyatt billiard balls for \$10.50, while the ivory set cost \$22 (the 2023 equivalent costs are \$325.65 and \$682.32, respectively) (**Fig. A1.25**). The technical and economic advantages of Hyatt's composite enticed the growth of pool and snooker, which required more balls. In 1928, B-B-C sold 16-ball ivory pool sets for \$130-\$285, while sets made of ivorylene were available at \$20-\$25 (\$2315.01-\$5075.21 versus \$356.15-\$445.19 in 2023, respectively), **Fig. A1.26**. A new generation of players who learned to play with composition balls ultimately led to the complete transition from ivory to plastic [13]. In 1926, the Billiard Association and the Control Council, responsible for the regulation and organization of English billiards and snooker, adopted crystalate balls for amateur championships. Finally, in 1929 it was pronounced that for the professional championship of English billiards, "all games to be played with crystalate" [35].

The discovery of the bone-celluloid composite success brings an entirely new set of questions. In 1883, billiard balls of pure celluloid (with no fillers) and bonsilate, another composite

material reportedly developed by Hyatt and co-workers, were produced in Albany [36]. If a substitute for ivory billiard balls had been achieved as early as 1868, why did John Wesley Hyatt continue experimenting (and likely fail) with other compositions? Building on the methodology developed in this study, we will pursue further investigation into the diverse formulations of billiard balls to gain a comprehensive understanding of the evolution of their development, manufacture, and use. This research will contribute to a deeper understanding of the social and environmental impact of ivory consumption and the past efforts for its replacement. The pigments used to color the balls are fascinating and, on their own, bring us a chronology, as they have been replaced over time. Ultimately, we can only interpret and preserve these significant historical objects with a complete study of their materiality.

2.4 Materials and Methods

2.4.1 Historical billiard balls

NMAH has 10 billiard balls identified in their records as cellulose nitrate or celluloid. The Celanese Corporation donated the Hyatt's 1868 billiard ball, studied in this work (ID number CH.334311, diameter 57 mm, 187g). The ivorylene billiard ball studied (ID number 1997.0071.08, 57mm) is part of an 11 billiard ball collection donated by the Albany International, former Albany Billiard Ball Company, in 1997. The interest in analyzing 1997.0071.08 came from the fact that it was already broken in halves and allowed the in-situ analysis of its interior. The bonzoline (48mm, 111.2g) and crystalate (41.5 mm, 73.2g \pm 0.2) billiard balls were acquired for analysis. Both sets are composed of three balls, two whites and one red, enclosed in their original box (**Figs. A1.21 and A1.27**). The bonzoline box mentions "made in England". Bonzoline started being manufactured in England in 1931 by the Composition Billiard Ball Supply Co., London. Crystalate billiard balls were manufactured until the development of Super Crystalate in 1972, a phenol-formaldehyde based material. For comparison with the ivorylene billiard ball, one of the bonzoline billiard balls was cut in half, using a regular saw and polished with a Micro-Mesh wet sanding cloth grit 8000. The densities of two NMAH's ivory billiards balls were measured, (ID Number CL.329507) 54mm and 143.8g and 57mm and 174.2g (**Fig. A1.28**).

2.4.2 X-Ray fluorescence spectroscopy (XRF)

A portable X-ray fluorescence spectrometer S1 Titan from Bruker was used on-site with the following experimental parameters: 40 kV, 6 μ A and acquisition times between 5 and 20s. The Micro X-ray fluorescence of the bonzoline and crystalate billiard balls were acquired on a

Bruker ArtTAX Pro spectrometer equipped with a Molybdenum (Mo) ampule, Peltier effect cooled Xflash 3001® semiconductor detector, and a movable arm. Experimental parameters: 40 kV, 300 μ A, 200 s, and helium atmosphere. Elements were identified by their characteristic X-ray emission lines using ARTAX software.

2.4.3 3D light microscopy and scanning electron microscope energy dispersive spectrometer (SEM-EDS)

NMAH microsamples (Hyatt's 1868 and ivorylene) were analyzed with focal stack visible light microscopy using a Hirox KH-8700 digital microscope. The compositional distribution of major and minor elements was collected at the micrometer to submicrometer scale using a Hitachi SEM and a Bruker XFlash 6|60 EDS detector. The detailed description of the method is described elsewhere [42].

2.4.4 Micro Fourier Transformed Infrared Spectroscopy (μ FTIR)

Infrared spectra were acquired on a Nicolet iS50 FT-IR spectrophotometer and a Nicolet Nexus spectrophotometer both equipped with a Nicolet Continu μ m (15 \times objective) microscope and a Mercury–Cadmium–Tellurium (MCT) detector cooled by liquid nitrogen. μ -samples were placed between diamond cells for sample compression and the spectra was acquired in transmission mode between the 4000–650 cm^{-1} , with a resolution of 8 cm^{-1} and 128 scans. μ -samples were collected using Ted Pella μ -tools a M8 Wild Heerbruug stereomicroscope (6x to 50x magnification) and a Leica MZ16 stereomicroscope (between 7.1 \times and 115 \times).

The quantification of the formulations was achieved by the development of calibration curves using the absorbance ratio method, ie, by mixing two components in different weight proportions: 1) for the quantification of the proportion of cellulose nitrate to ground bone; and 2) for the quantification of camphor to cellulose nitrate. For comprehensive details, please see the Supplementary Materials (Figs. A1.2, A1.3 and A1.13).

2.4.5 Raman spectroscopy

Raman MIRA DS is a handheld Raman spectrometer (Metrohm), operating with a diode laser (785nm, 100mW) and a 200–2300 cm^{-1} spectral range. The equipment provides a spectral resolution of 8-10 cm^{-1} and a spot size between 0.04-2.5 mm. The detection technique is Orbital Raster Scan (ORS), which scans a large area of the sample surface with a tightly focused beam that maintains the high spectral resolution, an advantage for heterogeneous materials without putting the material surface at risk. Micro Raman spectra were collected on a Labram 300 Jobin Yvon spectrometer equipped with a He-Ne laser (632.8 nm, 17mW) and a diode laser (785nm,

100mW). The laser beam was focused with an Olympus 100× lens with a spot size of 2 μ m. The conditions used are provided for each spectrum.

2.4.6 Peptide Mass Fingerprint (ZooMS)

Peptide Mass Fingerprint analysis involves the enzymatic digestion of proteins followed by Matrix Assisted Laser Desorption-Ionization Time of Flight mass spectrometric (MALDI) analysis of the resultant peptide mixture. Each protein as a unique sequence of amino acids, this, the mixture of peptides is unique – a “peptide mass fingerprint”. Marker ions in the MALDI spectra from known reference materials are compared with those from unknown samples for identification. The detailed description of the method is described elsewhere [43]. This analysis was performed to gain information on the origin of the bone found in the billiard balls. If the billiard balls contained ivory dust, ZooMS should have found elephant markers, or others ivory animal sources, namely as walrus, narwhal, hippopotamus, warthog, sperm whale or orca (30). PMF was the chosen method because of the small quantity of sample available (μ g).

2.4.7 Vickers hardness tests and density measurements

The micro-Vickers hardness of the bonzoline white ball was measured with a ZwickRoell ZHV μ micro-Vickers hardness tester, using a test force of 100gf, and performing 10 measurements in different areas. Density was measured considering that the billiard ball is a perfect sphere, mass/volume.

2.5 References

- [1] Ten Thousand Dollars for a Substitute for Ivory. *Scientific American*, 166 (1864).
- [2] R. Friedel, *Pioneer Plastic: The Making and Selling of Celluloid* (The University of Wisconsin Press, 1983).
- [3] M. I. Shamos, *The illustrated encyclopedia of billiards* (Lyons & Burford, 1993).
- [4] T. Palucka, *Artificial Billiard Balls*. *MRS Bull* 30, 614–614 (2005).
- [5] J. W. Hyatt, *Adress of Acceptance*. *Ind Eng Chem* 6, 168–170 (1914).
- [6] J. L. Meikle, *American Plastic: A Cultural History* (Rutgers University Press, 1997).
- [7] P. J. Morris, *Polymer Pioneers: A Popular History of the Science and Technology of Large Molecules* (Center for History of Chemistry, 1986).
- [8] S. Mossman, *Early plastics: perspectives 1850-1950* (Leicester University Press and Science Museum, 1997).
- [9] S. C. Rasmussen, *From Parkesine to Celluloid: The Birth of Organic Plastics*. *Angewandte Chemie* 133, 8090–8094 (2021).

- [10]. C. Everton, *The History of Snooker and Billiards* (Tbs The Book Service Ltd, 1986).
- [11] J. Roberts, *Modern Billiards*, F. M. Hotine, Ed. (C. Arthur Pearson Ltd., 1902).
- [12] R. Levi, *Billiards: the stokes of the game. Part III* (Riso Levi, 1916).
- [13] R. Levi, *Billiards In The 20th Century* (Riso Levi, 1931).
- [14] M. W. Broadfoot, *Billiards* (Longmans, Green and Co., 1896).
- [15] T. Reece, W. G. Clifford, *Billiards* (A. & C. Black, Ltd., 1915).
- [16] J. P. Mannock, *Billiards expounded to al degrees of amateur players* (Grant Richards, 1904).
- [17] N. Clare, *Die Geschichte des Billard- und Snookerspiels. Fortsetzung in billard* 16, 447 (1989).
- [18] G. Buxbaum, G. Pfaff, *Industrial Inorganic Pigments*, 3rd ed. (WILEY-VCH Verlag GmbH & Co KGaA, 2005).
- [19] T. C. Damen, S. P. S. Porto, B. Tell, *Raman Effect in Zinc Oxide*. *Physical Review* 142, 570 (1966).
- [20] J. Sun, Z. Wu, H. Cheng, Z. Zhang, R. L. Frost, *A Raman spectroscopic comparison of calcite and dolomite*. *Spectrochim Acta A Mol Biomol Spectrosc* 117, 158–162 (2014).
- [21] C. Selwitz, *Cellulose nitrate in conservation* (J. Paul Getty Trust, 1988).
- [22] E. M. Angelin, M. C. Oliveira, A. Nevin, M. Picollo, M. J. Melo, *To be or not to be an azo pigment: Chemistry for the preservation of historical β -naphthol reds in cultural heritage*. *Dyes and Pigments* 190, 109244 (2021).
- [23] P. Vandenabeele, L. Moens, H. G. M Edwards, R. Dams, *Raman spectroscopic database of azo pigments and application to modern art studies*. *Journal of Raman Spectroscopy* 31, 509–517 (2000).
- [24] F. Vollrath, M. Ruixin, D. U. Shah, *Ivory as an Important Model Bio-composite*. *Curator* 61, 95–110 (2018).
- [25] A. Quye, *Factors influencing the stability of man-made fibers: A retrospective view for historical textiles*. *Polym Degrad Stab* 107, 210–218 (2014).
- [26] L. J. H. Erkens, H. Hamers, R. J. M. Hermans, E. Claeys, M. Bijmens, *Lead chromates: A review of the state of the art in 2000*. *Surface Coatings International Part B: Coatings International* 84, 169–176 (2001).
- [27] B. Velde, *Composition and Mineralogy of Clay Minerals. Origin and Mineralogy of Clays*, 8–42 (1995).
- [28] O. E. Kiessling, *Minerals Yearbook 1932-33* (United States Government Printing Office, 1933).
- [29] O. E. Kiessling, *Mineral Resources of the United States 1930* (United States Government Printing Office, 1933).

- [30] B. Baker, R. Jacobs, M. J. Mann, E. Espinoza, Giavanna Grein, CITES Identification Guide for Ivory and Ivory Substitutes, C. Allan, Ed., 4th editio (World Wildlife Fund Inc., 2020).
- [31] C. C. M. Western, *The Practical Science of Billiards and It's Pointer* (Simpkin Marshall Hamilton Kent & Co Ltd, 1911).
- [32] *A complete handbook of standard rules of all the prominent games of billiards and pool* (The Brunswick-Balke-Collender Company, 1909).
- [33] B. Garno, *Modern Billiards: A complete textbook of the game, containing plain and practical instructions how to play and acquire skill at this scientific amusement* (The Brunswick-Balke-Collender Company, 1908).
- [34] R. H. Lafontaine, P. A. Wood, *History of Billiards Through Its Champions Part One. Studies in Conservation* 27, 109–117 (1982).
- [35] *The Billiards Association and Control Council: conditions for the professional championship of English billiards, 1929. The Billiard Player* (1928).
- [36] *The Billiard Ball: Its Process or Manufacture -- A Very Peculiar Industry. The Washington Post* (1877-1922) (1883).
- [37] G. Osmond, "Zinc Soaps: An overview of Zinc Oxide Reactivity and Consequences of Soap Formation in Oil-Based Paintings" in *Metal Soaps in Art*, F. Casadio, et al., Eds. (Springer, 2019), pp. 25–46.
- [38] I. Osticioli, et al., *Analysis of natural and artificial ultramarine blue pigments using laser induced breakdown and pulsed Raman spectroscopy, statistical analysis and light microscopy. Spectrochim Acta A Mol Biomol Spectrosc* 73, 525–531 (2009).
- [39] V. Otero, et al., *Nineteenth century chrome yellow and chrome deep from Winsor & NewtonTM. Studies in Conservation* 62, 123–149 (2016).
- [40] S. Brown, R. J. H. Clark, *Anatase: Important industrial white pigment and date-marker for artwork. Spectrochim Acta A Mol Biomol Spectrosc* 110, 78–80 (2013).
- [41] T. D. Chaplin, R. J. H. Clark, *Identification by Raman microscopy of anachronistic pigments on a purported Chagall nude: conservation consequences. Applied Physics A* 122.
- [42] E. P. Vicenzi, et al., *Major to trace element imaging and analysis of iron age glasses using stage scanning in the analytical dual beam microscope (tandem). Heritage Science* 10, 1–15 (2022).
- [43] D. P. Kirby, N. Khandekar, J. Arslanoglu, K. Sutherland, *Protein identification in artworks by Peptide mass fingerprinting in ICOM Committee for Conservation 16th Triennial Meeting, (Critério Artes Gráficas, Lda and ICOM Committee for Conservation, 2011).*

This is an accepted manuscript of an article published by Springer Nature in Heritage Science, on 11/07/23, available online:

Neves, A., Friedel, R., Callapez, M. E., Swank, S.

Safeguarding our dentistry heritage: a study of the history and conservation of 19th-20th century dentures, Heritage Science, 11:142

<https://doi.org/10.1186/s40494-023-00989-2>

SAFEGUARDING OUR DENTISTRY HERITAGE: A STUDY OF THE HISTORY AND CONSERVATION OF NINETEENTH-TWENTIETH CENTURY DENTURES

Abstract

In the 1870s, dentures were one of the first products made with celluloid, the first semi-synthetic plastic. Despite the significance of denture development in the history of celluloid and plastics, the chemical characterization of dentures in museum collections has never been attempted. It is urgent to assess the extent of celluloid heritage in denture collections due to the high degradation risk that this material imposes. In this work, 21 dentures from the National Museum of American History and from the Dr. Samuel D. Harris National Museum of Dentistry were characterized using a multi-analytical methodology using handheld Raman, X-Ray fluorescence, and micro-Fourier transformed infrared spectroscopies. All dentures were successfully characterized: 12 are made of celluloid, 4 of vulcanized rubber, 2 of phenol–formaldehyde, 2 of polyvinyl chloride—polyvinyl acetate copolymer (PVC-PVAc) and 1 of polymethyl methacrylate (PMMA). The identification of the dentures' base materials allowed a better understanding of their history and posed new questions about their conservation. Handheld Raman was demonstrated as an excellent in-situ tool for the study of polymeric materials.

3.1 Introduction

Developed in the USA in 1870 by John Wesley Hyatt, celluloid is a thermoplastic material composed of cellulose nitrate and camphor. Considered the pioneer of the plastics industry, celluloid was prized for its remarkable capacity to imitate natural materials, such as ivory or tortoiseshell. The advent of synthetic plastics eventually led to the gradual loss of celluloid's importance due to technical and economic reasons [1, 2]. Celluloid objects are now testimonies to a unique historical period: the transition from a society dependent on natural materials and their limitations to a society that synthesizes materials according to its needs. Today it can be difficult to identify this material: sometimes confused with the natural material it imitates; other times classified under the general term of plastic. While "hidden" in heritage collections, celluloid creates a problem: this material is inherently unstable, prone to degradation by the action of light, water, or heat, leading to the complete loss of the object's integrity, to the oxidation of materials by nitrous and nitric acid (HNO₃) and, potentially, to health problems [3-13]. Therefore, it is imperative to promptly identify the presence of celluloid in cultural heritage artifacts, and through examination of their history and degradation characteristics, develop sustainable methodologies for their preservation and exhibition.

The first successful use of celluloid was in the manufacture of billiard balls. The second was in the making of dentures. Hyatt introduced celluloid in the denture market in the early 1870s to challenge vulcanized rubber [1]. Despite the significance of celluloid dentures in the history and development of plastics, there is lack of material culture and conservation science studies that consider dentures in museum collections. However, several studies have been made on the history and chronology of materials used for dentures [14-20]. This creates a knowledge gap between the history of denture materials and the dentures that reside in the collections. This gap results in an extreme difficulty for museums in identifying the composition of dentures dated from the late nineteenth—early twentieth centuries, due to the variety and similar properties of the materials used by the industry. The problem extends to the interpretation, exhibition, and conservation of dentures. This is because the definition of the dentures' composition is essential in delineating their cultural significance, comprehending their physical-chemical changes over time, and determining the most suitable techniques for their preservation [13].

In this work, this issue is addressed by the analysis of two collections of dentures from the National Museum of American History (NMAH) and from the Dr. Samuel D. Harris National Museum of Dentistry (NMD) using a multi-analytical approach consisting of handheld

Raman X-ray fluorescence (XRF) spectrometers and micro-Fourier Transformed Infrared spectroscopy (μ FTIR).

Overall, our results demonstrate the importance of a spectroscopic approach to the identification of the materials that exist in denture collections. The identification of five different materials, namely celluloid, vulcanized rubber, phenol-formaldehyde plastic, polyvinyl chloride—polyvinyl acetate (PVC-PVAc) copolymer and polymethyl methacrylate (PMMA), broadened the understanding of these denture collections and posed new questions about their conservation.

In the next section, a brief historical overview of the development of dentures from the eighteenth to the twentieth centuries is presented. The chemical analysis of the dentures provided new information about the impact of different formulations and manufacturing methods on celluloid stability, on camphor substitution due to the bad taste and smell and on vermilion substitution due to toxicity.

3.1.1 Brief historical overview of the materials used in dental plates – from vulcanite to PMMA

In the eighteenth century, denture makers used ivory bases with human teeth, but both materials deteriorated in the mouth. In 1776, Alexis Duchateau and Dubois de Chémant invented a method to produce porcelain dentures that fitted well in the mouth and were aesthetically pleasing. However, no other dentist could replicate this process due to the unpredictable shrinkage of porcelain during firing. This led to the discontinuation of complete porcelain dentures by 1814. At this point, ivory dentures were still used, and gold was one of the preferred materials in denture making. However, both materials were costly, and the manufacturing methods were lengthy and complex. In 1844, the discovery of nitrous oxide as an anesthetic gas by Wells, allowing the painless extraction of teeth, increased the demand for dentures [14].

Charles Goodyear was granted a patent for the manufacture of vulcanite (vulcanized or hard rubber) dentures in 1855 [14]. Vulcanite was a cheap material, compared to ivory or gold, and allowed the enlargement of the dental plate market in the nineteenth century. It could be easily molded to the shape of the mouth with accurate surface detail. Still, vulcanite had problems: the natural color of vulcanized rubber is brown and very high quantities of vermilion (mercury (II) sulfide, α -HgS) were mixed to tentatively imitate the natural red color of the gums; it was a porous material leading to staining and cleaning problems [1, 14, 15]. Until 1881, the Goodyear company charged expensive fees to dentists who used vulcanite due to patent rights, leading them to search for alternatives. However, after the expiration of the patent in 1881, vulcanite became “universally employed” [21]. Vulcanized gutta-percha, known

as corallite, was also used for dental plates. Edwin Truman introduced it in 1851, but it was considered unstable, becoming brittle over time [15, 21].

Parkesine was the first cellulose nitrate plastic, invented in England by Alexander Parkes and introduced to the market during the 1860s [1]. Daniel Spill took an interest in Parkesine's potential and founded, with the inventor, a company with an initial capital of £10,000—the Parkesine Company Ltd. This company was unsuccessful and was liquidated in 1868, possibly due to these reasons: the use of low-quality raw materials, such as scraps of paper or rags, leading to a product with a "dirty" appearance; the flammability of the material; the use of large proportions of solvents combined with an insufficient drying process, leading to product deformation; and failure to conquer specific markets [1, 22,23,24].

John A. McClelland made the first attempt to use cellulose nitrate as a base for dentures in the 1860s [25]. In 1868, he patented dental plates using collodion mixed with gum copal, coloring matter, and an additive to reduce inflammability, namely ammonium phosphate, cadmium iodide or calcium oxalate [26]. This dental plate base was known as "Consolidated Collodion" or "Rose-Pearl". Advocated as being a superior base to vulcanite, some opposed it due to material shrinkage — "Rose-Pearl is pretty, but it shrinks" [27]. Considering the problems of Parkesine due to the high quantity of solvents used, it is possible that Rose-Pearl suffered from the same difficulties.

John Wesley Hyatt solved the solvent problem by mixing cellulose nitrate and camphor by mechanical means. He patented this innovative process in 1870 and, with his brother, Isaiah S. Hyatt, called this material "Celluloid". Celluloid had the advantage of being a thermoplastic material, meaning it becomes pliable above its glass transition temperature and solid upon cooling [camphor acts as a plasticizer for cellulose nitrate, decreasing its glass transition temperature (T_g) and increasing its flexibility; the secondary T_g of pure cellulose nitrate and celluloid (cellulose nitrate + 29% wt. camphor) are circa 100 °C and 53 °C, respectively [28, 29]]. This process can be repeated any number of times. Therefore, Hyatt was able to sell pre-made forms, the dental blanks, to manufacturers, who then used them to mold the dentures under heat and pressure from the mouth impressions of the patients. This strategy of distributing celluloid in pre-made forms, namely sheets, rods, and tubes, would eventually become the marketing strategy that led to its success. It was an advantage over vulcanite, a thermoset polymer that could not be reheated. Vulcanite denture manufacturers had to proceed with the vulcanization reactions themselves in apparatus called vulcanizers.

The formulation used by the Celluloid Manufacturing Company was 1 part of celluloid to 0.04 parts of vermilion [30]. Vulcanite dentures looked dull and unnatural due to their brown color and high vermilion content [48 parts of rubber to 36 parts of vermilion [21]]. Celluloid, on the other hand, had a truly natural appearance. Celluloid was so esthetically close

to human gum that it prompted S.S. White Dental Mfg. Co. to create a set of artificial teeth that better resembled human, a line called “natural forms” [25]. However, celluloid was more expensive than vulcanite and had stability problems, leading to color and dimensional changes. Furthermore, the taste of camphor was widely considered unpleasant [1].

In the nineteenth century, celluloid dentures were sold by the Celluloid Manufacturing Company and the American Zylonite Company. Other tradenames for celluloid dentures appeared in the twentieth century, such as Alcolite and Hecolite (invented in 1925), sold by the Alcolite Inc. and by the American Hecolite Denture Corporation, at least until the 1930s, **Figs. A2.1 and A2.2.**

Both vulcanite and celluloid were far from meeting the requirements for a perfect denture material. Therefore, with the advent of synthetic plastics, new materials were introduced in the denture market in the twentieth century. In 1927, the Dental Manufacturing Company Limited, London, started using Walkerite, a phenol–formaldehyde product. In 1933, the Bakelite Corporation introduced a material called Luxene. Several other phenol–formaldehyde dentures were commercialized, but these dentures showed color and dimensional change problems [18]. Vinyl dentures, made of mixtures of PVC and vinyl acetate started to be sold in 1932. S.S. White sold Resovin, marketed as “the highest quality denture material”, **Fig. A2.3.** Unfortunately, these vinyl dentures showed breakage problems in the mouth and fell into disuse [18]. The best replacement for vulcanite only appeared in 1936, with the commercialization of Vernonite, a polymethyl methacrylate (PMMA) denture [16]. This material fulfilled all the dental plate requirements and rapidly dominated the market. In 1938, a survey of dental plate materials used by dentists showed that 71% used vulcanite, 20% phenol–formaldehyde, 8% cellulose derivatives and 1% vinyl resins. In 1947, another survey concluded that 95% of all dentures were made of PMMA [14].

3.1.2 The manufacturing processes of celluloid dentures

There were three processes to mold dentures from the celluloid blanks: the oil-glycerin bath, the steam apparatus, and the “dry-heat” process [30]. The Hyatt brothers invented and patented the first two in 1871 and 1874, respectively [31, 32]. In the oil-glycerin bath, as the name indicates, the celluloid blanks were placed in metallic flasks (with the mold of the mouth made in plaster) immersed in a vegetable oil or glycerin bath heated to a temperature of 150 °C. Using the steam apparatus, the flasks were heated to a temperature between 100 and 150 °C and the pressure was regulated by a safety-valve, Fig. 1. The first “dry-heat” apparatus for the molding of celluloid dentures is attributed to R. Finley Hunt, an American dentist, living in Washington, D.C, patented in May 1875 [33, 34]. The second “dry-heat” apparatus was probably the one patented by Ferdinand Heindsmann, assignor to S.S. White, in July 1875 [35]. This

apparatus had the advantage of also being a vulcanizer and manufacturers could use it for either celluloid or rubber. The "Heidsmann's heater" was a dry oven in which the flasks with celluloid were heated to a temperature of 135 °C with an alcohol lamp [36], **Fig. 3.1**.

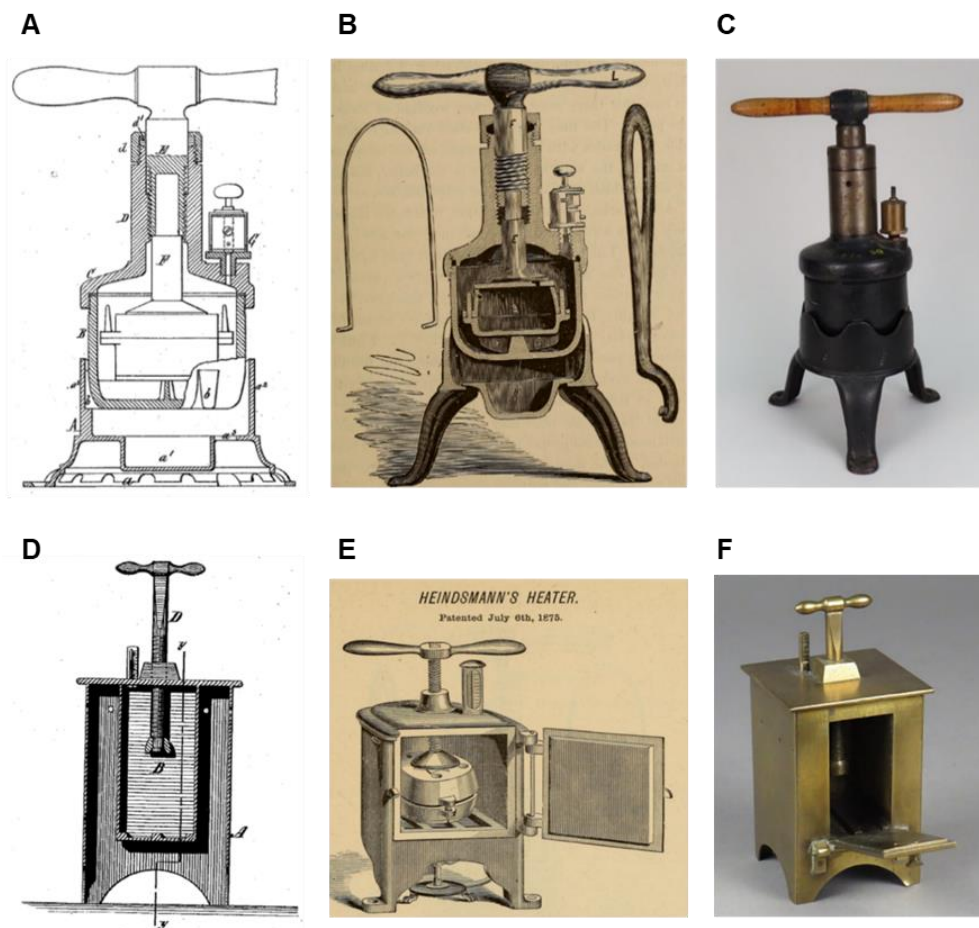


Figure 3.1. A) Scheme of the steam apparatus patented by the Hyatt brothers in 1874 [28]. B) Sectional view of the celluloid steam apparatus manufactured by the Celluloid Manufacturing Company and sold by S. S. White Dental Manufacturing Company [32], [33]. C) Example of one of these steam machines, collection of the National Museum of American History, catalog number M-08954. D) Scheme of the "dry-heat" apparatus patented by Ferdinand Heidsmann, assignor to S.S. White, in 1875. E) Patent model, NMAH collection, catalog number M-04242. F) "Heidsmann's heater" was manufactured and sold by S. S. White Dental Manufacturing Company in 1876 (Catalogue of dental materials, furniture, instruments, etc., for sale by Samuel S. White, 1876).

Although S.S. White Dental Mfg. Co. was granted in 1874 the exclusive right to sell the celluloid base, in 1878 the Celluloid Manufacturing Company distributed a pamphlet exposing the disadvantages of the "dry-heat" process, which was "manufactured by other parties" [30, 36]. The problems presented were the uneven heating of the dental blank and the need to use a wet plaster. In 1876, the "Heidsmann's heater" was sold at \$12 while the Hyatt's steam apparatus was sold at \$15. The possibility of acquiring a 2 in 1 celluloid and rubber apparatus at a lower price was a better deal for the dental plate makers [21]. The Celluloid Manufacturing

Company's need to send a message explaining their products' superiority is thus understandable.

In 1879, John S. Campbell, from New Jersey, invented an apparatus that superseded the previous ones, as pointed out by dentists in technical books [21, 34, 37]. It became known as the “New Mode Heater” and was also a vulcanizer. This apparatus had an outer compartment with steam to heat the dry inner chamber with the flasks. John Campbell combined the advantages of Hyatt’s and Heindsmann’s apparatus: the use of steam for a uniform heating and a dry chamber to avoid contact of celluloid with steam (which had a negative effect on color and porosity). Other devices of the same type were invented later, namely the W. W. Evan’s and Seabury’s vulcanizers [38, 39], the latter being commercialized by S.S. White Dental Mfg. Co. in 1894 [40].

An outcome of the “New Mode Heater” was that it allowed the development of vulcanite dentures with celluloid gums and porcelain teeth. This method became known as the “New Mode Continuous Gum” [16, 21]. For aesthetics, the vulcanite dentures could be covered with artificial gums made of porcelain, which also had a very natural look. However, this was a very difficult technique [15]. The “New Mode Continuous Gum” offered a more straightforward method using the same apparatus for molding vulcanite plates and veneering with celluloid.

In the 1920s and 1930s, the processes used were like the ones of the nineteenth century. For example, in a technical book for Hecolite dental plate manufacture, the apparatus described—the “Hecolizer”—was very similar to the Hyatt’s steam apparatus, with the difference of being built in aluminum and having a 110 V electric heater [20].

3.1.3 The vermilion problem

Vermilion (mercury (II) sulfide, α -HgS) was one of the most important red pigments until it stopped being produced in the twentieth century due to toxicity concerns [41]. Vermilion could be made by grinding mineral cinnabar or synthesized by the “dry” or “wet” methods. The wet method was invented in Germany in the seventeenth century by heating the black solid-phase form of mercury sulfide (metacinnabar, β -HgS) in a solution of ammonium and potassium sulfide. This process became the favorite in Europe and the USA [42]. Vermilion is a pigment known for its strong hiding power and high chroma. This pigment was blended with white pigments, such as lead or zinc white, to produce pink hues commonly used for flesh tones [42].

The use of this pigment in vulcanite and celluloid dentures raised the suspicion of mercury poisoning. The toxic effects were attributed to the liberation of mercury by the action of

saliva [43]. The worry of mercury poison led the Celluloid Manufacturing Company to advertise that celluloid had the advantage of only needing small amounts of vermilion compared to vulcanite [30]. The debate on vermilion toxicity in dentures extended to dentistry journals: Niles's (1881) opinion was that it could be prejudicial if the pigment derived from impurity-rich cinnabar by the existence of poisonous free mercury; high purity vermilion, synthesized by the "wet-process", would not cause any harm to the user. For him, the reason why celluloid and vulcanite led to problems in the mouth was related to the low heat conductivity of these materials compared to metals, thus his preference for metal plates [44]. Johnstone (1883) and Globenski (1889) maintained that vermilion was not harmful and added that cleanliness of the denture was a crucial factor in affecting the user's mouth health [45, 46]. The increasing concerns about vermilion toxicity in the twentieth century led to the invention of a celluloid formulation for dentures without vermilion. Hecolite was produced using a "a non-poisonous aniline instead of the toxic vermilion" [20]. It is unknown if any other products without vermilion were produced. In the twenty-first century, it was shown that α -HgS can be absorbed by the gastrointestinal tract and distributed to several tissues, including the brain [47]. Both the dry and wet synthesis processes can produce vermilion containing free mercury; the latter process in lower concentrations [48].

Due to its importance as an artistic material from antiquity to the nineteenth century, vermilion has been extensively studied [49-55]. Vermilion can darken if exposed to UV light by phase conversion of the red α -HgS to the black β -HgS. It was shown that chloride can act as a catalyzer of the light breakdown of α -HgS to metallic mercury (Hg), also leading to color changes. Raman spectroscopy was demonstrated as a technique with the potential to assess vermilion degradation by the shift and broadening of its characteristic peaks [51].

3.1.4 Aims of this research

The primary objective of this research was to characterize the formulations and conservation conditions of celluloid dentures. Consequently, the 21 dentures subjected to analysis in this investigation were chosen based on two criteria: (1) they were labeled as celluloid (NMD and NMAH), or (2) they were composed of an unidentified material yet exhibited comparable visual characteristics to those recognized as celluloid (NMD).

Due to camphor's undesirable odor and taste, celluloid dentures were an ideal case study to ascertain the extent to which camphor substitutes had been used to counteract this issue. Although camphor was considered the best cellulose nitrate plasticizer, several alternatives were tested from the 1880s to the 1920s. In addition to its unpleasant odor, camphor had other problems: its high melting point (175 °C), meaning that great care was required to apply the temperatures necessary to combine it with cellulose nitrate; the price fluctuations imposed

by the Japanese monopoly; and World War I supply shortages [13, 24, 56]. John Henry Stevens, the chief chemist of the Celluloid Manufacturing Company, started experimenting in the 1880s, testing several fragrant additives such as oil of cinnamon leaves or oil of wintergreen. In 1894, he patented acetanilide as a valid substitute for camphor: acetanilide had a melting temperature of 112°C and was odorless [24, 57, 58]. Later other chemicals were patented as total or partial camphor substitutes, such as oil of turpentine, triphenyl phosphate, or phthalates [13, 56-61].

Due to the concerns regarding the toxicity of vermilion and technical records mentioning the manufacture of celluloid dentures without vermilion, it was also useful to understand how vermilion was used and replaced in historical dentures.

Handheld Raman spectroscopy was used for the in-situ molecular characterization of the polymer matrix. To support the identification of cellulose nitrate, camphor, vermilion, and zinc oxide (the most common filler/stabilizer used in celluloid formulations), references of these materials were analyzed previously to the historical dentures. Micro sampling and microFTIR were performed on selected celluloid dentures to complement the formulation characterization and assess the conservation condition by quantifying the cellulose nitrate degree of substitution (DS) using calibration curves [62]. The degree of substitution of cellulose nitrate is defined as the number of nitrate groups attached per monomer (maximum of 3). Therefore, the quantification of the DS is an infrared tool to assess the polymer conservation condition since the decrease of DS (from 3 to 0) correlates with the scission of the nitrate group, i.e., degradation. According to the literature, the DS used to manufacture celluloid articles was 2.2 [63]. When the dentures were not made of celluloid, microFTIR was used to confirm the in-situ characterization made by handheld Raman. Portable XRF was used in-situ on the NMAH dentures to gain elemental information on inorganic additives, namely the fillers and pigments, such as zinc oxide and vermilion.

This work also provides insights into the materials used for the dentures' teeth. Because teeth were not the focal point of this research and due to analysis time restrictions, only one tooth of 6 different celluloid-labelled dentures was analyzed with handheld Raman spectroscopy.

3.2 Experimental

3.2.1 Collections from NMD and NMAH

This work analyzed 21 dentures, 15 from NMD and 6 from NMAH. Of NMD's 15 dentures, 5 were on display and described with a label (4 identified as celluloid and 1 as cellulose acetate;

identification method unknown) and the other ten were in storage and their materials unidentified. JUSTI 21, 23 and 24 were in the permanent exhibition and SSW 19 and 21 were in the exhibition “Tools of the trade: ancient Japanese dentistry” compiled by Dr. John Littlefield during an 1890–1892 world tour to introduce S.S. White Dental Manufacturing Company products to Australia and Asia. NMD’s dentures were analyzed by handheld Raman. Microsampling and μ FTIR were performed on 5 celluloid dentures based on their Raman spectra, dates, and conservation conditions. NMAH’s 6 dentures were selected based on their prior celluloid labelling. They were in storage and were analyzed using handheld Raman, μ FTIR and XRF.

3.2.2 Materials

The following materials were used as Raman and infrared material references: Pure cellulose nitrate membranes (AmershamTMProtran®, 0.2 μ m), camphor (96%, Sigma-Aldrich), zinc oxide (ZnO, Sennelier), vermilion (α -HgS, May & Baker LTD), PMMA sheet (unknown supplier), phenol–formaldehyde billiard ball (Aramith), 87% PVC- 13% PVAc copolymer (Aldrich Condensed Phase library, CAS number 9003-22-9) and calcium stearate [64].

3.2.2.1 Preparation of celluloid reference

A solution of 2% w/w of cellulose nitrate in methanol was prepared at room temperature and allowed to dissolve through the night (approx. 12 h). Cellulose nitrate-camphor (celluloid) films were obtained by adding camphor to the solution of 2% w/w cellulose nitrate in methanol. Camphor was added in 30% w/w to cellulose nitrate. Camphor was allowed to dissolve through the night (approx. 12 h). The solution was cast homogeneously over the surface of a microscope glass slide using a Pasteur pipette. The microscope glass slides were placed inside a desiccator with silica-gel and the solution left drying through the night (approx. 12 h). After drying, transparent cellulose nitrate-camphor (celluloid) films were obtained.

3.2.3 Characterization with handheld Raman MIRA DS

Handheld Raman spectra were acquired using Metrohm Raman MIRA DS. This Raman spectrometer operates with a diode laser with an excitation wavelength of 785 nm (100mW) and has a 200–2300 cm^{-1} spectral range. The equipment provides a spectral resolution of 8–10 cm^{-1} and a spot size between 0.04 and 2.5 mm. The detection technique is Orbital Raster Scan (ORS). The ORS scans a large area of the sample surface with a tightly focused beam that maintains a high spectral resolution, an advantage for heterogeneous materials and without putting the material surface at risk [65]. In this work, the laser power was set at maximum intensity (power

5) and with the maximum scans allowed by the software (10 scans) to obtain the best signal-to-noise ratio. The integration time was adjusted according to the response of the analyzed material, between 4 and 10 s. The measurements were collected using the 3 mm distance objective setting, i.e., without touching the object, **Fig. A2.4**. Variations in the microscale of the objective distance can be applied to increase the signal–noise ratio. For this purpose, a micrometric precision tripod (2 μm precision), with manual fine XYZ positioning, designed for MIRA DS was used. Sample curvature effects were minimized by testing different distances and positions and probing the spectrum intensity [66]. Cellulose nitrate, camphor, diethyl phthalate, zinc oxide and vermilion references were previously analyzed and supported the identification of these compounds, by comparison. Also, references for PMMA, using a sheet available at the laboratory (unknown supplier), and for phenol–formaldehyde resin, using a phenol–formaldehyde billiard ball (Aramith, made by Saluc, Belgium), were analyzed. Celluloid, cellulose acetate, polymethyl methacrylate (PMMA) and polyvinyl chloride (PVC) were also identified based on the literature [10, 60, 67,68,69]. Raman data for phenol–formaldehyde plastics (bakelite) or hard rubber (ebonite or vulcanite) identification was supported on [70, 71].

3.2.4 Characterization with μFTIR

3.2.4.1 Microsample acquisition

Microsamples were acquired from selected NMD and NMAH dentures using Ted Pella μ -tools. At NMD for magnification, a Dino-Lite digital microscope with magnification range 10x - 50x, 230x and 640 x 480 0.3MP image resolution was used. At NMAH was used a M8 Wild Heerbruug stereomicroscope (6x to 50x magnification). The dentures and sampling locations are shown, **Fig. A2.5** and **table A2.5**.

3.2.5 Micro Fourier Transform Infrared Spectroscopy (μFTIR)

Infrared spectra were acquired on a Nicolet iS50 FT-IR spectrophotometer equipped with a Nicolet Continuum (15 \times objective) microscope and a Mercury–Cadmium–Tellurium (MCT) detector cooled by liquid nitrogen. Micro samples were placed on a DC-3 diamond compression cell (Specac) and the spectra were acquired in transmission mode between the 4000–650 cm^{-1} , with a resolution of 8 cm^{-1} and 128 scans. Spectra are shown as acquired, without corrections or any further manipulation, except for removing the CO_2 absorption at approximately 2300–2400 cm^{-1} using OMNIC software. The degree of cellulose nitrate substitution was calculated using a calibration curve developed by Nunes et al. [62]. Celluloid, PVC–PVAc copolymer, PMMA and beeswax identification was based on the OMNIC spectra library and

literature [10, 72, 73]. The analysis of the spectra obtained from the hard rubber and phenol-formaldehyde dentures was more complex. Although identifying these materials can be made based on the literature [72, 74-77], it is difficult to understand what information can be extracted from the spectra. There is a lack of comprehensive work in the field of conservation science that explains the infrared spectral variations observed in the hard rubber and phenol-formaldehyde historical objects that may be related to synthesis or manufacturing differences, composition, or degradation. This problem has already been emphasized by Bell et al. [74].

3.2.6 Characterization with handheld X-Ray fluorescence spectroscopy

A portable/handheld X-ray fluorescence spectrometer S1 Titan from Bruker, from NMAH's National Numismatic Collection group, was used for the on-site elemental analysis, **Fig. A2.6**. Experimental parameters used were voltage of 40 kV, current of 6 μ A and acquisition times between 5 and 20s. The elements were identified by their characteristic X-ray emission lines using ARTAX software.

3.3 Results and discussion

3.3.1 Reference spectra by MIRA DS

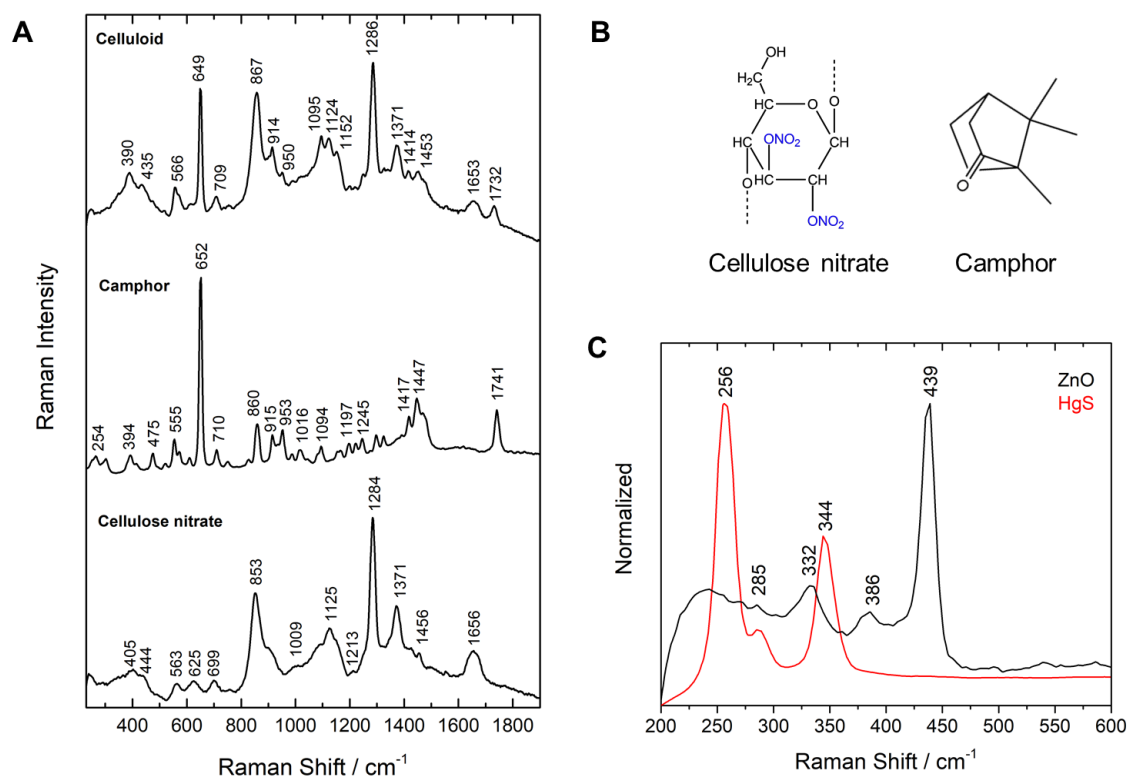


Figure 3.2. A) Raman spectra of a cellulose nitrate reference, camphor and celluloid (cellulose nitrate + 30% wt camphor). B) Cellulose nitrate and camphor chemical structures. Cellulose nitrate is showed with a degree of substitution 2 (on average, two nitrate groups and one hydroxyl group per monomer). Cellulose nitrate used for celluloid had a degree of substitution of 2.2. C) Raman spectra of vermilion (HgS, mercury sulfide) and zinc oxide (ZnO), also known as zinc white.

Two intense bands characterize cellulose nitrate Raman spectrum at 853 and 1284 cm⁻¹ attributed to the nitrate group stretching vibrations. Other bands from the nitrate groups are observed at 625, 699 and 1656 cm⁻¹. The bending vibrations of the CH and CH₂ groups are observed at 1371 and 1456 cm⁻¹, respectively. The bands observed between 1000 and 1215 cm⁻¹ are assigned to the cellulosic acetal structure, i.e., the ring ether and the glycosidic bond. The camphor spectrum is characterized by several bands, the most intense at 652 cm⁻¹ being attributed to the ring deformation of this compound. In the celluloid spectrum, the cellulose nitrate bands are influenced by camphor: in the region between 200 and 800 cm⁻¹ with the observation of the strong camphor band at 649 cm⁻¹; changes in the region between 900 and 1200 cm⁻¹; observation of two bands additional at 1414 and 1453 cm⁻¹; and the observation of

a band at 1732 cm^{-1} due to the camphor carbonyl group, **fig. 3.2A**[52], [55]. Vermillion is characterized by three bands at 256 , 285 and 344 cm^{-1} ; zinc oxide by bands at 285 , 332 , 386 and 439 cm^{-1} , **Fig 3.2C**.

3.3.2 Multianalytical characterization of NMD and NMAH dentures

All dentures, 21 in total, were successfully characterized: 12 are made of celluloid, 4 of vulcanized rubber, 2 of phenol-formaldehyde, 2 of polyvinyl chloride – polyvinyl acetate copolymer (PVC-PVAc) and 1 of polymethyl methacrylate (PMMA).

3.3.2.1 Celluloid dentures

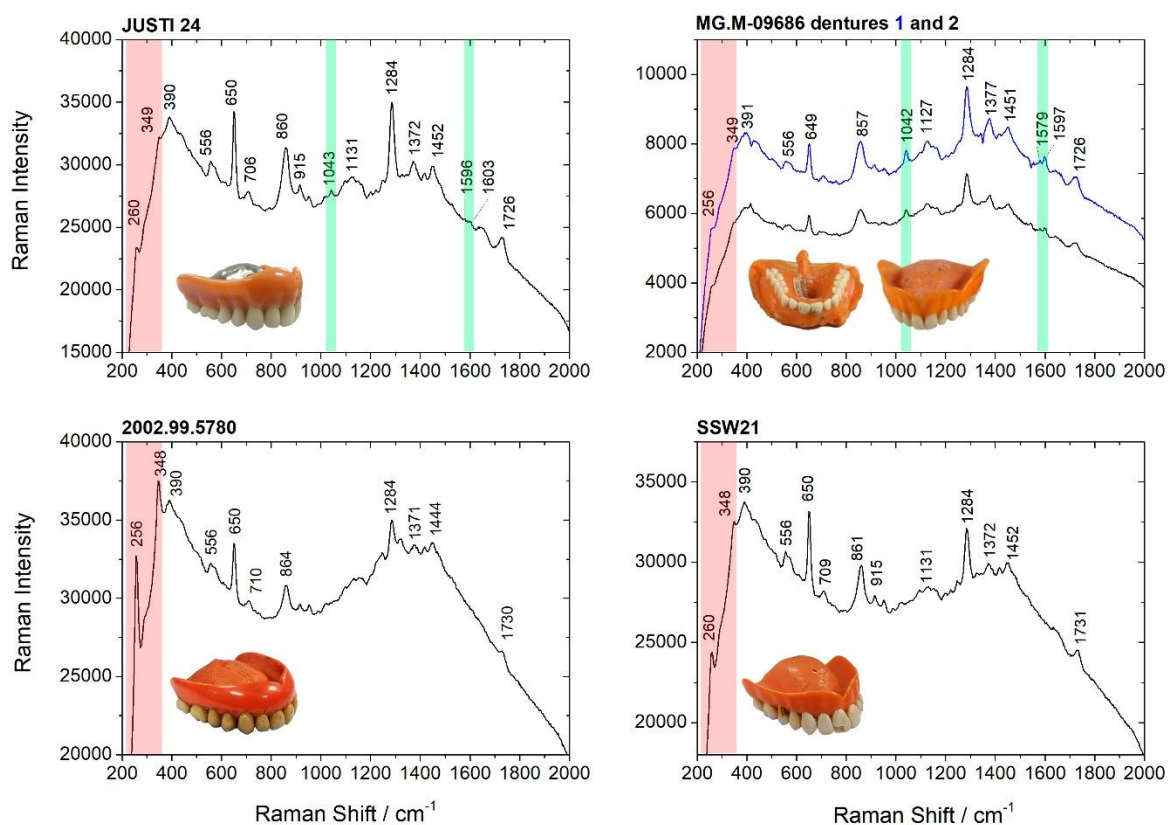





Figure 3.3. Raman spectra of celluloid (cellulose nitrate + camphor) dentures acquired with handheld Raman, using different acquisition times: JUSTI 24, 14 s acquisition time; MGM-09686 (denture 1 (black) and 2 (blue)), 3.5 s; 2002.99.5780, 6 s; SSW21, 10 s. Vermillion and phthalate peaks are highlighted in red and green, respectively.

Handheld Raman and μFTIR provided a straightforward identification of celluloid by detecting characteristic cellulose nitrate and camphor absorption bands. In the Raman spectra, all celluloid dentures (12 in total) showed similar absorptions: the three intense nitrate band vibrations around 1650 , 1280 and 840 cm^{-1} , the glycosidic structure vibrations between 1250 and 1000 cm^{-1} , and the camphor carbonyl stretching at 1730 cm^{-1} , C-H stretching and bending

vibrations between 3000 and 2800 and 1500–1300 cm^{-1} , respectively, **Fig. 3.3** and **Tables 3.1 and 3.2**. Raman spectra of JUSTI 24 and MG.M-09686 showed additional bands at 1043, 1596, 1603 and 1040, 1579, 1597 cm^{-1} , respectively, and a shift of the carbonyl bands to lower wavenumbers, **Fig. 3.3**. These features are characteristic of a phthalate plasticizer. Phthalate plasticizers started to be used in the 1920s, thus the Raman data correlates with the date proposed for JUSTI 24 (1930s). Phthalate bands were not observed in the infrared spectra, only a shift of the carbonyl band to lower wavenumbers was detected, **Tables 3.1 and 3.2**.

Table 3-1. Characterization of NMAH celluloid dentures (MG.M -09686 set) by handheld Raman, μ FTIR and XRF.






Object	NMAH Description	Handheld Raman		μ FTIR ^a	XRF
		Dental Plate	Tooth		
 Denture 1		Celluloid: 649, 710, 858, 918, 1124, 1284, 1377, 1453, 1642, 1722 cm^{-1} Phthalate: 1040, 1579, 1597, 1722 cm^{-1}	Porcelain: 460 cm^{-1} ; broad band between 1100-2200 cm^{-1}	Celluloid: 693, 750, 840, 1070, 1160, 1278, 1374, 1655, 1721, 2878, 2930, 2963 cm^{-1} <u>Degree of substitution:</u> 1.98	Zn and Hg
 Denture 2	Dentures; Donated by the Celluloid Corporation	Celluloid: 650, 710, 861, 914, 1124, 1284, 1377, 1451, 1642, 1723 cm^{-1} Phthalate: 1040, 1579, 1597, 1723 cm^{-1}	Not analyzed	Celluloid: 698, 750, 845, 1070, 1160, 1278, 1374, 1655, 1720, 2878, 2930, 2963 cm^{-1} <u>Degree of substitution:</u> 1.92	Zn and Hg
 Dental blank		Celluloid : 650, 710, 857, 918, 1124, 1284, 1377, 1450, 1642, 1725 cm^{-1} Phthalate: 1040, 1579, 1597, 1725 cm^{-1}	Not analyzed	Celluloid: 698, 750, 843, 1070, 1160, 1280, 1374, 1655, 1722, 2878, 2932, 2963 cm^{-1} <u>Degree of substitution:</u> 2.11	Zn and Hg





^aQuantification of cellulose nitrate degree of substitution (DS) was performed using an infrared calibration curve, developed by Nunes et al. (2020). Infrared spectra are showed in Fig.A2. 8.

All celluloid dentures showed the presence of vermilion (HgS) in the Raman spectra, **Fig. 3.3, Table 3.1 and 3.2** and **Fig. A2.7**. The first band of vermilion shifts from 263 to 256 cm^{-1} depending on the object, which can be related to pigment degradation. In the case of the MG.M-09686 set, the vermilion bands were barely visible, only confirmed by the presence of mercury (Hg) emission lines in the XRF spectra, **Figs. 3.3 and 3.4**. The main elements identified in this celluloid set, were zinc (Zn) and mercury (Hg). In the red gums of two vulcanite dentures, MG.291116.0049 and MG.291116.0046, Zn and Hg were also identified as the main

components, Fig. 3.4. It was possible to observe a higher intensity of the emission lines of Zn and Hg in the vulcanite dentures, indicating the higher concentration of these elements in comparison to celluloid. It was also observed that the concentration of Hg to Zn was higher in the vulcanite dentures, Fig. 3.4.

Table 3-2. Characterization of NMD celluloid dentures by handheld Raman and μ FTIR

Object	NMD description	Handheld Raman		μ FTIR ^a
		Dental plate	Teeth	
 SSW21	Full upper set of celluloid with human teeth. S.S. White 1890-1892	Celluloid: 556, 650, 709, 861, 915, 950, 1131, 1246, 1284, 1372, 1452, 1731 cm^{-1} Vermilion: 260, 348 cm^{-1}	Human teeth (hydroxyapatite): 432, 583, 961, and 1071 cm^{-1}	Celluloid: 840, 1064, 1278, 1657, 1730, 2963, 3452 cm^{-1} Degree of substitution: 2.12
 JUSTI 21	Maxillary dental plate with swaged gold base with celluloid overlay and porcelain teeth. Late 19th century	Celluloid: 555, 650, 706, 860, 915, 951, 1131, 1246, 1286, 1373, 1453, 1733 cm^{-1} Vermilion: 260, 349 cm^{-1}	Porcelain: 1408 and 1873 cm^{-1} ; broad bands between 1100-2200 cm^{-1}	Beeswax: 720, 1173, 1462, 1736, 2918, 2851, 2954 cm^{-1} (<i>superficial microsample</i>)
 JUSTI 24	Celluloid maxillary dental plate. Vitalium (chromecobalt alloy) cast base with porcelain teeth, circa 1930	Celluloid: 556, 650, 706, 860, 915, 951, 1131, 1251, 1284, 1372, 1452, 1726 cm^{-1} Phthalate: 1043, 1596, 1603, 1726 cm^{-1} Vermilion: 260, 349 cm^{-1}	Porcelain: 460 cm^{-1} ; broad band between 1100-2200 cm^{-1}	Celluloid: 839, 1063, 1278, 1657, 1729, 2963, 3473 cm^{-1} Degree of substitution: 2.03
 2002.99.5780	Taken out of storage. Had never been labelled	Celluloid: 556, 650, 710, 864, 917, 950, 1284, 1371, 1444, 1730 cm^{-1} Vermilion: 256, 348 cm^{-1}	Not analyzed	Celluloid: 843, 1066, 1280, 1649, 1730, 2963, 3452 cm^{-1} Degree of substitution: 1.87
 92.2.0924	Taken out of storage. Had never been labelled	Celluloid: 556, 652, 710, 862, 915, 951, 1131, 1246, 1284, 1371, 1445, 1728 cm^{-1} Vermilion: 256, 345 cm^{-1}	Not analyzed	Celluloid: 841, 1068, 1279, 1649, 1730, 2964, 3434 cm^{-1} Degree of substitution: 1.96

	Partial set of celluloid with porcelain teeth. S.S. White 1890-1892	Celluloid (cellulose nitrate + camphor): 556, 650, 706, 860, 915, 951, 1131, 1246, 1286, 1373, 1453, 1733 cm^{-1} Vermilion: 260, 349 cm^{-1}	Porcelain: 460 cm^{-1} ; broad band between 1100-2200 cm^{-1}	Not analyzed
SSW19				
	Taken out of storage. Had never been labelled	Celluloid: 556, 649, 709, 860, 915, 951, 1131, 1246, 1371, 1452, 1728 cm^{-1} Vermilion: 263, 349 cm^{-1}	Not analyzed	Not analyzed
2002.99.5287				
	Taken out of storage. Had never been labelled	Celluloid (cellulose nitrate + camphor): 556, 649, 710, 861, 915, 950, 1131, 1445, 1732 cm^{-1} Vermilion: 256, 348 cm^{-1}	Not analyzed	Not analyzed
2002.99.5818				
	Taken out of storage. Had never been labelled	Celluloid (cellulose nitrate + camphor): 556, 652, 710, 864, 917, 953, 1131, 1251, 1284, 1372, 1447, 1728 cm^{-1} Vermilion: 259, 349 cm^{-1}	Not analyzed	Not analyzed
2002.99.4726				

^aQuantification of cellulose nitrate degree of substitution (DS) was performed using an infrared calibration curve, developed by Nunes et al. (2020). Infrared spectra are showed in Fig. A2.8.

In the case of denture JUSTI 21, the microsamples acquired were very superficial, resulting in an unexpected infrared result, the identification of beeswax. This material could have been used to block celluloid camphoric taste, or it is a residue from a beeswax impression of the mouth (used until the 1880s by some dentists) [21], **Fig. 3.5**. The identification of celluloid by handheld Raman shows the capability of this technique to detect materials at greater depths and avoid superficial coatings.

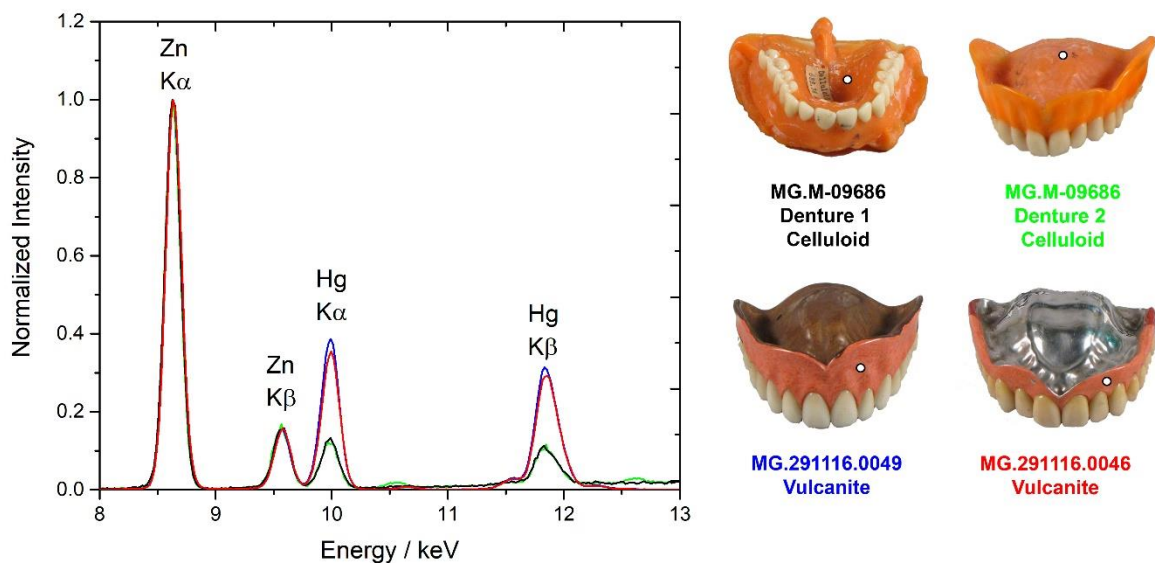


Figure 3.4. XRF spectra of celluloid dentures MG.M-09686 (dentures 1 and 2) and vulcanite dentures MG.291116.0046 and MG.291116.0049, normalized to the maximum (corresponding to Zn $K\alpha$ emission line). A higher relative intensity of vulcanite's Hg emission lines is observed. The analysis points are marked in the images of the dentures.

The degree of substitution of cellulose nitrate was calculated with infrared spectroscopy for 7 dentures, **Tables 3.1 and 3.2**. In the MG.M—09686 set, the dental blank showed a higher DS (2.11) than the dentures 1 and 2 (1.98 and 1.92). This decrease from one form to the other (dental blank to dental plate) can be related to the degradation induced by molding process (considering that in this case, they are all made from the same raw celluloid batch). The dental blank shows a DS value close to the stated by the literature for the manufacture of raw celluloid (2.2) [62]. The lower value (2.11) can be related to ageing but also to the initial process of transforming the celluloid sheet into a dental blank.

From the 7 plates, dental plate 2002.99.5780 was the one in worst visual conservation condition, with brown areas across the red gums and yellowed teeth with dark spots, **Table 3.2 and Fig. A2.9**. This dental plate showed the lowest DS value (1.87), which correlated with the visual observation. Denture 92.2.0924 showing localized dark spots associated to a pitting effect (possibly due to a technique to achieve a more natural imitation of the gums) had a DS of 1.96, **Table 3.2 and Fig. A2.10**. Dental plate JUSTI 24 (1930s), SSW21 (1890–1892) showed DS of 2.03 and 2.12 respectively, **Table 3.2**. According to the dates proposed for these dental plates, it would be expected for JUSTI 24 to be in better conservation condition than SSW19. This emphasizes the presence of the phthalate plasticizer, which might be accelerating the degradation of celluloid (the same goes for the MG.M–09686 set). Recently, it was shown that diethyl phthalate accelerates cellulose acetate degradation but for celluloid this investigation

as yet to be carried out [78, 79]. Lower DS can also be related to the cellulose nitrate manufacturing quality: phthalate plasticizers could be added for the manufacture of lower quality products. Lower manufacturing quality is also associated to the presence of residual sulfates due to an inadequate washing process, accelerating celluloid degradation [5, 6, 13].

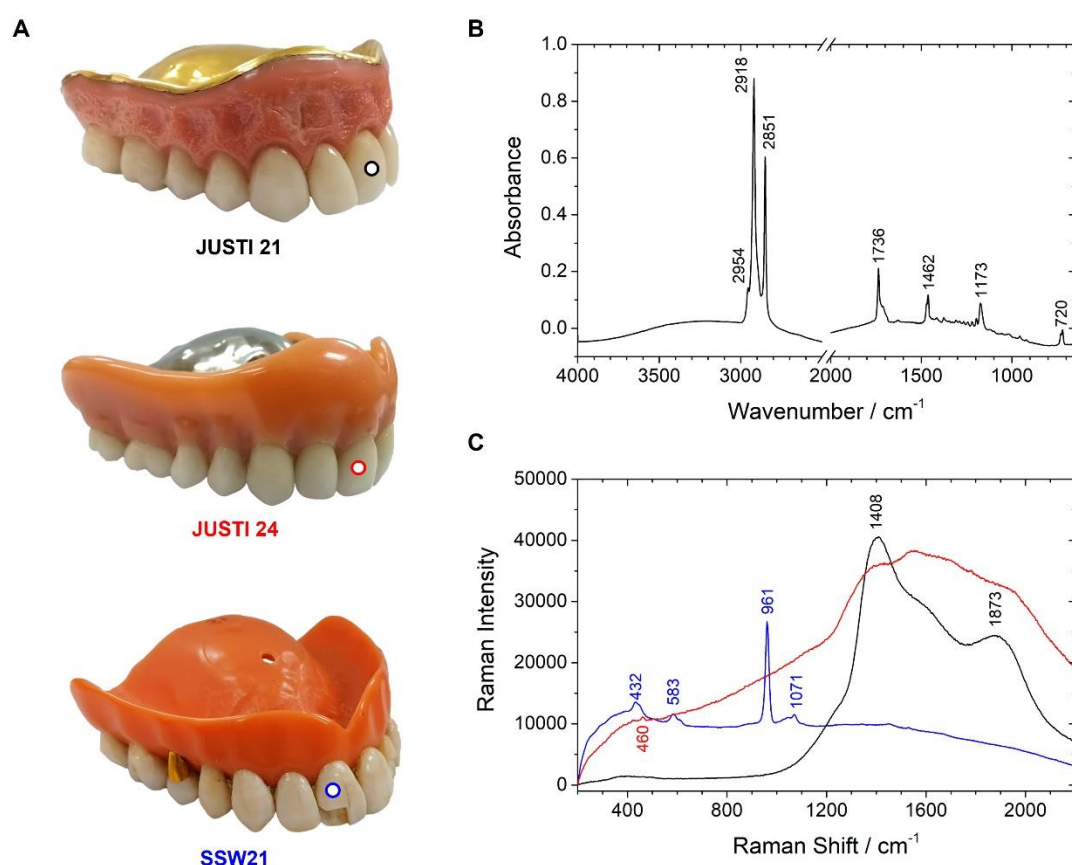


Figure 3.5. **A)** Photographs of dentures JUSTI 21, JUSTI 24 and SSW21, with indication of teeth analyzed with handheld Raman. **B)** Infrared spectra of JUSTI 21 beeswax coating. **C)** Raman spectra acquired from the porcelain teeth of JUSTI 21 (black, 1.2 s, 1 scans) and JUSTI 24 (red, 14 s, 10 scans) and from the human teeth of SSW21 (blue, 7 s, 10 scans).

3.3.2.1.1 Handheld Raman analysis of the celluloid dentures' teeth

The tooth of denture SSW21 was identified as a human tooth by the detection of the characteristic hydroxyapatite peaks at 432 $\nu_2(\text{PO})$, 583 $\nu_4(\text{PO})$, 961 $\nu_1(\text{PO}_4^{3-})$ and 1071 cm^{-1} $\nu_1(\text{CO}_3^{2-})$ [65], **Fig. 3.5** and **Table 3.2**. All the other teeth analyzed in this work with handheld Raman were identified as porcelain teeth by the detection of broad bands between 1100 and 2200 cm^{-1} , characteristic of the luminescence of rare earth elements when using a NIR excitation source to analyze glasses and ceramics [80], **Fig. 3.5**, **Tables 3.1** and **3.2** and **Fig. A2.11**. In the case of

dentures JUSTI 24, SSW19 and MG.M-09686 (dentures 1), it was possible to also identify the characteristic peak of α -quartz (SiO_2) at 460 cm^{-1} . Recently, it was demonstrated that the broad luminescence bands above 1100 cm^{-1} are due to the presence of glaze layers and their spectral profile change depends on the processing temperatures [81]. JUSTI 21 porcelain tooth showed better-resolved bands compared to the other dentures' porcelain teeth, which suggest a different manufacturing method, **Fig. 3.5**.

3.3.2.2 Vulcanized Rubber dentures

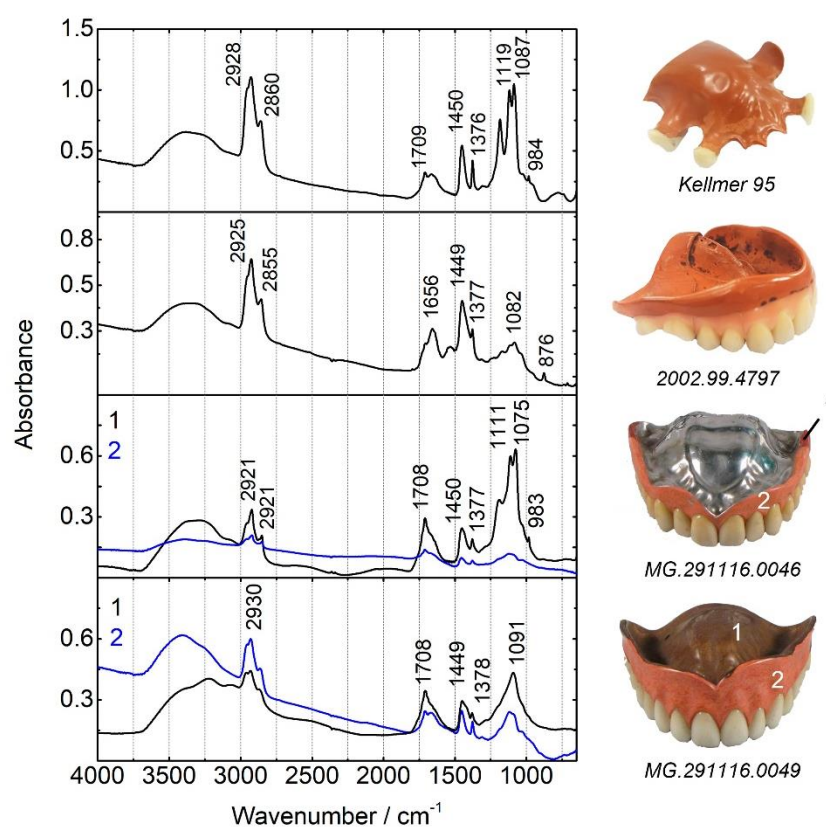






Figure 3.6. Infrared spectra acquired from the dentures identified as vulcanized rubber, by the detection of bands in the CH stretching ($3000\text{--}2800\text{ cm}^{-1}$) and bending regions ($1450\text{--}1375\text{ cm}^{-1}$). Denture 2002.99.4797 has porcelain gums. Dentures MG.291116.0046 and 0049 were micro sampled in different regions due to color differences, a dark and a light red, which showed spectral variations.

There were four dental plates, NMD's Kellmer 95 and 2002.99.4797 and NMAH's MG.291116.0046 and MG.291116.0049 where no peaks were observed in the Raman spectra. Kellmer 95 and 2002.99.4797 dental plates are very identical to each other having a dark brown color. MG.291116.0046 and MG.291116.0049 are also very identical in the appearance of the gums, an heterogeneous red mixture. All four were identified as vulcanized rubber, or hard rubber, by μFTIR , **Fig. 3.6 and Table 3.3**. The most characteristic bands of this compound are

the CH₂ and CH₃ stretching vibrations between 2930 and 2850 cm⁻¹ and bending vibrations at 1450–1375 cm⁻¹. However, several spectral differences were found in the four objects. Different fillers were identified: barium sulfate (BaSO₄) was identified in Kellmer 95 by its characteristic bands at 1185, 1119, 1087 and 984 cm⁻¹; this filler was also identified in the dark red of denture MG.291116.0046. Calcium carbonate was found in 2002.99.4797 by the bands at 876 and 712 cm⁻¹ (the broadening of 1449 cm⁻¹ is due to this compound which has a strong absorption at 1430 cm⁻¹). All vulcanized rubber dental plates exhibit a band at 1710–1705 cm⁻¹, which can be due to oxidation or due the presence of an additive. Broad bands between 1700 and 1500 cm⁻¹ suggests the presence of proteins.

Denture MG.291116.0046 metal plate is a nickel–chromium-based alloy by identification with XRF. The dark red area of this denture showed a complex X-ray fluorescence spectrum, with several bands attributed to zinc, selenium, strontium, cadmium, barium, and sulfur, **Table 3.3** and **Fig. A2.12**. Sulfur is from the vulcanized rubber structure. Barium correlated with the identification of barium sulfate by infrared spectroscopy. In the future, other complementary techniques may provide more information on the zinc, selenium, cadmium, and strontium compounds.

Table 3-3. Characterization of NMD and NMAH vulcanite dentures by handheld Raman, μFTIR and XRF.

Object	μFTIR	XRF
 Kellmer 95	Vulcanized Rubber: 1376, 1450 cm ⁻¹ Barium Sulfate (BaSO₄): 984, 1087, 1119, 1189 cm ⁻¹	Not analyzed
 2002.99.4797	Vulcanized Rubber: 1377, 1449 cm ⁻¹ Calcium carbonate (CaCO₃): 712, 876 cm ⁻¹	Not analyzed
 MG.291116.0046	Vulcanized Rubber (both light and dark red): 1377 and 1450 cm ⁻¹ Barium Sulfate (BaSO₄) (dark red): 983, 1075, 1111, 1189 cm ⁻¹	Light Red (XRF1): Zn and Hg Dark red (XRF2): Zn, Se, Sr, Cd, Ba, S Metal plate (XRF3): Cr, Fe and Ni
 MG.291116.0049	Vulcanized Rubber (both light and dark red): 1378 and 1449 cm ⁻¹	Light Red (XRF1): Zn and Hg <i>Not possible to acquire spectra from darker red top area</i>

3.3.2.3 Polyvinyl chloride - Polyvinyl acetate copolymer (PVC-PVAc) dentures

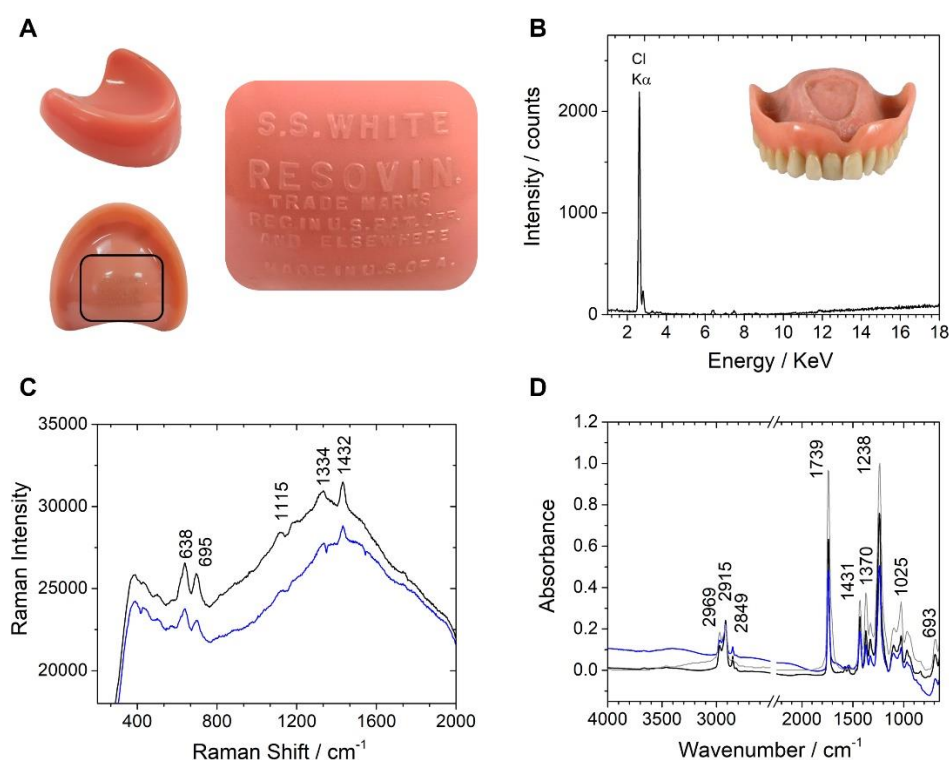




Figure 3.7. A) Dental blank 2002.99.5831 and detail of the inscription where it is possible to read “S.S. White Resovin. Trademarks. Rec. in U.S. Pat. Off. and elsewhere. Made in U.S. of A.”; B) XRF spectrum of MG.291116.0061, showing the strong emission of chloride. C) Raman of dental blank 2002.99.5831 (black, 4 s, 10 scans) and denture MG.291116.0061 (blue, 3 s, 10 scans). D) Infrared spectra of dental blank 2002.99.5831 (black) and denture MG.291116.0061 (blue), compared to a reference spectrum of 83% PVC:17%PVAc copolymer (grey).

NMD’s dental blank 2002.99.5831 was manufactured using Resovin, sold by S.S. White, **Fig. 3.7A**. With handheld Raman it was possible to identify the main peaks of PVC at 638, 695, 1115, 1334 and 1432 cm^{-1} . A similar spectrum was obtained for MG.291116.0061, a denture previously identified as celluloid, **Fig. 3.7C and Table 3.4**. μ FTIR provided more information; both were identified as PVC-PVAc copolymer. PVC main bands are observed at 1431 cm^{-1} attributed to the angular deformation of $\text{CH}_2\text{-Cl}$, at 1238 cm^{-1} to the CH-Cl out of plane angular deformation, between 1100 and 1025 to the C–C stretching, at 967 cm^{-1} to the C-H out of plane deformation; and at 831 and 692 cm^{-1} to the C–Cl stretching. PVAc is identified by its main bands at 1739 cm^{-1} of the carbonyl stretching and 1370 cm^{-1} of the CH_3 bending vibration [82]. The PVC-PVAc copolymer identified in both dentures has a higher PVC content compared to PVAc, by comparison with the $A_{1370\text{cm}^{-1}}/A_{1238\text{cm}^{-1}}$ band ratio of an IR reference spectrum of 83% PVC:17% PVAc copolymer, **Fig. 3.7D and Table 3.4**. The low content of PVAc is probably why handheld Raman was not able to identify bands from this polymer.

Both dentures 2002.99.5831 and MG.291116.0061 showed two additional infrared bands at 1575 and 1542 cm^{-1} , **Fig. 3.7D** and **Table 3.4**. These two bands, correlated with the sharp CH_2 asymmetric and symmetric stretching bands at 2915 cm^{-1} and 2850 cm^{-1} , indicate the presence of calcium stearate, a lubricant and stabilizer for PVC, **Fig. A2.13** [83].

Denture MG.291116.0061 was analyzed by XRF and chlorine (Cl) was found, correlating with the identification of PVC, **Fig. A3.7B**. According to Rueggeberg (2001) "By 1932, mixtures of PVC and vinyl acetate were available for use as denture base materials". This result shows that Resovin was one of these mixtures [16].

Table 3-4. Characterization of PVC-PVAc dentures from NMD and NMAH by handheld Raman, μFTIR and XRF.

Object	Handheld Raman	μFTIR	XRF
 2002.99.5831	PVC: 638, 695, 1115, 1334, 1432 cm^{-1}	PVC-PVAc copolymer: 692, 831, 967, 1025, 1100, 1238, 1371, 1431, 1739, 2969 cm^{-1} $A_{1370\text{cm}^{-1}}/A_{1238\text{cm}^{-1}} = 0.27^*$	Not analyzed
 MG.291116.0061	PVC: 637, 695, 1432 cm^{-1}	PVC-PVAc copolymer: 968, 1025, 1101, 1237, 1371, 1431, 1537, 1739, 2968 cm^{-1} $A_{1370\text{cm}^{-1}}/A_{1238\text{cm}^{-1}} = 0.28$	Cl
		Calcium Stearate: 2915, 2849, 1575 and 1542 cm^{-1}	
		Calcium Stearate: 2916, 2850, 1574 and 1540 cm^{-1}	

* 83% PVC:17% PVAc copolymer reference has a $A_{1370\text{cm}^{-1}}/A_{1238\text{cm}^{-1}} = 0.36$

3.3.2.4 Phenol-formaldehyde dentures

In the case of dental plate 2002.99.5459, a difficult-to-read inscription was found, being distinguishable the first three letters "LUX" and the last letter "E", **Fig. 3.8B**. The identification of the material as a phenol-formaldehyde resin, by the observation of Raman main bands at 1296 (CH_2 twisting), 1453 (CH_2 bending), 1610 cm^{-1} (ring stretching) and other minor bands, and by comparison with a phenol-formaldehyde resin billiard ball (Aramith), allows us to deduce that it is a Luxene dental plate manufactured by the Bakelite Corporation, **Fig. 3.8A and C**. Dental plate 2002.99.5524 was also identified as a phenol-formaldehyde but no inscriptions were found, **Fig. 8C** and **Table 3.5**. Denture 2002.99.5459 was also analyzed by infrared spectroscopy, validating the material characterization as a phenol-formaldehyde plastic, namely by the observation of bands between 1600 and 1300 cm^{-1} from the benzene ring stretching, the

CH₂ asymmetric and symmetric stretching at 2921 and 2864 cm⁻¹, the C = C stretching between 3100 and 3000 cm⁻¹ and the OH stretching with maximum at 3359 cm⁻¹, **Table 3.5** and **Fig. A2.14**.

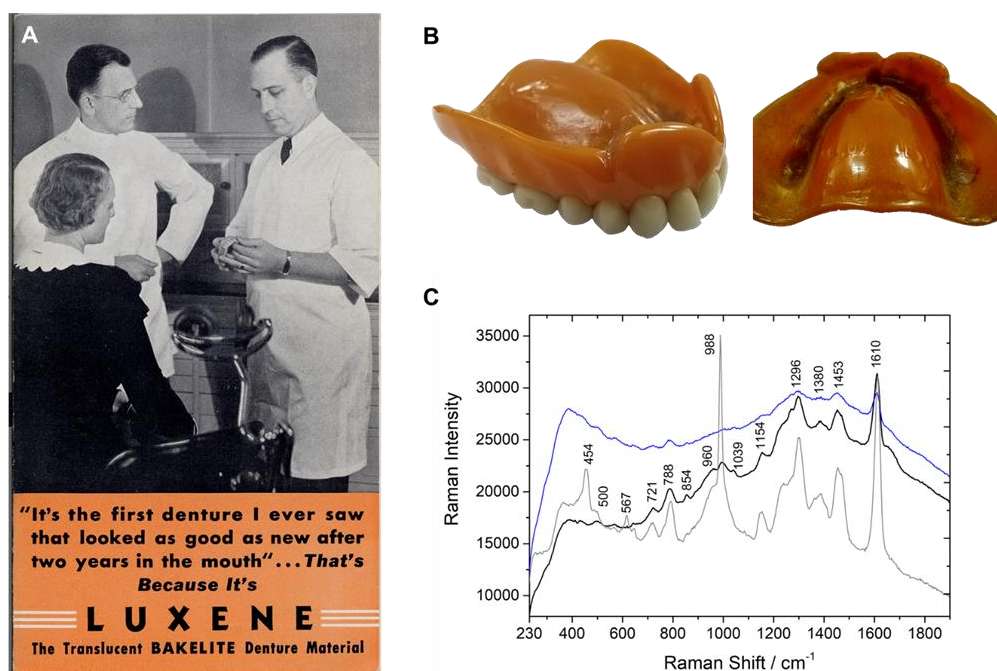




Figure 3.8. A) Advertisement of Luxene, Bakelite Corporation, circa 1940 (J. Harry DuBois Collection on the History of Plastics, NMAH.AC.0008). B) Photography and detail of the top of the denture 2002.99.5459 where the inscriptions “LUX” and “E” are read. C) Raman spectra (785nm, maximum power) of dentures 2002.99.5459 (black, 9s, 10scans), 2002.99.5524 (blue, 3s, 1 scan) and a phenol-formaldehyde Aramith billiard ball (grey, 8s, 1 scan).

Table 3-5. Characterization of NMD’s phenol-formaldehyde dentures by handheld Raman and μFTIR

Object	Handheld Raman	μFTIR
 2002.99.5459	Phenol-Formaldehyde: 500, 567, 721, 788, 854, 960, 991, 1039, 1154, 1296, 1380, 1453, 1610 cm ⁻¹	Phenol-Formaldehyde: 760, 885, 1071, 1154, 1216, 1271, 1380, 1455, 1484, 1602, 1657, 2864, 2921, 3359 cm ⁻¹
 2002.99.5524	Phenol-Formaldehyde: 500, 575, 721, 787, 1037, 1296, 1453, 1610 cm ⁻¹	Not analyzed

3.3.2.5 Polymethyl methacrylate (PMMA) denture

JUSTI 23, previously identified as cellulose acetate, was identified as PMMA by the observation of its main bands at 599 (C–C–O stretching), 813 (C–O–C stretching), 1451 (CH bending) and 1728 (carbonyl stretching) cm^{-1} and other minor bands, correlating with the Raman spectrum of a PMMA reference, **Fig. A2.9**. Raman was performed at both the transparent top and red gum area with the same results. With infrared spectroscopy, PMMA was also identified by the detection of characteristic bands from 2994 to 2844 the stretching vibration of the CH_3 and CH_2 ; at 1730 cm^{-1} the carbonyl stretching; between 1485 and 1385 cm^{-1} deformation of the CH_2 and CH_3 ; between 1300 and 950 cm^{-1} vibrations of the ester group; and at $841, 751 \text{ cm}^{-1}$ skeletal vibrations [75], **Table 3.6** and **Fig. A2.15**.

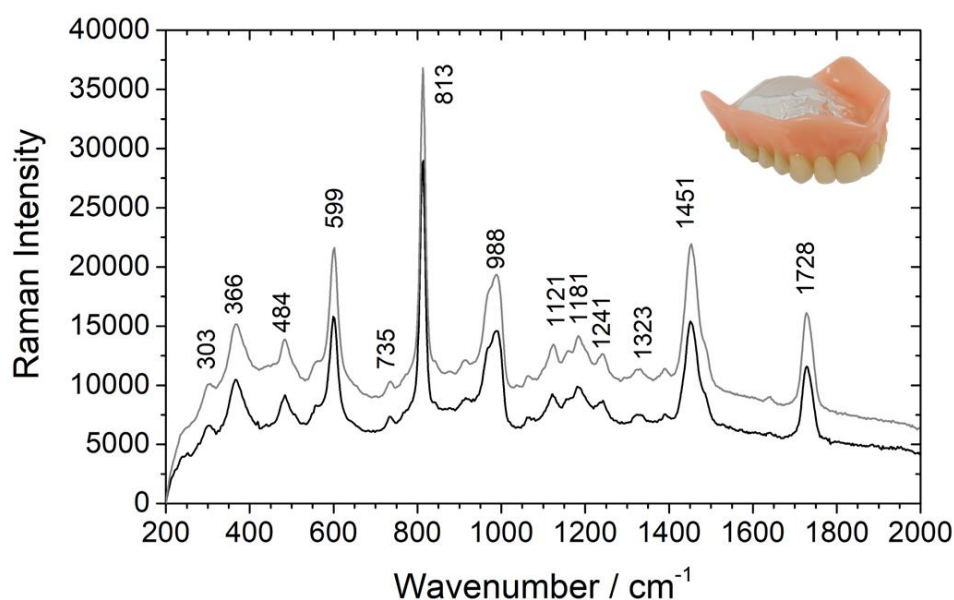



Figure 3.9. Raman spectra (785nm, maximum power) of JUSTI 23 (black, 10s, 10 scans) and of a PMMA reference (grey, 5s, 1 scan).

Table 3.6. Characterization of NMD’s PMMA denture by handheld Raman and μFTIR

Object	NMD original description	Handheld Raman	μFTIR
 JUSTI 23	Cellulose acetate maxillary dental plate made of safety celluloid as opposed to cellulose nitrate, which was flammable, circa 1920	PMMA: 303, 366, 484, 599, 735, 813, 988, 1221, 1181, 1242, 1324, 1390, 1451, 1728 cm^{-1}	PMMA: 751, 841, 966, 988, 1064, 1150, 1194, 1242, 1269, 1387, 1450, 1482, 1637, 1731, 2844, 2951, 2994, 3439, 3552, 3624 cm^{-1}

3.4 Conclusions

This work demonstrates the significance of celluloid in the denture market between the 1870s and the 1940s. The review of celluloid denture history shows that this material was an option aesthetically superior to vulcanite and easier to manufacture than porcelain. Patients who wanted a natural imitation of flesh and had the money for it could acquire a celluloid denture or a vulcanite/metal denture with celluloid gums. Celluloid impacted the development of denture manufacturing apparatus and induced the creation of new styles of porcelain teeth. Methods for making celluloid dentures were explained in several technical books, and prominent sellers sold the celluloid dental blanks in America and in Europe, namely S.S. White Manufacturing Company and Claudius Ash & Sons Company, respectively.

We demonstrate the importance of identifying the materials that exist in the collections of dentures. This approach broadened the understanding of celluloid denture history and the collections studied. The associations between material and appearance are now more evident. Five different materials were characterized in the collections of the National Museum of American History and the Dr. Samuel D. Harris National Museum of Dentistry: celluloid (12 dentures), vulcanized rubber (4 dentures), phenol–formaldehyde plastic (2 dentures), polyvinyl chloride—polyvinyl acetate copolymer (2 dentures) and polymethyl methacrylate (1 denture). All these materials represent different historical and physical experiences and conservation approaches. Special attention goes to the high number of celluloid dentures observed, which validated the importance of this material in denture development and commercialization. The high percentage of celluloid dentures identified in this collection, in contrast to the 1938 survey where cellulose derivatives constituted only 8%, suggests a larger use of celluloid dentures before the 1930s. However, it is necessary to consider that the dentures analyzed in this study were specifically selected based on their probability of being made with celluloid.

Collections worldwide holding historical dentures must pay attention to the presence of celluloid due to the risk of degradation and acid attacks. Signs of cellulose nitrate degradation include discoloration, brittleness, cracking, or weeping [72, 84, 85]. Yet, the celluloid dentures studied in this work are primarily in good conservation condition. They all showed similar compositions of cellulose nitrate, camphor, and vermilion. Those analyzed with XRF showed the presence of zinc, likely zinc oxide, which has a stabilizing effect on celluloid [5, 6]. The only formulation change appears to be the addition of phthalate plasticizers in the 1920s, probably to replace camphor partially. Calculation of the degree of substitution of cellulose nitrate suggests that the phthalate plasticizer may accelerate celluloid degradation or be associated to lower quality materials. Denture manufacturing processes can also play an essential role.

References should be produced following the historical formulations and aged to assess the degradation mechanisms and propose conservation guidelines.

Given the descriptions of complaints due to the bad taste and smell of camphor in celluloid dentures, it was interesting to observe that all celluloid dentures had camphor in their composition. This is not unexpected, as camphor was always considered the best plasticizer for cellulose nitrate. Furthermore, camphor may potentially yield beneficial outcomes owing to its antiseptic and antifungal properties. However, the impacts on the user's well-being necessitate further investigation given concerns surrounding its toxicity [86]. In the future, it would be useful to see if coatings, like beeswax, play a role in blocking taste, even though beeswax's presence is likely a vestige of a mouth impression using this material. This coating may have positive conservation impacts: JUSTI 21 is in excellent conservation condition. The conservation condition of JUSTI 21 can also be associated with its manufacturing quality. This denture's gold base is indicative of its high cost. The presence of beeswax and of unique porcelain teeth can also be markers denoting a product of exceptional quality.

Due to the discussions in the late nineteenth century about vermilion problems, it is also interesting to observe the ubiquity of vermilion in celluloid dentures, especially regarding the dentures dated from 1920s onward (plasticized with phthalate compounds). Based on the XRF results, vulcanized rubber dentures showed a higher concentration of vermilion than celluloid, in accordance with the technical literature of the late 19th-early twentieth century. Efforts were being made to replace vermilion in celluloid, but no substitutes were found. Other colorants appear to be used in the synthetic plastics, not by their identification but by the absence of vermilion bands in the Raman spectra. Chloride can act as a catalyst of vermilion degradation, a possible reason for its disuse in PVC-PVAc dentures.

Handheld Raman was demonstrated to be an excellent in-situ technique in identifying all the dentures' base materials, except for the vulcanized rubber (also known as vulcanite or hard rubber). In this case, identification was only achieved using μ FTIR. Handheld Raman was able to identify the phthalate plasticizers in celluloid dentures JUSTI 24 and MG.M-09686, dating them between the 1920s and the 1940s, from the start of phthalate plasticizer industrial use until the appearance of PMMA (which superseded all the previous materials). These phthalates were not detected by μ FTIR, showing how powerful handheld Raman spectroscopy is in detecting these additives.

Finally, we note that a systematic investigation of the vulcanized rubbers, phenol-formaldehyde, and polyvinyl chloride—polyvinyl acetate copolymer plastics should be performed. Only with a detailed study of the manufacturing processes and analysis of references will it be possible to extract more information from the spectroscopic data. In this work, it was possible to correlate tradenames with the material characterization: Resovin from S.S. White

with a PVC-PVAc copolymer; and Luxene from the Bakelite Corporation with a phenol-formaldehyde resin.

3.5 References

- [1] Friedel R. *Pioneer plastic: the making and selling of celluloid*. Madison: The University of Wisconsin Press; 1983.
- [2] Meikle JL. *American plastic: a cultural history*. New Brunswick: Rutgers University Press; 1997.
- [3] Thérias S, Bussière PO, Gardette M, Gardette JL, Lattuati-derieux A, Lavédrine B, et al. Degradation of celluloid in art works: a study of the mechanisms. *Actes du colloque Sciences des matériaux du patrimoine culturel*. 2012; 2:68–73.
- [4] Bussiere PO, Gardette JL, Therias S. Photodegradation of celluloid used in museum artifacts. *Polym Degrad Stab*. 2014; 107:246–54.
- [5] Quye A, Littlejohn D, Pethrick RA, Stewart RA. Investigation of inherent degradation in cellulose nitrate museum artefacts. *Polym Degrad Stab*. 2011; 96:1369–76.
- [6] Quye A, Littlejohn D, Pethrick RA, Stewart RA. Accelerated ageing to study the degradation of cellulose nitrate museum artefacts. *Polym Degrad Stab*. 2011; 96:1934–9.
- [7] Elsässer C, Micheluz A, Pamplona M, Kavda S, Montag P. Selection of thermal, spectroscopic, spectrometric, and chromatographic methods for characterizing historical celluloid. *J Appl Polym Sci*. 2021.
- [8] Kavda S, Micheluz A, Elsässer C, Pamplona M. Development of a gel permeation chromatography method for analysing cellulose nitrate in museums. *J Sep Sci*. 2021.
- [9] Valente M, Lozano C, Elsässer C, Angelin EM, Pamplona M. Shedding light on degradation gradients in celluloid: an ATR-FTIR study of artificially and naturally aged specimens. *Polymers*. 2023; 15:522.
- [10] Neves A, Angelin EM, Roldão É, Melo MJ. New insights into the degradation mechanism of cellulose nitrate in cinematographic films by Raman microscopy. *J Raman Spectrosc*. 2019; 50:202–12.
- [11] Neves A, Ramos AM, Callapez ME, Friedel R, Réfrégiers M, Thoury M, et al. Novel markers to early detect degradation on cellulose nitrate-based heritage at the submicrometer level using synchrotron UV–VIS multispectral luminescence. *Sci Rep*. 2021; 11:20208.
- [12] Curran K, Underhill M, Grau-Bové J, Fearn T, Gibson LT, Strlič M. Classifying degraded modern polymeric museum artefacts by their smell. *Angewandte Chemie Int Ed*. 2018; 57:7336–40.

- [13] Quye A. Quality matters for historical plastics: the past making of cellulose nitrates for future preservation. *Cahiers François Viète*. 2017; 2:45–65.
- [14] Murray MD, Darvell BW. The evolution of the complete denture base. Theories of complete denture retention a review. Part 1. *Aust Dent J*. 1993; 38:216–9.
- [15]. Engelmeier RL. The history and development of posterior denture teeth—introduction, part II: artificial tooth development in America through the Nineteenth Century. *J Prosthodont*. 2003; 12:288–301.
- [16] Rueggeberg FA. From vulcanite to vinyl, a history of resins in restorative dentistry. *J Prosthet Dent*. 2002; 87:364–79.
- [17] Ladha K, Verma M. Nineteenth century denture base materials revisited. *J Hist Dent*. 2011; 59:1–11.
- [18] Smith G. Denture Bases. *Australian Dental Mirror*. 1939; 5:14–32.
- [19] Kimball H. Modern denture base materials, and what to expect of them. *J Am Dent Assoc Dent Cosmos*. 1938; 25:243–52.
- [20] Underdahl L. The technique for hecolite. Portland: American Hecolite Denture Corporation; 1930.
- [21] Harris CA. The principles and practice of dentistry, including anatomy, physiology, pathology, therapeutics, dental surgery and mechanism. 13th ed. Philadelphia: P. Blakiston's Son and Co; 1913.
- [22] Yarsley VE, Flavell W, Adamson PS, Perkins NG. Cellulosic plastics. London: The Plastics Institute; 1964.
- [23] Mossman STI. Parkesine and celluloid. In: Mossman STI, Morris PJT, editors. The development of plastics. London: The Royal Society of Chemistry; 1994. p. 10–25.
- [24] Worden EC. Nitrocellulose industry. Volume II. London: Constable and Company Ltd, 1911.
- [25] A Catalog of the World's Premium S.S. White Porcelain Teeth. Philadelphia: The S.S. White Dental Manufacturing Company; 1911.
- [26] McClelland JA. Improved Material for Forming Dental Plates. USA: USP 77304, 1869.
- [27] Wright CM. Coming Base. *Transactions of the American Dental Association*. 1869;67–70.
- [28] Zhanning J. The glass transition temperature measurement of nitrocellulose by torsional braid analysis. *Propellants Explos Pyrotech*. 1992; 17:34–7.
- [29] Hamrang A. Using accelerated ageing process to predict the archival life of cellulose nitrate-based materials and historical objects. In: Haghi AK, editor. *Chemistry and chemical engineering research progress*. New York: Nova Science Publishers, Inc; 2010. p. 10–7.
- [30] Smith CS. Celluloid as a base for artificial teeth. Newark, New Jersey: Celluloid Manufacturing Company; 1878.

- [31] Hyatt JW, Hyatt IS. Improved Apparatus for Moulding Dental Plates. USA; USP 121522, 1871.
- [32] Hyatt IS, Hyatt JW. Apparatus and Processes for Molding Celluloids and the Coumpounds of Pyroxyline. USA; USP 152232, 1874.
- [33] Hunt RF. Process and Apparatus for Softening and Molding Celluloid. USA; 162752, 1875.
- [34] Evans WW. Celluloid and Zylonite. In: Essig CJ, editor. The American textbook of prosthetic dentistry. 2nd ed. Lea Brothers and Co: Philadelphia and New York; 1901.
- [35] Heindsmann F. Improvement in Dental Vulcanizing Apparatus. USA; USP 165328, 1875.
- [36] White SS. Catalogue of dental materials, furniture, instruments, etc., for sale by Samuel S. White. Philadelphia: The S.S. White Dental Manufacturing Company; 1876.
- [37] Gilbert SE. Vulcanite and celluloid: instructions in their practical working for dental purposes. Philadelphia: The S.S. White Dental Manufacturing Company; 1884.
- [38] Evans WW. Apparatus for forming dental plates. USA; USP 279365, 1883.
- [39] Seabury FW. Dental Vulcanizer. USA; USP 443699, 1890.
- [40] Vulcanizers, Celluloid Press, and Accessories. Philadelphia: S.S. White Dental Manufacturing Co.; 1894.
- [41] Radepont M. Understanding of chemical reactions involved in pigment discoloration, in particular in mercury sulfde (HgS) blackening. Antwerpen: Université Pierre et Marie Curie - Paris VI; Universiteit Antwerpen; 2013.
- [42] Gettens R, Feller R, Chase WT. Vermilion and Cinnabar. In: Roy A, editor. Artists' pigments: a handbook of their history and characteristic. Volume II. Washington, DC: National Gallery of Art; 1993. p. 159–82.
- [43] Goldwater L. Mercury in dentistry. *Clin Toxicol*. 1991; 29:151–64.
- [44] Niles ES. The compatibility of rubber and celluloid with the tissues of the mouth. *Dent Cosmos*. 1881; 23:458–61.
- [45] Johnstone A. Sore mouths from rubber and celluloid. *Items of interest*. 1883; 6:114–5.
- [46] Globensky S. Celluloid in mechanical dentistry. Is it to be recommended? *Dom Dent J*. 1889; 1:162.
- [47] Yen C-C, Liu S-H, Chen W-K, Lin R-H, Lin-Shiau S-Y. Tissue distribution of diferent mercurial compounds analyzed by the improved FI-CVAAS. *J Anal Toxicol*. 2002; 26:286–95.
- [48] Strahan D, Tsukada M. Measuring mercury emissions from cinnabar lacquer objects. *Stud Conserv*. 2016; 61:166–72.
- [49] Feller RL. Studies on the darkening of vermilion by light. *Rep Stud Hist Art*. 1967; 1:99–111.
- [50] Yu J, Warren WS, Fischer MC. Visualization of vermilion degradation using pump-probe microscopy. *Sci Adv*. 2019;5:eaaw313621.

- [51] Chiriu D, Pala M, Pisu FA, Cappellini G, Ricci PC, Carbonaro CM. Time through colors: a kinetic model of red vermilion darkening from Raman spectra. *Dyes Pigm.* 2020;2021(184):108866.
- [52] Miguel C, Pinto JV, Clarke M, Melo MJ. The alchemy of red mercury sulphide: the production of vermilion for medieval art. *Dyes Pigm.* 2014; 102:210–7.
- [53] Spring M, Grout R. The blackening of vermilion: an analytical study of the process in paintings. *Natl Gallery Tech Bull.* 2002; 23:50–61.
- [54]. Keune K, Boon JJ. Analytical imaging studies clarifying the process of the darkening of vermilion in paintings. *Anal Chem.* 2005; 77:4742–50.
- [55] Hogan C, Da PF. Colour degradation of artworks: an ab initio approach to X-ray, electronic and optical spectroscopy analyses of vermilion photodarkening. *J Anal At Spectrom.* 2015;30(3):588.
- [56] Sachs AP, Byron O. Camphor substitutes in the manufacture of celluloid. *Ind Eng Chem.* 1921;13(10):893–901.
- [57] Pereira A, Candeias A, Cardoso A, Rodrigues D, Vandenabeele P, Caldeira AT. Non-invasive methodology for the identification of plastic pieces in museum environment—a novel approach. *Microchem J.* 2016;1(124):846–55.
- [58] Mazurek J, Laganà A, Dion V, Etyemez S, Carta C, Schilling MR. Investigation of cellulose nitrate and cellulose acetate plastics in museum collections using ion chromatography and size exclusion chromatography. *J Cult Herit.* 2019; 35:263–70.
- [59] Salvant J, Sutherland K, Barten J, Stringari C, Casadio F, Walton M. Two László Moholy-Nagy paintings on Trolit: insights into the condition of early cellulose nitrate plastic. *e-Preserv Sci.* 2016; 13:15–22.
- [60] Paris C, Coupry C. Fourier transform Raman spectroscopic study of the first cellulose-based artificial materials in heritage. *J Raman Spectrosc.* 2005; 36:77–82.
- [61] Stewart RA. *Analytical Studies of the Degradation of Cellulose Nitrate Artefacts* [Doctor of Philosophy]. University of Strathclyde; 1997.
- [62] Nunes S, Ramacciotti F, Neves A, Angelin EM, Ramos AM, Roldão É, et al. A diagnostic tool for assessing the conservation condition of cellulose nitrate and acetate in heritage collections: quantifying the degree of substitution by infrared spectroscopy. *Herit Sci.* 2020;8:1–14.
- [63] Reilly JA. Celluloid objects: their chemistry and preservation. *J Am Inst Conserv.* 1991; 30:145.
- [64] Otero V, Sanches D, Montagner C, Vilarigues M, Carlyle L, Lopes JA, et al. Characterisation of metal carboxylates by Raman and infrared spectroscopy in works of art. *J Raman Spectrosc.* 2014; 45:1197–206.

- [65] Geravand A, Hashemi Nezhad SM. Simulation study of the Orbital Raster Scan (ORS) on the Raman spectroscopy. *Optik*. 2019;1(178):83–9.
- [66] Bowie BT, Chase DB, Lewis IR, Griffiths PR. Anomalies and artifacts in Raman Spectroscopy. In: Chalmers JM, Griffiths PR, editors. *Handbook of vibrational spectroscopy*. Chichester: John Wiley & Sons; 2002.
- [67] Madden O, Cobb KC, Spencer AM. Raman spectroscopic characterization of laminated glass and transparent sheet plastics to amplify a history of early aviation “glass.” *J Raman Spectrosc*. 2014; 45:1215–24.
- [68] Kilsinska-Kopacz A, Lydzba-Kopczynska B, Czarnecka M, Kozlecki T, del Melendez JH, Mendys A, et al. Raman spectroscopy as a powerful technique for the identification of polymers used in cast sculptures from museum collections. *J Raman Spectrosc*. 2019; 50:213–21.
- [69] Babo S, Ferreira JL, Ramos AM, Micheluz A, Pamplona M, Casimiro MH, et al. Characterization and long-term stability of historical PMMA: impact of additives and acrylic sheet industrial production processes. *Polymers*. 2020; 12:2198.
- [70] Monni J, Niemela P, Alvila L, Pakkanen TT. Online monitoring of synthesis and curing of phenol—formaldehyde resol resins by Raman spectroscopy. *Polymer*. 2008; 49:3865–74.
- [71] Hendra PJ, Jackson KDO. Applications of Raman spectroscopy to the analysis of natural rubber. *Spectrochim Acta*. 1997; 50:1987–97.
- [72] Shashoua Y. *Conservation of plastics: materials science, degradation and preservation*. Amsterdam: Elsevier Ltd; 2008.
- [73] Derrick MR, Stulik D, Landry JM. *Infrared spectroscopy in conservation science*. Los Angeles: The Getty Conservation Institute; 1999.
- [74] Bell J, Nel P, Stuart B. Non-invasive identification of polymers in cultural heritage collections: evaluation, optimisation and application of portable FTIR (ATR and external reflectance) spectroscopy to three—dimensional polymer—based objects. *Herit Sci*. 2019; 7:1–18.
- [75] de Sá SF, da Cruz SM, Callapez ME, Carvalho V. Plastics that made history—the contribution of conservation science for the history of the Portuguese Plastics Industry. *Conservar Património*. 2020; 35:85–100.
- [76] Connors SA. *Chemical and physical characterization of the degradation of vulcanized natural rubber in the museum environment*. Kingston: Queen’s University; 1998.
- [77] Linnig FJ, Stewart JE. Infrared study of some structural changes in natural rubber during vulcanization. *J Res Natl Bur Stand*. 1934;1958(60):9–21.
- [78] Mohtar AA, Nunes S, Silva J, Ramos AM, Lopes J, Pinto ML. First-principles model to evaluate quantitatively the long-life behavior of cellulose acetate polymers. *ACS Omega*. 2021; 6:8028–37.

- [79] Mohtar AA, Pinto ML, Neves A, Nunes S, Zappi D, Varani G, et al. Decision making based on hybrid modeling approach applied to cellulose acetate based historical films conservation fourier transform infrared spectroscopy. *Sci Rep.* 2021; 11:16074.
- [80] Carter EA, Wood ML, Waal D, Edwards HGM. Porcelain shards from Portuguese wrecks: Raman spectroscopic analysis of marine archaeological ceramics. *Herit Sci.* 2017; 5:1–8.
- [81] Kamura S, Tani T, Matsuo H, Onaka Y, Fujisawa T, Unno M. New probe for porcelain glazes by luminescence at near-infrared excitation. *ACS Omega.* 2021; 6:7829–33.
- [82] Abdelghany AM, Meikhail MS, Asker N. Synthesis and structural-biological correlation of PVC-PVAc polymer blends. *J Market Res.* 2019; 8:3908–16.
- [83] Gönen M, Ozturk S, Balköse D, Okur S, Ulkü S. Preparation and characterization of calcium stearate powders and films prepared by precipitation and Langmuir Blodgett techniques. *Ind Eng Chem Res.* 2010; 49:1732–6.
- [84] Quye A, Williamson C. *Plastics: collecting and conserving.* Edinburgh: NMS Publishing Limited; 1999.
- [85] POPART: A European Project on the preservation of plastic Artefacts in Museum Collections. <https://popart-highlights.mnhn.fr/>. Accessed 31 May 2023.
- [86] Santos CD, Cabot JC. Persistent effects after camphor ingestion: a case report and literature review. *J Emerg Med.* 2015;1(48):298–304.

This is an accepted manuscript of an article published by OpenEdition Journals in Ler História, available online:

Neves, A and Callapez, E.

For the history of celluloid: evolution of the comb industry in Portugal, 1880-1970

Published in Portuguese and translated here to English by the authors.

FOR THE HISTORY OF CELLULOID: EVOLUTION OF THE COMB INDUSTRY IN PORTUGAL, 1880-1970

Abstract

In this article, we address the evolution of the comb industry in Portugal from 1880 to 1970 with the aim of understanding the technological, economic, and social impact of celluloid in the national context. We explain, from historical and statistical sources and chemical analysis of Portuguese combs with historical significance, from the collections of Sociedade Martins Sarmento and Casa da Memória de Guimarães, that the introduction of celluloid by the comb industry of Guimarães, in 1895, revolutionized the industrial context of Guimarães, transforming it into a center to produce (semi)synthetic plastics from the 1950s onwards. Celluloid had impact on the imitation tortoiseshell market, sought by social classes with low economic power, and coexisted industrially and commercially with horn, the traditional material used in combmaking. The comb industry in Guimarães had a unique evolution in the national and international context of the history of plastics.

4.1 Introduction

“What is the place for the comb in the Museum of History? Do we at least know the history of its industry?”. António Lopes de Carvalho⁵ asked these questions in his famous work

⁵ Born in 1881, known by the initials A. L. de Carvalho, he was a writer, publicist, and journalist. He was one of the founders of the “Centro Republicano Vimaranesense” in 1906, President of the

“Mesteres de Guimarães” (Masters of Guimarães), published in 1943 [1]. After almost 80 years, little has been written about the history of comb-making in Portugal. To our knowledge, the most significant contribution was that of Teresa Costa (2006) on the comb industry in Guimarães, the city identified as the place of origin of the Portuguese comb [2]. This article seeks to contribute to a broader knowledge of this industry in a period of great technological and social transformations from 1880 to 1970. One of the primary agents of this transformation was what we call “plastics”.

Today, “plastics” are essential materials in the consumer market, representing around 5% of Portuguese sales in 2020 [3]. The term “plastics” is recognized as “a class of synthetic organic polymers that pass through the plastic state, i.e., a moldable state between liquid and solid” [4]. Currently, the market is dominated by several materials that fit this definition, such as polypropylene (PP), polyethylene (PE), polyvinyl chloride (PVC) and polyethylene terephthalate (PET). However, the use of these materials raises controversial questions about pollution and the destruction of ecosystems on a global scale. Therefore, alternatives and substitutes to synthetic plastics have been sought, for example, in the development of bioplastics [5]. However, as alerted by Altman (2021), “although bioplastics represent a growing segment within the industry, they are not a new idea and have a long history, often neglected and misunderstood” [6].

Celluloid, coined by Robert Friedel (1983) as the “pioneer plastic”, was a bioplastic⁶ composed of cellulose nitrate (semisynthetic polymer) and camphor. It was developed in 1870 by John Wesley Hyatt (1837-1920) in the United States of America (USA) to replace the ivory used in billiard balls. The imitative properties of this new material were remarkable, and it was later used as a substitute for many other precious biomaterials, such as tortoiseshell or mother-of-pearl [7].

The comb industry was one of the first industries to adapt this material in its production processes. Robert Friedel (1983) used two examples, Leominster (USA) and Oyonnax (France), two major comb production centers in the 19th century, to demonstrate how the adaptation of celluloid profoundly altered the economic and technological contexts of these two cities, even when the shape and function of the combs remained the same. Combs became just one of several products that were part of the emerging plastics industry at the beginning of the 20th century. Instead of the product, it was the material that came to dominate industrial life due to its unique characteristics [7].

municipality of Guimarães from May to December 1922, was part of the Board of the “Sociedade Martins Sarmiento” and was director of the “Jornal de Guimarães” [57]

⁶ Considering the IUPAC definition [58]

In Portugal, recent studies have shown that celluloid was introduced in Guimarães by the “Fábrica de pentes a vapor da Madroa” (Madroa Steam Comb Factory) in 1895, but the technological, economic, and social impacts of using this material in the context of the Portuguese comb industry has not been explored [8], [9]. Therefore, the main objective of this article is to understand this impact on the panorama of the comb industry in Guimarães, to understand its implications for the development of the plastics industry in Portugal and to make a comparison with the international context.

This work is divided into four sections. First, and given that information about the comb industry in Portugal is scarce, the evolution of the number of factories and workshops specialized on manufacturing combs was analyzed based on data found in the Static Yearbooks of Portugal from 1879 to 1916. Given the relationship between the comb and cutlery industries, a comparison of the yearbook data with the observations of Cordeiro and Costa (2014) was made [10]. Finally, to understand the 19th-century context of comb-making in Guimarães, the reports on the Guimarães Industrial Exhibition of 1884 proved to be valuable.

The second section discusses the evolution of the materials used in the comb industry, from horn, through celluloid, to plastic. Two comb collections, from “Casa da Memória de Guimarães” and “Sociedade Martins Sarmiento”, two important cultural institutions of Guimarães, were studied, **fig. A3.1 and A3.2**. Two significant factories made the combs of these collections, “Fábrica do Carregal” and “Fábrica de Plásticos Pátria”. The molecular characterization of the materials that compose these collections was performed *in situ* using a handheld Raman spectrometer MIRA DS.

In the third section, data, from the Comercial Statistics of Portugal, on the importation of plastic materials by Portugal, from 1923 to 1960, was analyzed and compared with the evolution of the comb industry considering both the national and international contexts. The last section analyzed data from the Portuguese National Institute of Statistics (INE) on the number of plastics factories and the quantity of cellulosic plastics produced in Portugal between 1955 and 1968. This provided a base for comparing the industrial panorama of Guimarães with other primary plastics industrial centers in Portugal: Lisboa, Leiria, Porto e Aveiro. This comparison was completed based on the literature: Callapez [4] on the history of plastics in Portugal; Miranda [8] on the plastics industry in Aveiro; Gomes [11] and Beira [12] on the mold industry for plastics in Marinha Grande and Oliveira de Azeméis.

4.2 Celluloid and the comb industry of Guimarães

Guimarães is located in the hydrographic basin of Vale do Ave, which encompasses several other municipalities, including Póvoa de Lanhoso, Póvoa de Varzim and Santo Tirso. The

water supply and driving energy provided by rivers Ave and Vizela, alongside the geographically promoted cattle-raising tradition, led to the establishment of the tannery, cutlery, and comb-making workshops since medieval times. Historical records indicate that in Guimarães the profession of comb-making already existed in the 14th century [2], [13].

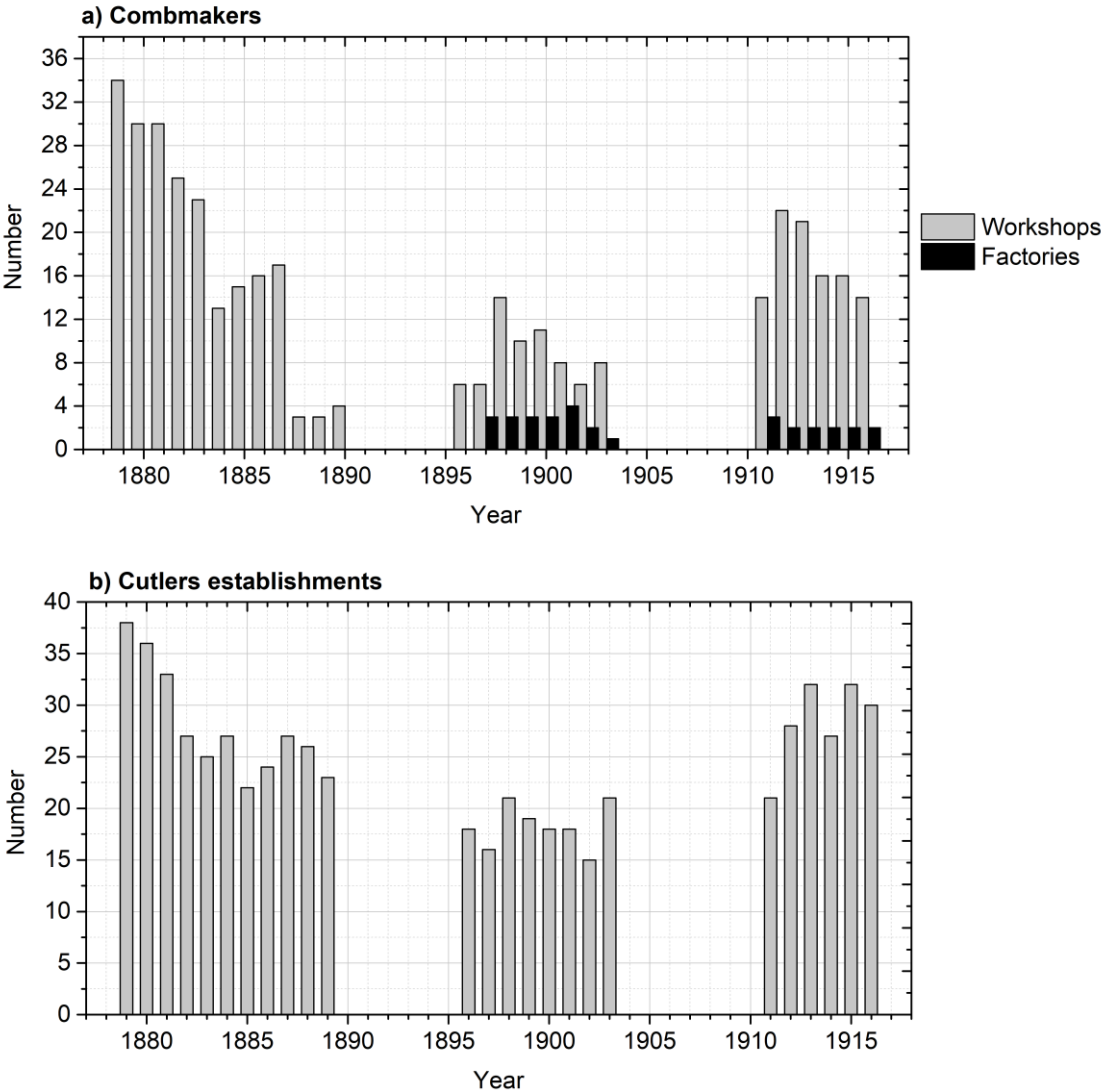


Figure 4.1. Number of comb workshops and factories in Portugal from 1879 to 1916. There is no information between 1891-1895 and 1904-1910 and after 1916. Source: Portuguese statistical yearbooks (INE).

After centuries of prosperity, these activities stagnated in the 19th century due to a lack of technological and organizational innovation [10]. According to the Portuguese commercial yearbooks, nationwide, in 1879, there were 34 workshops specialized in comb-making, **Fig. 4.1a**. In 1881, 15 were settled in Guimarães, a proportion that evidences this city as the significant comb-making center in Portugal [14]. In 1890, there were only three workshops,

demonstrating the state of economic suffocation in which these workshops operated. Of these three, only one was registered in the district of Braga, which encompasses Guimarães⁷, **Table 4.1**.

Table 4-1. Evolution of the number of comb workshops and factories in the districts of Lisbon, Viseu, Porto and Braga, between 1890 and 1916. Data for these districts was only registered for the years described. Source: Portuguese statistical yearbooks (INE).

Year	Workshops				Factories			
	Lisbon	Viseu	Porto	Braga	Lisbon	Viseu	Porto	Braga
1890	0	0	2	1	No factories nationwide			
1900	4	5	2	0	0	0	1	2
1903	2	1	3	2	0	0	0	1
1915	0	2	8	6	0	0	0	2
1916	0	1	6	7	0	0	0	2

If we compare the number of cutlery workshops over time, we observe a less accentuated decrease, **Fig. 4.1b**. According to Cordeiro and Costa [10], the cutlery workshops were small, poor, unhealthy, with archaic artisanal processes, and did not produce enough profits to allow the owner to invest in their modernization. The same seems true for comb workshops but on a larger scale.

For the comb-making sector, the pronounced decrease in the number of workshops is also associated with the external dependence of the Portuguese economy, resulting from protectionist policies that limited innovation and the diversity of national products [15]. The workshops could not compete with the quantity and quality of mechanically produced combs imported abroad. The workshops that survived probably sold at a regional or local level. About the decadent state of the Portuguese comb industry in this period, it is interesting to read the report written by the commissioner who visited the 1884 Guimarães Industrial Exhibition, in which the traditional horn combs were exhibited:

The cause of the decadence is the competition with similar foreign products, which, being obtained by improved processes, come to compete advantageously with ours; however, industrialists fight against this competition, lowering prices and increasing the number of working hours, which reach eighteen per day (Pombeiro, 1884, 1) [16]

⁷ The difference between workshop and factory is not explicit but the difference is associated with the number of workers and the use of steam machines [59]

Between 1892 and 1898, there was substantial capital investment in machinery importation at the national level [17]. This investment was felt in the district of Braga. In the comb industry, the creation of the first factories and growth in the number of workshops can be observed (figure 1a). In 1900, of the three new factories in Portugal, two were headquartered in the Braga district, **Table 4.1**.

The first contact of a comb-maker from Guimarães with celluloid may have occurred in 1876. In that year, the Guimarães industry was represented at the Centennial Exhibition in Philadelphia in 1876 with 10 exhibitors: one of them by Augusto Mendes da Cunha in the “fancy goods” sector, exhibiting bone combs [18]. One of the commemorative objects of this event was a comb made of celluloid (today belonging to the collection of the Henry Ford Museum, Michigan, USA).

However, celluloid was only introduced in Portugal in 1895, the year in which the Madroa Steam Comb Factory was installed in Guimarães under the firm *Dias, Silva e Lerdeira*, surnames of the founders Francisco Dias de Castro, José da Silva Guimarães and José Lerdeira Guimarães⁸. Since there was no knowledge in the Portuguese industrial context for such a project, it was necessary to resort to foreign expertise. A French technician named Edmond Chevrey was hired and machinery was ordered from Genffeny & Sons, located in one of the main comb production centers in France, Ezy-sur-Eure. In addition to the introduction of celluloid, the new factory was a pioneer in producing combs from cattle hoofs [19]. It is important to note that the importation of French technical knowledge was not uncommon. It was a need shared by other European countries, such as Germany or Italy [9] The celluloid for the combs was imported from France as square blocks or sheets.

The factory was successful and quickly exhibited its products at industrial exhibitions, participating in the Portuguese Industrial Exhibition held in 1897 at the Palácio de Cristal, in the city of Porto, and winning a silver medal. In 1899, the factory had 40 workers and produced 1800 combs a day, selling them in the markets of Lisbon and Porto. In 1900, this company was selected to participate in the Paris Universal Exhibition, representing the Guimarães industry at Portugal’s Pavilion [18]. No information about this factory in the 20th century was found. In 1903, only one comb factory was registered in the national yearbooks and sources indicate that it would be the factory “Costa, Lerdeira and Commandita”.

The request for the establishment of this factory was made to the administrator of the municipality of Guimarães, Manuel de Castro Sampaio, in 1897. A license was requested to produce horn combs using a steam machine and other accessories. The request was classified

⁸ The Portuguese statistical yearbooks only provide numbers for the first comb factories in 1897.

in a specific class due to the smoke and danger of explosion [20]⁹. In 1898, the factory was installed in Rua da Caldeira, Guimarães [21]. In 1909, it produced horn and celluloid combs, cutlery “in all kinds” and “many other articles from the Guimarães industry” [22]. This company participated in the Agricultural and Industrial Exhibition of Guimarães in 1923, exhibiting several celluloid combs and other celluloid, galalith and horn articles, such as shoehorns and “toilet cases”, **Fig. 4.2**. Other three firms, “Eduardo & Silva”, “Emprêsa Industrial de Guimarães” and “Machado & Pinto”, also displayed celluloid items [23].



Figure 4.2. “Costa, Cerdeira and Commandita” celluloid combs and articles factory at the Guimarães Industrial and Agricultural Exhibition in 1923. Source: Photo library of Sociedade Martins Sarmento.

Overall, from 1911 onwards, there was an increase in the number of comb makers in Portugal. In 1916, of the 14 workshops in operation, six were based in the district of Braga, as well as the only two Portuguese factories. In 1923, four companies from Guimarães exhibited combs and other celluloid articles. This evolution evidences the positive impact of celluloid on the comb industry in Portugal. It is in line with the assertion of Schmitt [24], writer of an essential technical book on the production of combs, which states that the use of celluloid induced the global growth of this industry.

⁹ The request was specific for the production of horn combs but is important to note that celluloid was a flammable material, for example, leading to fires in factories in comb factories in Brooklyn, USA, and Mümliswil, Switzerland.

In 1928, the Costa Lerderia e Commandita factory had five steam factories (plus one in Vizela) and ten artisanal workshops in Guimarães, which supplied the country [2]. The innovative character of this company, not very common in the Portuguese industrial context, was one of the reasons for its success and longevity. This is exemplified by the two patents found in the Industrial Bulletins of 1929 and 1930 related to a hot stamping process on celluloid combs and an improvement in a mechanical system to produce combs [25],[26]. It is still not known when this company closed its doors.

After 1916, the Portuguese statistical yearbooks or industrial statistics stopped showing data on the comb industry. However, in the 1940 and 1950 national censuses, it was possible to verify that the district of Braga continued to be the main comb production center: respectively 88% and 62% of the total number of combs makers nationwide [27], [28].

4.3 Horn, celluloid and plastic

Until the 19th century, comb manufacturers preferred the following raw materials: boxwood, bone, ivory, mother-of-pearl, and tortoiseshell [29]. These materials, of vegetable and animal origin, were chosen because they are rigid, easy to work in cutting and polishing operations, and dimensionally stable under humidity and temperature fluctuations [24]. In Portugal, some of these materials were significant in 16th to 18th-century comb making, mostly related to the manufacture of combs in Lisbon: ivory had a strong presence in the goods produced by the “Real Fábrica de Pentas de Marfim, Caixas de Papelão e Vernizes” (Royal Factory of Ivory Combs, paper boxes and varnishes), founded in 1764 in Lisbon by the French industrialist Gabriel de la Croix, as part of a reformist initiative by the Marquis of Pombal; personal hygiene combs made of bone, ivory and tortoiseshell were found in archaeological works at the Convent of Santana, Lisbon, dated between the 16th and 18th centuries¹⁰ [30]; In 1833, tortoiseshell and horn combs were manufactured in Lisbon, as described in a proclamation of the Senate of the Lisbon Chamber of that year about a request from the “Juizes do Ofício de Penteeiro” for regulatory measures on the market of combs in these two materials¹¹.

In the 19th century, horn became the most used material to manufacture combs. The technological advances developed in Leominster, USA, were fundamental in achieving an efficient transformation of this material. Of note was the invention of a press, between 1798 and 1812,

¹⁰ The discovery of ivory and tortoise shell combs for personal hygiene indicates the presence of a class of high social status and financial power.

¹¹ “Juizes do Ofício de Penteeiro”, which can be translated as the “Judges of the Combmaker Craft”, was a guild of the “Casa dos Vinte e Quatro” (House of the Twenty-Four), an administrative body of the municipality of Lisbon (Arquivo Municipal de Lisboa, AML-AH, Chancelaria da Cidade, Coleção de editais da Câmara Municipal de Lisboa, 1823-1833, doc. 216 (15 de junho 1833))

which allowed the horn to be smoothed and cut into squares, a necessary format for the remaining production stages. In addition, cutting, intercutting or polishing machines were invented for both horn and tortoiseshell, which sped up the production processes. Methods for coloring the horn and obtaining several different effects were also developed, the most important being the imitation of tortoiseshell [29].

In Guimarães, a city located in one of the leading cattle production centers in Portugal, the sources evidence horn as the primary raw material [2]. The report “Industrial Exhibition of Guimarães” in 1884 informs us about the use of this material and its target market:

Even today, there is an important trade in the most ordinary combs, which are widely consumed by the popular classes due to their low price and duration. The raw material is cattle horn. Before, consumption was so prominent that it was necessary to import horn, from Lisbon and other lands (Comissão Central, 1884, 246) [31].

In the work of A.L. de Carvalho, the “Mesteres de Guimarães”, it is possible to read a transcription of a horn comb-making process used in this city during the 19th century [1]. Despite mentioning a wooden press to flatten the horn, all other operations were handmade. On this issue, it is worth reading another paragraph from the report written in “Comércio de Guimarães” on the combs on display at the Guimarães Industrial Exhibition in 1884:

It is a pity that the comb-makers are not taught the processes used abroad.; because, despite all the difficulties they are struggling with, the products have improved a lot in terms of quality; and in the exhibition there were samples of combs and other objects made of horn, imitating tortoiseshell, which were not inferior to those coming from abroad (Pombeiro, 1884,1) [16]

One of the comb-makers present at this exhibition mentioned to the commission in charge of the report that he did not have any machinery, other than a hand saw, to produce horn combs imitating tortoiseshell, an arduous task and that in the making of small combs, it tired the eyes [31]. Therefore, it is relevant to highlight the quality of the horn combs imitating tortoiseshell. This demonstrates the knowledge of Portuguese comb-makers in the processes of clarifying and dyeing the horn. These processes were simple, but the quality of the imitation depended on the craftsman's skill¹².

Horn and using methods to imitate tortoiseshell were crucial factors for introducing celluloid in this Guimarães industry. Horn and tortoiseshell are materials composed of keratin and have thermoplastic properties, i.e., they can be molded when subjected to heat and

¹² For example, to give the horn a tortoise-like appearance, it could be applied a mixture of orpiment and lime with a brush [24].

pressure. Williamson [32] explained that advances in compression molding of horn motivated the market for low-cost molded articles. This market would later be dominated by (semi) synthetic thermoplastic materials, the first of which was celluloid. Freinkel [33] referred to horn as a “natural plastic”. The processes used by Portuguese comb-makers in the 19th century did not include compression molding. Still, experience with horn prepared them to work with and understand the thermoplastic properties of celluloid.

Westmont [34] used the example of celluloid tortoiseshell imitation combs to show how this material allowed the rural population, with low purchasing power, of Eckley, Pennsylvania, USA, to fulfill their material desires [34]. Celluloid, used to imitate precious natural materials, conveyed a level of social status and sophistication that surpassed the role of the comb as a purely functional object. In Guimarães, the market for this type of “fake” material already existed with horn in 1884, 11 years before the introduction of celluloid in the Portuguese industry.

Friedel [7] showed, for three companies headquartered in New York, USA, between 1877 and 1912, that the price of horn combs was always lower than that of celluloid. Considering the high horn availability in Guimarães, this price ratio was likely the same, even though a horn comb imitating a tortoiseshell was more costly than a regular one [24]. However, celluloid was technically and commercially advantageous, as it allowed for faster and more efficient manufacturing processes, consistent results, and several colors and patterns.

Horn preparation was a job requiring physical exertion and skill. Joseph Collyer (1748-1827) wrote that the craft of the horn, though stinking, required more skill than strength¹³. One of the first steps was the selection of the horn based on its shape and weight. Afterwards, the worker, in charge of the smoothing step, had to cut the horn into blocks with great care, following the natural curvature of the horn. Finally, these blocks were heated and pressed between two hot iron plates. The final thickness was regulated according to the applied force. Celluloid eliminated this process. The licensed factories received the material in uniform sheets with predefined dimensions and thicknesses, which were easily cut.

The artisanal results obtained with the horn were variable with a limited range of effects. In addition to the tortoiseshell effect, Schmitt [24] explains methods to change horn color to black, white or red. Celluloid allowed for a better-quality imitation of tortoiseshell. The celluloid imitations were exceptional, even fooling the most experienced eye. Furthermore, celluloid was soluble in many organic solvents, which allowed coloration with a wide variety of pigments and dyes. The effects commercialized were numerous, the most important being ivory, tortoiseshell and mother-of-pearl, and even horn, with variations within each group.

¹³ Apud [61]

The variability and limitations inherent to a natural material were overcome by the uniformity, availability, and solutions offered by celluloid [7].

In Leominster, USA, and Oyonnax, France, factories were established to supply raw celluloid to the comb factories. Two examples are the Viscoloid Company in Leominster (1901) and Société Oyonnaxienne (1902) in Oyonnax. Their construction required substantial capital investment. These factories carried out all stages of celluloid production, from the synthesis of cellulose nitrate to the cutting and distribution of sheets for comb-making. In these two production centers, celluloid replaced appear to have replaced horn [7].

In Guimarães, the tradition of horn transformation coexisted with celluloid, as observed by the chemical analysis of comb collections from Casa da Memória de Guimarães and Sociedade Martins Sarmiento. This is due to 1) lack of technical knowledge and of capital to build factories for the production and distribution of raw celluloid, and 2) to the livestock of the region of Guimarães.

There are no records of raw celluloid production in Portugal. António Rio de Janeiro, technical manager of the factory “Sociedade Portuguesa do Celulóide” (Portuguese Celluloid Society), was the first Portuguese to patent a process on a novel method to produce raw celluloid in Portugal [8], [9]. This factory exhibited toys made of celluloid paste at the Guimarães Agricultural Industrial Exhibition in 1923 [23]. The use of celluloid paste was not common which suggests that Rio de Janeiro’s factory can have produced its own raw material on a small-scale following his patent. However, for comb-making purposes, the established practice was to use celluloid sheets.

In 1943 and 1956, the district of Braga had the largest cattle herd in the country: 13.1% and 13.6% of the total heads of cattle nationwide [35], [36]. Only the frontier districts of Porto and Viana do Castelo competed with these numbers. If we add these three districts, we account for the same years, 36.9% and 35.9% of the total heads of cattle nationwide, respectively. These numbers support that the supply of horn continued to exist in the region of Guimarães throughout the 20th century and this promoted the preservation of horn comb-making. To understand the difference with the American case, Friedel [7] suggests that the increasing use of refrigeration processes, allowing the transport of meat from the center to the east coast of the USA, led to a decrease of the livestock in the region close to Leominster and boosted the transition to celluloid.

In the 1930s, there were disputes between comb-makers from Guimarães for the acquisition of horn, such was the demand for this material. In 1935, comb-makers organized a society, called “União de Fabricante de Pentas” (Union of the comb-makers), to regulate the horn market. However, this regulatory attempt failed shortly after [2], [37]. In the collection of “Fábrica de Plásticos Pátria”, a celluloid barber's comb in imitation horn suggests that comb-

makers could have resorted to this solution in case of difficulty in obtaining real horn. The demand for celluloid due to the unavailability of horn is something completely different from that observed in Leominster, USA, or Oyonnax, France, where celluloid was introduced to replace horn due to the technical and commercial advantages it offered [7].

The dynamics of knowledge transmission also played an important role in the preservation of horn transformation in Guimarães. Knowledge was transmitted from generation to generation, by observation. It is necessary to consider that the illiteracy rate in the district of Braga was 72% in 1900 and 47% in 1950 [28], [38]. The mechanical properties of celluloid allowed it to be adapted without radically changing the traditional manufacturing processes. This is exemplified by the case of João Teixeira's factory, "Fábrica do Carregal".

Born in the 1920s, João Teixeira learned the craft of the comb-maker from his father, watching him work in his small workshop. In this workshop, the combs were produced using traditional processes, by artisanal cutting and polishing processes. In the 1950s, João Teixeira decided to establish his own comb factory in Guimarães. At its peak, the factory employed 80 people and produced an average of 1000 combs a day. In 2006, he manufactured combs with his son. According to T. Costa [2], the manufacturing process continued to be "very similar to the primitive" and horn was the preferred material. João Teixeira had machinery powered by diesel and electricity, typical of a technological system of a comb factory from the first half of the 20th century. From the Raman spectroscopy analyzes carried out on the combs from João Teixeira's factory, belonging to Casa da Memória, it was possible to identify horn and celluloid. It was not possible to specify the date of these objects, but this material characterization reflects the significance of these two materials in the Guimarães comb industry. For its low cost and durability, horn was used for the personal hygiene combs. Celluloid, due to its imitative qualities, was used for decorative combs, as shown by the tortoiseshell imitation combs in **Fig. 4.3** and **Fig. A3.3 and A3.4**.



Figure 4.3. Combs from the João Teixeira's factory, from Casa da Memória collection. Left, horn combs. Right, celluloid combs in imitation of tortoiseshell.

In the 1940s, there were 13 comb factories in Guimarães, which used horn and celluloid [2]. Fábrica de Plásticos Pátria, with one foot in the past, with the production of horn and celluloid combs, and other in the future by producing of cellulose acetate and polystyrene objects, is a prime example of the role of celluloid in the transition from natural to synthetic materials. Founded in the 1950s, it was one of the largest exporters of plastics nationwide, having closed its doors in 2009. The former factory facilities were transformed into what is now "Casa da Memória de Guimarães". Casa da Memória and Sociedade Martins Sarmiento have collections with various objects produced by this factory, from different types of combs, toys, and religious articles. These collections are representative of the transition from a comb industry with traditional processes, as observed at Fábrica do Carregal, to the modern plastics industry, using injection molding and mass production. Two dandruff combs, with the same shape and function, are an excellent example of how different materials tell us the story of this industrial evolution, **Fig. 4.4**.

The celluloid comb was probably produced from a sheet of transparent orange celluloid, following the processes established in the late 19th- early 20th centuries, **Fig A3.5**. The cellulose acetate comb was produced by injection molding, recognized by the sprue imperfection on the side of the comb (the circles at the top are also indicative of this process), **Fig A3.6**. Cellulose acetate is used as the tortoiseshell imitation. Here, celluloid gains a new aesthetic dimension, used with an intense and artificial tonality, characteristic of the new post-World War II synthetic world. This factory also produced imitation tortoiseshell and imitation horn combs (the

largest number of celluloid combs in this collection are imitation tortoiseshell), **Fig. A3.7**. It was this versatility of celluloid, to imitate and create artificial effects, at low cost, that revolutionized the comb industry. The modernization with the adoption of injection molding, of the production of cellulose acetate, but mainly of polystyrene goods, was a natural step in an industry that had already surpassed the limits of nature, **Fig. A3.8**.

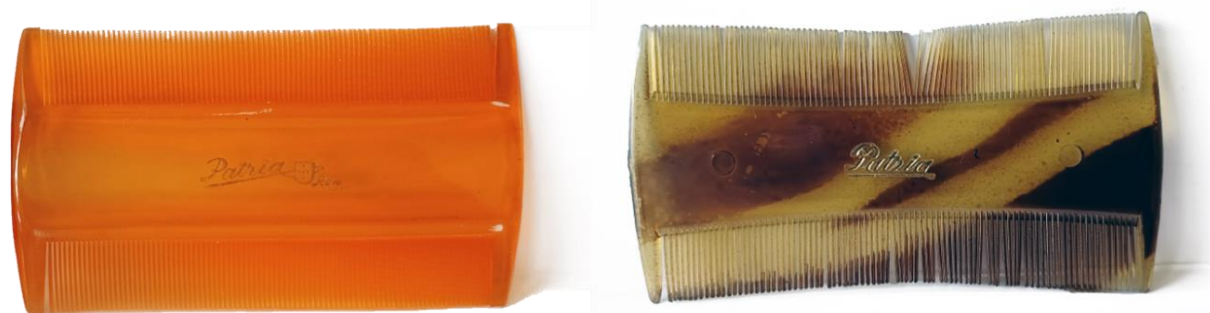


Figure 4.4. Dandruff combs made from celluloid (left) and cellulose acetate (right). They were produced by Fábrica de Plásticos Pátria and are from the collection of Sociedade Martins Sarmento. This factory advertised its combs as “The best Portuguese comb”.

4.4 Importation of plastic materials from 1923 to 1960

The importation of semi-synthetics, such as celluloid and Galalite, and synthetic plastic materials, such as Bakelite, polymethyl methacrylate (PMMA), show the development of the plastics industry in Portugal and its relationship with the Guimarães comb-making tradition, **Fig. 4.5**. Imports of celluloid (raw and as finished product) start to be registered in 1923.

Together with the 1923 “Guimarães Agricultural Industrial Exhibition”, which had 5 companies exhibiting celluloid articles, and the publication, in that same year, of the first Portuguese patent to produce celluloid, these factors demonstrate the growth of this material’s industrial and commercial importance in Portugal. With lack of data prior to 1923, it is difficult to understand the impact of the First World War, but the growth trend is related to the positive economic cycle observed in the country in the 1920s and to the evolution of the industry of celluloid in the international [15].

Emil Ott [39] showed, based on data from the North American census, that the price of cellulose nitrate decreased by 40% from 1917 to 1918. This decrease is related to the increased production of guncotton, a flammable material composed of trinitrate of cellulose, for military purposes during the First World War. After the war, there was a surplus of unused cellulose nitrate. Factories were created to produce celluloid, such as the case of the “Società Italiana Della Celluloide”, founded in 1922 by the Mazzucchelli brothers in Castiglione Olona, Italy [40]. In the USA, Ott [39] observed that in 1918, were produced 8.1 million tons of raw material

were produced; in 1923, 12.7 million tons, corresponding to an increase of 56.7%. In Germany, the European country where celluloid production was most developed, production rose from 25 tons/day in the pre-war years to 52 tons/day in 1923, corresponding to an increase of 108% [41]. This growth in German production had an impact on the Portuguese industrial context: of the total raw celluloid imported by Portugal between 1923 and 1926 (about 121.3 tonnes), 71% was imported from Germany (about 86 tonnes).

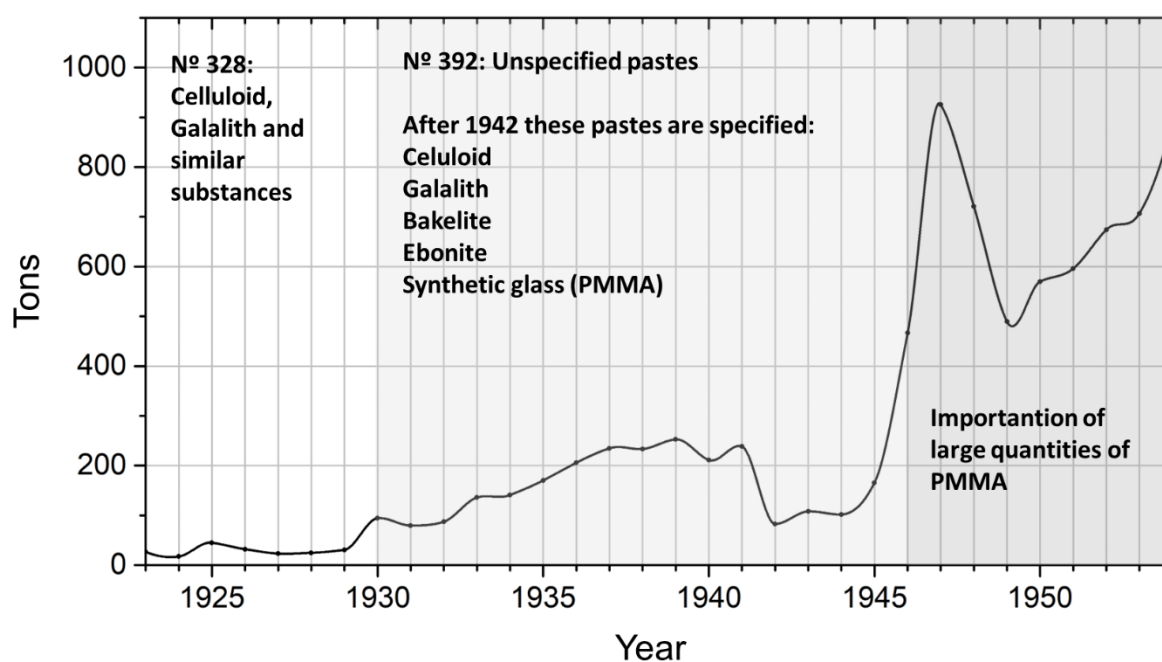


Figure 4.5. Evolution of the importation of plastic materials in Portugal. Source: Foreign trade reports from 1923 to 1954 (INE).

In the USA and France, despite the global growth of the celluloid industry, comb production centers were motivated to diversify their product due to a crisis of lack of demand. Social movements for women's emancipation led to revolutionary changes in women's fashion [42]-[44]. The “crazy 20s”, with the popularization of short hair resulted in a decrease in the demand for adornment combs. It is interesting to note that in Guimarães this diversification occurred only on a small scale in Costa, Lerdeira and Commandita. Guimarães comb industry was the primary supplier of combs in Portugal, either for personal hygiene and to hold or to adorn the hair. As a tool for hair hygiene, the comb was an essential everyday object [46].

In 1930, the first record of Bakelite importation occurs. From this year onwards, there is an increase in the importation of plastic materials. The importation growth agrees with Callapez argument [4]. She demonstrated the significant industrial dynamics prevalent in the plastics transformation sector during this decade, despite a special industrial policy imposed by

the Portuguese dictatorship in 1931 which constrained industrial growth¹⁴. This dynamism is associated with the increase of the number of factories in Lisbon, Leiria, Aveiro and Porto established to transform celluloid, Galalith and Bakelite [4], [9]. Noted by Joaquim do Vale in 1952, in a critic to the imposed industrial regime, written in “Notícias de Guimarães”, the dynamics of the comb industry resulted in technological innovation due to foreign competition:

It is said that this industrial regime promotes technical progress. This is not observed. Technical progress develops with competition. Look to what happened with the comb industry. The Americans flooded the market with plastic combs sold at competitive prices. How did our industrialists react? They equipped themselves with modern machines. Now they produce combs in abundance, for very cheap prices. This is due to competition, because, if not, they would continue with the same old processes (Vale, 1952, 1-2) [46].

In 1946, the first import of “plastic” appears, included in category 392, the same as celluloid. In 1948, the term “plastic” disappears, being replaced by synthetic glass, which meant polymethyl methacrylate (PMMA). The book “Matérias Plásticas” (Plastic Materials), the first Portuguese technical book on the plastics industry, written by António Rio de Janeiro, and published in 1950, describes production processes for celluloid, Galalith, synthetic glass (PMMA) and Bakelite, which, in the importation records, are the most significant plastic materials in the Portuguese economy during this period [48].

From 1946 to 1948, an increase in plastic materials importation is observed, such as celluloid, Galalith and PMMA, due to the demand created after the shortage caused by the Second World War. In 1943, 40 tons of celluloid were imported; in 1947 that number rose to 85 tons. Celluloid was bought at higher prices between 1946 and 1948 due to postwar increased demand [15]. In 1949, demand dropped by 18% compared to the previous year, with repercussions on the price: in 1948 celluloid cost 74,000 escudos/ton and in 1949, 60,000 escudos/ton. After 1949, importations rose for all plastic materials, denoting the growth of the plastics industry in Portugal. From 1947 onwards, the plastics industry was no longer limited by the special industrial regime of 1931, which contributed significantly to this evolution [4]. In 1959 a total of 106.4 tons of celluloid were imported.

The growth of the plastics industry is reflected by the advances on the technical-scientific terms used in importation records, which also relates to the first Portuguese technical book

¹⁴This regime ruled that all industrial actions had to be sanctioned by the central government. This created obstacles for the establishment of new factories and modernization of the existent ones. Only the industrialists with good political connections took advantage of this regime.

“Materias Plásticas” (1950). In 1951, the importation records show a new category – N° 389 “Raw artificial plastic materials, whether or not incorporating paper, fabric or other substances”. This category included celluloid, PMMA and cellulose acetate. In 1960, there were significant changes in the organization of the data. For the first time, the importation of synthetic polymers, such as polyethylene (PE), polyvinyl chloride (PVC) and polystyrene (PS) is described. After this year, no specific data was found for the importation of celluloid, which relates to the decrease of its commercial interest worldwide. Due to its technical and economic disadvantages, celluloid could not compete with synthetic plastics. As an example, in France, raw celluloid ceased to be produced in 1968 [41].

4.5 The singularity of the plastics industry in Guimarães

The metamorphosis of the Portuguese comb industry into the plastics industry was noted in 1954 by António Lopes de Carvalho in the 1953 “Guimarães Industrial and Agricultural Exhibition”:

But let us contemplate. We are attracted by the comb makers. Between what they were and what they are there is a great difference. By successive paths the comb makers have walked. From animal horn, they reached celluloid and Galalith. From these more or less transparent and elastic pastes, they arrived, through a liquefied product, at the most synthetic of materials (...) The old industry of combs has finally metamorphosed into the brand-new industry of plastics. Industrial entrepreneurs, studied, traveled, and reformed. And they achieved a “miracle”, the rebirth of the old industry that seemed to be sinking. What their machines produce today ranges from combs to the most beautiful things found in trinket bazaars (Carvalho, 1954, 1) [50]

António Lopes de Carvalho mentions four comb factories and two industrialists as the main figures of this transition: “Xavieres Limitada”, José Teixeira from “Fábrica de Pentes do Ribeirinho” and José Mendes de Oliveira from “Fábrica dos Pentes da Caldeiroa” (the name of the fourth factory is not identified, probably the Fábrica de Plásticos Pátria, given its relevance in this sector) [51]. José Mendes de Oliveira was an important figure in the comb industry from Guimarães, but no additional information has yet been found about his role, beyond that written by A. L. de Carvalho: “when the history of the introduction of plastic in the national industry is made, the name of this man from Guimarães will have to be mentioned as a testament to the hardworking spirit of progress that accompanies so many of our industrialists” [51]. This industrialist is associated, by this author, with the “Fábrica dos Pentes da Caldeirôa”. It will be important to understand if there is a connection between this factory and

Costa, Lerderia and Commandita, which was headquartered in Caldeirôa street, Guimarães. “Fábrica de Pentes do Ribeirinho” was founded in 1905 by Manuel Teixeira to produce horn combs and hairpins, having diversified its product in the 1940s with the production of toys¹⁵. In 1954, José Teixeira, son of Manuel Teixeira, becomes one of the first industrialists from Guimarães to buy a modern injection molding machine to produce toys and other utilitarian objects [52]. Xavieres Limitada had 800 employees working in the transformation of synthetic plastic materials and the technical knowledge was acquired in internships in Germany [53].

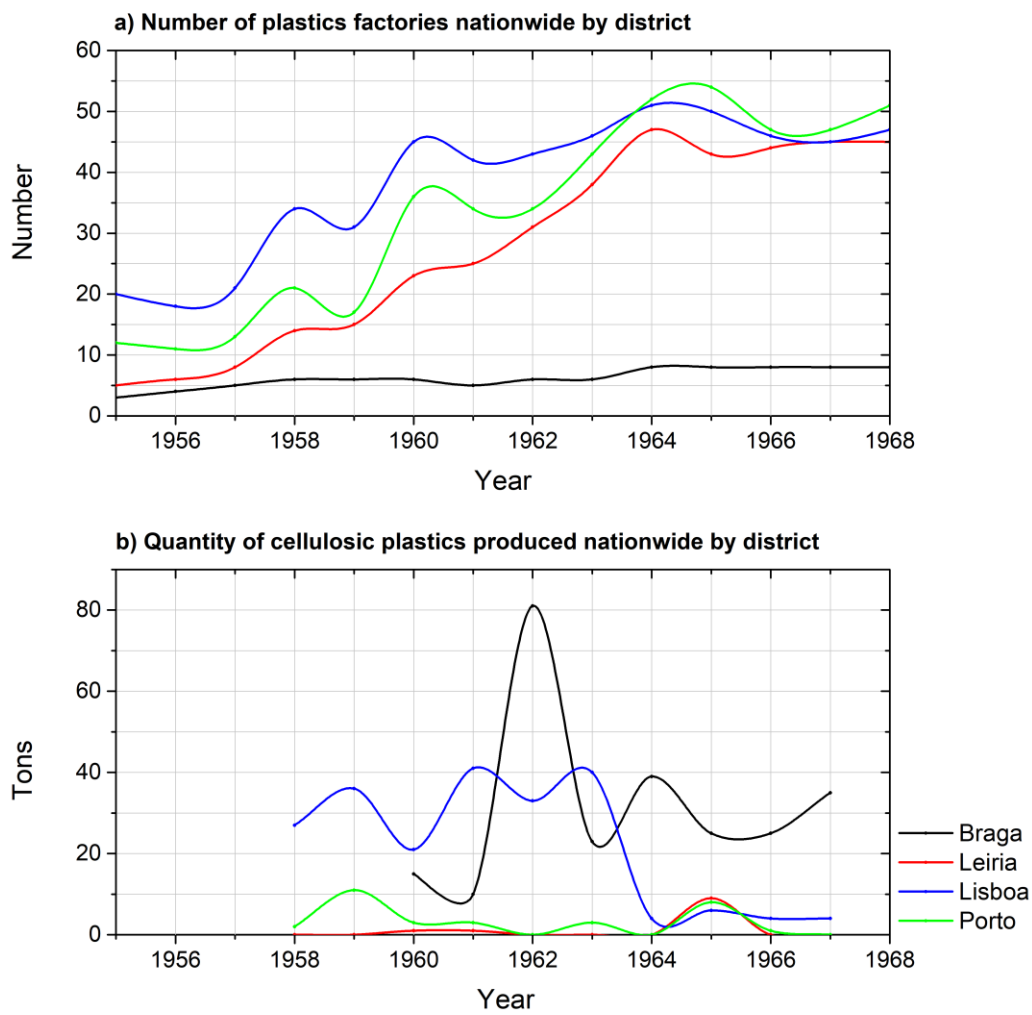


Figure 4.6. Evolution of the number of plastics factories and the quantity of cellulosic plastic materials produced in Portugal by the districts of Braga, Leiria, Lisbon and Porto. Source: Industrial Statistics from 1955 to 1967 (INE)

¹⁵ After World War II, the sale of plastic toys skyrocketed due to the high birth rate (the “baby boom”) [33]

The particularity of these four factories is that they are all directly linked to the Guimarães tradition of combs. This tradition had significant impact on the evolution of the city's plastics industry. Data on the number of plastics factories and quantity of cellulosic articles produced at national level, found in the Industrial Statistics of INE (1958-1967), in the section "Manufacture of Articles from Plastic Materials", show the singularity of the district of Braga, **Fig. 4.6**.

The growth rate of plastics factories in the district of Braga was much lower than that observed in the districts of Lisbon, Porto and Leiria, but the production of articles with cellulosic plastic materials remained relevant. If we consider the smaller number of factories nationwide in the district of Braga, the importance of factories from Guimarães in the transformation of cellulosic materials in Portugal is evident. The cellulosic plastics group is not specified; however, the importation data shows celluloid and cellulose acetate as the most significant. Regardless of this specification, this was the legacy of celluloid in the plastics industry of Guimarães; it was the most important district for the production of cellulosic plastics from 1964 to 1967 in Portugal.

We observe that in the district of Leiria the transformation of cellulosic plastics was not found. In this city, the first plastic used was Bakelite, introduced by the company Nobre & Silva, founded in 1927. In 1936, the factory was modernized and began to produce plastic stoppers, lids, and ashtrays in Bakelite, using compression processes. Due to the "synthetic" legacy of Nobre & Silva and the proximity to the plastic molds industrial center, Marinha Grande, in the following decades, there was a notable growth of plastic factories in the region [54]. It was synthetic materials such as polystyrene, polyethylene and polypropylene that dominated production in Leiria.

Despite not being included in the national industrial statistics, the city of Espinho, in the district of Aveiro, was an important center for the production of celluloid articles from 1930 onwards. "Luso-Celulóide" and "Hércules", were two factories which produced toys and religious articles in celluloid, cellulose acetate and polystyrene at a large scale. As happened with Guimarães in 1895, in Espinho the industrial knowledge to produce celluloid articles is brought by Leon Petit, a Frenchman from Oyonnax, where the family had a workshop manufacturing combs, spectacles and trinkets in bone, horn and celluloid. In 1930, he founded a company for the production and commercialization of celluloid articles in collaboration with the Henriques brothers, who owned a toy store in Espinho under the brand name "Pencudo". In 1931, the Henriques brothers separated from Leon Petit and created "Luso-Celulóide", which manufactured celluloid toys and religious articles. In comparison with Guimarães, horn was never part of the manufacturing processes of Espinho's celluloid factories, either at "Luso-Celulóide" or at "Hércules", which was founded in 1947 by one of the Henriques brothers, Artur Henriques [8]. Although celluloid was introduced by a comb-maker, Leon Petit, this

craft had an indirect role in the development of the plastics industry in Espinho. Regarding the transformation processes, in 1951, “Luso-Celulóide” operated several Eckert & Ziegler injection machines, developed in Germany in 1926 for the injection of polystyrene. It also had two horizontal alternative screw injection machines [55]. The materials used by this factory were those used by “Fábrica de Plásticos Pátria”, indicating similar transformation processes.

This similarity of transformation processes is also evidenced by the connections between Guimarães, Aveiro and Leiria with the industry of plastics molds in Marinha Grande and Oliveira de Azeméis. “Anibal H. Abrantes”, the first Portuguese factory to produce molds for injection moulding, was founded in 1945 in Marinha Grande. Between 1945 and 1956, the main clients were “Luso-Celulóide” and “Hércules” (Espinho), “Baquelite Liz” and “Matérias Plásticas Lda.” (Leiria) and “Fábrica de Pentes do Ribeirinho” (Guimarães) [11]. “Moldoplástico”, the first plastic molds factory in Oliveira de Azeméis, founded in 1955, sold molds to “Fábrica de Pentes do Ribeirinho”, “Xavieres Lda.” and for “Fábrica de Plásticos Pátria”, and for factories in Leiria and Aveiro [12]. It is important to mention the role of Guimarães workers in the development of the plastic mold industry, namely in Oliveira de Azeméis. António Silva, one of the founders of the firm “A. Silva Godinho”, an important plastics mold factory founded in 1964, recalled that “Fábrica de Plásticos Pátria had the best mold making artists” (Beira, 2007, 92). One of these artists, Alfredo Frias, left this factory to later form a partnership with António Loura at the “Metaloura” factory in Oliveira de Azeméis. António Rodrigues, leader of Simoldes Plásticos, one of the most important plastic mold factories in Portugal, mentioned that his “uncle Gabriel” had an “impressive expertise: he made molds for combs by hand, with a steel punch and without a pantograph for Pátria, a factory in Guimarães” (Beira, 2007, 185-186). It was still not possible to determine the role of celluloid in this mold making school of Guimarães.

Between 1958 and 1967, the production of cellulosic plastics in Porto was low. From 1960 to 1964, there was competition between the districts of Lisbon and Braga. Information on the use of celluloid in Lisbon is scarce. In the 1920s, “Sociedade Portuguesa do Celulóide” was headquartered in Lisbon. In this decade, “Cunha Costa & Companhia” produced dolls in celluloid paste [8]. More intriguing for us was the discovery of a small notice in 1933, with the title “A curious case!!!”, which refers to a French manufacturer of Oyonnax, “Mr. E. Potard, who operates (...) a factory of celluloid articles in Benfica (Lisbon)” [56]. Again, we find a relationship between the emigration of a French industrialist, from a region known for its combs, and the use of celluloid in Portugal. E. Potard Lda. was a factory operating in the plastics industry from 1945 onwards [4]. Plastics factories like this one may have contributed to the production of cellulose in Lisbon during the period analyzed. But the dynamics of

introduction of this industry is closer to the case of Aveiro than Guimarães, in which the Portuguese tradition of comb-making played a preponderant role.

4.6 Conclusion

As observed in international context, celluloid introduction in Portugal was a technological advance of great importance in the evolution of the comb industry. However, the dynamics of horn replacement, traditionally used in Guimarães for the production of combs, differs from the experience in Leominster, USA and from Oyonnax, France. In these two centers, factories to produce raw celluloid were created, which made the material available in uniform sheets, with pre-defined sizes, in a wide range of colors and patterns. In Portugal, there was no technical-scientific knowledge for a project of this type: the production of raw celluloid was a chemically complex process, required substantial capital investment and given the flammability of the material, safety rules were strict. However, with regard to the transformation of celluloid, there was already knowledge based on the long tradition of horn transformation since both materials are thermoplastic. Nevertheless, the entrepreneurship of the industrialists from Guimarães was notable, namely in the search for this knowledge through missions and circulation abroad and by the unprecedented investment of capital in modern machinery, creating the first comb factories in the country to transform celluloid. However, contrary to what happened in the American and French comb centers, in Portugal celluloid did not replace horn.

Celluloid offered technical and economic advantages: it eliminated all stages of the difficult preparation of horn, speeding up processes and reducing the wage bill. However, in Guimarães, raw celluloid had to be imported. No comparative data was found between the costs of horn and celluloid for Portugal, but if we consider the proximity and availability of horn as opposed to dependence on a foreign supplier, transport costs and customs fees of celluloid importation, it is conclusive why Guimarães comb-makers kept using horn.

Celluloid was mostly used to imitate tortoiseshell in the comb collections of the João Teixeira's factory and "Fábrica de Plásticos Pátria". These two significant examples of comb-making in Guimarães, are evidence that celluloid was introduced in Portugal to replace the imitations made with horn. The market for imitations of tortoiseshell made with horn is a topic that the scientific community has paid little attention to. It is generally assumed that the replacement of tortoiseshell started to be significant with the introduction of celluloid. The Portuguese problem with foreign competition in this imitation tortoiseshell market, referred in the "Guimarães Industrial Exhibition Report" in 1884, suggests the existence of celluloid combs in the Portuguese territory as early as the 1880s, imported from the USA, England or France, countries that began to produce celluloid in the 1870s.

Making a horn comb in imitation tortoiseshell was a slow process; the craftsman had to transform the horn through arduous processes and change its color, with a limited set of effects, with variable results. Raw celluloid was imported from the factory already resembling tortoiseshell, with a range of variations to choose from, in large sheets that allowed the production of several combs. Furthermore, with good quality celluloid the imitation could be so perfect as to fool the most trained eye.

The success of celluloid combs produced by Portuguese factories, from 1895 onwards, specially by “Fábrica de pentes a vapor da Madroa” and “Costa, Lerdeira and Commandita”, show the importance of this imitation market in the late 19th-early 20th centuries, where the target markets were the classes with low purchasing power. As observed with the American rural population, as discussed by Westmont [34], the Portuguese also sought out these imitations as a means of increasing their social status.

The advantages of the transformation of celluloid by mechanical processes to produce combs is demonstrated by comparing Guimarães with Lisbon. In the early 19th century, tortoiseshell and horn combs were manufactured in the Portuguese capital. In 1903, only two comb-making workshops existed and in 1916 there were neither workshops nor factories in Lisbon’s district. Lisbon was probably one of the primary ports of entry for foreign celluloid combs, which promoted the closure of the local comb workshops.

The notion that celluloid, a semi-synthetic plastic material, allowed superior technical and commercial solutions to horn, a natural plastic material, transformed the traditional comb industry of Guimarães into the “new” plastics industry. Thus, as explained by Friedel (1983) with respect to international contexts, we find that in Portugal celluloid had the same legacy: the modern idea of “plastic”. This is exemplified by the classification of imported materials: celluloid, classified since 1923, shared the class of Bakelite, the first synthetic plastic, from 1930 to 1950. From 1950 onwards, “Fábrica de Plásticos Pátria” used celluloid for combs to imitate horn, tortoiseshell or with artificial colors that no longer resembled the natural materials. Polystyrene, a synthetic plastic, became the material produced in greater quantity, transformed by injection molding with dies made in Portugal, namely in Marinha Grande and Oliveira de Azeméis. This technological innovation, that of synthetic plastics and injection molding, was again due the entrepreneurial spirit of the industrialists from Guimarães in seeking technical knowledge abroad. Guimarães became one of the centers of Portuguese plastic production, along with Lisbon, Porto, Leiria and Aveiro. However, the preservation of the comb-making tradition, with the specialization of imitation tortoiseshell and pioneering use of celluloid, transformed Guimarães into a singular industrial center of nationwide importance. By the end of the 1960s, it was the largest center producing cellulosic plastics nationwide.

In short, and in response to António Lopes de Carvalho, the comb will have a prominent place in the Museum of the History of Portugal. It was the comb that opened the door to the new world of plastics- and this comb was from Guimarães.

4.7 References

- [1] A. L. de Carvalho, *Os Mesteres de Guimarães, Volume IV*. Instituto Nacional do Trabalho, 1943.
- [2] T. Costa, «Guimarães: A indústria de pentes artesanais em chifre», em *As artes e as mãos da história*, I. M. Fernandes, M. J. Meireles, e P. Moscoso, Eds. Guimarães: Oficina, 2006, pp. 90–103.
- [3] Instituto Nacional de Estatística, *Estatísticas da Produção Industrial - 2020*. Lisboa: Instituto Nacional de Estatística, 2021.
- [4] M. E. Callapez, «A origem da indústria transformadora de plásticos em Portugal», Universidade Nova de Lisboa, Faculdade de Ciências e Tecnologia, 1998.
- [5] S. Kakadellis e G. Rosetto, «Achieving a circular bioeconomy for plastics», *Science*, vol. 373, n. 6550, pp. 49–50, 2021.
- [6] R. Altman, «The myth of bio-based plastics», *Science*, vol. 373, n. 6550, pp. 47–49, 2021.
- [7] R. Friedel, *Pioneer Plastic: The Making and Selling of Celluloid*. Madison: The University of Wisconsin Press, 1983.
- [8] M. Miranda, «Fantástico Plástico: Notas sobre o fabrico do brinquedo de plástico no século XX português», *Mínia*, n. 14, pp. 133–150, 2019.
- [9] A. Neves, M. E. Callapez, M. J. Melo, e R. Friedel, «On the Trail of Celluloid in Portugal», in *Proceedings of the Plastics Heritage Congress 2019, March 29-31, Lisbon, Portugal, 2020*, pp. 29–48.
- [10] J. M. L. Cordeiro e F. S. Costa, «A indústria de cutelarias em Guimarães: um património a conhecer e a valorizar», em *'A Jangada de Pedra'. Geografias Ibero-Afro-Americanas. Atas do XIV Colóquio Ibérico de Geografia*, 2014, pp. 1107–1112.
- [11] N. Gomes, «A Indústria Portuguesa de Moldes para Plástico: História, Património e sua Musealização», *History*, vol. Masters, 2005.
- [12] E. Beira et al., *Indústria de moldes no Norte de Portugal. Protagonistas: uma coleção de testemunhos*. Oliveira de Azeméis: CENTIMFE - Centro Tecnológico da Indústria de Moldes, Ferramentas Especiais e Plásticos, 2007.

- [13] P. Moscoso, «Cutileiros: uma arte medieval que chegou até nós», em *As artes e as mãos da história*, P. M. Isabel Maria Fernandes, Maria José Meireles, Ed. Guimarães, 2006, pp. 36–45.
- [14] A. J. F. Caldas, *Guimarães: apontamentos para a sua história*, 2a edição. Guimarães: Sociedade Martins Sarmento, 1996.
- [15] L. F. Costa, S. M. Miranda, e P. Lains, *História Económica de Portugal 1143-2010*, 2a edição. Lisboa: A Esfera dos Livros, 2011.
- [16] B. de Pombeiro, «Relatorio do comissário que visitou a Exposição Industrial de Guimarães», *O Commercio de Guimarães*, Guimarães, 12 de novembro de 1884.
- [17] A. Castro, *A revolução industrial em Portugal no século XIX*. Lisbon: Lumiar, 1978.
- [18] P. R. Nogueira, D. R. Martins, C. Fiolhais, e G. Santos, «Indústria Têxtil: expor Guimarães ao mundo desde o século XIX», em *II Internacional Historical Congress. As cidades na História: Sociedade*, 2017.
- [19] A. A. das Neves, «As Indústrias Vimaraneses em 1899», *Memórias de Araduca*, 2017. <http://araduca.blogspot.com/2017/11/as-industrias-vimaraneses-em-1899-1.html> (acedido 12 de setembro de 2019).
- [20] M. de C. Sampaio, «Edital», *O Commercio de Guimarães*, Guimarães, p. 3, 28 de janeiro de 1897.
- [21] F. J. Freitas, *Almanak de Guimarães: Commercial, burocrático, descriptivo, chrographico e historico para 1899*. Famalicão: Typhographia Minerva, 1898.
- [22] Costa Lerdeira e Commandita, «Fábrica a Vapor de Pentes e Cutelarias de Guimarães», *O Regenerador*, p. 4, 1909.
- [23] F. Martins, *Guimarães: O labor da Grei*. Guimarães: Tipografia Minerva Vimaranesense, 1928.
- [24] F. Schmitt, *Manuel du Fabricant de Peignes*. Paris: Librairie J.-B. Baillièere et fils, 1923.
- [25] Costa Lerdeira e Commandita, «Aperfeiçoamento no sistema mecânico de dentear travessas e pentes para o cabelo», Patent N° 16:041, 1929
- [26] Costa Lerdeira e Commandita, «Processo e máquina própria para a estampagem a quente em prateado ou dourado de ornamentos ou dizeres, sobre travessas e pentes em celulóide ou substância análoga», Patent N° 16:356, 1930
- [27] Instituto Nacional de Estatística, *VIII Recenseamento Geral da População no Contiente e Ilhas Adjacentes em 12 de dezembro de 1940*. Lisboa: Imprensa Nacional de Lisboa, 1945.

- [28] Instituto Nacional de Estatística, IX Recenseamento Geral da População no Continente e Ilhas Adjacentes em 15 de dezembro de 1950. Lisboa: Bertrand (Irmãos), Lda., 1953.
- [29] P. Walton, *Combmaking in America*. Boston: Viscoloid Company, Inc., 1925.
- [30] M. V. Gomes, R. V. Gomes, e J. Gonçalves, «Objectos produzidos em matérias duras de origem animal, do Convento de Santana, de Lisboa», em *I Encontro de Arqueologia de Lisboa: Uma Cidade em Escavação*, 2015, pp. 85–105.
- [31] Comissão Central, «Relatório da Exposição Industrial de Guimarães em 1884», Typographia de António José da Silva Teixeira, Porto, 1884.
- [32] C. J. Williamson, «The Victorian Plastics - Foundations of an Industry», em *The Development of Plastics*, S. T. I. Mossman e P. J. T. Morris, Eds. London: The Royal Society of Chemistry, 1994, pp. 1–9.
- [33] S. Freinkel, *Plastics: A Toxic Love Story*. Boston and New York: Houghton Mifflin Harcourt, 2011.
- [34] V. C. Westmont, «Faux materials and aspirational identity: Celluloid combs and working-class dreams in the Pennsylvania anthracite region», *Journal of Material Culture*, vol. 25, n. 1, pp. 93–107, 2019.
- [35] Instituto Nacional de Estatística, *Estatística Agrícola 1943*. Lisboa: Sociedade Astória, Limitada, 1945.
- [36] Instituto Nacional de Estatística, *Estatística Agrícola 1956*. Lisboa: Bertrand (Irmãos), Lda., 1957.
- [37] A. J. da S. B. Júnior, «União dos Fabricantes de Pentes, Limitada», *Notícias de Guimarães*, p. 4, 16 de Dezembro de 1935.
- [38] Direcção Geral da Estatística e dos Proprios Nacionaes, *Censo da População do Reino de Portugal no 1o de dezembro de 1900*. Lisboa: Typographia da «A Editora», 1906.
- [39] E. Ott, «Cellulose Derivatives as Basic Materials for Plastics», *Industrial and Engineering Chemistry*, pp. 1641–1647, 1940.
- [40] C. Cecchini, «Dalla celluloid alla plastica bio: 150 anni di sperimentazione materiche lette attraverso l'azienda Mazzucchelli azienda italiana 1849», em *Italian Material Design: imparando dalla storia*, G. Bosoni e M. Ferrara, Eds. Associazione italiana degli storici del design, 2014, pp. 9–32.
- [41] J.-M. Michel, *Contribution à l'histoire industrielle des polymères en France: Les sociétés étrangères*. Societé Chimique de France, 2013.

- [42] J. L. Meikle, *American Plastic: A Cultural History*. New Brunswick: Rutgers University Press, 1997.
- [43] V. Kollmann-Caillet, «The Museum of the Comb and Plastics Industry in Oyonnax», *e-plastory*, n. 5, pp. 1–8, 2017.
- [44] W. Rodrigues, I. Rodrigues, T. Requejo, e R. Neto, «Moda e “Élites”, nos anos 20», em VI Jornadas de Comunicação e Cultura no ISCTE, 1987, pp. 193–206.
- [45] J. R. Pita e A. L. Pereira, «Traços de higiene e cosmética no Portugal Novecentista», em *O Corpo Feminino em Revista: Alimentação, Higiene e Cosmética em Portugal e no Brasil (séculos XIX-XX)*, Évora: Publicações do Cidehus, 2022.
- [46] M. A. P. de Almeida, «As epidemias nas notícias em Portugal: cólera, peste, tifo, gripe e varíola, 1854-1918», *História, Ciências, Saúde – Manguinhos*, vol. 21, n. 2, pp. 687–708, 2014.
- [47] J. do Vale, «Daqui não saio... O condicionamento industrial», *Notícias de Guimarães*, Guimarães, pp. 1–2, 27 de janeiro de 1952.
- [48] A. R. de Janeiro, *Indústrias Plásticas: Celulóide, Galalite, Vidro Plástico e Baquelite*. Lisboa: Livraria Bertrand, 1950.
- [49] M. F. F. G. Rollo, «Portugal e a Reconstrução Económica do Pós-Guerra: O Plano Marshall e a economia portuguesa dos anos 50 Portugal e a Reconstrução Económica do Pós-Guerra. O Plano Marshall e a economia portuguesa dos anos 50», Faculdade de Ciências Sociais e Humanas da Universidade Nova de Lisboa, 2004.
- [50] A. L. de Carvalho, «Labor: do passado oficial ao industrialismo presente», *Notícias de Guimarães*, Guimarães, p. 1, 27 de junho de 1954.
- [51] A. L. de Carvalho, «Aquela Fábrica», *Noticias de Guimarães*, Guimarães, 20 de Maio de 1956.
- [52] Sofia Pires, «Bem-vindo ao Fabuloso Mundo Vimaranense dos Brinquedos Antigos», *Mais Guimarães: A Revista da Cidade Berço*, pp. 18–19, 2016.
- [53] L. Freitas, «António Xavier em entrevista: uma viagem no tempo», *Mais Guimarães: A Revista da Cidade Berço*, 13 de dezembro de 2017.
- [54] M. E. Callapez, «Plásticos na sociedade portuguesa rural», *Revista Brasileira de História da Ciência*, vol. 3, n. 2, pp. 200–210, 2010.
- [55] Henriques e Irmão Lda, *Fábrica Luso-Celulóide de Henriques e Irmão*. Lisboa: Tipografia Casa Portuguesa, 1951.
- [56] “Um caso curioso!!!”, *Diário de Lisboa*, Lisboa, p. 7, 25 de junho de 1933.

- [57] A. Costa, «António Lopes de Carvalho», *Guimarães na República: Guimarães, o País e o Mundo na imprensa vimaranense da 1ª República*, 12 de Fevereiro de 2010
- [58] M. Vert et al., «Terminology for biorelated polymers and applications (IUPAC recommendations 2012) », *Pure and Applied Chemistry*, vol. 84, n. 2, pp. 377–410, 2012.
- [59] L. Caetano, «A Classificação Estatística das Indústrias: elementos para a sua caracterização», *Finisterra*, vol. 42, pp. 311–381, 1986.
- [60] J. L. Hull, «Compression and Transfer Molding», em *SPI Plastics Engineering Handbook of the Society of the Plastics Industry, Inc.*, M. L. Berins, Ed. Boston: Springer, 1991, pp. 251–288.
- [61] P. Hardwick, *Discovering horn*. Southampton: Lutterworth Press, 1981.
- [62] I. I. Rubin, «Injection Molding of Thermoplastics», em *SPI Plastics Engineering Handbook of the Society of the Plastics Industry, Inc.*, M. L. Berins, Ed. Boston, MA: Springer US, 1991, pp. 133–178.

~

*This is an accepted Manuscript of an article published
by Nature in Scientific Reports, on 12/10/21, available online
Neves, A., Ramos, A. M., Callapez, M. E., Friedel, R., Réfrégiers, M., Thoury, M., & Melo, M. J.
Novel markers to early detect degradation on cellulose nitrate-based heritage at the submicrometer level
using synchrotron UV–VIS multispectral luminescence. Scientific Reports, 11(1), 1–13.
<https://doi.org/10.1038/s41598-021-99058-6>*

**NOVEL MARKERS TO
EARLY DETECT DEGRADATION ON
CELLULOSE NITRATE-BASED HERITAGE:
AT THE SUBMICROMETER LEVEL
USING SYNCHROTRON UV-VISIBLE
MULTISPECTRAL LUMINESCENCE**

Abstract

Cellulose nitrate (CN) is an intrinsically unstable material that puts at risk the preservation of a great variety of objects in heritage collections, also posing threats to human health. For this reason, a detailed investigation of its degradation mechanisms is necessary to develop sustainable conservation strategies. To investigate novel probes of degradation, we implemented deep UV photoluminescence micro spectral imaging, for the first time, to characterize a corpus of historical systems composed of cellulose nitrate. The analysis of cinematographic films and everyday objects dated from the 19th c. / early 20th c. (Perlov's collection), as well as of photoaged CN and celluloid references allowed the identification of novel markers that correlate with different stages of CN degradation in artworks, providing insight into the role played by plasticizers, fillers, and other additives instability. By comparison with photoaged references of CN and celluloid (70% CN and 30% camphor), it was possible to correlate camphor concentration with a higher rate of degradation of the cinematographic films. Furthermore, the present study investigates, at the sub-microscale, materials heterogeneity that correlates to the artworks' history, associating the different emission profiles of zinc oxide to specific color formulations used in the late 19th and early 20th centuries.

5.1 Introduction

5.1.1 A pioneer plastic in peril



Figure 5.1. Objects from Perlov's celluloid collection that consists of 300 everyday celluloid objects, donated by Amy Schenkein and Dadie Perlov, American collectors and majority donors of the Smithsonian Institute's celluloid collection. Containing several objects of different types, from razor blades, fans, pins, postcards or advertising items, this collection is significant of the American technological advances in the celluloid industry from the 1890s to the 50s. The objects showed were studied in the framework of this research: a 1901 postcard (A), two undated advertisement pins, hereby called the holy bible pin (B) and the American flag pin (C), and an 1899 calendar (D).

Cellulose nitrate is considered the first semisynthetic polymer and was trademarked as Parkesine and, later in the USA, as Celluloid by John Wesley Hyatt [1], [2]. Its flexibility and dimensional stability led to its extensive use as a new photographic and cinematographic medium for films, being present in image heritage collections in archives and museums [3], [4]. It was also widely used between the 1890s and 1920s for design pieces and everyday objects, all testimonies of our material culture, **Figs. 5.1 and 5.2**. Celluloid also attracted artists like Naum Gabo and Antoine Pevsner to creating sculptures that are now preserved in museums [5]. This heritage may be at risk, as we do not yet know what factors trigger an irreversible degradation leading to the total loss of these precious objects. It is for this reason that cellulose nitrate is considered an intrinsically unstable material in heritage collections, posing also risks

to human health. To slow down degradation, low-temperature storage is accepted by the conservation community [6], but these solutions prohibit public access, are price-sensitive, have high energy costs and there are concerns about its effects on the physical stability and material lifetime [7], [8]. Important insights on its degradation were achieved over the last decade [7-32], but a full elucidation of its mechanisms is still required to develop sustainable conservation strategies as in the NEMOSINE project, by developing a smart modular package with the main goal of energy-saving and extent conservation time [33]–[35]. **Fig. 5.2.**

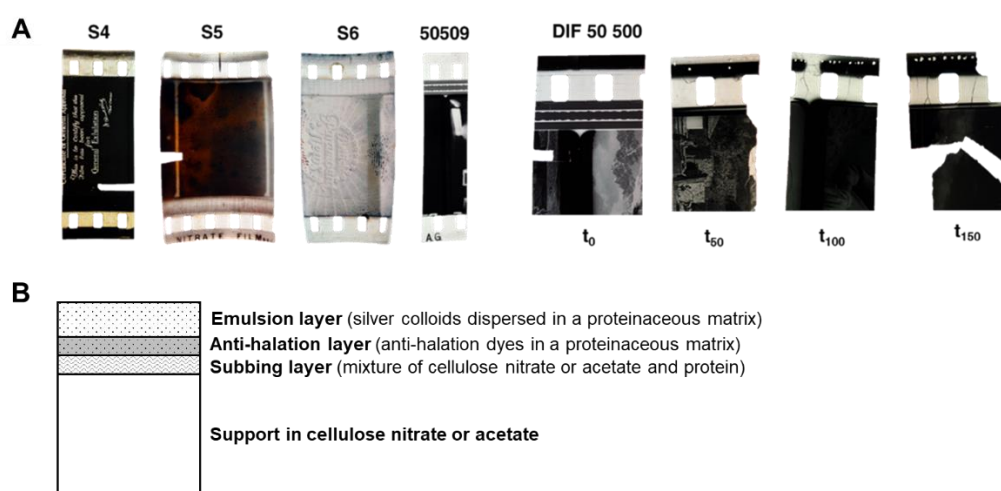


Figure 5.2. A) Cinematographic film samples S4, S5, S6, 50509 and DIF 50 500. DIF 50 500 was artificially aged ($\lambda \geq 280$ nm, 40 °C): at 50 hours of irradiation the film was yellowed and fragile; at 100h presented cracking; and at 150h the film lost its integrity. B) Multi-layer structure of a generic cinematographic film. The cellulose nitrate is the thickest layer and it is the support of the image. The image is formed by silver colloids dispersed in a proteinaceous matrix which is adhered to the support by another thin layer, the subbing layer. Finally, the anti-halation layer prevents light to be reflected in the image layer causing a halo effect.

5.1.2 Celluloid in private and public collections of plastics

During its heyday (roughly from 1880 to the 1920s) celluloid was used for an astonishing array of toiletries, novelties, and “fancy goods”. It was prized particularly for the ease with which it could be made to imitate semi-precious materials like ivory, tortoiseshell, coral, and mother-of-pearl [36]. Almost every article of commerce that could be made of these materials was fabricated from celluloid, and generally (but not always) sold more cheaply than they. For the most part, celluloid was not in any way functionally inferior to the materials it replaced, and it was frequently aesthetically equivalent [36]. In some forms, its cost was so low that it could be used in large volume for ephemeral articles—often advertising novelties (such as pocket calendars, rulers, book-marks, trade cards, and the like) [1]. Because these pieces were both more durable and more handsome than the card or paper items they replaced, they were often kept and stashed away rather than disposed of. Larger objects, such as combs, brushes, and

other toiletry items, were often passed down as heirlooms, much as their ivory or tortoiseshell models would have been.

In the 20th century, celluloid was almost everywhere eclipsed by newer and generally less expensive plastics. Even in photography and cinema, the material was replaced by the less flammable acetate films. In consumer goods, from toys to toiletries to tools, celluloid gave way to the products of chemical industry, led at first by phenol-formaldehyde (introduced as Bakelite) and then in even greater volume by a host of synthetic polymers, mostly made from petrochemicals. Celluloid became almost quaint as its uses fell away, until by mid-century not much more than table tennis balls and guitar picks remained [36]. But celluloid remains well represented in private and public collections of plastics, and the objects found in those collections raise a host of issues for understanding both the behavior of the material and the ways in which we use the material and the objects for historic preservation and representation.

Table 5-1. Description and degree of substitution (DS) of the cinematographic films and celluloid objects studied (Perlov’s celluloid collection).

Samples	DS [§]	Thickness (µm)	Date	Manufacturer	Description
S4	2.15	193	1932-42	Kodak	35mm black and white cinematographic film with no sound
S5	2.20	187	1933-42	Kodak	
S6	2.06	205	N.A.	Agfa	35mm black and white cinematographic films with sound
50509	2.18	147	1930	Kodak	
DIF 50 500	1.71	175	1940-60	Kodak	
Postcard	2.06	300	Possibly from 1901	N.A.	Celluloid postcard with floral and landscape-colored reliefs. Handwritings in French. In the upper part of the postcard, the date “30-09-1901” is written.
Holy Bible Pin	2.00	400	N.A.	N.A.	A celluloid pin with a metallic needle. On the back has the inscription “Made in the USA”.
American Flag Pin	2.01	300	N.A.	Bastian Bros, New York	A celluloid pin with a metallic needle. This pin belonged to the Grand Army of the Republic (G.A.R.).
Calendar	1.88	1000	1899	The Whitehead and Hoag Co., New Jersey	An 1899 celluloid year calendar with an advertisement to The Packer Manufacturing company in New York.

[§]Degree of substitution calculated by µFTIR using the calibration curve described in Nunes et al. [33]

The study here attempts to demonstrate methods for investigating the historical and physical experience of this first plastic in cinematographic films (dated from 1925 to 1960) and

objects, **Fig. 5.2 and Table 5.1**. The objects are part of a collection that originated with the private efforts of Dadie Perlov, who collected a wide range of small celluloid articles, largely from the northeastern United States during the last decades of the 20th century. Items from Perlov's collection constitute the primary celluloid holding in the museums of the Smithsonian Institution, in Washington, D.C [36]. Other items have ended up in other museums, and about 304 have been donated to Portuguese institutions, and these have been the basis of the study here.

5.1.3 Synchrotron deep UV photoluminescence micro spectral imaging to safeguard celluloid heritage.

Celluloid nitrate absorbs and can be excited in the UV (Supplementary Fig. S1), emitting in the UV-VIS region [37]; early degradation products that are formed in extremely low concentrations are also prone to show specific luminescence signals, making photoluminescence techniques very adapted to identify chemical changes [38]. In this work, we propose to assess the level of degradation by the use of luminescent chemical markers that are excited in the deep UV (DUV) using two instruments operating between 200 and 800 nm. The first endstation is dedicated to raster micro-scanning photoluminescence spectroscopy using a confocal configuration (POLYPHEME). The second one is a multispectral imaging system based on a full-field configuration (TELEMOS) [39], [40]. In this specific configuration, using synchrotron beam as a source of light to generate photoluminescence imaging, the limit of detection can be approached to 100 nM, enabling to detect intermediates and products that will be invisible to most spectroscopy techniques, due to their very low concentration [38].

In addition, the possibility to retrieve centimetric fields of view at sub-micrometer lateral resolution has shown to be extremely efficient for tackling the intrinsic heterogeneity of the historical objects [39], [40], such as those studied in this work, which can be described as intrinsically heterogeneous systems, **Table 5.1 and Figs. 5.1 and 5.2**. Cinematographic films can be described as multilayer systems in which CN-based polymers are used as image support: pigments or fillers are not expected in this type of matrix. In contrast, in the celluloid artworks from the Perlov's collection, fillers and pigments are present, admixed with celluloid. The analysis of these complex historical samples is supported by highly characterized reference materials, artificially aged, which will be studied both using DUV micro-imaging and UV-VIS spectrofluorimetry. Historical films were also artificially aged to simulate longer periods of natural ageing.

In this work, the level of degradation assessed by the luminescent markers is compared with the degree of substitution (DS) of CN calculated by infrared spectroscopy, since DS decreases with ageing [20], [26], [28], [29], [33], [41]. This decrease in DS in CN-based polymers,

is a consequence of the first phase of the degradation mechanism, which occurs through homolytic scission of the nitrate groups [19], [26]. In a pristine matrix used as support for cinematographic films, the DS is expected to be ca 2.26 [33], [42], and its decrease is a consequence of the scission of the nitrate group and its substitution by hydroxyl groups as depicted in Fig. 6.3. In the first phase of degradation, this leads to an increase and broadening of the carbonyl band at 1740 cm^{-1} alongside the increase of the OH absorption between 3700 and 3100 cm^{-1} , in the infrared spectrum [26], [32], [33]. For more details, please see next section.

The data acquired by synchrotron deep UV photoluminescence micro spectral-imaging (DUV- μ PL), will be for the first time used to identify alteration markers in historical objects made from CN. This knowledge can support the development of early warning tools to monitor CN degradation in heritage collections.

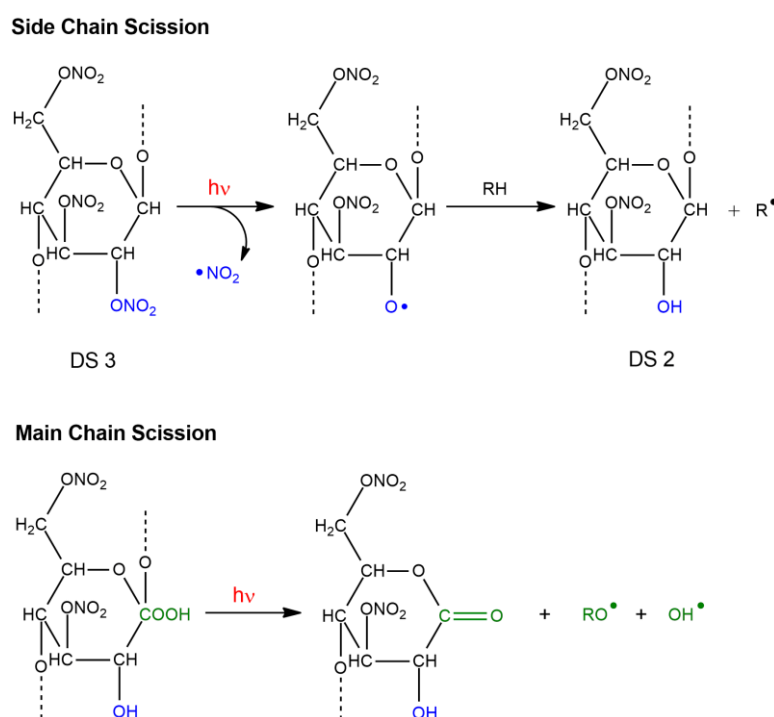


Figure 5.3. Cellulose nitrate side-chain scission starts with de-nitration, by the homolysis of a nitrate group in C2 or C3 and the release of $\bullet\text{NO}_2$ (inducing a DS decrease). In a second phase, hydroperoxides formed in C1, lead to main chain scission through cleavage of the glycosidic bond, with the formation of a gluconolactone as the primary degradation product. This mechanism, triggered by light, produce excited states that can simulate the natural ageing.

5.1.4 Photooxidation of cellulose nitrate to elucidate its degradation mechanism

Recent insights into the degradation mechanism of cellulose nitrate and celluloid were achieved by S. Therias, J.L. Gardette *et al.*. These authors showed that CN and celluloid present a common degradation mechanism, being proved that photodegradation ($\lambda_{\text{irr}} > 300$ nm) simulates the natural ageing mechanism [19], [26], [32]. In a first phase, for CN, the results show that the main degradation mechanism is based on de-nitration, followed by the formation of oxidation products exhibiting lactone and anhydride functions detected by their infrared carbonyl band at 1735-1740 cm^{-1} and 1760 cm^{-1} , respectively. Gluconolactone is identified “as the primary degradation product”, **Fig. 5.3**. In a second phase, these oxidized chemical structures will react, provoking side and main chain scissions, leading to physical modifications, which include embrittlement and yellowing [26], [32]. In addition, Thérias *et al.* correlated changes in the molecular weight distribution with the “loss of the pyranose and acetal structures and the formation of the gluconolactone”, by calculating the average number of chain scissions per chain [26]. Based on this research, an integrated version of the degradation mechanism of CN is presented in **Fig. A4. 1 and Fig. A4.2**, which is summarized in **Fig. 5.3**. In our ageing experiments, irradiation is carried out at $\lambda_{\text{irr}} > 280$ nm because it simulates the mechanism observed by irradiating at $\lambda_{\text{irr}} > 300$ nm.

5.2 Results and discussion

5.2.1 Alteration markers in reference samples

Fluorescence emission and excitation spectra collected on artificially aged reference samples show that different stages of CN degradation correlate with the detection of luminescent intermediates that display specific spectra, **Fig. 5.4**. A fluorescence excitation spectrum mimics the UV-VIS absorption spectrum of the chromophore that emits, and these were acquired using spectrofluorimetry (spot analyses, $10 \times 2 \text{mm}^2$ using a Jobin Yvon spectrofluorometer). Originally, an unreacted CN film is characterized by a broad excitation spectrum centered at 320 nm, which during the first 20h of irradiation shifts to shorter wavelengths (290 nm) and only then it will evolve continuously to longer wavelengths, starting at 50h of irradiation with a maximum at circa 300 nm, **Fig. 5.4 (left)**. The first shift to 290 nm can result from the degradation of chromophores formed in the dark. In the films that have suffered extensive degradation, a strong shift to higher wavelengths is observed in the excitation spectra; for example, at 130h of irradiation, several oxidized functions are identified by the presence of emission bands whose maxima are at 266, 325, 366 and 400 nm **Fig. 5.4 (right)**.

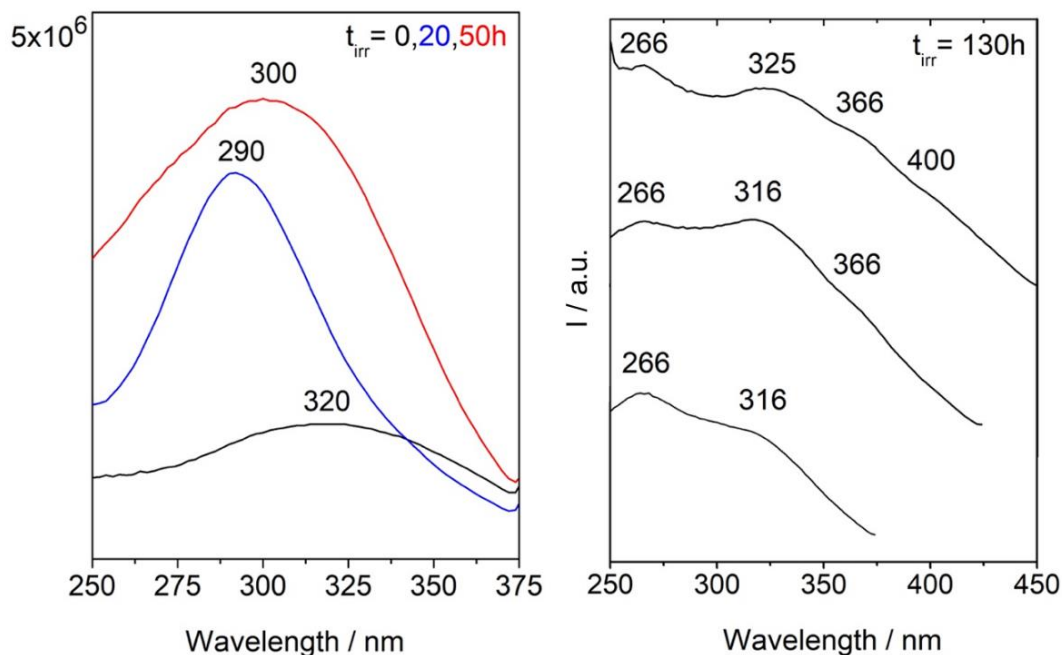


Figure 5.4. Irradiation of cellulose nitrate films followed by luminescence. Left, unreacted CN film is characterized by a broad excitation spectrum centred at 320 nm ($\lambda_{em} = 390$ nm), and in the first 20h of irradiation the maximum is shifted to shorter wavelengths (290 nm) and then evolve to a maximum at circa 300 nm at 50h of irradiation, which will continue to shift to longer wavelengths. Right, at 130h of irradiation several oxidized functions are observed described by maxima at 266, 325, 366 and 400 nm ($\lambda_{em}=390, 450$ and 480 nm). This agrees with the yellowing observed in the film.

This agrees with the yellowing observed in the cellulose nitrate films. Based on the excitation spectra collected on the various samples, we selected the excitation wavelength of 290 nm to acquire maps of emission spectra with the DUV micro-imaging set-up of the DISCO beamline, **Fig. 5.5**. The overall signal collected at the microscale is consistent with the averaged signal collected using spectrofluorimetry, **Fig. A4.3**. With an important advantage, the emission spectra obtained having a better resolution, it was possible to discriminate two bands in aged samples, in what was seen by spectrofluorimetry as an unresolved broad band, **Fig. A4.3**. For this reason, we will only discuss the emission spectra acquired using synchrotron radiation. An important first result was to prove that degradation is homogeneous in the reference films, which was achieved by showing that the average spectrum obtained with POLYPHEME mapping is representative of the luminescence of each pixel, **Fig. 5.5B**. POLYPHEME shows that CN at t_0 is characterized by a weak emission at 425 nm, this band increases during irradiation (I_{max} ca. 2600 cps). Also, a second band is formed, and its intensity increases over time in comparison to the first band at 420 nm, being visible at 150h of irradiation with maximum at 510-520 nm. This is an important result that was tested to assess the conservation condition of CN

by plotting this ratio $I_{425\text{nm}}/I_{510\text{nm}}$ versus irradiation time. We observed a linear correlation between those two parameters showing that quantification of the degradation state of CN can be assessed through the ratio between these two bands ($I_{425\text{nm}}/I_{510\text{nm}}$), **Fig. A4.4**: the higher the intensity of the CN2 band at 510-520 nm over the first band CN1 (*ca.* 420 nm), the higher the extent of degradation when compared with the DS values obtained by infrared spectroscopy. In future work, more irradiation times will be measured (shorter and longer) for CN and celluloid, to assess whether different mechanisms are at play.

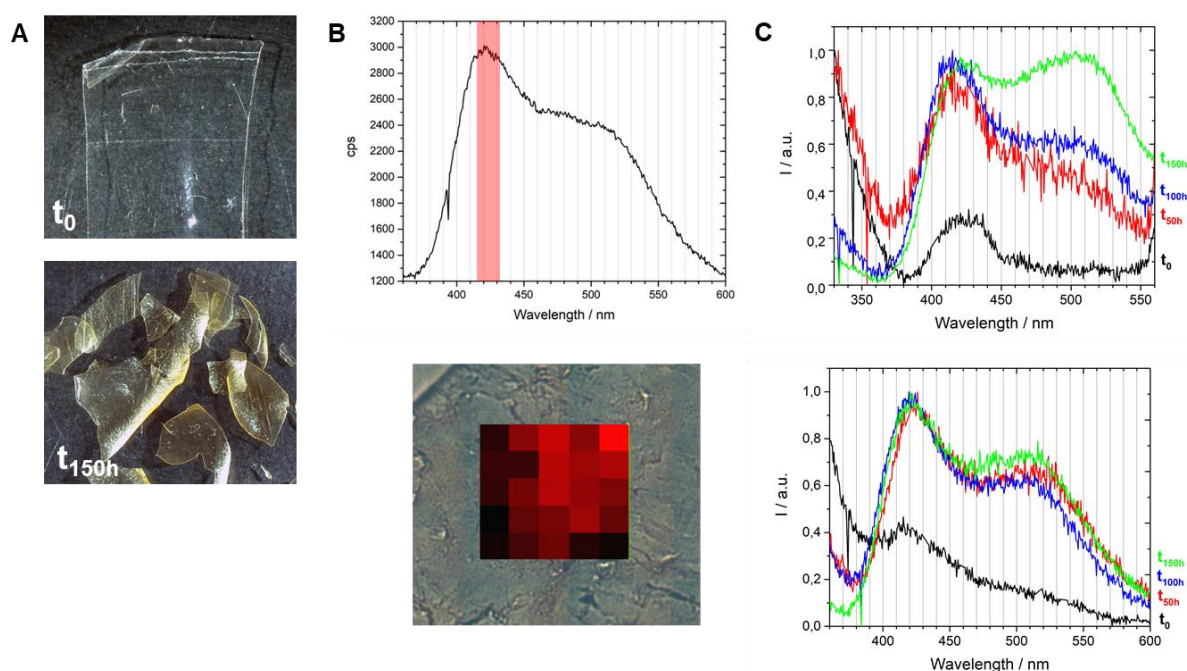


Figure 5.5. A) Microscope images (7.1x magnification) of cellulose nitrate homogeneous thin films (150 μm) used as reference films before (t_0) and after 150h of irradiation. B) POLYPHEME raster scanning map of a 150h aged celluloid reference ($\lambda_{exc} = 330\text{nm}$, 20 μm step, 5s acquisition time), together with the average, representative, emission spectrum. Intensity variations of the probed region between 415 and 425nm are due to the topography of the sample. C) Normalized emission spectra of artificially aged cellulose nitrate (top, $\lambda_{exc} = 290\text{nm}$) and celluloid (bottom, $\lambda_{exc} = 330\text{nm}$) irradiated during 50h, 100h and 150h.

When exciting at 290 nm, the spectrum of celluloid is dominated by the emission of camphor (I_{max} *ca.* 1900 cps). To avoid it and to collect only the CN emission, excitation was performed at 330 nm for celluloid references. As observed for CN, degraded celluloid is also characterized by a first band at 420 nm and a second one at 510-520 nm, **Fig. 5.5C**. However, the $I_{425\text{nm}}/I_{510\text{nm}}$ ratios indicate that comparing to CN, celluloid has degraded more rapidly: celluloid value of 3.25 at 50h of irradiation is similar to CN at 100h of irradiation, 3.07.

In summary, the studies on reference samples identified relevant markers to probe alteration in CN films. To assess the relevance of those markers in naturally aged samples, we performed similar analytical procedures in the cinematographic films and celluloid artworks.

5.2.2 Cinematographic films dated from 1925 to 1960, naturally and artificially aged

The observation of the stratigraphy of the cinematographic films studied shows that they are composed of the celluloid support and the image layer, **Fig. 5.2B**, which is a proteinaceous matrix with dispersed silver particles [43]. On naturally aged DIF-50500 cross-section, the spatial distribution of luminescent species collected using POLYPHEME allows to distinguish three regions by their specific emission spectra, **Fig. 5.6**: *i*) in the proteinaceous material, the image layer was characterized by a band at 412 nm. This emission can be associated with collagen as it was made from animal sources, principally calfskin [44]; *ii*) in the celluloid support, the emission spectra presented a band at 425 nm and a shoulder at higher wavelengths (*ca.* 510 nm) that compare well with the 150 h irradiated celluloid reference (**Fig. 5.5C**) and, agree with the degree of substitution of 1.71 calculated for this film by infrared spectroscopy (indicative of a degraded CN) [33], Table 1; *iii*) at the support interfaces, with air and with the image layer, the spectra presented two bands at 420 nm and 538 nm; this second band is more shifted and intense than the second band produced during degradation of celluloid references (centered at *ca.* 510-520 nm), and can represent other types of degradation products. This emission at 538 nm can be related to a more extensive degradation or a different mechanism, **Fig. 5.6**. This degradation trend was confirmed in the cinematographic films S4, S5, S6 and 50509, where a more intense emission in the region between 500-550 nm at the interfaces was also observed, **Fig. A4.5**.

DIF-50500 samples artificially aged ($\lambda \geq 280$ nm, 40 °C, 150h) were analyzed in situ since it was not possible to prepare a cross-section due to the film brittleness, **Fig. 5.2**. After 150h of irradiation, the emission spectrum acquired was very similar to that of the 150h artificial aged cellulose nitrate reference emission, **Fig. A4.6**. This behavior comparable to cellulose nitrate is probably due to the low amount of camphor in DIF-50-500, *ca.* 6% w/w, estimated by infrared spectroscopy [26], **Fig. A4.7**. This further strengthens the results obtained in the reference samples, proving that the concentration of camphor increases the degradation rate of celluloid.

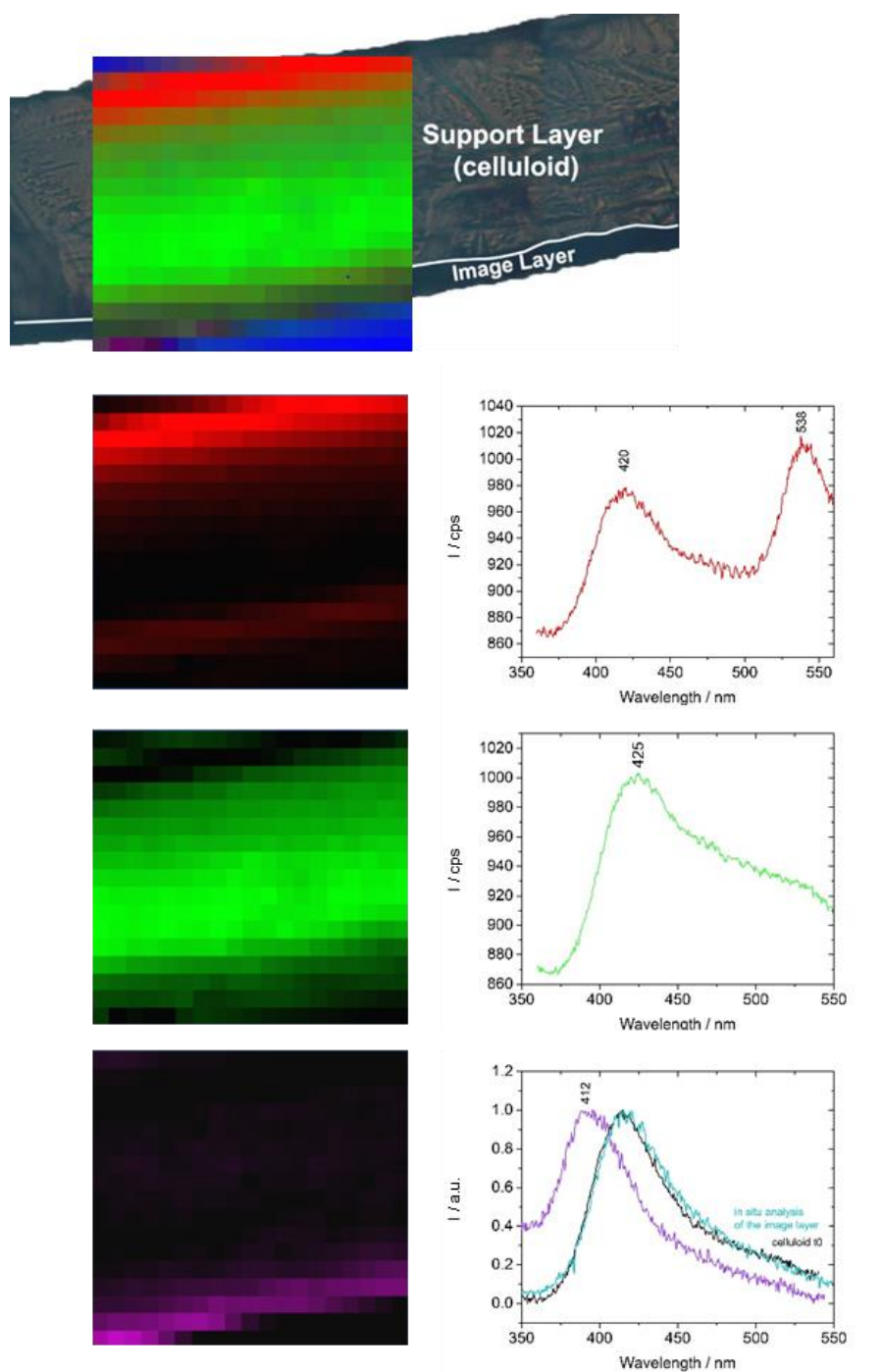


Figure 5.6. POLYPHEME raster scanning map (10 mm step, 5s acquisition time, $\lambda_{exc} = 330$ nm) of the cinematographic film DIF 50 500. Three regions of interest were distinguished based on characteristic emission spectra: the proteinaceous image layer, with a band at 412 nm; the support layer with a band at 425 nm and a shoulder at higher wavelengths; and other products at the interfaces, air-support, and support-image, characterized by a band at 538 nm.

5.2.3 19th c./early 20th c. celluloid everyday objects collection

Zinc oxide (ZnO) was the main pigment used to produce the ivory-like color and it was identified by its emission at 380 nm, in all the objects studied [39], [40], [45]–[47]. Zinc oxide is a semiconductor having a first narrow UV emission band at *ca.* 380 nm, assigned to the band-gap transition, and “its intensity represents a direct measure of the crystal quality” [48]. One or more emission bands in the visible region that tend to be broad and centered at *ca.* 425 nm and 510 nm [40], [46], [48] can be attributed to defects or impurities that are related to levels located within the bandgap (trapped states). The ratio between the UV and visible bands can vary enormously in historical paints and may be used to distinguish between them [40], [46], **Fig. A4.8**.

In the case of the celluloid objects of the Perlov collection, following excitation at 290 nm, the three bands described for ZnO were observed, **Fig. 5.7** and **Figs. A4.8-14**. These bands were identified with maxima at *ca.* 380 nm (ZnO1), at *ca.* 418 nm (ZnO2) and at *ca.* 507 nm (ZnO3), **Fig. A5.8**. Every pixel of the POLYPHEME maps performed has a significant contribution of the 380 nm emission, even for those with higher intensity emissions above 400 nm, confirming the ubiquitous presence of this pigment in the samples. The ratios between the three bands varied from pixel to pixel, in the same sample and within samples, showing the heterogeneity of this ZnO-polymer systems, **Fig. 5.7** and **Figs. A4.8-15**. However, for each of the objects studied, characteristic trends were observed, which will be discussed below.

The ZnO band at *ca.* 380 nm does not overlap with the CN emission, **Fig. 5.5C**. On the other hand, considering that these objects have an estimated camphor concentration between 20-15% w/w, **Fig. A4.12**, the emission of this plasticizer at *ca.* 420 nm can contribute to an intensity increase in this region.

Overall, the four objects analyzed showed different emission profiles: in the 1901 postcard the emission at 510 nm (ZnO3) dominates over the other two bands; the 1899 calendar is characterized by a highly heterogeneous system with high-intensity emissions from the three bands; for the Holy Bible Pin and the American Flag Pin, the band at 380 nm displays the highest intensity, **Fig. 5.7** and **Figs. A4.13-15**.

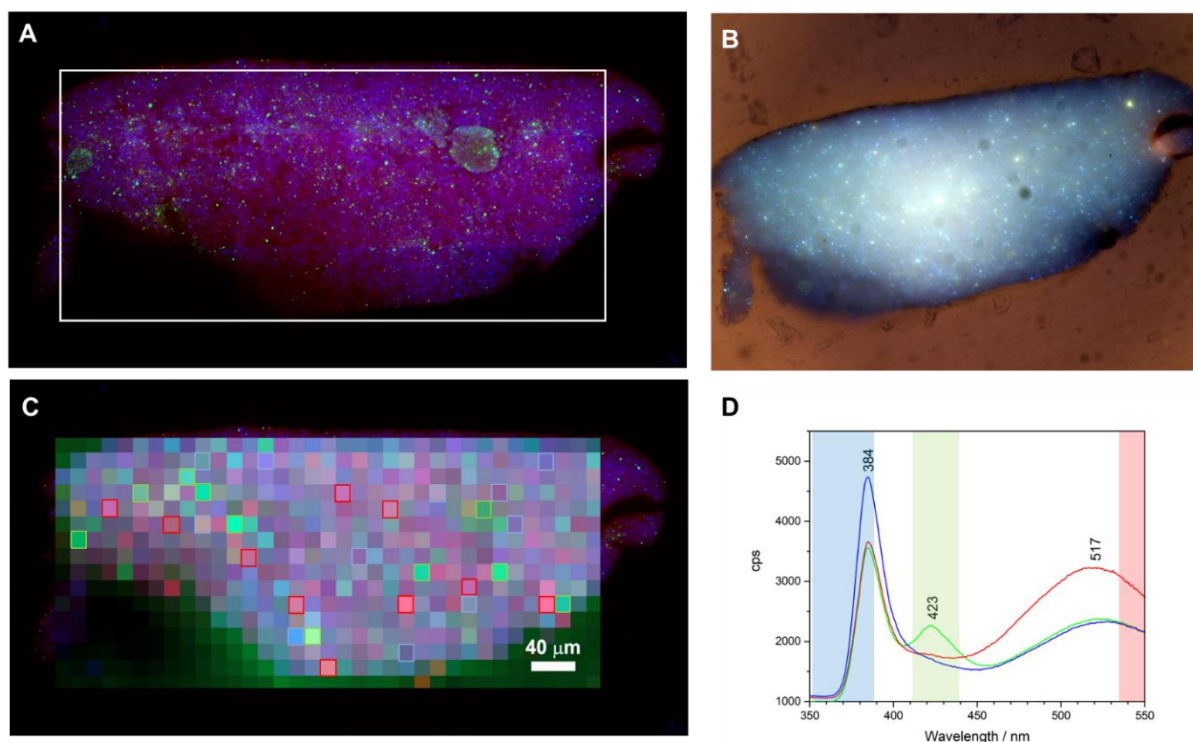


Figure 5.7. **A)** Full-field luminescence imaging by TELEMOS of the American flag celluloid advertisement pin ($\lambda_{exc} = 290$ nm, 40x objective). Emission bandpass filters used: 352-388 nm (blue); 412-438 nm (green); 535-607 nm (red). The white-square marks indicate the POLYPHEME map area. **B)** Spatially registered false-colour RGB image of the emission at excitations of 365 (blue), 385 (green) and 405 nm (red) with emission bandpass filter 514 nm (30 nm FWHM). **C)** Raster scanning map by POLYPHEME ($15 \times 15 \mu\text{m}^2$, 5s, 2 accumulations, $\lambda_{exc} = 290$ nm). Colors were designated as follows: blue for the band edge emission at 385 nm, green for the spectral region between 400-450 nm; red for the region between 510-550 nm. **D)** Average spectra calculated from 10 points for each designated color: strong near band edge emission (blue); contributions of ZnO crystal defect emissions between 400-450 nm (green) and strong green band emission (red). The spectral points used are marked in the POLYPHEME map (C) with squares of the correspondent color. The spectral regions viewed using TELEMOS setup are highlighted, with colours corresponding to the bandpass filters used.

The American flag advertisement pin mappings were characterized by the strong emission of zinc oxide particles, **Fig 5.7**. The heterogeneity of the system was observed on images collected with the full field endstation TELEMOS, by designating colors to each emission bandpass filter used: blue for the 352-388 nm range to image zinc oxide (ZnO); green for the 412-438 nm range to image ZnO trapped states, cellulose nitrate degradation, camphor, or other admixed materials; and red for the 535-607 nm range to image the ZnO trapped states and cellulose nitrate degradation, **Fig. 5.7**. In future work, we will investigate the origin of these differences by studying a set of aged and unaged reference samples. In this work, we will examine in more detail the American Flag Pin to better understand the information it is possible to extract based on the luminescent properties of ZnO, CN and camphor. The results

correlated with POLYPHEME mapping in which we observed, spatially, spectral variations related to the main emission features, **Fig. 5.7C**. These emission features can be represented by three average spectra (calculated from 10 selected pixels) and are characterized by 1) 380 nm emission, accounting for 67% of the mapped area, 2) emissions between 400-450 nm (10%) and 3) ZnO trapped state emission above 500nm (23%), **Fig. 5.7D** and **Figs A4.9-10**. To better understand the causes of these variations, preliminary Raman and infrared analyzes were carried out. The main results are summarized in **Table A4.1**. μ Raman analysis of whitish particles in the American flag pin, studied by TELEMOS and depicted with a strong blue luminescence in **Fig. 5.7**, confirmed the presence of ZnO by its characteristic peaks at 330 and 475 cm^{-1} and identified a peak at 1054 cm^{-1} indicative of cerussite (PbCO_3), **Fig. A4.11** and **table A4.1**. This also agrees with the identification of Zn, Pb and Ca by EDXRF. Zinc stearate was also detected by Raman peaks at 1062, 1094, 1127, 1296 and 1445 cm^{-1} , its presence is confirmed by FTIR-ATR by comparison with a reference, **Fig A4.11-12**. It was also possible to identify peaks related to the polymer matrix, namely the nitrate groups (864, 1286, 1652 cm^{-1}) and camphor (650 cm^{-1}) main vibration. Zinc stearate and cerussite are compounds that can be responsible for the variations observed between the ZnO1 emission at 385 nm and the ZnO3 trapped state broad emission between 500 and 550 nm [40], [46], [49], [50], **Fig. 6.7**. Emissions between 400 and 450 nm can be due to ZnO defect-associated emissions, camphor, or localized cellulose nitrate degradation [46], [48]. Future work will investigate more in-depth the origin of these emissions and if they can be related to specific formulations of ZnO that could be used as a signature to a technological process (for colour production).

In summary, it was possible to visualize at the macro and sub microscale, the heterogeneity of these complex mixture of ZnO with celluloid. Three spectral regions of interest were identified: the ZnO1 (385nm) and ZnO3 (500-550nm) emissions whose intensity variations can be influenced by the presence of organic functionalized ZnO and other inorganic additives or impurities; and the 400-450 nm regions whose contributions can be due to ZnO crystal defects (ZnO2) or to the polymer associated emissions, either camphor or cellulose nitrate degradation. Comparing POLYPHEME results for the four objects analyzed it was possible to observe differences in their spectral signatures and spatial distribution at the submicrometric scale, **Fig. 5.7** and **Figs. A4.13-15**. The different emission features of these two objects can be due to formulation differences, shown by Raman analysis, which identified massicot/litharge (PbO) and zinc stearate for the 1901 postcard and anatase (TiO_2) and azurite for the holy bible pin, **Table A4.1**. These results will be further explored in future work, but already show the potentiality of this technique to distinguish color formulations that can also be linked with the three different ZnO manufacturing methods employed in the late 19th early 20th centuries.

5.3 Conclusions

The present study here describes the implementation of synchrotron deep UV photoluminescence micro spectral-imaging for investigating (DUV- μ PL), at the sub-microscale, cellulose nitrate-based objects' material heterogeneity that correlates to its history (of alteration and manufacture). The investigation of cellulose nitrate and celluloid luminescence properties using DUV excitation has revealed the presence of markers that can be used for the detection of the degradation process at the early stage. By using excitation between 250 and 300nm, DUV- μ PL has allowed visualizing the distribution of degradation products in cinematographic films, with very high resolution, providing new insights into their degradation mechanisms. During degradation, the emission spectra of cellulose nitrate in the UV-VIS modifies markedly; the initial low emission at 420 nm increases and a new band at 510-520 nm appears. The higher the intensity of the band at 510-520 nm over the first band (*ca.* 420 nm), the higher the extent of degradation. Importantly, we proved that the evolution of the ratio between the two bands ($I_{425\text{nm}}/I_{510\text{nm}}$) correlates with DS calculated by infrared spectroscopy, increase in this ratio with decrease in DS, showing that it is possible to monitor the level of degradation of CN by DUV- μ PL. This tool allowed another important discovery: the higher the camphor concentration the higher the degradation rate both in reference samples and on cinematographic films. This crucial information will be next tested within an extended set of historical objects possibly using a chemometrics approach. Future experiments will also test an extended set of CN and celluloid samples, aged with shorter irradiation times, to better discuss the chromophores that give rise to the emission bands at 425 and 510 nm. At this point, it is not possible to attribute them to the excited state emission of the key intermediates formed during degradation: alcohols, hydroperoxides or lactones depicted in **Fig. 5.3**.

We also demonstrate the asset of these techniques to characterize and map, by combining spectral and spatial information, the heterogeneous microenvironments of the zinc oxide-based pigment in celluloid heritage. Due to the intrinsically heterogeneous nature of the objects in the Perlov collection, the variations observed in the luminescence of zinc oxide could be linked to the presence of lead carbonate or with the lead (identified by Raman microscopy), and as such to a specific color formulation [46]. Overall, this study shows that DUV- μ PL, due to its unique detection limit and high spatial resolution, is a fundamental technique for the study of cellulose nitrate-based heritage and plastic heritage, in general.

Finally, this work shows how the collection of celluloid objects donated by Perlov is a valuable historical source. Each object offers a biography that represents a valuable way of informing its past. The object's biography is a necessary research tool to understand and contextualize the relationships between people and the meaning, purpose, and use of an object. It

is also an effective didactic tool used in museums for teaching history. To write these biographies, POLYPHEME and TELEMOS have the potential to provide important data on manufacturing particularities. Knowing more about the object's materiality is also necessary to better preserve it in a historical and material sense.

5.4 Methods

5.4.1 Cinematographic films and objects from Perlov's collection and sample preparation

The cinematographic films were provided by the Austrian Academy of Sciences and the German Film Institute, partners of the NEMOSINE project. The selected celluloid objects belong to the Perlov's collection, a collection that consists of 300 everyday celluloid objects, donated by Amy Schenkein and Dadie Perlov, American collectors and majority donors of the Smithsonian Institute's celluloid collection.

Cross-sections of the cinematographic films were prepared by using a Leica RM 2155 rotary microtome equipped with low profile blades Leica DB 80 LX. To do so, a small sample was removed from the border of the cinematographic films (about 2 × 2 mm). This fragment was taped over a small piece of polymethylmethacrylate (PMMA) to hold it steady (the glue did not enter in contact with the sampling area). The PMMA was previously cleaned with ethanol. This assembly was fixed in the microtome clamping system. 15 µm slices were cut by using a clean portion of the blade for each cut and making a quick but relatively gentle motion (to get a clean cut and avoid ridges and fractures). The cuts were controlled by using a stereomicroscope. The sample cross-sections were placed over a microscope slide. This method allows the proper observation of the stratigraphic layers of the cinematographic films without the use of embedding resins.

Cross-sections of the celluloid objects were prepared by microsampling using Ted Pella µ-tools and a Leica MZ16 stereomicroscope. Since the objects studied have thicknesses below 1mm, the micro samples were cut from the corners of the objects from one end to the other (cross-section). The cross-sections were embedded in a polyester resin (Clear Casting Polyester Resin AM) so that the areas in contact with the resin corresponded to the surface of the object and the interior of the cross-section to the object's bulk. The samples were wet ground on a polishing wheel to expose the cross-section. Micro-Mesh® sheets with grit 8000 were used for dry polishing.

5.4.2 Reference samples preparation

Cellulose nitrate films were obtained from a solution of 4% (w/v) in methanol, prepared at room temperature (20 °C) and allowing cellulose nitrate to dissolve through the night (approx. 12 hours). This solution was homogeneously poured over a porcelain vessel using a Pasteur pipette and placed inside a desiccator with silica gel. The solution was left drying for 3 hours. After drying, a transparent cellulose nitrate film was peeled off the vessel with Ted-Pella micro tweezers. Samples with an area of 2.5x1 cm² were cut with a scalpel. The thickness of these reference films was 150 µm (approaching the thickness of the polymeric support of a cinematographic film). Celluloid films were obtained by adding camphor to the previous solution, in a ratio of 70/30 (cellulose nitrate/camphor) in weight. They were prepared following the same methodology used for the cellulose nitrate films.

5.4.3 Artificial Ageing

The irradiation of the cellulose nitrate and celluloid reference films and the cinematographic film DIF 50 500 (cut in pieces with dimensions of ca. 2x1cm²) was carried out in a CO.FO.ME.GRA accelerated aging apparatus (SolarBox 3000e) equipped with a Xenon-arc light source, an outdoor filter $\lambda \geq 280$ nm, with constant irradiation of 800 W/m² and a temperature of 40°C. The films were irradiated for a maximum period of 150h (total irradiance = 365 MJ/m²). To avoid sample movement inside the irradiation apparatus, the samples were placed inside “homemade” glass boxes with a quartz plate over (100mm x 100mm x 3mm thick, UQG Optics Limited).

5.5 Instrumentation

5.5.1 Optical microscopy

Microsampling of the celluloid objects was performed with Ted Pella µ-tools using a Leica MZ16 stereomicroscope. This microscope has a 7.1x to 115x zoom range lens, equipped with an integrated Leica ICD digital camera and a Leica KL 1500 LCD external cold light source with two flexible optic fibre cables. Microphotographs of the cinematographic cross-section were acquired using a Axioplan 2ie Zeiss microscope equipped with 10x ocular lenses and a 20x Epiplan objective, an incident halogen light illuminator (tungsten light source, HAL 100) and a digital Nikon camera DXM1200F, with Nikon ACT-1 software.

5.5.2 Spectrofluorimetry

Cellulose nitrate excitation spectra were acquired using a Jobin Yvon/Horiba SPEX Fluorog 3-2.2 spectrofluorometer with a 450W xenon lamp and a double-grating monochromator. Measurements with the spectrofluorometer were performed at front-face (ff). In this technique, the incident excitation beam is focused on the front surface of the samples and the fluorescence emission is acquired from the same region at an angle of 22.5° , which minimizes reflected and scattered light. To ensure that different samples were analysed in the same area, the reference films were placed on quartz demountable cells (Lightpath Optical (UK) Ltd.) and mounted in a cell holder for short path length cells (Lightpath Optical (UK) Ltd.), with the film surface directly facing the beam. Corrected emission and excitation spectra were collected using 3 mm entrance and exit slits, an integration time of 0.2 seconds, an increment of 2 nm. Excitation spectra were recorded collecting the signal at 390, 450 and 480 nm. To ensure the reproducibility of the results, 2 sets of four samples of irradiated cellulose nitrate and celluloid were analyzed.

5.5.3 UV-Vis spectroscopy

Ultraviolet-visible absorption spectra were recorded on a Varian-Cary 100 Bio spectrophotometer, between 200 and 800 nm with air as a reference and a constant temperature of $20 \pm 1^\circ\text{C}$. To ensure that different samples were analysed in the same area, the reference films were placed on quartz demountable cells (Lightpath Optical (UK) Ltd.) and mounted in a cell holder for short path length cells (Flightpaths Optical (UK) Ltd. To obtain absorbances <2 , the films were prepared with thickness $<10\mu\text{m}$ using solutions of 1.85% (w/v) in methanol applying the methodology described in *Reference samples preparation*.

5.5.4 μ Infrared spectroscopy

All samples were analyzed by μ Fourier Transform Infrared Spectroscopy for molecular characterization of the polymer matrix. Infrared spectra were acquired on a Nicolet Nexus spectrophotometer equipped with a Nicolet Continuum (15 \times objective) microscope and a Mercury-Cadmium-Tellurium (MCT) detector cooled by liquid nitrogen. Micro samples were placed on a diamond cell and the spectra were acquired in transmission mode between the $4000\text{--}650\text{ cm}^{-1}$, with a resolution of 8 cm^{-1} and 128 scans. Spectra are shown as acquired, without corrections or any further manipulation, except for the removal of the CO_2 absorption at approximately $2300\text{--}2400\text{ cm}^{-1}$.

5.5.5 μ Raman microscopy

Celluloid cross-sections were analyzed by μ Raman to obtain further information on inorganic additives in correlation with Micro-energy dispersive X-ray fluorescence analysis. The Raman spectra were collected on a Labram 300 Jobin Yvon spectrometer equipped with a He-Ne laser operating at 632.8 nm. The laser beam was focused with an Olympus 100 \times lens with a spot size of 2 μ m. The laser was used at maximum power (without the use of filters), with a collection time of 15-20s performing 20 to 30 scans. It was used a high-resolution grating (1800 grooves/mm).

5.5.6 Micro-energy dispersive X-ray fluorescence

X-ray fluorescence of the celluloid objects was performed in situ with a Bruker ArtTAX Pro spectrometer equipped with a Molybdenum (Mo) ampule, Peltier effect cooled Xflash 3001[®] semiconductor detector and a movable arm. The experimental parameters used were voltage of 40 kV, current of 300 μ A, acquisition time of 180s.

5.5.7 Micrometer

Sample thickness was measured using a TOPEX 31C629 micrometer, which has a length measurement from 0 to 25 mm and an accuracy of $10 \pm 5 \mu$ m.

5.5.8 Synchrotron deep UV-excited photoluminescence

Samples were analyzed at the POLYPHEME and TELEMOS end-stations of the DISCO beamline (Synchrotron SOLEIL, Gif-sur-Yvette, France). POLYPHEME was used to perform hyperspectral photoluminescence micro-imaging and acquire full emission spectra with high spectral resolution; TELEMOS for full-field luminescence microscopy [39], [52].

5.5.8.1 POLYPHEME

Emission spectra were recorded on an Olympus IX71 inverted microscope with lens replacement to be transparent in the deep UV range, a 40 \times Zeiss Ultrafluar UV-transmitting immersion objective, with monochromatic excitation wavelengths of 290 and 330nm, an emission wavelength range of 320–640, using integration times between 5 – 20s per spectrum. We tested our experimental conditions and found that no degradation is induced in the samples, with the excitation beam; thus, we did not observe changes in the fluorescence of the references after repeated irradiation at 290 nm and 330 nm in the same point of analysis. Raster scanning maps were performed with integration times of 5s (2 accumulations) and 10s (1 accumulation), in areas between $280\mu\text{m}^2 - 1.25 \text{ mm}^2$ using 2 to 15 μ m steps. In **Fig. 5.5C**, the emission data

was normalized to the range 0 to 1 applying the function *normalize to [0, 1]* ($y = \frac{y-y_{min}}{y_{max}-y_{min}}$) using Origin2016 Pro software.

References and cinematographic cross-sections were analysed between two 170 μ m quartz coverslips. Embedded celluloid cross-sections were placed on top of a 170 μ m quartz coverslip. During the experiments, the in-situ analysis of the 1899 calendar was tested with success.

Data acquired were pretreated in Labspec for the removal of cosmic spikes using a top-hat filter and map colour assignments. For the quantification of the emission contributions for each pixel in the American flag pin POLYPHEME mapping, **Fig. 5.7C**, a direct classical least squares (DCLS) modeling using Labspec 5 was performed. Three average spectra, each one calculated from 10 spectra characterized by 1) strong near band edge emission (blue loading), 2) ZnO crystal defect emissions between 400-450 nm (green loading), and 3) strong green band emission (red loading), were used as reference component spectra (loadings) **Fig 5.7D**. For each pixel, the model finds a linear combination of the reference component spectra which best fits the raw data. Using three loadings (blue, green, and red) with scores (x, y and z) the sum, S, of the linear combination is represented by: $S = [x * \text{blue}] + [y * \text{green}] + [z * \text{red}]$. The model provides the scores in percentage and data was normalized so that the combination of all scores adds to 100%. The bigger the score the bigger the similarity with the loading. An example of the model output for an emission spectrum is given in **Fig. A1.9**. This procedure was used to identify the distribution of the reference component spectra within the spectral array to create a profile based on each component distribution, **Fig. A1.10**. Based on the scores obtained for each pixel (448 pixels out of a total of 560 due to resin emission, not showed in **Fig. A1.17**) the total averages were calculated for the entire map. Blue loading accounted for 67% of the mapped area, the green loading accounted for 10%, and the red loading for 23%. The error map for this model is showed in **Fig. A1.16**.

5.5.8.2 TELEMOS

Images acquired were collected using an Axio ObserverZ1 microscope (Carl Zeiss MicroImaging) with a 40x Zeiss Ultrafluar UV-transmitting immersion objective, with a monochromatic excitation wavelength of 290nm and a dichroic mirror with a cut-off wavelength at 300 nm. Fluorescence was collected using four emission bandpass filters: 352-388 nm; 412-438 nm; 535-607 nm. Acquisition time was set at 10s for all channels. Images obtained were treated with ImageJ software: a BASIC corrected DW processing was used to remove the artefacts; the false-color images were created by associating a designated color to each channel (blue, green, and red) and manipulating the color balance. This method allowed localizing areas with the highest fluorescent signals.

5.6 References

- [1] R. Friedel, *Pioneer Plastic: The Making and Selling of Celluloid*. Madison: The University of Wisconsin Press, 1983.
- [2] S. T. I. Mossman, "Parkesine and Celluloid," in *The Development of Plastics*, S. T. I. Mossman and P. J. T. Morris, Eds. The Royal Society of Chemistry, 1994, pp. 10–25.
- [3] Y. Shashoua, *Conservation of Plastics: Materials science, degradation and preservation*. Elsevier Ltd, 2008.
- [4] B. Lavédrine, *A Guide to the Preventive Conservation of Photograph Collections*. Getty Publications, 2003.
- [5] M. Derrick and D. Stulik, "Deterioration of Cellulose Nitrate Sculptures Made by Gabo and Pevsner," in *Proceedings of a Conference Symposium – Saving the Twentieth Century*, Sept. 15-20, 1991, 1993.
- [6] P. Z. Adelstein, *IPI Media Storage Quick Reference*. Rochester: Image Permanence Institute, 2009.
- [7] Y. Shashoua, "Modern plastics: Do they suffer from the cold?," *Stud. Conserv.*, vol. 49, pp. 91–94, 2004.
- [8] I. R. Ahmad, D. Cane, J. H. Townsend, C. Triana, L. Mazzei, and K. Curran, "Are we overestimating the permanence of cellulose triacetate cinematographic films? A mathematical model for the vinegar syndrome," *Polym. Degrad. Stab.*, vol. 172, p. 109050, 2020.
- [9] A. Quye, D. Littlejohn, R. A. Pethrick, and R. A. Stewart, "Accelerated ageing to study the degradation of cellulose nitrate museum artefacts," *Polym. Degrad. Stab.*, vol. 96, no. 10, pp. 1934–1939, 2011.
- [10] A. Quye, "Quality Matters for Historical Plastics: The Past-Making of Cellulose Nitrates for Future Preservation Anita Quye*," *Cah. François Viète*, vol. 2, no. III, pp. 45–65, 2017.
- [11] A. Quye, D. Littlejohn, R. A. Pethrick, and R. A. Stewart, "Investigation of inherent degradation in cellulose nitrate museum artefacts," *Polym. Degrad. Stab.*, vol. 96, no. 7, pp. 1369–1376, 2011.
- [12] J. Rychly, A. Lattuati-Derieux, L. Matisova-Rychla, K. Csomorova, I. Janigova, and B. Lavedrine, "Degradation of aged nitrocellulose investigated by thermal analysis and chemiluminescence," *J. Therm. Anal. Calorim.*, vol. 107, no. 3, pp. 1267–1276, 2012.

- [13] A. Neves, E. M. Angelin, É. Roldão, and M. J. Melo, "New insights into the degradation mechanism of cellulose nitrate in cinematographic films by Raman microscopy," *J. Raman Spectrosc.*, vol. 50, no. June 2018, pp. 202–212, 2018.
- [14] H. Chai, Q. Duan, H. Cao, M. Li, and J. Sun, "Effects of nitrogen content on pyrolysis behavior of nitrocellulose," *Fuel*, vol. 264, no. November 2019, 2020.
- [15] H. Chai et al., "Experimental study on the effect of storage conditions on thermal stability of nitrocellulose," *Appl. Therm. Eng.*, vol. 180, p. 115871, 2020.
- [16] X. Gao, L. Jiang, Q. Xu, W. Wu, and R. Afriyie Mensah, "Thermal kinetics and reactive mechanism of cellulose nitrate decomposition by traditional multi kinetics and modeling calculation under isothermal and non-isothermal conditions," *Ind. Crop. Prod.*, vol. 145, no. January, p. 112085, 2020.
- [17] J. Salvant, K. Sutherland, J. Barten, C. Stringari, F. Casadio, and M. Walton, "Two László Moholy-Nagy Paintings on Trolit : Insights into the condition of early cellulose nitrat plastic," *e-Preservation Sci.*, vol. 13, pp. 15–22, 2016.
- [18] A. Espinosa and C. D. L. R. Anaya, "Neutralizing the sulfate of nitrate: An opportunity for restoration," in *Sustainable Audiovisual Collections Through Collaboration: Proceedings of the 2016 joint technical symposium*, D. S. Rachael Stoeltje, Vicki Shively, George Boston, Lars Gaustad, Ed. Indiana: Indiana University Press, 2017, pp. 188–195.
- [19] S. Thérias et al., "Degradation of celluloid in art works : a study of the mechanisms" *Actes du Colloq. Sci. des matériaux du Patrim. Cult.*, vol. 2, pp. 68–73, 2012.
- [20] M. Edge, N. S. Allen, M. Hayes, P. N. K. Riley, C. V. Horie, and J. Luc-Gardette, "Mechanisms of deterioration in cellulose nitrate base archival cinematograph film," *Eur. Polym. J.*, vol. 26, no. 6, pp. 623–630, 1990.
- [21] C. Selwitz, *Cellulose nitrate in conservation*. The Getty Conservation Institute, 1988.
- [22] M. Derrick, V. Daniel, and A. Parker, "Evaluation of storage and display conditions for cellulose nitrate objects," *Stud. Conserv.*, vol. 207–211, no. August, 1994.
- [23] C. Elsässer, A. Micheluz, M. Pamplona, S. Kavda, and P. Montag, "Selection of thermal, spectroscopic, spectrometric , and chromatographic methods for characterizing historical celluloid," *J. Appl. Polym. Sci.*, pp. 1–19, 2021.
- [24] F. C. Izzo et al., "Elucidating the composition and the state of conservation of nitrocellulose-based animation cells by means of non-invasive and micro-destructive techniques," *J. Cult. Herit.*, vol. 35, pp. 254–262, 2019.

- [25] M. Schilling, M. Bouchard, H. Khanjian, T. Learner, A. Phenix, and R. Rivenc, "Application of Chemical and Thermal Analysis Methods for Studying Cellulose Ester Plastics," *Acc. Chem. Res.*, vol. 43, pp. 888–896, 2010.
- [26] S. Berthumeyrie, S. Collin, P. O. Bussiere, and S. Therias, "Photooxidation of cellulose nitrate: New insights into degradation mechanisms," *J. Hazard. Mater.*, vol. 272, no. 2, pp. 137–147, 2014.
- [27] K. Curran, A. Mo, M. Underhill, L. T. Gibson, T. Fearn, and M. Strlič, "Cross-infection effect of polymers of historic and heritage significance on the degradation of a cellulose reference test material," *Polym. Degrad. Stab.*, vol. 107, no. 2, pp. 294–306, 2014.
- [28] E. Ciliberto, P. Gemmellaro, V. Iannuso, S. La Delfa, R. G. Urso, and E. Viscuso, "Characterization and weathering of motion-picture films with support of cellulose nitrate, cellulose acetate and polyester film," *Procedia Chem.*, vol. 8, pp. 175–184, 2013.
- [29] J. Mazurek, A. Laganà, V. Dion, S. Etyemez, C. Carta, and M. R. Schilling, "Investigation of cellulose nitrate and cellulose acetate plastics in museum collections using ion chromatography and size exclusion chromatography," *J. Cult. Herit.*, vol. 35, pp. 263–270, 2019.
- [30] É. Roldão, "A contribution for the preservation of cellulose esters black and white negatives," NOVA School of Science and Technology, PhD thesis 2018.
- [31] É. Roldão, A. J. Parola, M. Vilarigues, B. Lavédrine, and A. M. Ramos, "Unveiling the Colours of Cellulose Nitrate Black and White Film-based Negatives in Colonial Photography," *Stud. Conserv.*, vol. 65, pp. 118–126, 2020.
- [32] P. O. Bussiere, J. L. Gardette, and S. Therias, "Photodegradation of celluloid used in museum artifacts," *Polym. Degrad. Stab.*, vol. 107, pp. 246–254, 2014.
- [33] S. Nunes et al., "A diagnostic tool for assessing the conservation condition of cellulose nitrate and acetate in heritage collections: quantifying the degree of substitution by infrared spectroscopy," *Herit. Sci.*, vol. 8, pp. 1–14, 2020.
- [34] J. Kammer et al., "Quantitative and qualitative assessment of VOCs emitted from cellulose acetate movie films by PTR-ToF-MS," *J. Cult. Herit.*, vol. 47, pp. 50–58, 2020.
- [35] A. Al Mohtar, S. Nunes, J. Silva, A. M. Ramos, J. Lopes, and M. L. Pinto, "First-Principles Model to Evaluate Quantitatively the Long-Life Behavior of Cellulose Acetate Polymers," *ACS Omega*, vol. 6, pp. 8028–8037, 2021.
- [36] R. Friedel, "Is It Real? Imitation and Originality in Plastics," in *The Age of Plastic: Ingenuity and Responsibility*, O. Madden, A. E. Charola, K. C. Cobb, P. T. DePriest, and R. J. Koestler, Eds. Washington D.C.: Smithsonian Institution Scholarly Press, 2017, pp. 51–60.

- [37] D. N. S. Hon and T. L. Gui, "Photodegradation of cellulose nitrate," *Polym. Photochem.*, vol. 7, no. 4, pp. 299–310, 1986.
- [38] J. Lemaire, J.-L. Gardette, J. Lacoste, P. Delprat, and D. Vaillant, "Mechanisms of Photooxidation of Polyolefins: Prediction of Lifetime in Weathering Conditions," in *Polymer Durability*, 1996, pp. 577–598.
- [39] M. Thoury et al., "Synchrotron UV-visible multispectral luminescence microimaging of historical samples," *Anal. Chem.*, vol. 83, no. 5, pp. 1737–1745, 2011.
- [40] L. Bertrand, M. Refregiers, B. Berrie, J. Echard, and M. Thoury, "A multiscale photoluminescence approach to discriminate among semiconducting historical zinc white pigments," *Analyst*, vol. 138, pp. 4463–4469, 2013.
- [41] A. Quye, "Quality Matters for Historical Plastics: The Past-Making of Cellulose Nitrates for Future Preservation," *Cah. François Viète*, vol. série III, no. 2, pp. 45–65, 2017.
- [42] R. A. Stewart, "Analytical Studies of the Degradation of Cellulose Nitrate Artefacts," University of Strathclyde, PhD thesis, 1997.
- [43] S. Fujita, *Organic Chemistry of Photography*. New York: Springer-Verlag Berlin Heidelberg, 2004.
- [44] United States Tariff Commission, "Glues, gelatins & related products. A survey of the production of glues, gelatins, and related products in the principal producing countries, their process of manufacture, use, and distribution.," Washington D.C., 1940.
- [45] S. Hageraats, K. Keune, M. Réfrégiers, A. van Loon, B. Berrie, and M. Thoury, "Synchrotron Deep-UV Photoluminescence Imaging for the Submicrometer Analysis of Chemically Altered Zinc White Oil Paints," *Anal. Chem.*, vol. 91, p. 14887–14895, 2019.
- [46] C. Clementi, F. Rosi, A. Romani, R. Vivani, B. G. Brunetti, and C. Miliani, "Photoluminescence Properties of Zinc Oxide in Paints: A Study of the Effect of Self-Absorption and Passivation," *Appl. Spectrosc.*, vol. 66, no. 10, pp. 1233–1241, 2012.
- [47] M. Thoury, A. van Loon, K. Keune, J. J. Hermans, M. Réfrégiers, and B. Berrie, "Photoluminescence Micro-Imaging Shed New Light on the Development of Metal Soaps in Oil Paintings," in *Metal Soaps in Art*, F. Casadio, K. Keune, P. Noble, A. van Loon, E. Hendriks, S. A. Centeno, and G. Osmond, Eds. Springer, 2019, pp. 211–226.
- [48] M. Zhang, F. Averseng, J.-M. Krafft, P. Borghetti, G. Costentin, and S. Stankic, "Controlled Formation of Native Defects in Ultrapure ZnO for the Assignment of Green Emissions to Oxygen Vacancies," *J. Phys. Chem. C*, vol. 124, pp. 12696–12704, 2020.

- [49] A. Artesani, F. Gherardi, A. Nevin, G. Valentini, and D. Comelli, "A Photoluminescence Study of the Changes Induced in the Zinc White Pigment by Formation of Zinc Complexes," *Materials (Basel)*, vol. 10, p. 340, 2017.
- [50] V. Gonzalez, D. Gourier, T. Calligaro, K. Toussaint, G. Wallez, and M. Menu, "Revealing the origin and history of Lead-white pigments by their photoluminescence properties," *Anal. Chem.*, vol. 89, pp. 2909–2918, 2017.
- [51] G. Osmond, "Zinc Soaps: An overview of Zinc Oxide Reactivity and Consequences of Soap Formation in Oil-Based Paintings," in *Metal Soaps in Art*, F. Casadio, K. Keune, P. Noble, A. Van Loon, E. Hendriks, S. A. Centeno, and G. Osmond, Eds. Springer, 2019, pp. 25–46.
- [52] F. Jamme et al., "Synchrotron UV Fluorescence Microscopy Uncovers New Probes in Cells and Tissues," *Microsc. Microanal.*, vol. 16, pp. 507–514,

CONCLUSIONS

6.1 Discussion

Celluloid has been renowned for its remarkable ability to closely resemble the visual characteristics of a range of natural materials. However, despite its remarkable aesthetic similarities, celluloid has been found lacking in its capacity to replicate the corresponding physical properties of these natural substances accurately. This is largely due to a lack of recognition of celluloid as a composite material. Typically perceived as a cellulose nitrate-camphor matrix with additives for stabilization and coloration purposes (such as zinc oxide), celluloid was often dismissed as a viable substitute for ivory in billiard balls, as the properties of its primary component, cellulose nitrate, markedly differ from those of ivory. This idea endured because the composition of celluloid billiard balls was never characterized by modern analytical techniques. This thesis' novel perspective, which conceptualizes celluloid as a composite material, bears substantial implications for historical interpretation and conservation practices.

Using a multi-analytical approach, this work shows that celluloid billiard balls invented by John Wesley Hyatt, and sold from the 1870s to the 1950s, were consistently made with a mixture of ground bone, cellulose nitrate, and camphor (and likely aluminosilicates). The weight proportions of the components were measured by infrared spectroscopy, and the results correlated with Hyatt's patent of May 6, 1869 (USP 89582): 25% of cellulose nitrate to 75% of ground bone. Nowadays, ivory has been termed as a "model biocomposite" composed of complex structure of hydroxyapatite (~70%) and an organic matrix (~30%). Ivory bio-inspired synthesis is an ongoing research field to save elephants. One of the approaches for developing synthetic bio-inspired ivory is using bio-inspired ratios: "bio-inspired synthetic ivory may actually be possible if and when the right component chemistry and ratios can be mixed and ivory's micro- and nanostructure can be copied into the composite" [1]. During the 19th century, Hyatt demonstrated a notable achievement by combining hydroxyapatite and cellulose

nitrate in comparable amounts to those found in ivory. This composite was used as a substitute for ivory in billiards. Therefore, it is crucial for contemporary researchers seeking alternatives to ivory to acknowledge the triumphs of this inventor.

The acceptance of celluloid by the sport's elites was difficult. The ivory balls were the standard material and symbol of prestige for the professionals. The celluloid billiard balls, as *bonzoline*, were cheaper and had slightly different mechanical properties. Players who learned with ivory and played with it for a long time had difficulty handling the *bonzoline* billiard balls in their first attempts. However, evidence was found suggesting that two factors contributed to the entry of celluloid into the professional circuits: its higher stability in India's climate and its use by famous billiard champions. These two factors seem to be linked [2-5] and should be further investigated. Ultimately, the popularization of the game of pool and snooker in the late 19th century was enhanced by celluloid billiard balls. These games require a high number of balls (16 for pool and 22 for snooker), and the lower price of celluloid was preponderant. As a result, the number of billiard, pool, and snooker halls increased, which induced a higher number of amateur players who learned to play with ivory substitutes. Finally, with the arrival of a new generation of players who have never experienced playing with ivory, the switch to plastic substitutes became complete [6], [7].

The advantages of an approach that combine the history of science and technology and conservation science to understand the significance of objects and materials was further demonstrated with the research on denture collections. This work broadened the understanding of celluloid denture history and the collections studied. The associations between material and appearance are now more evident, which will help curators and conservators in the future. Material and historical evidence shows that celluloid dentures were significant in the market from the 1870s to the 1940s and that the compositions were consistent through time: cellulose nitrate, camphor, and vermilion (with the addition of phthalate plasticizers after the 1920s).

These two case studies, the billiard balls, and dentures, show the importance of identifying materials and that it continues to be necessary to create procedures that allow cultural institutions to assess the materiality of their plastics collections in a simple, straightforward, economical, and efficient ways. This is more evident when dealing with smaller cultural institutions, such as the Casa da Memória de Guimarães and Sociedade Martins Sarmento of Guimarães, Portugal. Through the solo utilization of handheld Raman MIRA DS for material characterization, it was determined that the comb collections under examination are of considerable importance to the history of Portuguese plastics and need immediate preservation measures. The research on the evolution of the Portuguese comb industry, based on these two collections, show evidence that celluloid was introduced to face the importation of imitation

tortoiseshell combs. Robert Friedel (1983) mentioned that the relationship between the economic position of celluloid and horn was complex [8]. The Portuguese example is interesting because celluloid and horn appear to have coexisted in their market niches. Celluloid substituted horn when it required a tortoiseshell imitation. For hygiene combs, horn sufficed because of its economic advantages over celluloid. As observed for Leominster (USA) and Oyonnax (France), the introduction of celluloid in Guimarães promoted the transition of the combs industry into a plastic industry in the 1950s. Still, horn continued to be a significant material in producing combs.

The use of handheld Raman MIRA DS for successfully characterizing a wide variety of objects proved its potential for the in-situ analysis of contemporary materials in collections. Raman MIRA DS allows the fast and reliable acquisition of spectra, and it's a versatile and easily transportable tool (tested in the USA and Portugal).

Finally, this work shows that Deep UV synchrotron multispectral luminescence spectroscopy successfully characterized cellulose nitrate and celluloid degradation. The ability of these techniques to identify luminescent intermediaries and to map their spatial distribution with very high resolution, provides new insights into the degradation mechanisms of heterogeneous multilayer systems in cultural heritage. Overall, it is demonstrated DUV luminescence microscopy is a fundamental technique that should be implemented in conservation labs for the study of cellulose nitrate-based heritage and plastic heritage in general.

6.2 Future perspectives

The knowledge gained in this work with the celluloid billiard balls implies a question: What do we really know about the celluloid objects in our heritage collections? This work shows a knowledge gap related to celluloid in sports or dentistry. But the composition and development of other celluloid applications have also been overlooked, particularly in music or medicine. Future research should address celluloid in all its material dimensions. The extent to which we possess knowledge about the materiality of celluloid is crucial for the preservation of its heritage.

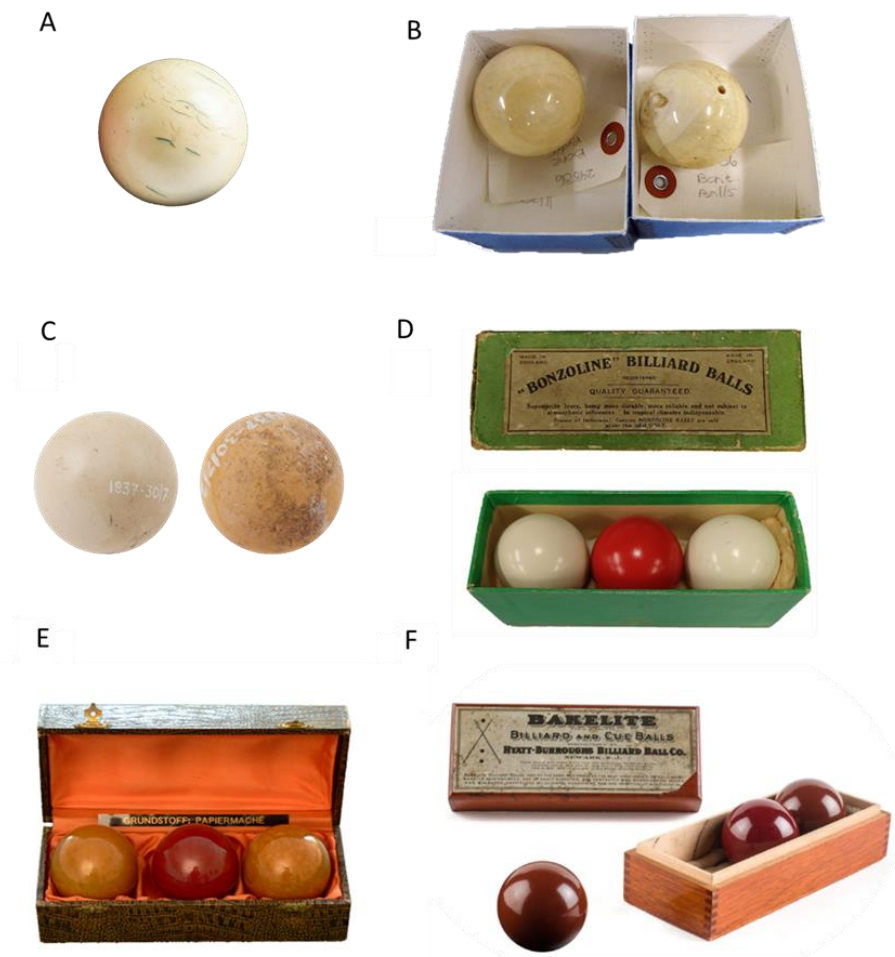


Figure 6.1. A) Ivory ball 1875-1920, NMAH B) Bone billiard balls, unknown date, Smithsonian Institution, NMAH C) Billiard balls made from Parkesine (c. 1860), Science Museum (UK); B) Bonzoline billiard balls acquired during this work (1930s); C) Papier-Mache billiard balls from the Billiard Museum Weingartner, Austria, Vienna (undated). D) Bakelite billiard balls sold by Hyatts-Burroughs Billiard Ball Co (1910s), Smithsonian Institution, NMAH.

There is still so much more to discover about the history of billiard balls. The NMAH has ivory balls in their collection and two “bone balls”. Although ivory was the standard material, affordable bone balls seem to have been used. However, records about their use were not found. It will be interesting to understand if Hyatt's experimentation with ivory dust and bone dust has any relationship with the markets for these two types of balls. Another exciting question relates to billiard balls from the Science Museum (UK) claimed to be made from Parkesine, c. 1860. Naturally, there is a curiosity about these object's compositions and how their properties compare with the material invented by Hyatt. Furthermore, there are other compositions in billiard ball museums, namely made of paper-mâché, a composite material. Finally, what is the relationship between the celluloid billiard balls and the Bakelite billiard balls sold by the Hyatts-Burroughs Billiard Ball Co? It is known that Bakelite was used with fillers. These questions emphasize our limited understanding of the materials utilized in inventing composites and how they replaced the natural ones, **Fig. 6.1**. The billiard balls serve as a prime case study due to the complex dynamics involved in developing a substitute for ivory, introducing it to the market, and ultimately being used in billiard tables. As sports objects, the billiard balls acceptance depends on the dialogue between the sporting world (athletes, trainers, technical staff), the sports federations and the engineers [9], [10].

The mechanical properties of the celluloid and other significant billiard balls will be measured. This will provide insight into the players' perceptions of each material's physical properties while playing. In addition, the measurements will help create a virtual environment for testing the different mechanical properties, preferentially as a playable didactic tool [11], [12].

The preservation of celluloid billiard balls and dentures is now an urgent challenge to address. There is a need for further investigation into the stability of early celluloid formulations and to understand the degradation processes involving, for example, the interactions of bone and cellulose nitrate and cellulose nitrate and vermillion. The comparison of the stability of these celluloid formulations will shed light on the behavior of celluloid billiard balls in tropical climates in comparison to ivory and on understanding the advantages or disadvantages of celluloid compared to vulcanite, PVAc-PVC copolymers or bakelite. Most importantly, this research is fundamental in developing effective methods to preserve these early celluloid objects.

The research of celluloid in Portugal will continue in a project financed by the Portuguese Foundation for Science and Technology entitled “The Plastics Metamorphoses - the reality and the multiple approaches to a material”. This will be an interdisciplinary project which will address the history of plastics in many dimensions. One of this project's tasks will be to focus on the study of the Portuguese celluloid Perlov Collection, namely its interpretation,

degradation, and exhibition; this project aims to create an exhibition on the history of early and plastic materials. Therefore, the research on early plastics in Portugal must be extended to other materials, for example, Galalith. Galalith is a material that has not received much attention from academia worldwide. During this research, sources from the Portuguese National Institute of Statistics were found showing that this casein-formaldehyde plastic was produced in the Portuguese national context. It is still widely used for buttons.

Within the NEMOSINE European project (nemosineproject.eu), an infrared DS quantification method was used as the basis for the construction of a predictive degradation model for cellulose acetate, built on a first-principles model considering the hydrolysis of the polymer in a neutral and acidic medium. This predictive model was coupled with sensors to detect and quantify the concentration of acetic acid, allowing the end-user to determine the effect of each storage parameter, like temperature, relative humidity, and the presence of an adsorbent on the material lifetime [13]-[15]. In this European project, sensors for detecting NO_x gases emitted during cellulose nitrate degradation were also developed. However, without a degradation model. The data collected with Deep UV synchrotron multispectral luminescence spectroscopy showed the enormous potential of this technique as an alternative to the NO_x sensor for the detection of cellulose nitrate degradation. In the future, inspired by the results from NEMOSINE, a system based on the luminescence of celluloid objects, combined with the NO_x sensor and a predictive model for cellulose nitrate degradation, will be of utmost relevance to the preservation of celluloid heritage.

Deep UV synchrotron multispectral luminescence spectroscopy variations observed in the luminescence of zinc oxide need to be explored to learn more about the role of this additive in the stability of celluloid and the manufacture and processing of the objects studied. Ongoing research is testing this technique to study transparent 3D celluloid objects to understand the overall mechanism of degradation and the role of camphor.

Portable UV-VIS luminescence spectrometers should be tested as an in-situ alternative to DUV luminescence microscopy. This equipment allows the sample to be excited in the UV (>200 nm) using fiber optics. A portable multi-analytical approach combining luminescence with handheld Raman, such as MIRA DS, and portable ATR-FTIR and XRF, could be established for the in-situ study of celluloid objects and plastics in general.

6.3 References

- [1] F. Vollrath, M. Ruixin, and D. U. Shah, "Ivory as an Important Model Bio-composite," *Curator*, vol. 61, pp. 95–110, 2018.
- [2] J. Roberts, *Modern Billiards*. London: C. Arthur Pearson Ltd., 1902.

- [3] C. Everton, *The History of Snooker and Billiards*. West Sussex: Tbs The Book Service Ltd, 1986.
- [4] C. D. Locock, *Side and Screw: Notes on the Theory and Practice of the Game of Billiards*. New York: Longmans, Green and Co., 1901.
- [5] C. C. M. Western, *The Practical Science of Billiards and It's Pointer*. London: Simpkin Marshall Hamilton Kent & Co Ltd, 1911.
- [6] R. Levi, *Billiards: the stokes of the game. Part III*. Manchester: Riso Levi, 1916.
- [7] R. Levi, *Billiards In The 20th Century*. Manchester: Riso Levi, 1931.
- [8] R. Friedel, *Pioneer Plastic: The Making and Selling of Celluloid*. Madison: The University of Wisconsin Press, 1983.
- [9] P. Trabal, "Resistance to technological innovation in Elite sport," *Int Rev Sociol Sport*, vol. 43, no. 3, pp. 313–330, Sep. 2008,
- [10] W. E. Bijker, *Of Bicycles, Bakelite and Bulbs: Toward a Theory of Sociotechnical Change*. Massachusetts: MIT Press, 1997.
- [11] A. Silva, D. Malhadas, and A. R. Fernandes, "Poolimmersion: A Realistic Physically Based Billiards Simulation," in *24º Encontro Português de Computação Gráfica e Interação (EPCGI)*, 2017.
- [12] B. Thompsett, A. Harland, and J. Roberts, "Investigating the Relationship between Physical Properties of a Football and Player Perceptions," *Procedia Eng*, vol. 147, pp. 519–525, 2016.
- [13] S. Nunes et al., "A diagnostic tool for assessing the conservation condition of cellulose nitrate and acetate in heritage collections: quantifying the degree of substitution by infrared spectroscopy," *Herit Sci*, vol. 8, pp. 1–14, 2020.
- [14] J. L. Abeer Al Mohtar, S. Nunes, J. Silva, A. M. Ramos, and M. L. Pinto, "First-Principles Model to Evaluate Quantitatively the Long-Life Behavior of Cellulose Acetate Polymers," *ACS Omega*, 2021
- [15] A. al Mohtar et al., "Decision making based on hybrid modeling approach applied to cellulose acetate based historical films conservation Fourier Transform Infrared spectroscopy," *Sci Rep*, pp. 1–13, 2021.

APPENDICES

Appendix 1.

The best billiard ball in the nineteenth century: composite materials made of celluloid and bone as substitutes for ivory

Supporting Information Text

Materials

For the construction of the infrared calibration curves were used the following materials: Bovine femur (Talhos Silau, Portugal), pure cellulose nitrate membranes (AmershamTMProtranTM Cytiva), camphor (Sigma-Aldrich, 96%), methanol (Sigma-Aldrich, HPLC grade).

Bovine bone powder preparation

The bovine (cow) bone powder was prepared by grinding a fresh femur bone, supplied by a local butcher. In the first stage, the femur bone was hand sawed into smaller pieces (circa 5x2cm), using an 300mm standard metal saw (Dexter). The soft tissues were mechanically removed using a scalpel and a spoon and the bone cleaned in a surfactant solution of 0.1 wt.% in water (Teepol). To further reduce the particle size, the bone pieces were sawed again and hammered (<1cm). Finally, the bone was ground in an agate pestle and mortar for 20min (Retsch Mortar Grinder RM 200).

Preparation of bovine bone powder – cellulose nitrate samples

A solution of 2% w/w of cellulose nitrate in methanol was prepared at room temperature and allowing cellulose nitrate to dissolve through the night (approx. 12 hr). The bovine bone powder was mixed with this solution in different proportions by weight of bone and cellulose nitrate: 80%, 70%, 60% and 50% w/w bone to 20%, 30%, 40% and 50% w/w cellulose nitrate, respectively. The solution was stirred with a magnetic stirrer and the solvent allowed to evaporate until a homogenous dough was obtained (2-4h, higher times for higher amounts of cellulose nitrate/methanol). This dough was dried through the night (approx. 12h) in a desiccator with silica-gel. After drying, homogenous references of bone and cellulose nitrate were obtained.

Preparation of cellulose nitrate-camphor (celluloid) films

Cellulose nitrate-camphor (celluloid) films were obtained by adding camphor to a solution of 2% w/w cellulose nitrate in methanol. Camphor was added in different proportions by weight to cellulose nitrate: 10%, 20% and 35% w/w camphor to and 90%, 80% and 65% w/w cellulose nitrate, respectively. Camphor was allowed to dissolve through the night (approx. 12 hr). The solution was cast homogeneously over the surface of a microscope glass slide using a Pasteur pipette. The microscope glass slides were placed inside a desiccator with silica-gel and the solution left drying through the night (approx. 12 hr). After drying, transparent cellulose nitrate-camphor (celluloid) films were obtained.

Construction of the bovine bone powder – cellulose nitrate μ FTIR calibration curves

A bone micro-particle was collected from the 1868 Hyatt billiard ball, and the infrared spectrum acquired: it was possible to observe the strong PO_4^{3-} vibration band at 1036 cm^{-1} , the amide I (C=O stretching), amide II (mixed C-N stretching and N-H in plane bending) and amide III (mixed C-N stretching (18%-40%) and N-H in plane bending (40-60%) and additional contributions of C-C stretching) bands at 1644 , 1551 and 1238 cm^{-1} , respectively, the CO_3^{2-} vibrations at 1451 , 1418 (this doublet is due to B type substitution by CO_3^{2-} , the major substitution in bone and dentine) and 873 cm^{-1} , in the region between 3600 and 3000 the amide A and amide B and OH stretching, (**Fig. S2**). The carbonate content ($\text{CO}_3^{2-}:\text{PO}_4^{2-}$) and the mineral to matrix ratios (Amide I: PO_4^{2-}) of the reference and "original" billiard ball bone samples were measured with FTIR following the method by [1] (**Fig. S2**). The carbonate content is related to crystallinity and the mineral to matrix ratio to the amount of collagen to the amount of hydroxyapatite. Both ratios decrease with the decrease of the particle size. For the cow bone reference, the $\text{CO}_3^{2-}:\text{PO}_4^{2-}$ was of $0.26 (\pm 0.05, 3\text{ spectra})$ and the Amide I: PO_4^{2-} of $0.33 (\pm 0.04, 3\text{ spectra})$. For the original billiard ball, $0.22 (\pm 0.04, 2\text{ spectra})$ and $0.30 (\pm 0.02, 2\text{ spectra})$, respectively. These values evidence similar properties and particle sizes.

Infrared spectrum of cellulose nitrate was characterized by bending of the CH and CH_2 bonds between 1500 - 1300 cm^{-1} , respectively, the strong vibrations of the nitrate groups at 1651 ($\nu_s\text{NO}_2$), 1280 ($\nu_a\text{NO}_2$) and 842 (νNO) cm^{-1} , and the cellulosic vibrational envelope, i.e., the stretching of the inter and intra ether bonds, between 1200 and 900 cm^{-1} . The infrared spectrum of the bovine bone was characterized the amide I (1650 cm^{-1}), amide II (1550 cm^{-1}) and amide III (1240 cm^{-1}) bands of collagen, the strong absorption of the apatitic phosphate of hydroxyapatite with maximum at 1036 cm^{-1} (νPO_4^{3-}), the ν_3 and ν_2 bands of the carbonate ions (CO_3^{2-}) in hydroxyapatite at 1451 and 873 cm^{-1} . By mixing both materials, changes are more evident in the regions of strong absorption of the nitrate and phosphate groups. For the development of the calibration curve the ratio $\nu_a\text{NO}_2/\nu\text{PO}_4^{3-}$ was plotted in function of the % w/w of cellulose

nitrate in the mixture. The absorbances of both bands was measured using OMNIC software by applying a baseline correction. Baselines were delineated using the band height tool and the absorbance calculated from the maximum of the band to the corresponding baseline: for the $\nu_{\text{a}}\text{NO}_2$, the baseline was delineated between 1800 and 1220 cm^{-1} ; for the νPO_4^{3-} , the baseline was delineated between 1185 and 925 cm^{-1} . For each bovine bone powder-cellulose nitrate sample, 6 infrared spectra were collected and used. In **Fig. S2B**, the average of the 6 infrared spectra for each sample and the absorbance measuring methodology is shown. A linear regression of the data was calculated using OriginPro 2016. The calibration curve obtained coefficient of determination (R^2) of 0.983 (**Fig. S3**).

Construction of the cellulose nitrate-camphor μFTIR calibration curves

When mixed with cellulose nitrate, the influence of camphor in cellulose nitrate infrared spectrum is observed by the appearance of the carbonyl band ($\nu\text{C}=\text{O}$) at 1730 cm^{-1} and minor changes related to the vibrations of the CH bonds in and 1500-1330 cm^{-1} . The relative absorbance of the carbonyl band increases with the increase of camphor concentration. For the development of the calibration curve, the ratio $\nu\text{C}=\text{O}/\nu_{\text{a}}\text{NO}_2$ was plotted in function of the % w/w of camphor in the mixture. The absorbances of both bands was measured using OMNIC software by applying a baseline correction. A baseline was delineated using the band height tool, between 1520 and 1220 cm^{-1} , and the absorbance calculated from the maximum of the band to the corresponding baseline. For each cellulose nitrate-camphor reference sample, 3 infrared spectra were collected and used. The average of the 3 infrared spectra for each sample and the absorbance measuring methodology is shown. A linear regression of the data was calculated using OriginPro 2016. The calibration curve obtained had a coefficient of determination (R^2) of 0.975 (**Fig. S13**)

SUPPLEMENTARY FIGURES

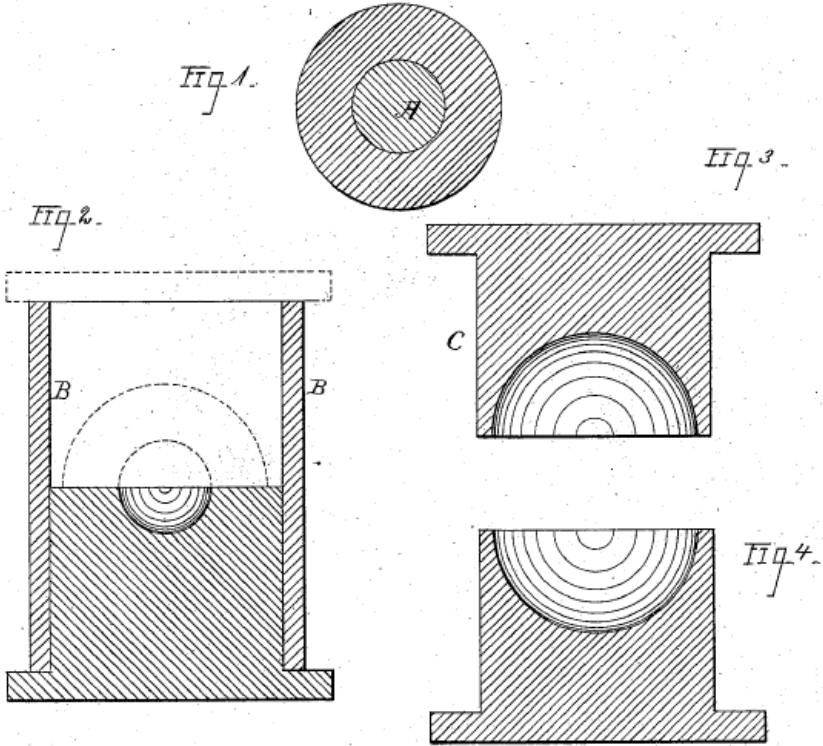


Figure A1. 1. Scheme of Hyatt's US Patent 259984 of 1882. Fig.1 is the central section of a billiard-ball made according to the invention, where A is the core and B is "a wall or shell adapted to fit over the core-set, the nature and construction of which is sufficiently illustrated in Fig. 2."

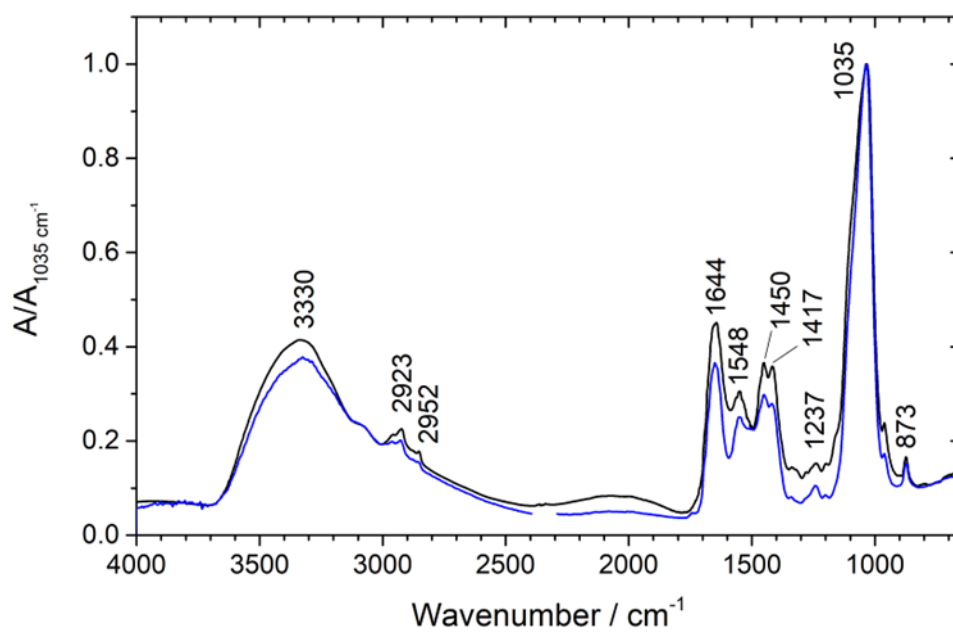


Figure A1.2. Infrared spectra of a bone micro-particle collected from the 1868 billiard ball (black) and from the ground cow femur bone (blue).

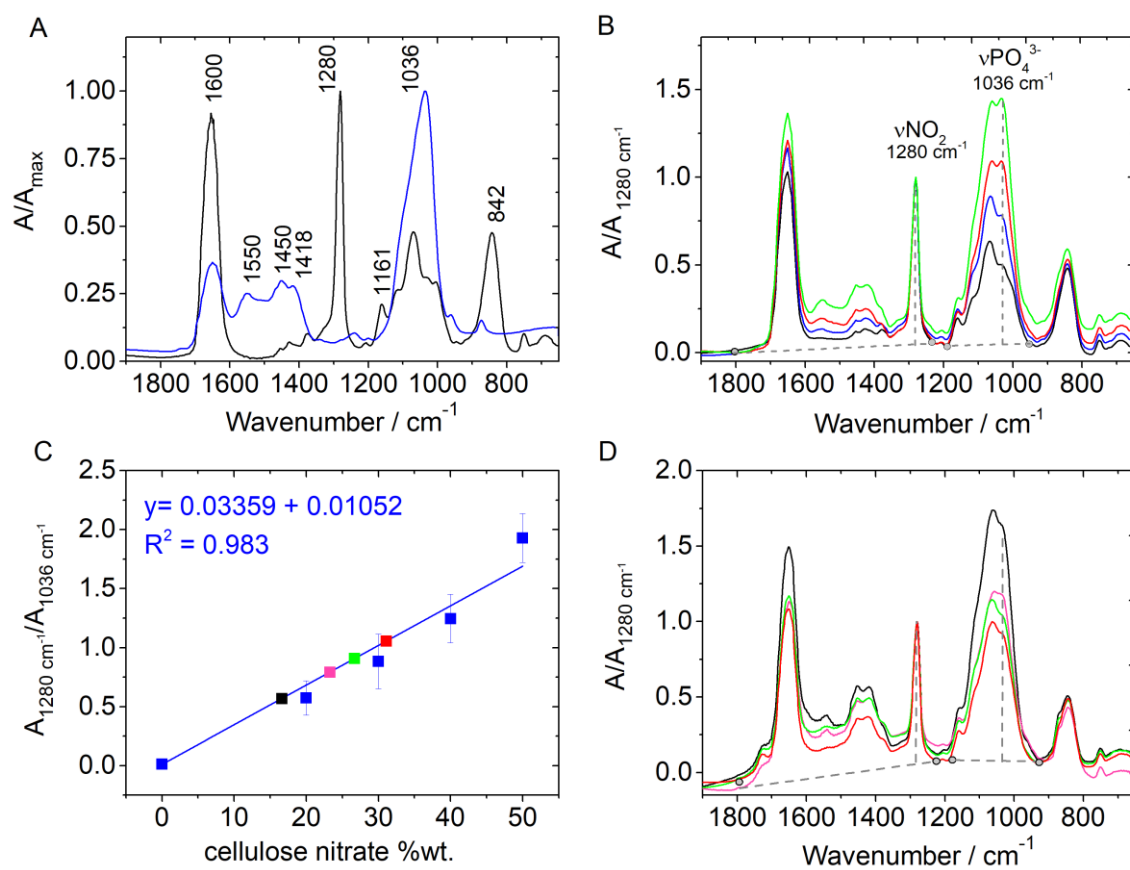


Figure A1.3. Development of the bone-cellulose nitrate calibration line and quantification of the mixture in the 1868 billiard ball. A) Infrared spectra of the ground cow bone femur (blue) and cellulose nitrate references (black) between 1900 and 650 cm^{-1} ; these materials were used for the development of the calibration curve. B) Overlay of the infrared spectra of the bovine bone-CN reference mixtures, normalized to the $\nu_s\text{NO}_2$ (1280cm^{-1}) band (%wt bone/cellulose nitrate): 80/20 (green), 70/30 (red), 60/40 (blue), 50/50% (black). C) The data shows the average ratio and the standard deviation calculated from 6 infrared spectra collected for each reference (blue). The cellulose nitrate concentrations calculated for 4 spectra of the 1868 billiard ball are showed (average 23%, standard deviation 6%). D) Overlay of the infrared spectra used for the quantification of the bone-celluloid mixture in the 1868 billiard ball. The colors correspond to the points in C. The spectra are normalized to the $\nu_s\text{NO}_2$ (1280cm^{-1}) band. Acquired from 4 different microsamples collected from the surface of the object.

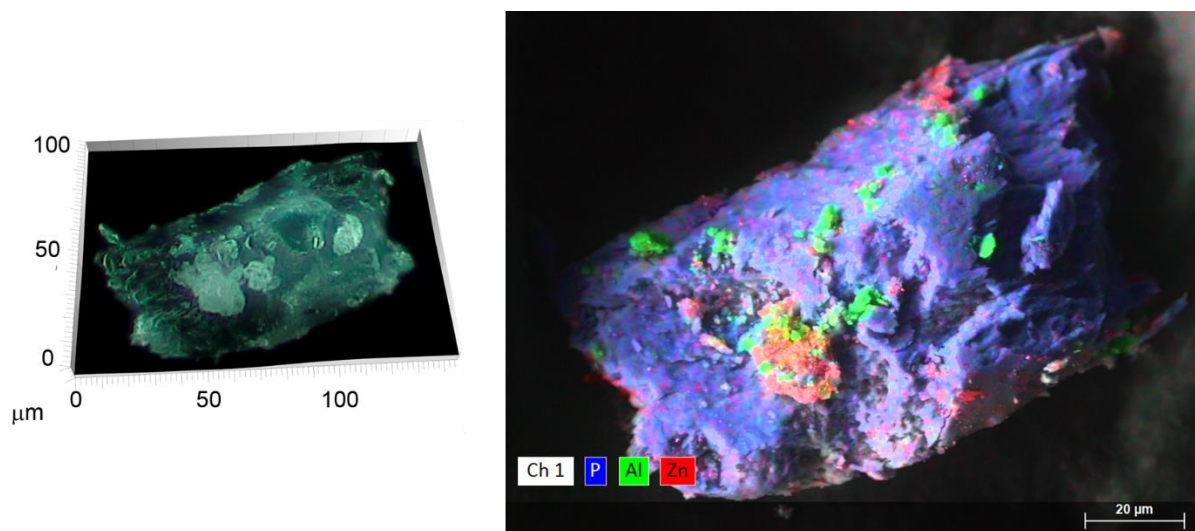


Figure A1.4. SEM-EDS imaging of a bone particle acquired from the 1868 billiard ball sample. The distribution of phosphorous (P), aluminum (Al) and zinc (Zn) is showed. It is possible to observe the homogenous distribution of phosphate in the bone matrix. At the surface of the bone particle, aluminum (Al) particles were found, related to the presence of aluminosilicates. Furthermore, it was possible to observe a homogenous mass adhered to the sample of the bone particle attributed to presence of zinc (Zn), possibly from the celluloid zinc oxide mixture.

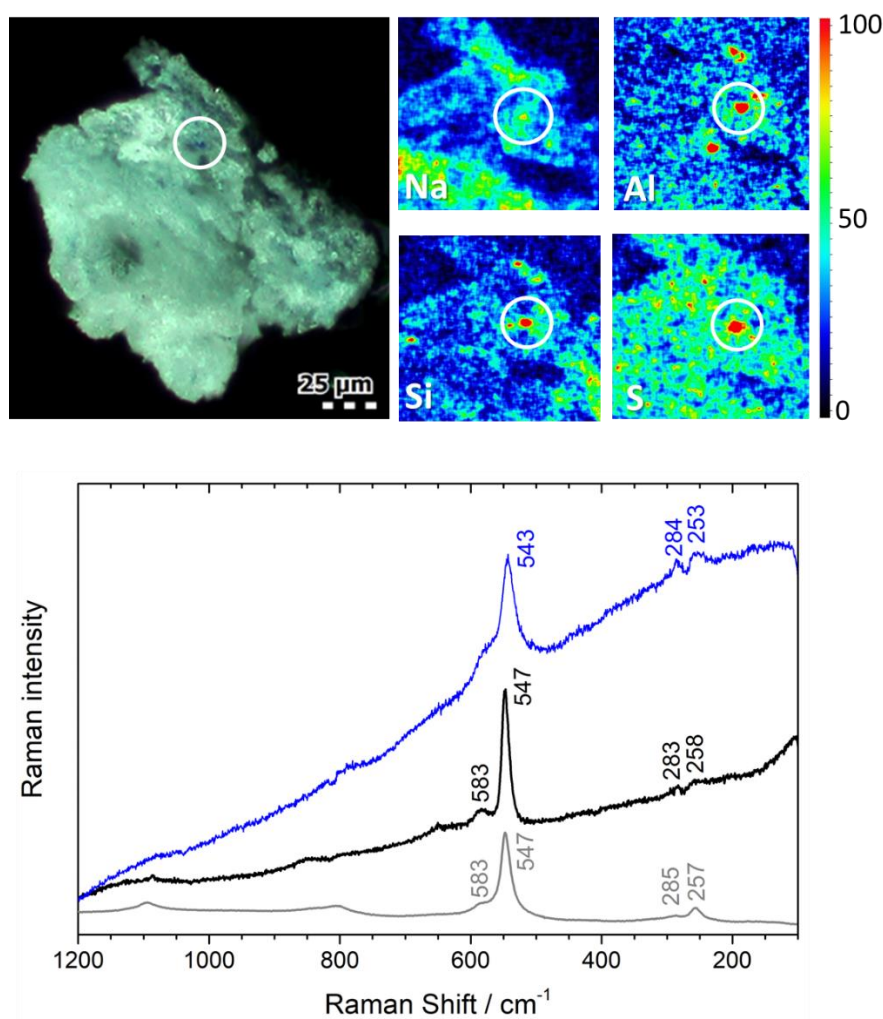


Figure A1.5. SEM-EDS and Raman spectrum of the blue particle found in the 1868 hyatt billiard ball sample. The SEM-ED component images show a zoom of the area where the blue particle was found, where it is possible to detect strong emission from sodium (Na), aluminium (Al), silicon (Si) and sulfur (S). The blue particle was analyzed with μ Raman (blue spectrum, 785nm laser, 4.35mW, 20s, 10 cycles) and a strong band was observed at 543 cm^{-1} . Another blue particle was found in a different microsample and analyzed with μ Raman (black spectrum, 785nm laser, 4.35mW, 150s, 5 cycles). This sample was compressed providing a better-quality Raman spectrum, with the detection of a strong band at 547 cm^{-1} . This band is attributed to the ultramarine blue's symmetric stretching vibration (ν_1) of S^{3-} , as it is possible to compare with a reference Raman spectrum (grey, Casa Ferreira). Other bands were detected at $253\text{-}257\text{ cm}^{-1}$ attributed to the bending vibration (ν_2) of S^{3-} and a unattributed shoulder at 583 cm^{-1} .

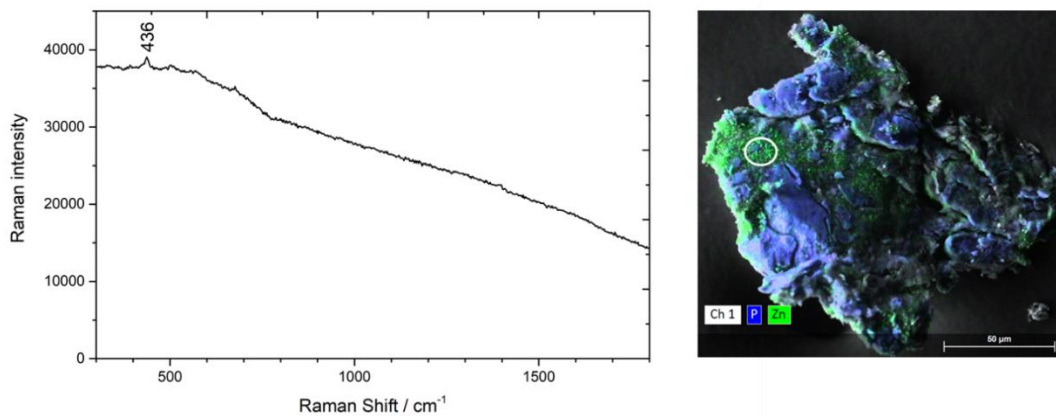


Figure A1.6. μ Raman spectra of the zinc particles (left) found in a microsample of the 1868 billiard ball imaged with SEM-EDS (right). (633nm laser, 4.25 mW, 120s x 5 acquisition time). False color image of the SEM-EDS electron beam-induced X-ray imaging: phosphorous from hydroxyapatite in blue, zinc from ZnO in green. The region of μ Raman analysis is marked by the white circle. Due to the fluorescence detected it was necessary to reduce the laser power and use longer acquisition times.

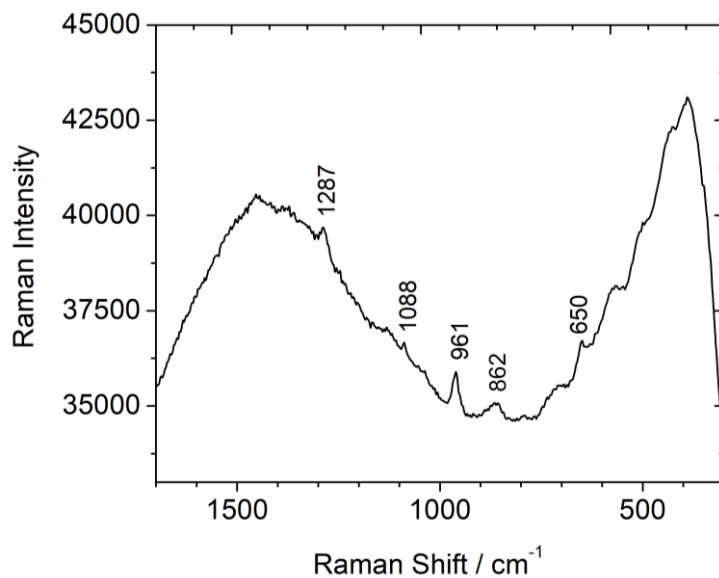


Figure A1.7. Raman MIRA DS spectra obtained from the in-situ analysis of the 1868 billiard ball. Conditions: 1.20s acquisition time, 10 cycles. It was only possible to identify the most intense bands for each of bone, cellulose nitrate, and camphor. This is due to strong background noise. Since this effect was not observed when analyzing pure bone powder, and laser 785nm this does induce strong bone fluorescence this is probably due to another minor component in the mixture, such as a surface treatment, or due to degradation. Calcite (CaCO_3) was also detected by the observation of the characteristic symmetric stretching of the carbonate ($\nu_s\text{CO}_3^{2-}$) at 1088 cm^{-1} . This mineral carbonate does not exist in bone, meaning that it was intentionally admixed, possibly as chalk.

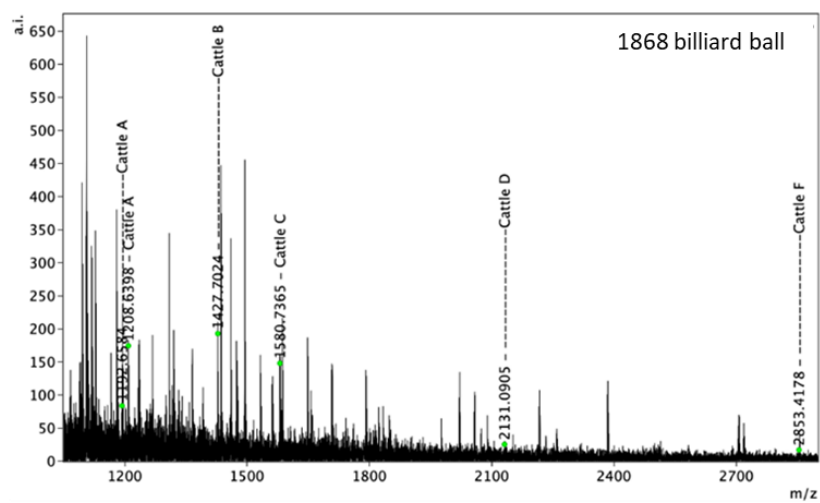


Figure A1.8. Peptide Mass Fingerprint MALDI spectra of the 1868 billiard ball. The cattle markers are indicated in the spectra.

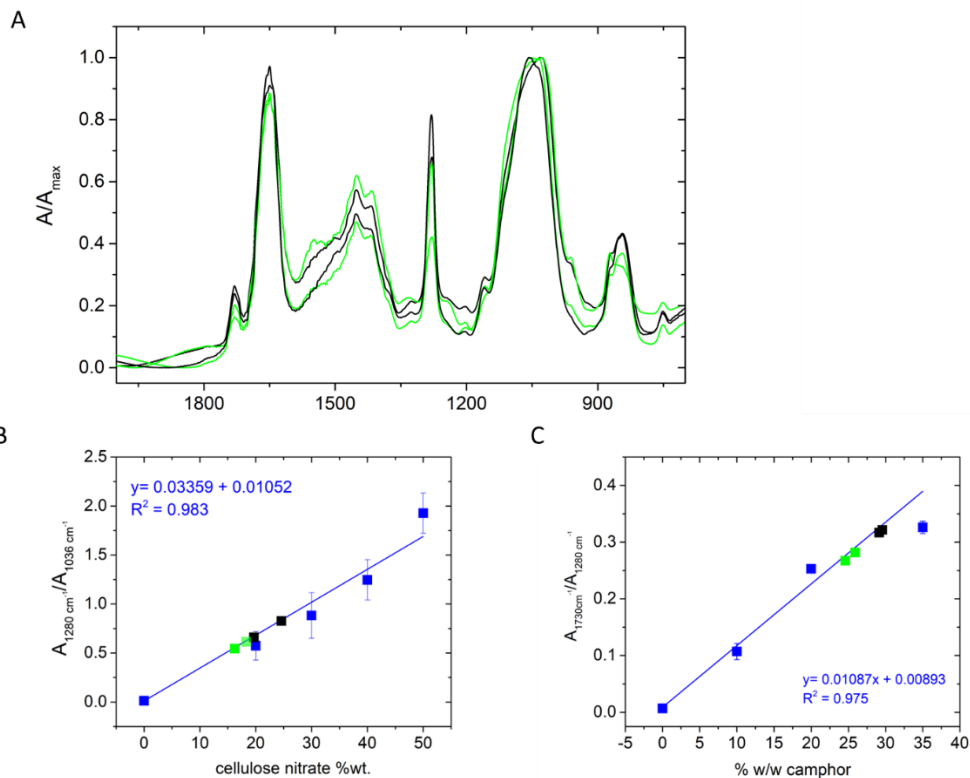


Figure A1.9. Quantification of the bone-cellulose nitrate and camphor-cellulose nitrate formulation of the bonzoline billiard ball. A) Overlay of the infrared spectra of the four microsamples used for the quantification of bonzoline formulation, 2 from the surface (green) and 2 from the interior (black). The spectra are normalized to the maximum (νPO_4^{2-} ($\sim 1036 \text{ cm}^{-1}$) band. C) The cellulose nitrate concentration calculated for the two regions are showed (average 20%, standard deviation 2%). D) The camphor concentrations calculated for the three regions are showed (average 27%, standard deviation 2%).

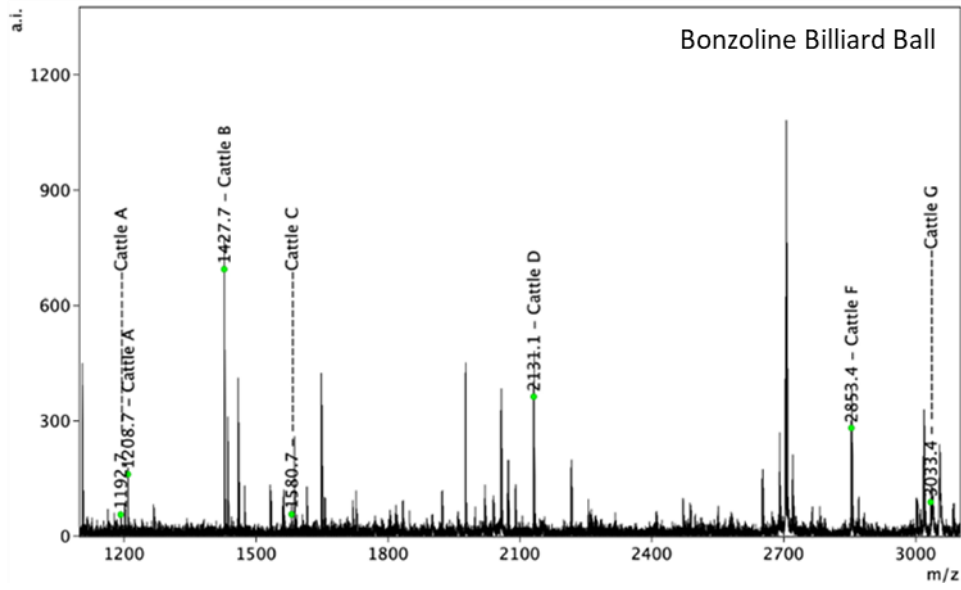


Figure A1.10. Peptide Mass Fingerprint MALDI spectra of the bonzoline billiard ball. The cattle markers are indicated in the spectra.

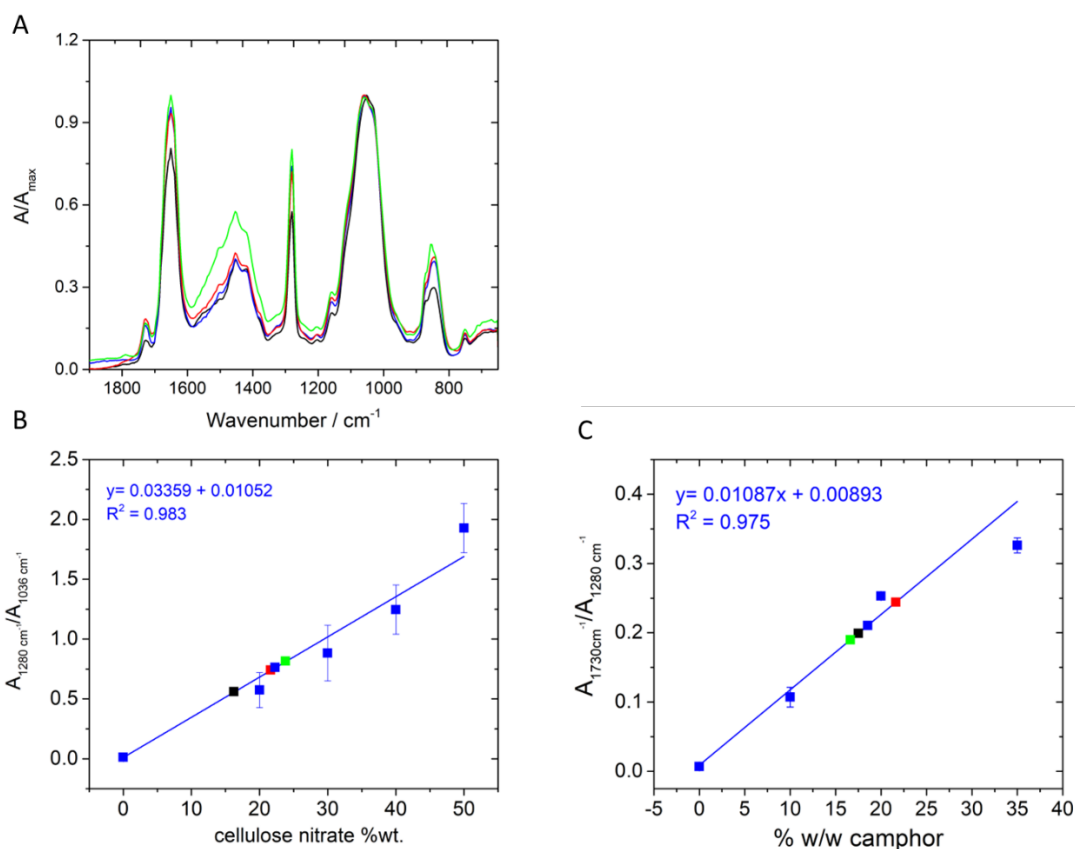


Figure A1.11. Quantification of the bone-cellulose nitrate and camphor-cellulose nitrate formulation of a white crystalate billiard ball. A) Overlay of the infrared spectra of the four microsamples used for the quantification of crystalate formulation, all acquired for the surface of the ball. The spectra are normalized to the maximum (νPO_4^{2-} ($\sim 1036 \text{ cm}^{-1}$) band. C) The cellulose nitrate concentration calculated for the four samples are showed (average 21%, standard deviation 2%). D) The camphor concentrations calculated for the three regions are showed (average 19%, standard deviation 1%).

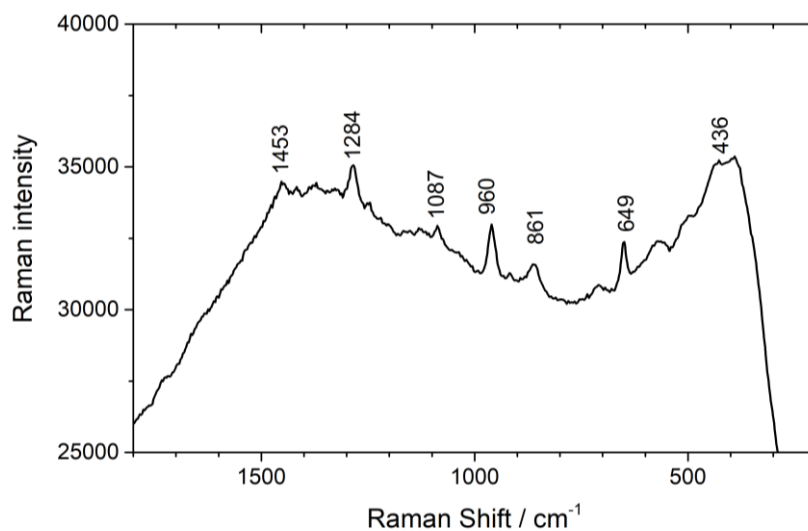


Figure A1.12. Handheld Raman Mira DS spectrum of the white bonzoline billiard ball. (785nm, 7s acquisition time, 10 cycles). The bands of cellulose nitrate groups are observed at 861, 1284 and 1453 cm⁻¹, of camphor at 649 cm⁻¹, hydroxyapatite at 960 cm⁻¹, calcite at 1087 cm⁻¹ and zinc oxide at 436 cm⁻¹.

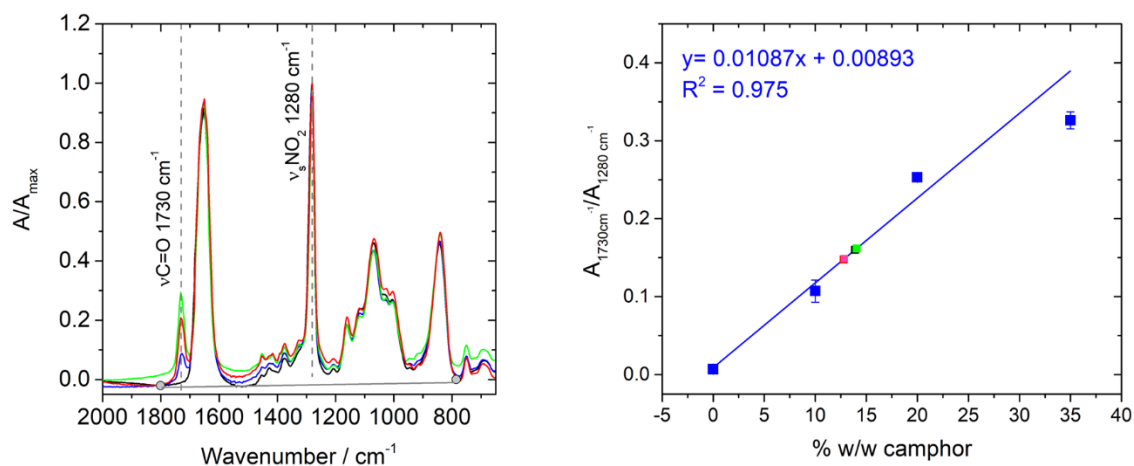


Figure A1.13. Development of the camphor-cellulose nitrate calibration line and quantification of the plasticizer concentration in the 1868 billiard ball. A) Overlay of the infrared spectra of the cellulose nitrate-camphor mixtures, normalized to the maximum (1280cm^{-1}) (%wt. camphor/cellulose nitrate): 100% cellulose nitrate (black), 10/90 (blue), 20/80 (red), 35/65% (green). For the calibration curve, it was used the ratio between the carbonyl band of camphor, at 1730 cm^{-1} , and the $\nu_{\text{a}}\text{NO}_2$ band of the cellulose nitrate, at 1280 cm^{-1} . B) Calibration curve and respective equation and coefficient of determination (R^2) for the linear fitting of the $\nu\text{C}=\text{O}$ 1730 cm^{-1} / νNO_2 1280 cm^{-1} ratio calculated from μFTIR in function of the % w/w of camphor. The data shows the average ratio and the standard deviation calculated from the 3 infrared spectra collected for each reference. The colored points are the quantification of camphor in the 1868 billiard ball based on the analysis of 4 microsamples (average 13%, standard deviation 1%).

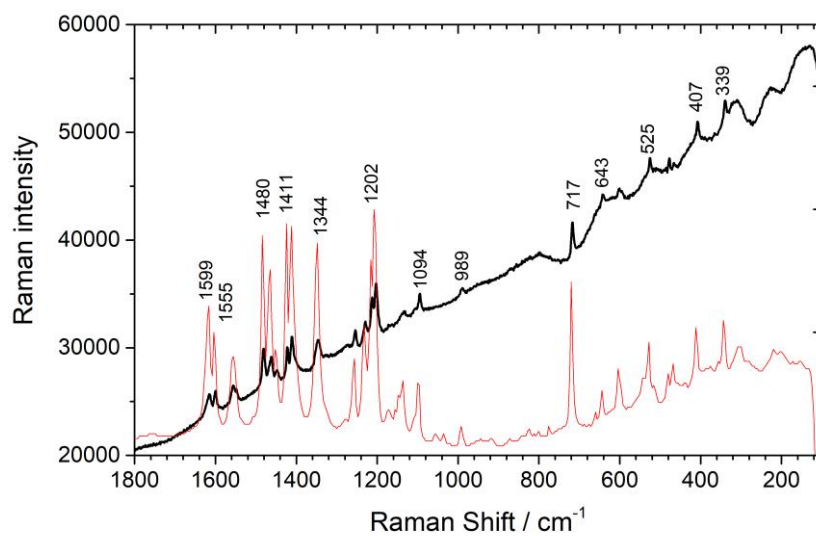


Figure A1.14. μ Raman spectrum of the red bonzoline ball at surface. Conditions: 633nm laser, 4.25 mW, 10s x 5 cycles acquisition time. Compared with a barium lithol red reference. Source: Herbst synthetic pigment database (in red, 633 nm).

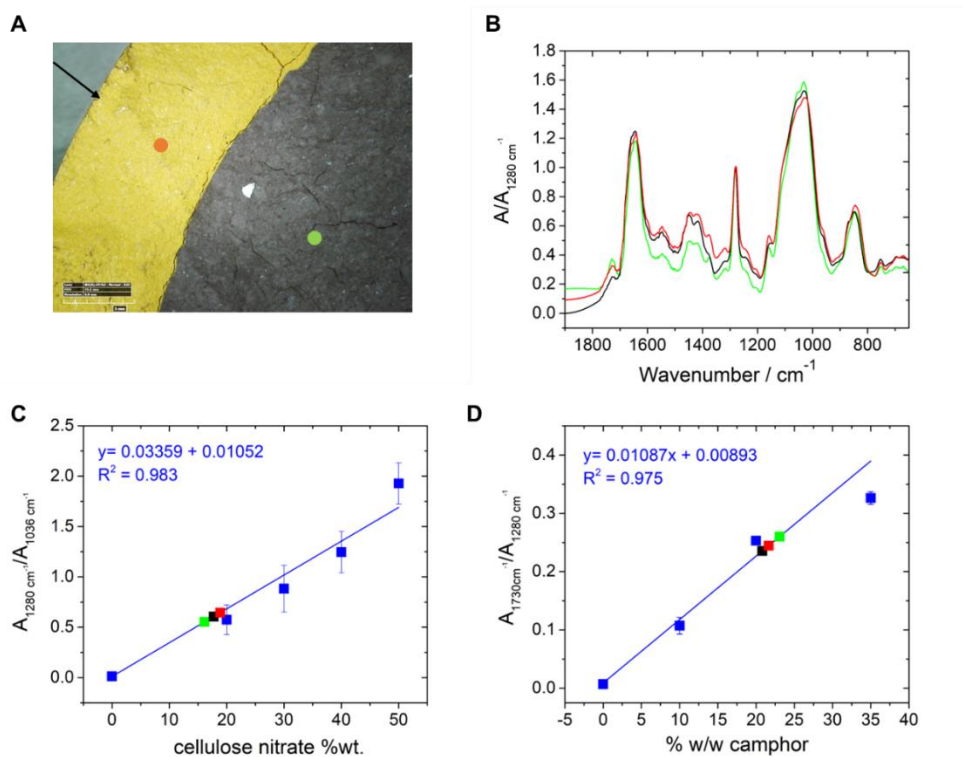


Figure A1.15. Quantification of the bone-cellulose nitrate and camphor-cellulose nitrate formulation of the ivorylene billiard ball. A) Areas of microsampling: surface (black), interior yellow (red) and brown core (green). B) Overlay of the infrared spectra of the three microsamples used for the quantification of ivorylene formulation. The spectra are normalized to the $\nu_s\text{NO}_2$ (1280cm^{-1}) band. C) The cellulose nitrate concentration calculated for the three regions are showed (average 17%, standard deviation 1%). D) The camphor concentrations calculated for the three regions are showed (average 22%, standard deviation 2%).

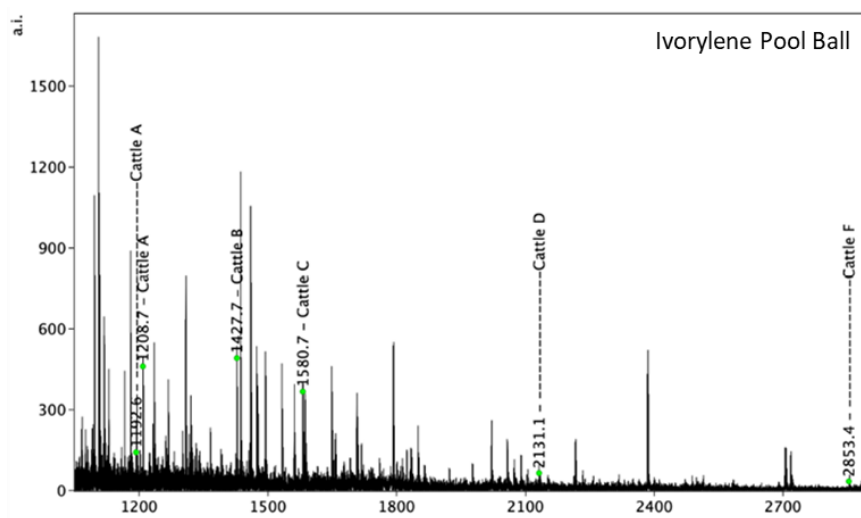


Figure A1.16. Peptide Mass Fingerprint MALDI spectra of the ivorylene pool. The cattle markers are indicated in the spectra.

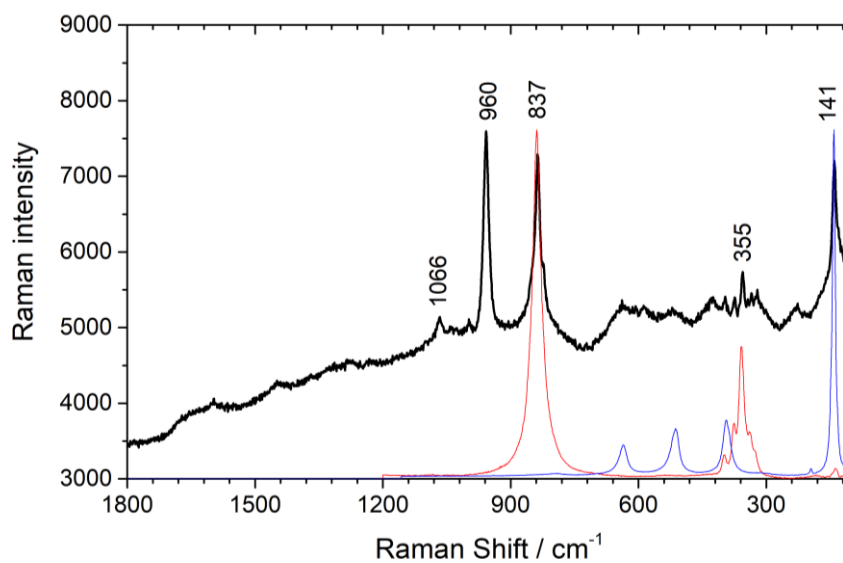


Figure A1.17. μ Raman spectrum of the yellow ivorylene. Conditions: 633nm laser, 4.25 mW, 40s x 5 cycles acquisition time. Compared with a chrome yellow deep ($\text{PbCr}_4\text{O.PbO}$) reference. Source: UCL London (in red, 633nm); and with and anatase (TiO_2) reference. Source: Jobin-Yvon database (in blue, 633 nm). In more detail, chrome yellow was detected through its μ Raman spectra by the observation of the chromate symmetric stretching $\nu_1(\text{CrO}_4^{2-})$ at 837 cm^{-1} and the symmetric bending $\nu_4(\text{CrO}_4^{2-})$ at 355 cm^{-1} , (2). Anatase (TiO_2) was identified by the detection of the characteristic strong and sharp band of the E_g mode at 140 cm^{-1} (3).

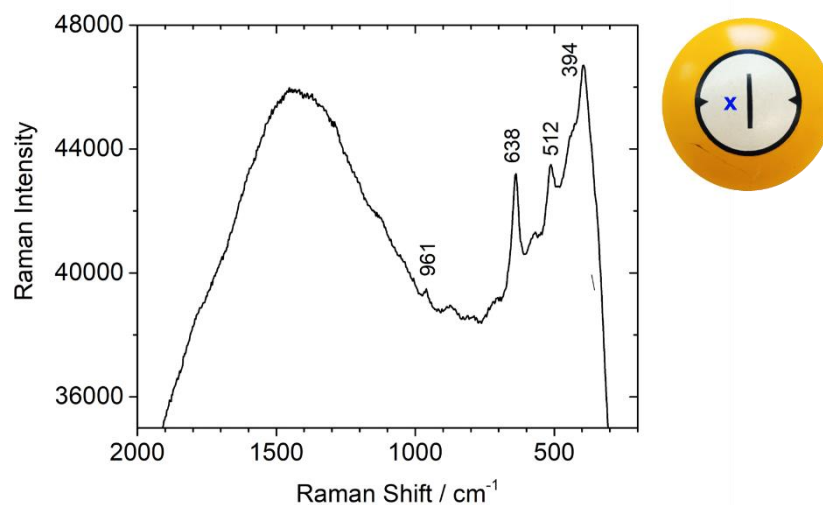


Figure A1.18. Raman MIRA DS spectra obtained from the in-situ Raman MIRA DS analysis of the ivorylene pool ball white number region. The point of analysis is marked with a blue X on the pool ball image. Conditions: 0.5s acquisition time, 10 cycles. It was possible to detect anatase (TiO₂), by the observation of bands at 394, 512 and 638 cm⁻¹ (the strong band at 140 cm⁻¹ is not observed due the equipment specificities). Raman MIRA DS was as an excellent tool to identify in-situ, bone, celluloid, chrome yellow and anatase in complex mixture.

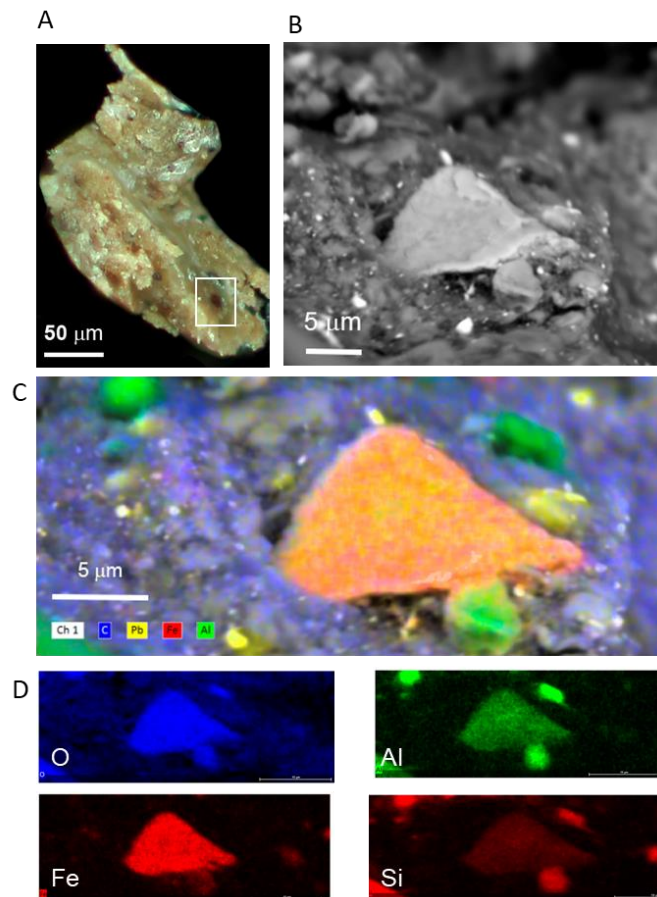


Figure A1.19. SEM-EDS imaging of a dark particle observed in ivorylene's brown core sample. A) Microscope visible light image by SEM of the sample showing the location of the particle. B) Magnification showing the particle's morphology. C) SEM-EDS electron beam induced X-Ray imaging showing the distribution of carbon, lead, iron and aluminum. D) Elemental component images, showing the emission of oxygen (O), aluminum (Al), iron (Fe) and silicon (Si). The dark particle showed significant concentrations of iron (Fe), aluminum (Al) and oxygen (O). Fe/Al oxides have dark toned colors, which correlated with the visual observation of the particle and overall core. These oxides are clay minerals, which indicates to the use of this material in the core of the ball. Around this particle were also found particles of lead (Pb), possibly from chrome yellow, and other unidentified aluminosilicates. In this ivorylene core region, EDS quantification of the concentration of magnesium (Mg) in the bone Ca-P rich phase (correlated to the overall distribution of oxygen) was found to be circa 0.3% mass% (elephant ivory has a higher concentration, around 4 %).

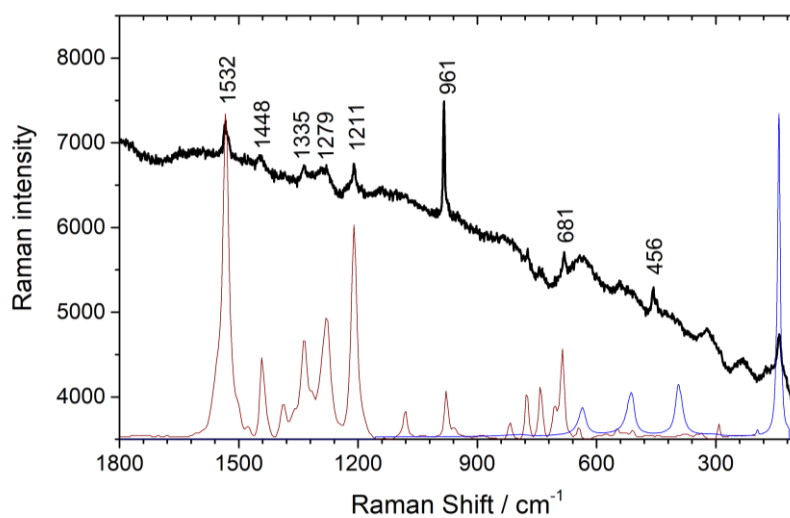


Figure A1.20. μ Raman spectrum of the brown ivorylene core. Conditions: 633nm laser, 4.25 mW, 15s x 5 cycles acquisition time. Compared with copper phthalocyanine green G (PG7) reference. Source: UCL London (in brown, 633nm); and with anatase (TiO₂) reference. Source: Jobin-Yvon database (in blue, 633 nm).



Figure A1.21. Photograph of the Bonzoline Billiard Balls set acquired in this work. In the top lid it is possible to read “Superior to ivory, being more durable, more reliable, and not subject to atmospheric influences. In tropical climates Indispensable.” The bonzoline billiard balls started being manufactured in England in 1931 by the Composition Billiard Ball Supply Co., Stratford, London. Before that they were manufactured in the USA by the Albany Billiard Ball Company.

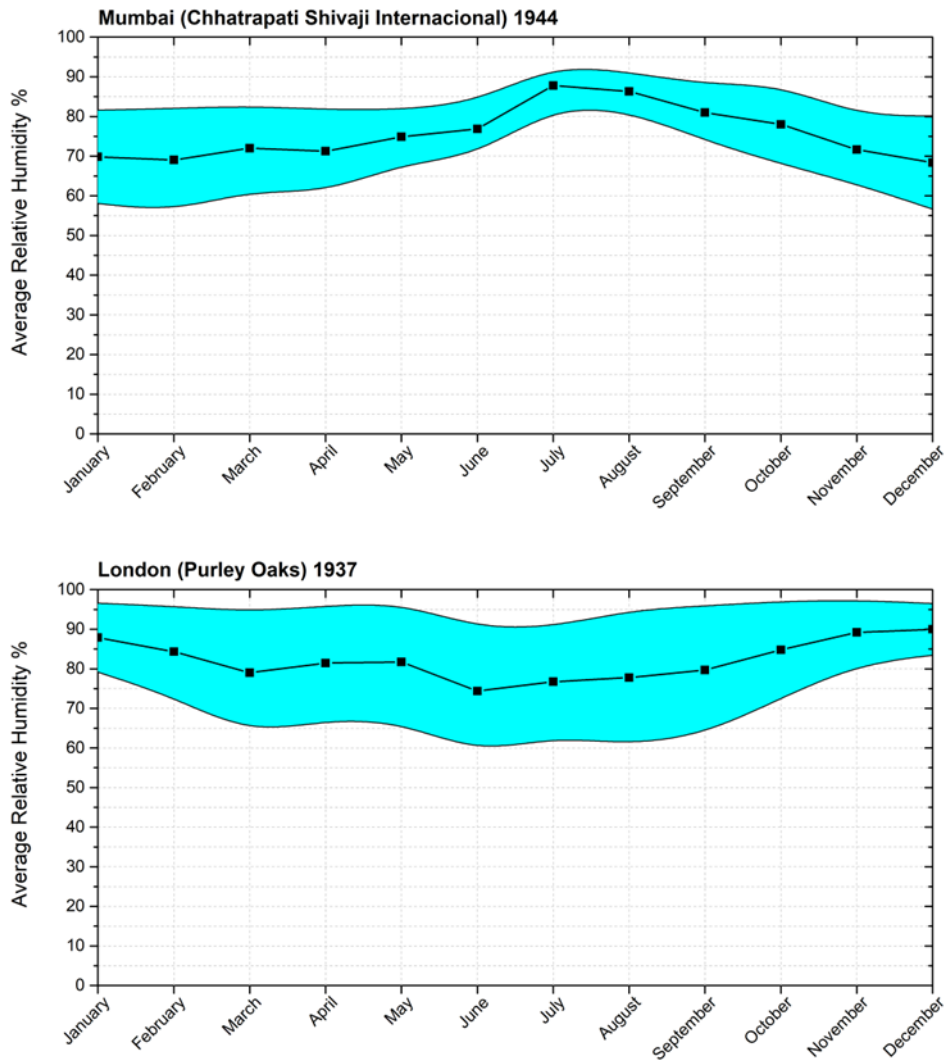


Figure A1.22. Yearly humidity variations (monthly averages and standard deviations) in Mumbai, India, and London, UK, in the years of 1944 and 1937, respectively. The annual standard deviation for Mumbai was 6.3% and for London 4.8%, which is demonstrative of the more prominent humidity fluctuations in the former. Data was acquired from Integrated Surface Dataset (Global) available at National Centers for Environmental Information. The stations (Chhatrapati Shivaji International and Purely Oaks) were selected based on their proximity to the city centers, and the years selected were the oldest available.



Bonzoline Billiard Balls.



**BEST SUBSTITUTE FOR IVORY.
KNOWN ALL OVER THE WORLD.**

To the Bonzoline Manufacturing Company.

"DEAR SIRS,—I have played with all makes of composition billiard balls, and in my opinion

BONZOLINE BILLIARD BALLS
are far the best substitute for ivory, and the most reliable.

"Yours faithfully,

"C. DAWSON (Champion).

"September 22, 1903."

MORE THAN A MILLION BALLS IN DAILY USE.

**10s. 6d. per Ball; Size $2\frac{1}{8}$. Any Colour.
OF ALL BILLIARD FIRMS.**

WHOLESALE ONLY FROM

**The Bonzoline Manufacturing Co., Ltd.,
34 Queen Street, London, E.C.**

Figure A1.23. Charles Dawson, English billiard champion who defended ivory billiard balls in 1899 but later, in 1904, supported the sales of bonzoline. Right, photo of Charles Dawson taken from the book he authored in 1904 "Practical Billiards". Advertisement to the Bonzoline Billiard Balls in 1904, where it is possible to read the supportive statement of the Charles Dawson.



H. W. STEVENSON, Ex-Champion.
The first Player to make 1000 break. 1016 with Bonzoline Balls.
Thurston's, London, October, 1916.

CRYSTALATE  

BILLIARD BALLS. 

*THE ONLY COMPOSITION BILLIARD BALL
MADE IN ENGLAND.*

With these Balls . . .

H. W. STEVENSON,
EX-CHAMPION,
made his **GREAT RECORD BREAK** of
703
at Free Trade Hall, Manchester,
December, 1903, in a match
STEVENSON v. HARVERSON, 9000 UP,
under Association Rules.

"The performances of the Ball speak volumes, and I predict
a great future for it." H. W. STEVENSON, Ex-Champion.

Professionals, the principal Amateurs, and the
Press, all affirm that "Crystalate" is the finest
Billiard Ball in the World.

Sold by Billiard Houses and Sports Depôts throughout the Empire.

. . . THE . . .

ENDOLITHIC MANUFACTURING Co., Ltd.,
POMONA BUILDINGS, LONDON, E.C.

Figure A1.24. Henry W. Stevenson, English billiards champion who played with crystalate and bonzoline balls. Left, Henry W. Stevenson in 1916 when he made the first 1000 break with bonzoline billiard balls. Right, 1904 advertisement to the Crystalate billiard ball with the referral to Henry W. Stevenson.

BAR COUNTERS, BACK BARS, MIRRORS, WINE AND BEER COOLERS

THE BRUNSWICK-BALKE-COLLENDER CO.'S

PRICE LIST OF MATERIALS, 1885-1886.



To prevent your communication falling into hands of unscrupulous imitators be particular to address plainly our full company name on your envelope.

THE BRUNSWICK-BALKE-COLLENDER CO.

Every article mentioned in this Price List with price attached, is warranted for convenience of our customers when ordering. By this arrangement it becomes unnecessary to write the name or description of the goods desired; the number is all that is required. By paying attention to this you will save time and annoyance, but no mistake will be avoided.

BILLIARD CLOTHS TO FIT TABLES

Real Simonis (Guaranteed Genuine).

Number Size of Table.	Exact Size of Bed of Table.	First Quality.	Second Quality.	Third Quality.
5x10	5x9.8	For bed, 17.00 " custom, 8.00	15.00 4.00	12.50 3.00
4.5-2x9	4.4x8.8	For bed, 22.00 " custom, 4.00	19.50 3.50	16.00 3.25
4x8	4.2x8	For bed, 20.00 " custom, 2.50	17.00 3.00	15.00 2.75

PRICE PER YARD.
No. 1. 24 inches wide, per yard \$6.00
No. 2. 24 inches wide, per yard 5.50
No. 3. 24 inches wide, per yard 5.00

SEMONIS CLOTH.

It is not surprising that unappreciated parties have put upon the market an imitation of the celebrated "Simonis" cloth. On the continent of Europe, in England and America, the imitations of Simonis have come into existence, and have succeeded in imitating the genuine so closely in appearance only, that one must be a good judge to detect the difference and determine its value. These imitated productions are imported into this country and offered for sale by small billiard cloth cutters, and respectable dealers of billiard materials, who too often succeed in persuading their patrons, who pay for "the best cloth made," and who seem too little that they have been deceived into purchasing an inferior, short lived, and comparatively worthless cloth.

BILLIARD AND POOL TABLES.

HYATT PATENT BALLS.

We are Sole and Exclusive Agents in the United States for the Manufacture of Billiard and Pool Balls which can only be obtained from the different houses of The Brunswick-Balke-Collender Co.

We hardly see other competition bill from the fact that some give satisfaction when they see the HYATT. These are the only balls we can procure. In case the competition breaks within one year from date of purchase within the term of guarantee, positively be returned balling new balls are forwarded as exchange. Any others, unless authorized as above, will not be considered.

The new style-said throughout will never chip or burn, and are in every respect superior to any.

Important Feature.—They are not affected by temperature or climate and can be safely used at all seasons of the year. They always remain perfectly spherical, and retain their balance, have the same texture, slick, and durability as the best ivory.

No.	HYATT PATENT BILLIARD BALLS.	per set
55	1-2 inch Billiard Balls	\$13.00
56	" " " "	12.50
57	" " " "	11.50
58	" " " "	10.50
59	" " " "	9.50
60	" " " "	8.50
61	" " " "	7.50

LATEST COMBINATION.

Owing to the increased cost of ivory balls, it would not be a bad idea to use, in pairs of four ivory balls, two Hyatt Combination billiard balls, light and dark, and two clear ivory for the cue balls. The combination balls never need combination set, complete.

No. 62. 2.3-Balls, standard size \$18.00
No. 63. 2.7-Balls 19.00

Remember, that by remitting cash, draft, or post office order, with order as per Price List, you save express charges for return of money. Address plainly, THE BRUNSWICK-BALKE-COLLENDER CO.

HYATT PATENT POOL BALLS.

No. 64	3.0 inch, Sixteen Balls	per set	\$45.00
65	" " " "	"	40.00
66	" " " "	"	35.00
67	" " " "	"	30.00
68	" " " "	"	25.00
69	" " " "	"	20.00
70	" " " "	"	15.00
71	" " " "	"	10.00
72	Coloring and Numbering Fancy	per set of 16	5.00
73	" " " "	"	4.00
74	" " " "	"	3.00
75	" " " "	"	2.00
76	" " " "	"	1.00
77	" " " "	"	0.50
78	" " " "	"	0.25
79	" " " "	"	0.10

IVORY BILLIARD BALLS.

None Shipped Unless Thoroughly Seasoned. We use nothing but the superior Zambian soft Ivory, the only such suitable for Billiard Balls. The Egyptian Ivory is not handled by us at all, being in its nature too brittle, although less expensive.

PRICES FOR SINGLE BALL.

No. 80	2.0-3.0 inch, per set of 4	\$25.00
81	" " " "	24.00
82	" " " "	23.00
83	" " " "	22.00
84	" " " "	21.00
85	" " " "	20.00
86	" " " "	19.00
87	" " " "	18.00
88	" " " "	17.00
89	" " " "	16.00
90	" " " "	15.00
91	" " " "	14.00
92	" " " "	13.00
93	" " " "	12.00
94	" " " "	11.00
95	" " " "	10.00
96	" " " "	9.00
97	" " " "	8.00
98	" " " "	7.00
99	" " " "	6.00
100	" " " "	5.00
101	" " " "	4.00
102	" " " "	3.00
103	" " " "	2.00
104	" " " "	1.00

All Clear Balls per set, \$2 extra for every size. Season-Checked Balls, 30 per cent. less.

IVORY FIFTEEN-BALL POOL BALLS.

No. 105	2.3-3.0 inch Fifteen-Ball Pool Balls	per set of 15	\$95.00
106	" " " "	"	90.00
107	" " " "	"	85.00
108	" " " "	"	80.00
109	" " " "	"	75.00
110	" " " "	"	70.00
111	" " " "	"	65.00
112	" " " "	"	60.00
113	" " " "	"	55.00
114	" " " "	"	50.00
115	" " " "	"	45.00
116	" " " "	"	40.00
117	" " " "	"	35.00
118	" " " "	"	30.00
119	" " " "	"	25.00
120	" " " "	"	20.00
121	" " " "	"	15.00
122	" " " "	"	10.00
123	" " " "	"	5.00
124	" " " "	"	0.00

IVORY PIGEON-HOLE BALLS.

No. 125	2 inch Pigeon-Hole Balls (20)	per set	\$13.00
126	" " " "	"	12.00
127	" " " "	"	11.00
128	" " " "	"	10.00
129	" " " "	"	9.00
130	" " " "	"	8.00
131	" " " "	"	7.00
132	" " " "	"	6.00
133	" " " "	"	5.00
134	" " " "	"	4.00
135	" " " "	"	3.00
136	" " " "	"	2.00
137	" " " "	"	1.00
138	" " " "	"	0.50
139	" " " "	"	0.25
140	" " " "	"	0.10

BALL RACKS.

No. 141	10 Ball Pool Rack, New York Style, side Rack	per set	\$5.00
142	" " " "	"	4.00
143	" " " "	"	3.00
144	" " " "	"	2.00
145	" " " "	"	1.00
146	" " " "	"	0.50
147	" " " "	"	0.25
148	" " " "	"	0.10
149	" " " "	"	0.05
150	" " " "	"	0.02

BRUSHES.

No. 151	Brushes, each	No. 1, \$2.00. No. 2, \$1.60. No. 3, \$1.00.
152	Brushes of extra fine quality	No. 1, \$2.00. No. 2, \$1.60. No. 3, \$1.00.

BILLIARD HALL CHAIRS.

These chairs are manufactured expressly for The Brunswick-Balke-Collender Co. As per price list, you will observe the magic chair seat and rollers, per dozen less than the usual, although they are made in the same style and pattern, the extra price being only one cent of the more expensive model.

SOLID WELAUX, NO. 1 FINISH.

No. 153	Double Cane Seat and Back, Plain Arm	Chair No. 104	\$24.00
154	" " " "	"	22.00
155	" " " "	"	20.00
156	" " " "	"	18.00
157	" " " "	"	16.00
158	" " " "	"	14.00
159	" " " "	"	12.00
160	" " " "	"	10.00
161	" " " "	"	8.00
162	" " " "	"	6.00
163	" " " "	"	4.00
164	" " " "	"	2.00
165	" " " "	"	1.00
166	" " " "	"	0.50
167	" " " "	"	0.25
168	" " " "	"	0.10
169	" " " "	"	0.05
170	" " " "	"	0.02

Remember, that by remitting cash, draft, or post office order, with order as per Price List, you save express charges for return of money. Address plainly, THE BRUNSWICK-BALKE-COLLENDER CO.

Figure A1.25. Page from the Brunswick – Balke – Collender Co. 1885 catalog with the price information for "Hyatt Patent Balls" and ivory balls (source: Brunswick digital library).

Ivorylene Pocket Balls

The Popular Pocket Billiard Ball

Furnished in
two sizes,
2¼-inch
standard size,
\$20.00
per set
and
2⅝-inch
professional
size,
\$25.00
per set

Genuine Ivory Pocket Balls

16 to a Set

No.	Size	Clear	Enameled		Seasoned	Checked and Sand Cracked
3-7	2¼-in.	\$220.00	\$154.00	3-7	2¼-in.	\$130.00 to \$212.00
3-7	2⅝-in.	284.00	200.00	3-7	2⅝-in.	156.50 to 240.00

Figure A1.26. Clippings from the Brunswick – Balke – Collender Co. 1928 catalog with the prices of ivorylene and ivory pool sets (source: Brunswick digital library).



Figure A1.27. Photograph of the Bonzoline Billiard Balls set acquired in this work. Weights from left to right: 73.559g, 73.348g, 73.089g.



Figure A1.28. Photograph of the NMAH's ivory billiards balls, dated from 1875-1920 (ID Number CL.329507). The dimensions and weight of left and right billiard balls were measured: 57mm and 174.2g; 54mm and 143.8g, respectively.

Table A1.1. Transcriptions of the formulations for the manufacture of billiard balls and imitation ivory patented by John Wesley Hyatt and co-inventors from 1865 to 1915.

Title	Formulation	Patent	Com- pany
<i>Billiard-Balls</i>	<i>I take shellac dissolved in alcohol and mix with it a sufficient quantity of ivory-dust, or bone-dust, or other ingredients, so as to form a paste which can be spread. For white balls I take bleached shellac and mix some white lead or other white paint with the ivory or bone-dust; and for colored balls I mix vermilion or other colored paint with the above-described composition. For colored balls the shellac may be dark</i>	J.W. Hyatt, 1865, USP 50359	-
<i>Improve- ment in composi- tions for billiard balls and other arti- cles</i>	<i>First, I take paper-pulp, thoroughly saturated with water, so that it is in a semi-fluid condition. While in this condition I mix with it the flour of gum-shellac, or any other similar fusible water-proof gum, by thoroughly stirring them together. The proportions of the gum to the paper-pulp are about equal in quantity by weight in a dry state(...)The specific gravity of the composition may be adjusted by the addition of white lead, or any suitable pigment, to the gum (...)To color the composition, the pulp may be colored as desired before use, or aniline red, or other coloring matter which will dissolve in alcohol (...)</i>	J.W. Hyatt, 1868, USP 76765	-
<i>Improved molding composi- tion to imi- tate ivory and other composi- tions</i>	<i>Take any kind of fibrous vegetable, animal, or even mineral matter, such, for instance, as paper, leather-chips, or asbestos, and reduce the same to a very fine state (...) I also use gum-shellac, or any other solid, fusible, and adhesive gum or substance (...) and reduce the same to a very fine powder. This cement I thoroughly intermix (...) both being in as dry a state The proportions of the cementing substance to the fibrous material are about equal in quantity by weight, although I do not confine myself to these proportions (...) If desirable, the specific gravity of the article or articles can be regulated by the use of white lead or other suitable pigment.</i>	J.W. Hyatt, 1869, USP 88633	The Hyatt Mfg. Co., Albany, New York
<i>Improved method of</i>	<i>I take a ball which is made of composition, or a substance of inferior appearance, and suspend it between two points, so that it can be rotated freely about its axis. While thus held</i>	J.W. Hyatt, 1869, USP 88634	The Hyatt Mfg.

coating bil- liard-balls	<i>the ball is dipped into a solution of collodion, and when re- moved therefrom it is rotated slowly, to cause the collodion to flow evenly over its surface, and when dry to form thereon a thin skin or coating.</i>			Co., Al- bany, New York
Improved compound of ivory dust and other mate- rials	<i>We form the collodion by taking say, one pound of guncotton and dissolving it in a mixture of equal parts of alcohol and ether, in sufficient quantity to produce a thick solution. With this solution we mix three pounds of ivory-dust, pulverized very fine and purified, forming the whole into a plastic mass.</i>	J.W. Hyatt and D. Blake, 1869, USP 89582	-	
Improved method of making solid collo- dion	<i>We place soluble cotton, pyroxyline, or prepared cellulose into a strong cylinder or suitably-shape mold. With the py- roxyline may be mixed ivory-dust, bone-dust, asbestos, flake- white, or any other desirable substance, according to the na- ture of the product required (...) the proportion of the solvent the pyroxyline is as five to ten, seven to ten, or equal parts, by weight, according to the nature and proportions of the compound. When pyroxyline is used alone, from one-half to three-fourths, by weight, of solvent will be sufficient; but when ivory-dust or another material is added, a somewhat greater proportion of solvent will be required.</i>	J.W. Hyatt and I.S. Hyatt, 1869, USP 91341	-	
Improve- ment in treating and mold- ing pyroxy- line	<i>(...) we mix therewith finely pulverized gum-camphor in about the proportions of one part (by weight) of the camphor to two parts of the pyroxyline when in a dry state. This pro- portions may somewhat be varied with good results.</i>	J.W. Hyatt and I.S. Hyatt, 1870, USP 105338	-	
Improve- ment in processes of coating bil- liard-balls, knife-han- dles and other arti- cles	<i>I prepare the collodion by mixing sufficient alcohol and ether with guncotton to make a thick plastic mass, something like the consistency of dough, and then mold it upon the article to be coated therewith.</i>	J.W. 1871, 114945	Hyatt, - USP	

<i>Improve- ment in factitious ivory</i>	<i>We take, say, one hundred parts by weight of ivory dust, one hundred parts of pyroxyline,(by which term we mean soluble nitrocellulose), and fifty parts of powdered gum-camphor.</i>	J.W. Hyatt and I.S. Hyatt, 1874, USP 156354	The Celluloid Mfg. Co., New York
<i>Improve- ment in si- licious ma- terials to imitate ivory and similar substances</i>	<i>To finely-pulverized bone, horn, hoof, ivory, ivory-nut, or other similar substance containing gluten, albumen, and animal oils (...) added two (2) equal portions, by weight, of a solution of any of the alkaline silicates - silicate of soda preferred – the silicate being of the consistency of syrup or molasses</i>	J.W. Hyatt and C. M. Hyatt, 1878, USP 201348	-
<i>Factitious material to imitate ivory, horn, etc.</i>	<i>The complete formula, therefore, will be, of bone-dust, seventeen parts; of the solution of gum (four parts of bleach shellac, one part of borax and six parts of water), twenty-one parts; of boracic acid, one and one-half part.</i>	J.W. Hyatt, C.S. Lockwood, J.H. Stevens, 1880, USP 236034	Bon-silate Company, Newark, New Jersey
<i>Manufac- ture of a factitious material to imitate ivory</i>	<i>(...) The solution will consist of eight parts of shellac, thirty-two parts of ammoniacal water, and forty parts of zinc oxide.</i>	J.W. Hyatt, 1881, USP 239794	-
<i>Plastic composi- tion for the cores of bil- liard balls and for</i>	<i>In practicing the method last above referred to, I take a good article of glue, preferably in the form of powder, which is dissolved in a proper quantity of water by means of heat. After a solution has been formed, I add a percentage of glycerine, together with comminuted bone or its equivalent, and mix the elements in the most</i>	C.S. Lockwood, 1882, USP259878	Bon-silate Company, (Lim-ited), Albany,

<i>other purposes</i>	<i>thorough manner possible, adding a pigment, earth or mineral matter, or coloring agent, if desired (...)</i>		New York
<i>Process of and apparatus for molding plastic materials</i>	<i>The invention has relation to an improved process and apparatus to be used in the application of an exterior section or coating to articles having a core or interior portion made of material different from the exterior part. (no formulation is given)</i>	J.W. Hyatt, C.S. Lockwood, 1882, USP 259984	Bonsilate Company, (Limited), Albany, New York
<i>Plastic material</i>	<i>In practicing my invention, I take, say, eight pounds of bone, ivory, horn, fish scales, quills, or other materials from the same nature (...) two ounces of phosphate of ammonia (...) two pounds of shellac (...) and mix the elements thoroughly together.</i>	C.S. Lockwood, 1883, USP 283793	Bonsilate Company, (Limited), Albany, New York
<i>Plastic material</i>	<i>The ingredients having been prepared, I take about eight pounds of pulverized bone and add to it about two ounces of phosphate of ammonia.</i>	C.S. Lockwood, 1884, USP 283793	Bonsilate Company, (Limited), Albany, New York
<i>Game-Ball with composition coating</i>	<i>This invention relates to the manufacture of balls having a composition coating which is molded while in a plastic condition upon a hard core and allowed to harden and season there on. Celluloid, casein compounds, hard rubber, and other compositions are used for such purposes.</i>	J.W. Hyatt and C. H. Hyatt, 1915, 1156144	-

SI References

1. I. Kontopoulos, S. Presslee, K. Penkman, M. J. Collins, Preparation of bone powder for FTIR-ATR analysis: The particle size effect. *Vib Spectrosc* 99, 167–177 (2018).
2. L. Monico, K. Janssens, E. Hendriks, B. G. Brunetti, C. Miliani, Raman study of different crystalline forms of PbCrO_4 and $\text{PbCr}_{1-x}\text{SxO}_4$ solid solutions for the noninvasive identification of chrome yellows in paintings: a focus on works by Vincent van Gogh. *Journal of Raman Spectroscopy* 45, 1034–1045 (2014).
3. T. Ohsaka, F. Izumi, Y. Fujiki, Raman spectrum of anatase, TiO_2 . *Journal of Raman Spectroscopy* 7, 321–324 (1978).

Appendix 2.

Safeguarding our dentistry heritage: a study of the history and conservation of nineteenth-twentieth century dentures

"You'll Come Out Smiling"

Modern Pain Reducing Methods Used in My Office

WHY suffer? Are you troubled with a run-down, sluggish feeling, rheumatism, stomach trouble, indigestion, headaches or many other ills of your body and **WONDER WHY?**

DOCTORS, life insurance companies and other authorities on human health will tell you that long life depends largely on good teeth. Why risk your health? Every day you let your teeth go, the larger your dentist bill will be.




Set of Teeth
My Regular \$20
Value—Special Price



\$15

\$25 Set of Teeth	\$20
\$35 Set of Teeth	\$25
Gold Crowns	\$5
Bridgework	\$5
Fillings from	\$1

Extractions, \$1 and \$2
These plates are guaranteed to fit and the teeth set to look natural.

Hecolite Plates



The Most Natural and Beautiful Teeth Made. All Pink Natural Gums Special for One Month

\$27.50 per plate

There is no reason why you shouldn't have one of these plates.
SEE OUR SAMPLE AND BE CONVINCED

Personal Attention Given by Dr. Leon
33d Year of Practice

GAS \$2 Per Administered 2 Tooth Plates Repaired While you \$1.50 wait 1 up

Advice Free
Work Guaranteed
Extraction Free
When New Teeth are Ordered

TERMS MAY BE ARRANGED

Dr. LEON Cor. 7th & E Sts. N.W.
Entrance on 7th St. Over Liggett's Drug Store

OPEN EVENINGS. Hours: 9 A.M. to 8 P.M.; Sunday, 10 A.M. to 1 P.M.

Figure A2.1. Advertisement for Hecolite in the Evening Star, Washington, D.C, Friday, February 8, 1935.

DR. EITELJORG and Associated DENTISTS
Indiana's Oldest and Largest Dental Office

3 WHOLE FLOORS
3 OFFICES in 1

Complete X-RAY
Full Mouth
 Why take chances with your teeth and health when you can have a reg. \$10 X-RAY EXAM. for.....
\$1.50

Nature's Closest Competitor
Alco-Lite PLATE
*Beautiful as a Pink Shell
 Light Weight and Very Strong
 More Comfortable to Wear*
 Now at the Lowest Price in History

\$13.50
\$15.00
\$17.50

A New Special PLATE
 Now you can enjoy the pleasure of a quality plate, guaranteed to fit, at the lowest price we've ever offered,
\$9.00
 Worth at Least \$15
 What a Value

Our Super-Special PLATE
 We used to get \$20 for this fine plate—and it's worth it. Made in our own lab. Guaranteed to fit.
\$10

22K CROWNS BRIDGES
 Highest quality workmanship. Low as.....
\$4

Safe, Painless EXTRACTION FREE
with Plates or Brackets

34 Years Here

EASY PAYMENTS IF DESIRED
DR. EITELJORG
and Associated Dentists

2 Doors East of Meridian St. 8 E. WASH. ST. Telephone Riley 7010

Figure A2.2. Advertisement for Alcolite in the Indianapolis Times, March 21, 1933



Figure A2.3. Resovin dental plate from the Smithsonian Collection, ID number MG.260892.295.









Figure A2.4. Raman MIRA DS analysis of the swaged gold and celluloid dental plate JUSTI 21 from NMD (left) and of the vulcanized rubber and Vitallium alloy denture MG.291116.0046 from NMAH (right), using the 3mm distance objective set up.



Figure A2.5. NMAH's dentures and micro sampling location. Denture photographs source: Smithsonian Institution.

Table A2.1. NMD’s denture and sampling location. The microscope images were collected with a DINO-LITE digital microscope.

Denture and sampling location	Microscope image of sampling location
 <p data-bbox="199 831 335 864">Kellmer 95</p>	
 <p data-bbox="199 1249 351 1283">2002.99.4797</p>	
 <p data-bbox="199 1809 351 1843">2002.99.5496</p>	



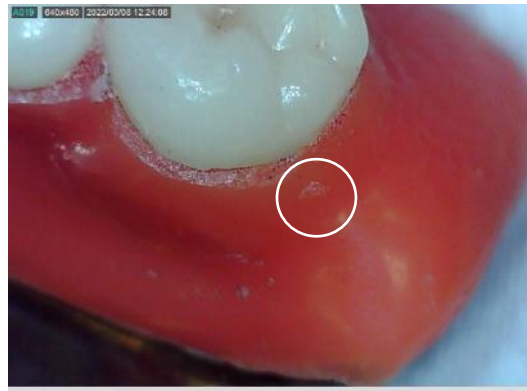
2002.99.5831



JUSTI 23



JUSTI 24



SSW21





92.2.0924



2002.99.5780





Figure A2.6. Right, celluloid denture inside the X-ray fluorescence spectrometer S1 Titan analysis chamber. The analysis area where the x-ray beam interacted with the object is beneath the denture. The chamber lid was closed for analysis. Left, different view where it is possible to see the X-ray fluorescence spectrometer S1 Titan beneath the analysis chamber. The trigger had to be pressed during the analysis; the time corresponding to the acquisition time.

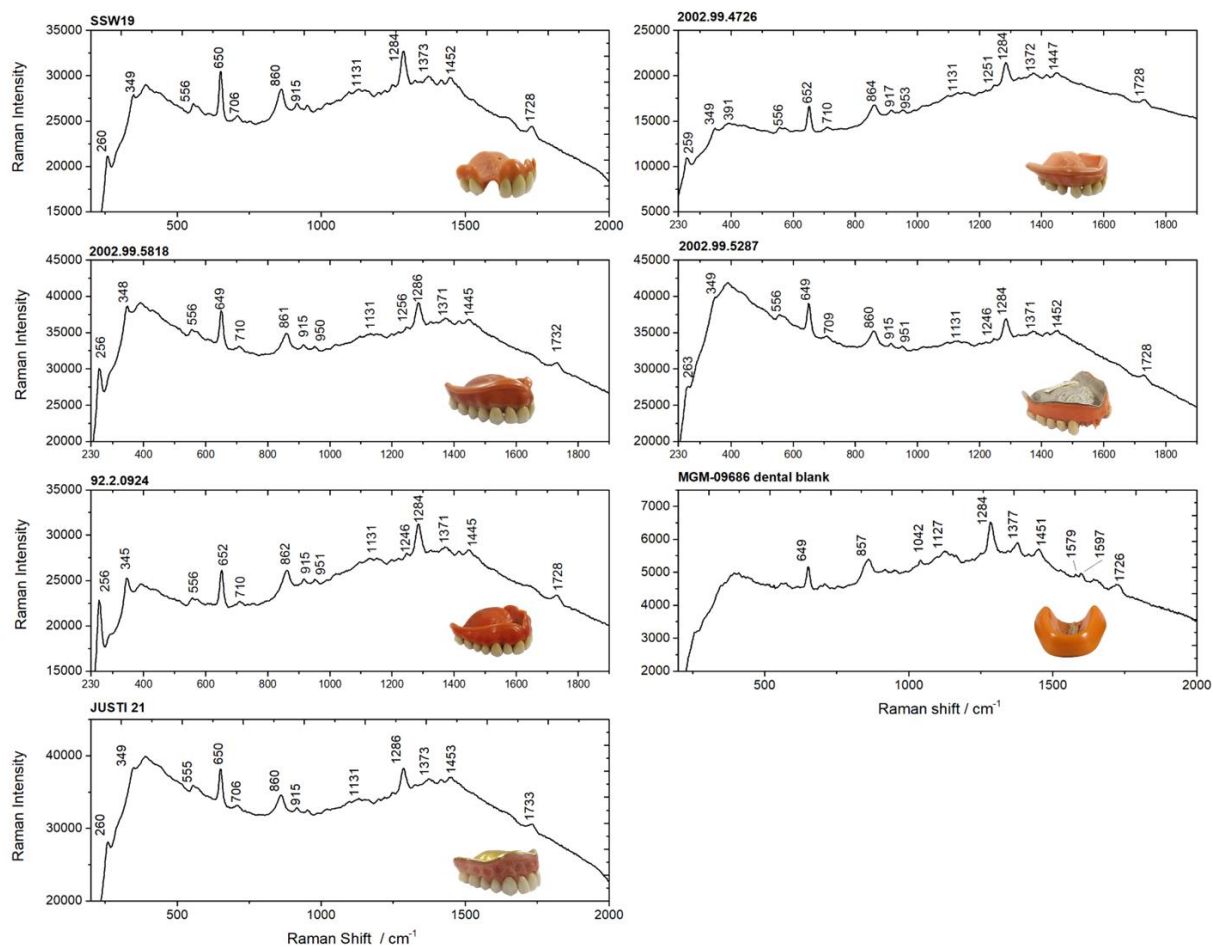


Figure A2.7. Handheld Raman spectra of the celluloid dentures' from NMD and NMAH, namely SSW19 (10s), 2002.99.4796 (7s), 2022.99.5818 (8s), 2022.99.5287 (6s), 92.2.0924 (10), MG.M-09686 dental blank (2.6s) and JUSTI 21 (7s)

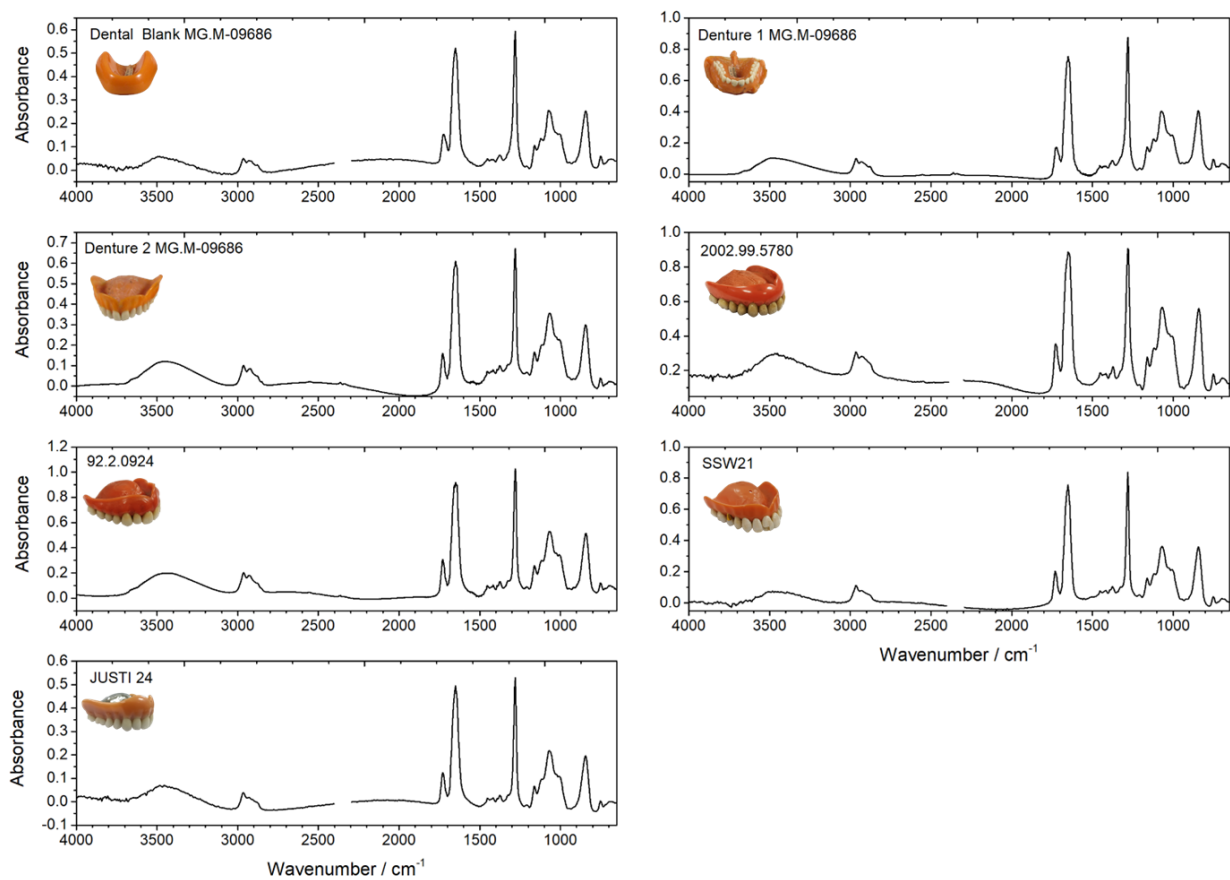


Figure A2.8. Infrared spectra of the celluloid dentures' microsamples from NMD and NMAH.



Figure A2.9. Photographs with a 65MP camera (top) and with a Dinolite USB digital microscope AM2111-0.3MP (bottom) showing the conservation condition of 2002.99.5780.

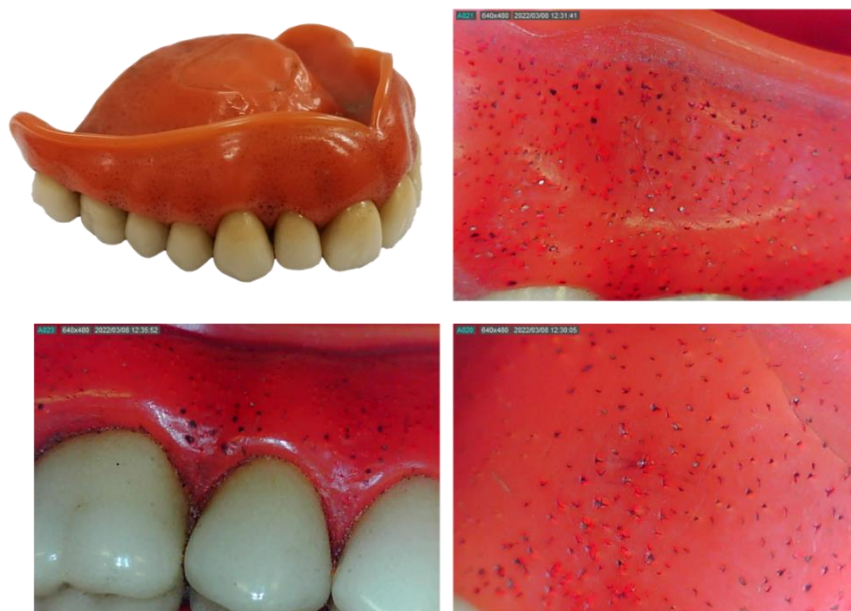
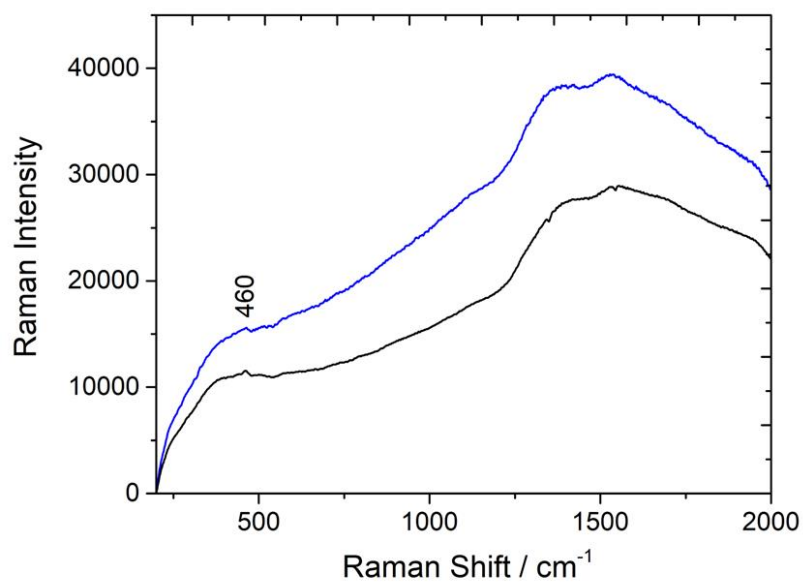


Figure A2.10. Photographs with a 65MP camera (top) and with a Dinolite USB digital microscope AM2111-0.3MP (bottom) showing the conservation condition of 92.2.0924, namely the pitting effect at the celluloid gums.



SSW19



MG.M-09686 denture 1

Figure A2.11. Handheld Raman spectra of the teeth of celluloid dentures SSW19 (2s) and MG.M-09686 denture 1 (3.7s). The tooth analyzed for each denture is identified with a circle.

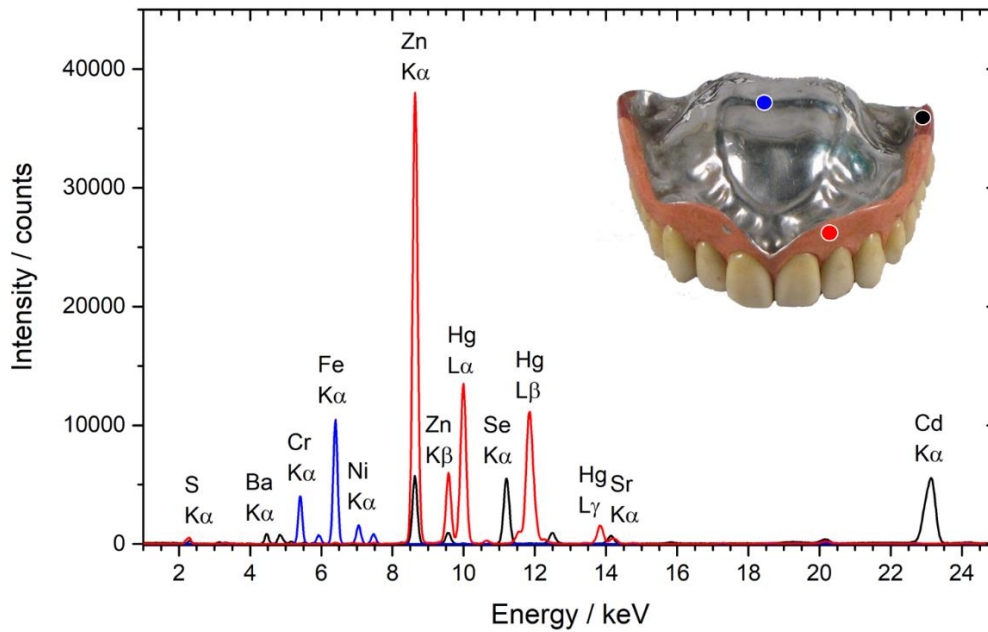


Figure A2.12. XRF spectrum of NMAH’s vulcanized rubber denture MG.291116.0046 in three different points, marked in the denture’s photograph.

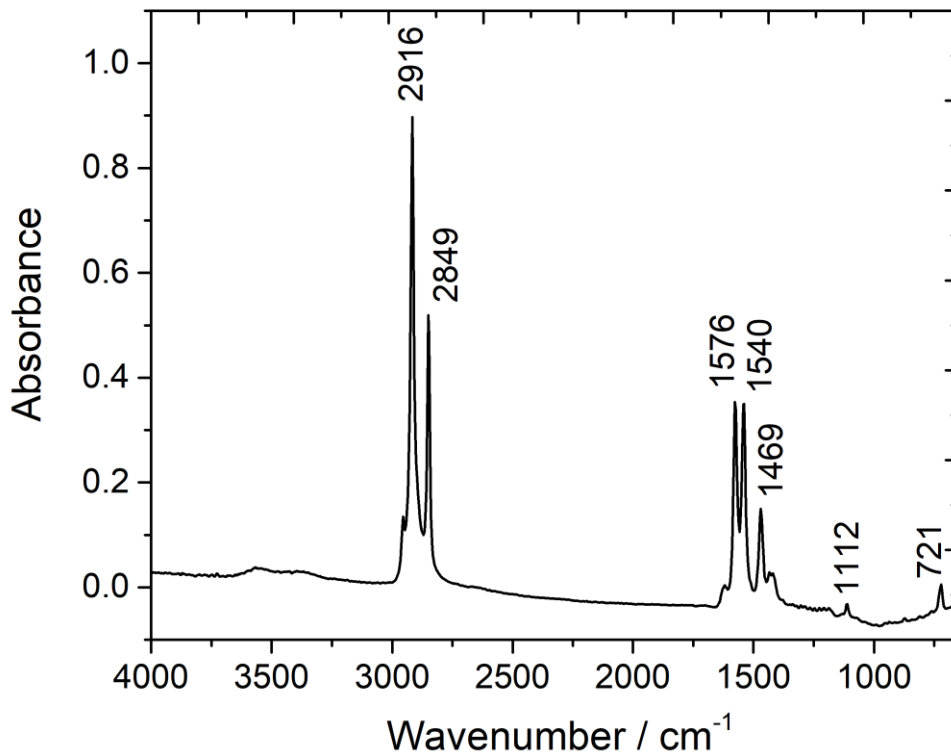


Figure A2.13. Infrared spectrum of a calcium stearate reference, for more details on this reference preparation and characterization please see Otero et al. (2014).

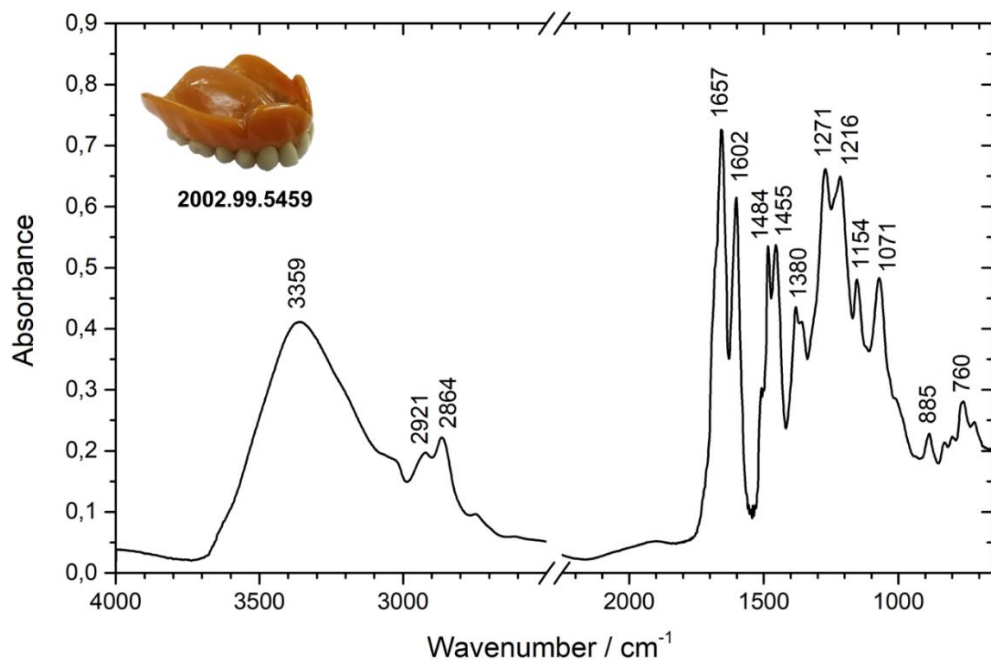


Figure A2.14. Infrared spectra of NMD dental plate 2002.99.5496 (probably a *Luxene* dental plate from the Bakelite Corporation).

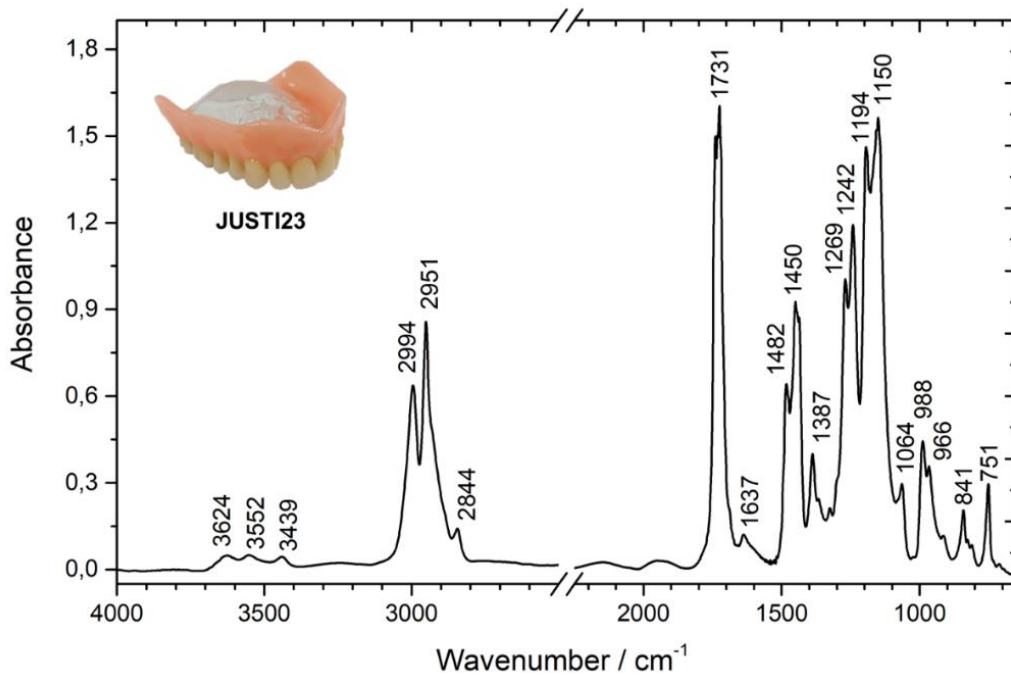


Figure A2.15. Infrared spectra of NMD dental plate JUSTI 23 identified as PMMA. Bands at 1731 and 1150 cm⁻¹ are saturated.

Appendix 3. The materiality of the “best Portuguese comb”: Evolution of the comb industry in Portugal, c. 1880-1970.

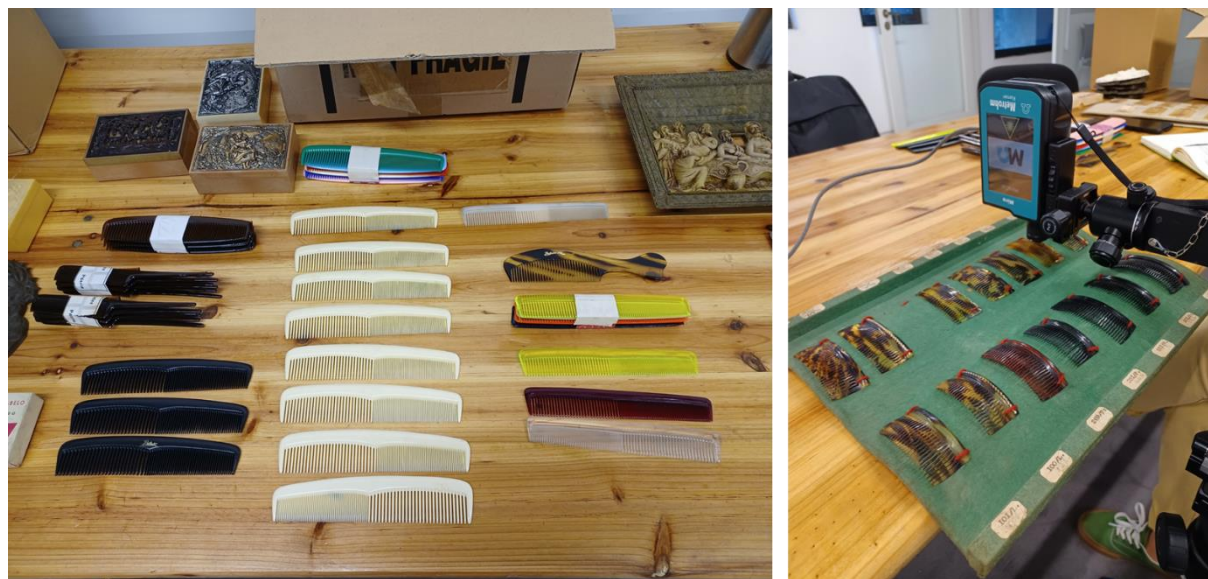


Figure A3.1. Left, overall view of some of the objects from “Fábrica de Plásticos Pátria” from Casa de Memória de Guimarães. Right, the analysis with Raman MIRA DS of celluloid imitation tortoiseshell combs from João Teixeira’s collection in Casa de Memória de Guimarães.



Figure A3.2. Overview of some of the objects from “Fábrica de Pentes Pátria” and their Raman MIRA DS analysis at Sociedade Martins Sarmento, Guimarães.

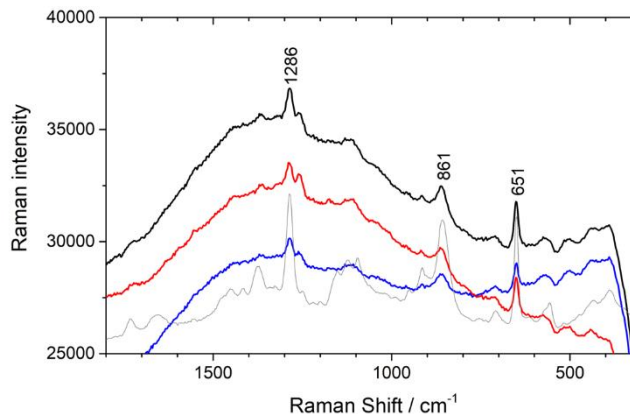


Figure A3.3. Raman MIRA DS spectra of the celluloid tortoiseshell imitation combs from João Teixeira's collection in Casa da Memória, Guimarães. Identification of celluloid is made by the detection of the strong nitrate bands at 1286 and 861 cm^{-1} and camphor sharp fingerprint band at 651 cm^{-1} . The Raman spectra of the combs are compared with a celluloid reference (in grey, cellulose nitrate + 30% camphor wt.)

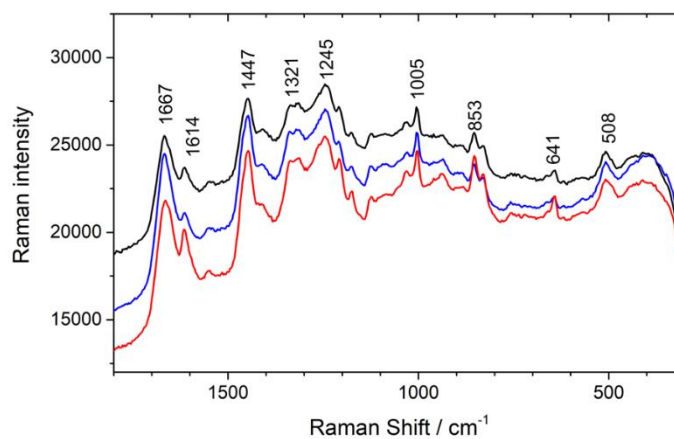


Figure A3.4. Raman MIRA DS spectra of the horn combs from João Teixeira's collection in Casa da Memória, Guimarães. Horn is identified by the detection of the $\nu\text{C}=\text{O}$ amide I (1667 cm^{-1}), νCC (1614 cm^{-1}), δCH_2 scissoring (1447 cm^{-1}), δCH_2 deformation (1321 cm^{-1}), δCH_2 wagging (1245 cm^{-1}), νCC aromatic (1005 cm^{-1}), νCCH aromatic (853 cm^{-1}), νCS (641 cm^{-1}), $\nu\text{S-S}$ (508 cm^{-1}) [1]. Oral information obtained by Teresa Costa (2006) from João Teixeira is clear that horn was a preponderant material in comb manufacture [2].

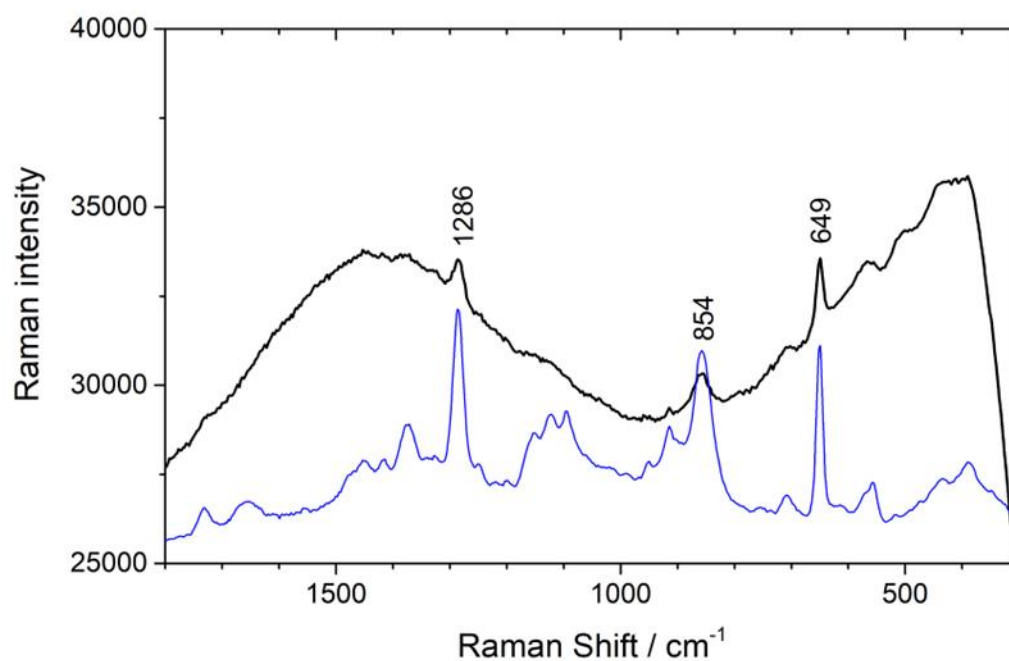


Figure A3.5. Raman MIRA DS spectrum of the orange transparent celluloid comb of the “Fábrica de Plásticos Pátria” collection from Sociedade Martins Sarmento, Guimarães. Celluloid is identified by the detection of strong nitrate bands at 1286 and 854 cm^{-1} and camphor sharp fingerprint band at 649 cm^{-1} . The Raman spectra of the combs are compared with a celluloid reference (in blue, cellulose nitrate + 30% camphor wt.).

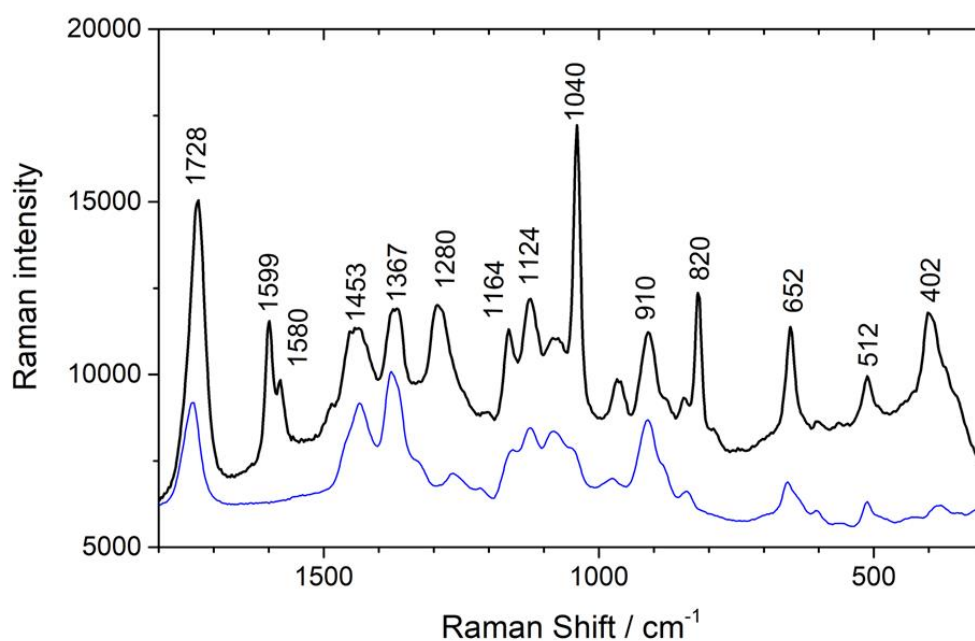


Figure A3.6. Raman MIRA DS spectrum of the cellulose acetate tortoiseshell imitation comb of the “Fábrica de Plásticos Pátria” collection from Sociedade Martins Sarmento, Guimarães. Cellulose acetate is primary identified by the stretching band of the carbonyl group at 1728 cm^{-1} , and the methyl (CH_3) deformations at 1453 and 1367 cm^{-1} . The identification of additional bands at 1599 , 1580 , 1040 , 820 and 652 cm^{-1} are due to the presence of a phthalate plasticizer, leading also to the shift of the carbonyl stretching band [3]. The Raman MIRA DS spectrum of a cellulose acetate (degree of substitution 2.4) reference is shown (blue).

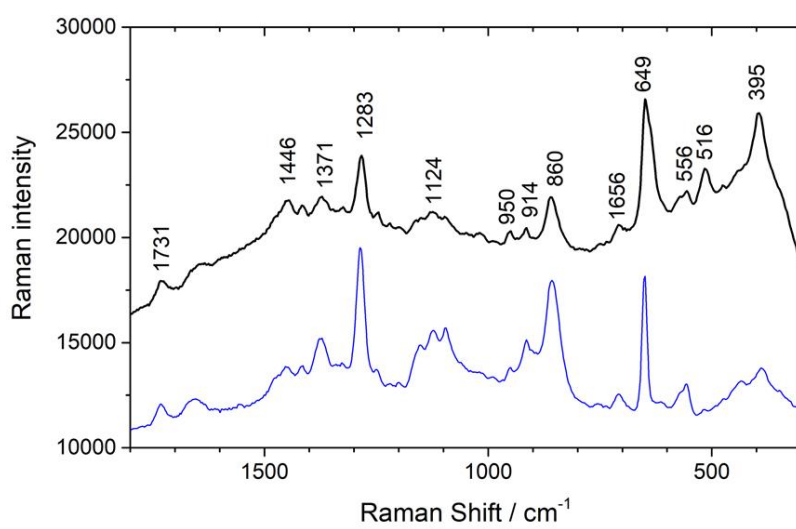


Figure A3. 7. Raman MIRA DS spectrum of an celluloid comb imitating horn with the brand name “Aravil”. The Raman spectra of the combs are compared with a celluloid reference (in blue, cellulose nitrate + 30% camphor wt.).

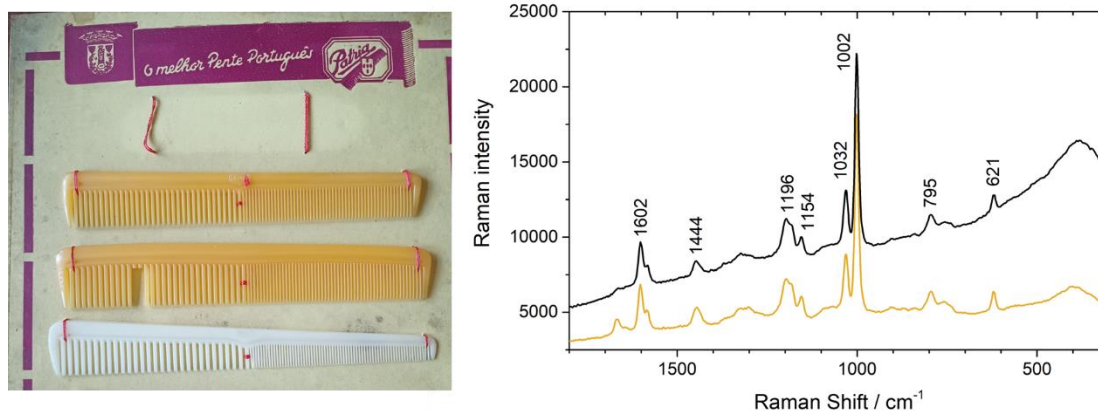


Figure A3.8. Raman MIRA DS spectra of two polystyrene combs of “Fábrica de Plásticos Pátria” from the collection of Sociedade Martins Sarmento, Guimarães (black spectrum from the white comb and the yellow from the first yellow comb). The Raman spectrum of polystyrene is well known in the literature and identification can be made by band comparison [4].

Supporting information:

The condition of celluloid objects from “Fábrica de Plásticos Pátria” collection from Sociedade Martins Sarmento, Guimarães.

Celluloid is a chemically unstable material that degrades under the influence of light, temperature, and water. At the molecular level, the cleavage of the polymer chains leads to material cracking and the release of hazardous acids, nitrous acid (HNO_2), and nitric acid (HNO_3), which attack both the polymer itself and neighboring materials. Over the long term, these degradation mechanisms can lead to the total loss of the material. Therefore, it is essential to identify the materials that make up plastic collections, with a primary focus on celluloid. In the Casa de Sarmento collection, three celluloid combs were found, two imitating tortoise shell and one imitating horn (**Fig. A3.9**). All show typical cracking patterns of celluloid degradation. The paper where these combs are attached is degraded, showing stains due to the release of acids from both the celluloid and the paper itself. From a conservation point of view, it is important to separate the combs from the paper. The combs should be stored in an isolated, dark, and well-ventilated location. The relative humidity should be around 50-55%, and the temperature should not exceed 20°C [5]. The combs could be wrapped in 100% cotton paper that allows the emission of volatiles. Recently, the European project NEMOSINE

(<https://nemosineproject.eu/>) developed intelligent boxes for the conservation of celluloid and cellulose acetate. When the boxes are available, this will be a recommended option.

It is important to note that the precautions to be taken with celluloid also apply to cellulose acetate, which degrades through similar mechanisms and releases acetic acid. Polystyrene is chemically more stable, but its preservation should also be planned. This study demonstrates the importance of identifying the materials in collections, as different materials represent different historical interpretations and conservation methodologies.



Figure A3.9. Celluloid combs from the of “Fábrica de Plásticos Pátria” from the collection of Sociedade Martins Sarmento, Guimarães, where it is possible to see the cracking pattern of extreme celluloid degradation.

References

- [1] H. G. M. Edwards, D. E. Hunt, and M. G. Sibley, “FT-Raman spectroscopic study of keratotic materials: Horn, hoof and tortoiseshell,” *Spectrochim Acta A Mol Biomol Spectrosc*, vol. 54, no. 5, pp. 745–757, 1998.
- [2] T. Costa, “Guimarães: A indústria de pentes artesanais em chifre,” in *As artes e as mãos da história*, I. M. Fernandes, M. J. Meireles, and P. Moscoso, Eds. Guimarães: Oficina, 2006, pp. 90–103.
- [3] C. Paris and C. Coupry, “Fourier transform Raman spectroscopic study of the first cellulose-based artificial materials in heritage,” *Journal of Raman Spectroscopy*, vol. 36, no. 1, pp. 77–82, 2005.

- [4] J. R. Anema, A. G. Brolo, A. Felten, and C. Bittencourt, "Surface-enhanced Raman scattering from polystyrene on gold clusters," *Journal of Raman Spectroscopy*, vol. 41, no. 7, pp. 745–751, 2010.
- [5] Y. Shashoua, *Conservation of Plastics: Materials science, degradation and preservation*. Elsevier Ltd, 2008.

Appendix 4. Novel markers to early detect degradation on cellulose nitrate-based heritage at the submicrometer level using synchrotron UV-Visible multispectral luminescence.

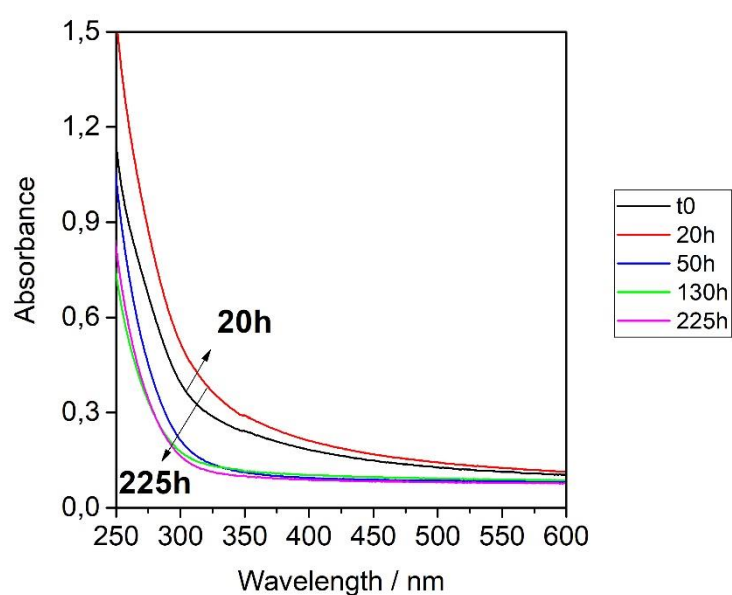
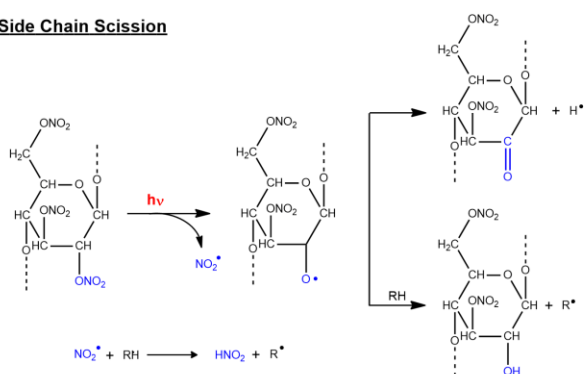
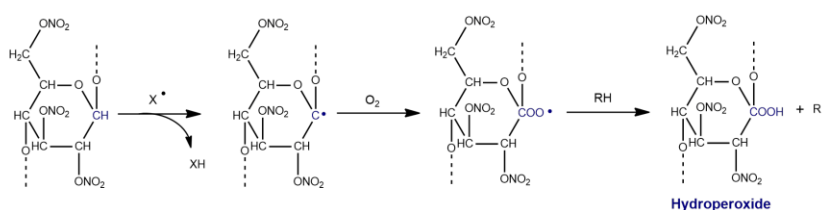


Figure A4.1. UV-VIS absorption spectra of cellulose nitrate films (ca. 1 μ m), irradiated at 20h, 50h, 130 and 225 ($\lambda_{irr} \geq 280$ nm, 60°C).

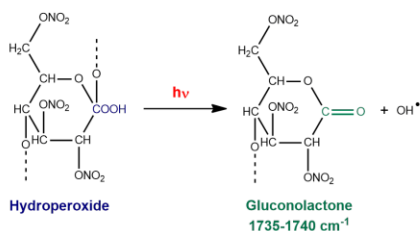
Side Chain Scission



Hydroperoxide Formation at C1



Main Chain Scission



Anhydride Formation

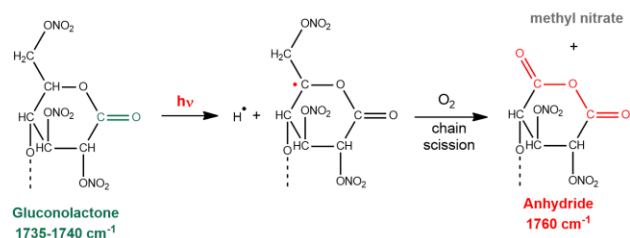


Figure A4.2. Cellulose nitrate side-chain scission starts with de-nitration, by the homolysis of a nitrate group in C2 or C3 and the release of $\bullet\text{NO}_2$. The alkoxy radical formed can be converted into a ketone or hydroxyl group. X^\bullet is defined as any radical which will promote H^\bullet , namely $\bullet\text{NO}_2$ or RO^\bullet , which lead to the formation of nitrous acid (HNO_2) or a hydroxyl group (ROH) respectively. C1H is the most labile hydrogen and thus the most easily abstracted. *Hydroperoxide formation at C1* will occur, in the excited state, by reaction of the produced macroradical with oxygen and further H^\bullet abstraction. This leads to the formation of the hydroperoxide and to the formation of another macroradical R^\bullet in the cellulose nitrate structure. *Cellulose nitrate main chain scission* occurs due to the decomposition of the excited state hydroperoxide, leading to scission of the glycosidic bond and formation of a gluconolactone (detected in the infrared at 1735cm^{-1} - 1740cm^{-1}). *Anhydride formation* will occur in a second step, following light absorption, in which the macroradical produced at C5 will react with oxygen, leading to the formation of a carbonyl at C5 and the release of $\bullet\text{CH}_2\text{ONO}_2$, which converts into a final product,

methyl nitrate, by H^\bullet abstraction. This anhydride function if detected in the infrared at 1760cm^{-1} ^{19,26}. For more details on the degradation mechanism of CN, please see p. 144 in ref. 26.

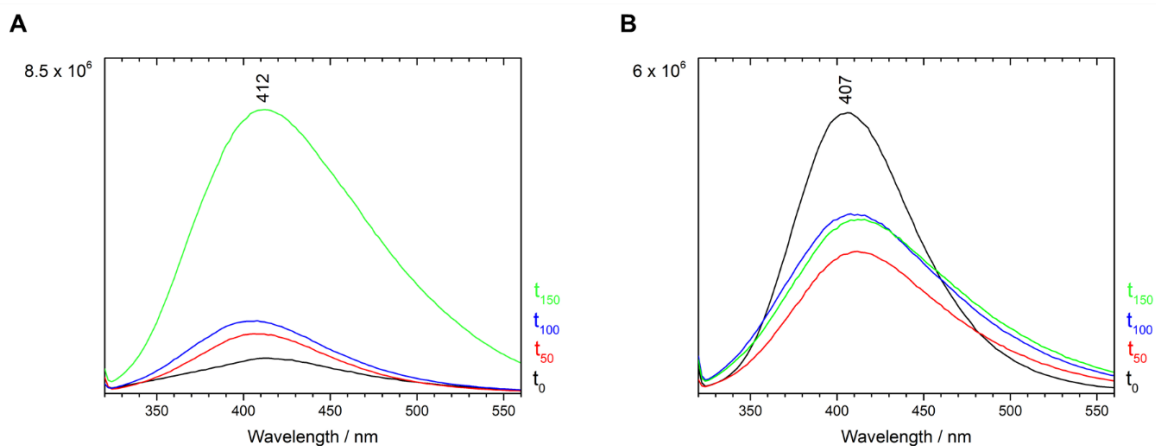


Figure A4.3. Emission spectra ($\lambda_{\text{exc}} = 290\text{nm}$) of artificially aged references irradiated during 50h, 100h and 150h ($\lambda_{\text{irr}} \geq 280\text{nm}$, 60°C), using a spectrofluorometer, in A) cellulose nitrate and B) celluloid (70% cellulose nitrate and 30% camphor w/w).

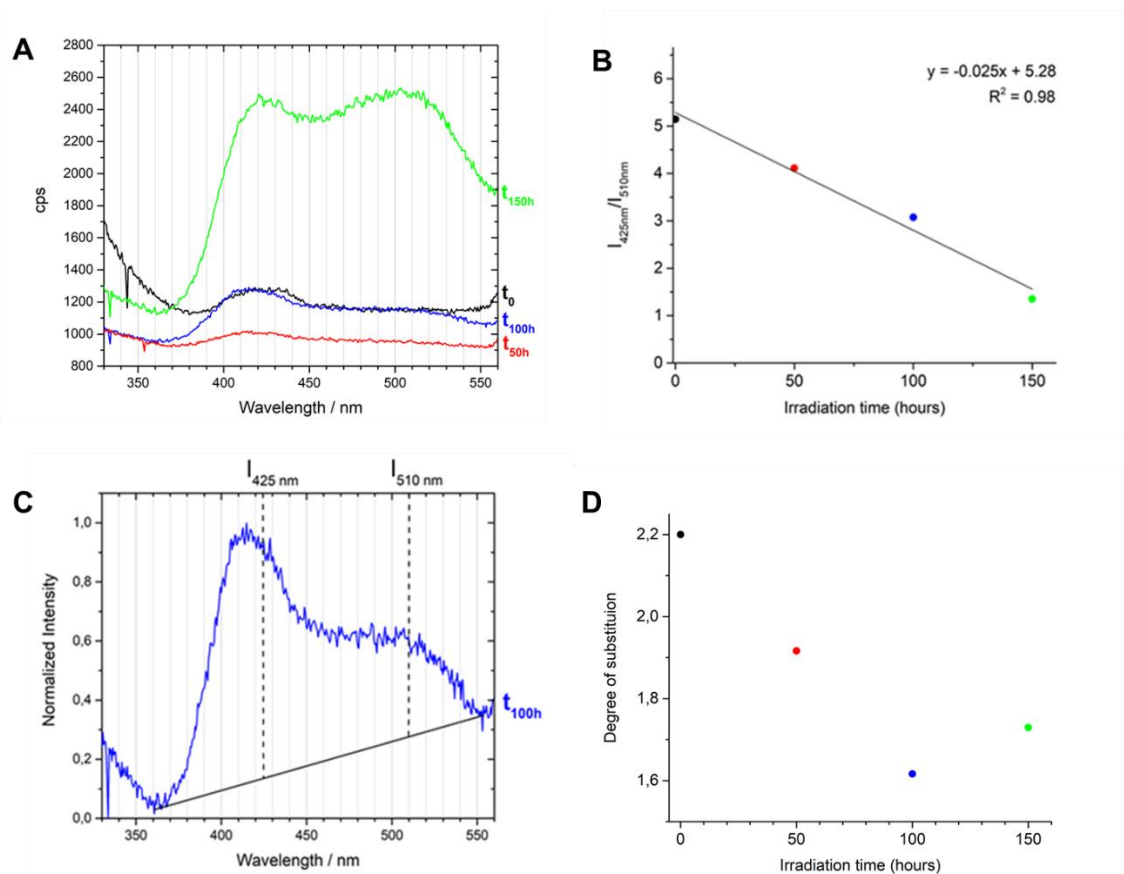


Figure A4.4. A) Emission spectra ($\lambda_{exc} = 290\text{nm}$) of artificially aged cellulose nitrate irradiated during 50h, 100h and 150h. B) The ratio $I_{425\text{nm}}/I_{510\text{nm}}$ was plotted over irradiation time and a linear regression was calculated. C) $I_{425\text{nm}}$ and $I_{510\text{nm}}$ were calculated as exemplified for $t_{100\text{h}}$, the intensities were corrected for each spectrum by applying a baseline between 360 nm and 550 nm. D) The degree of substitution of the artificially aged cellulose nitrate references was plotted over the irradiation time. At 150h of irradiation, main chain scission leads to the decrease of the νCOC band (1070 cm^{-1}) which is the reference band used for the DS calculation, resulting in higher DS values. Although this measuring technique shows this limitation for high degradation times, below 100h of irradiation the expected DS decrease was observed. In the future, shorter irradiation time intervals will provide more details on how DS correlates with the emission of cellulose nitrate at early stages of degradation ($< 100\text{h}$).

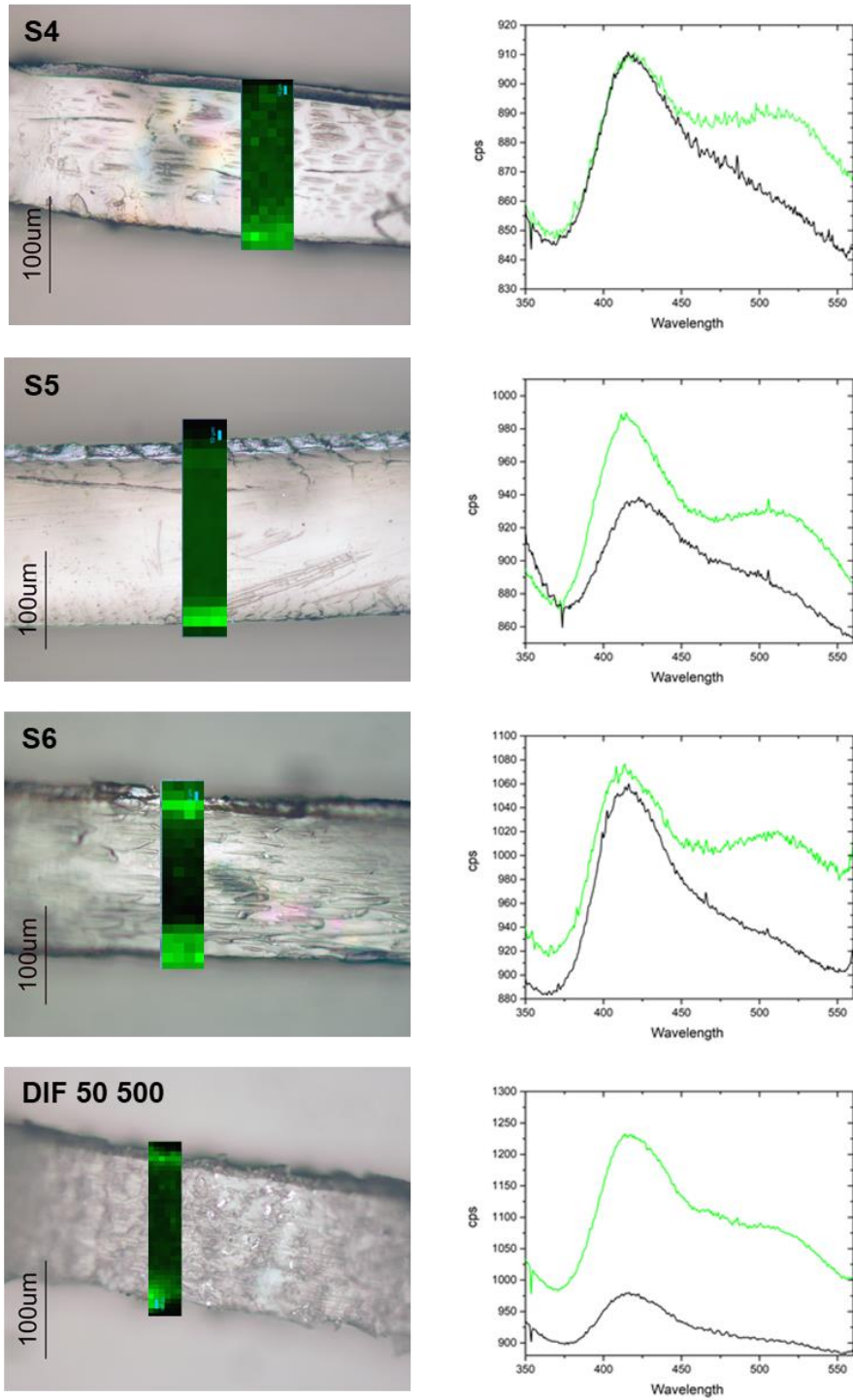


Figure A4.5. POLYPHEME raster scan mapping of cinematographic films S4, S5, S6 and 50509. The maps show the intensity variation of the emission band between 500 and 550 nm. Emission spectra collected at the interfaces (green) and the interior (black) of the cross-sections are shown.

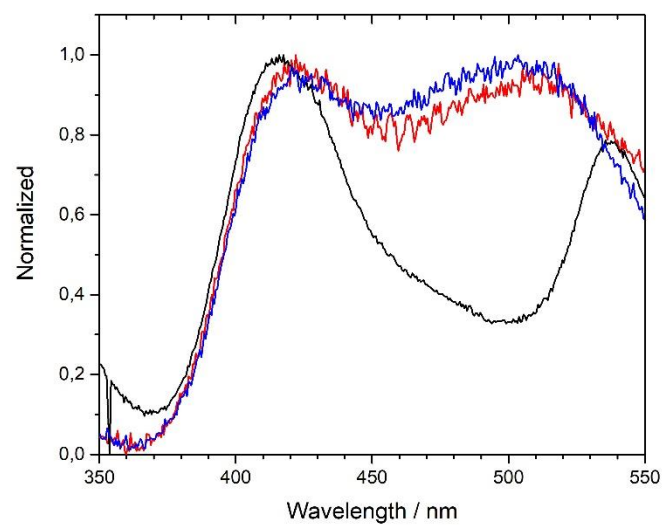


Figure A4.6. Normalized emission spectra of DIF 50 500 cellulose nitrate support at t_0 (black line) and 150h of irradiation (red line). The spectra are compared with the emission spectrum of cellulose nitrate artificial aged reference irradiated during 150h (blue line).

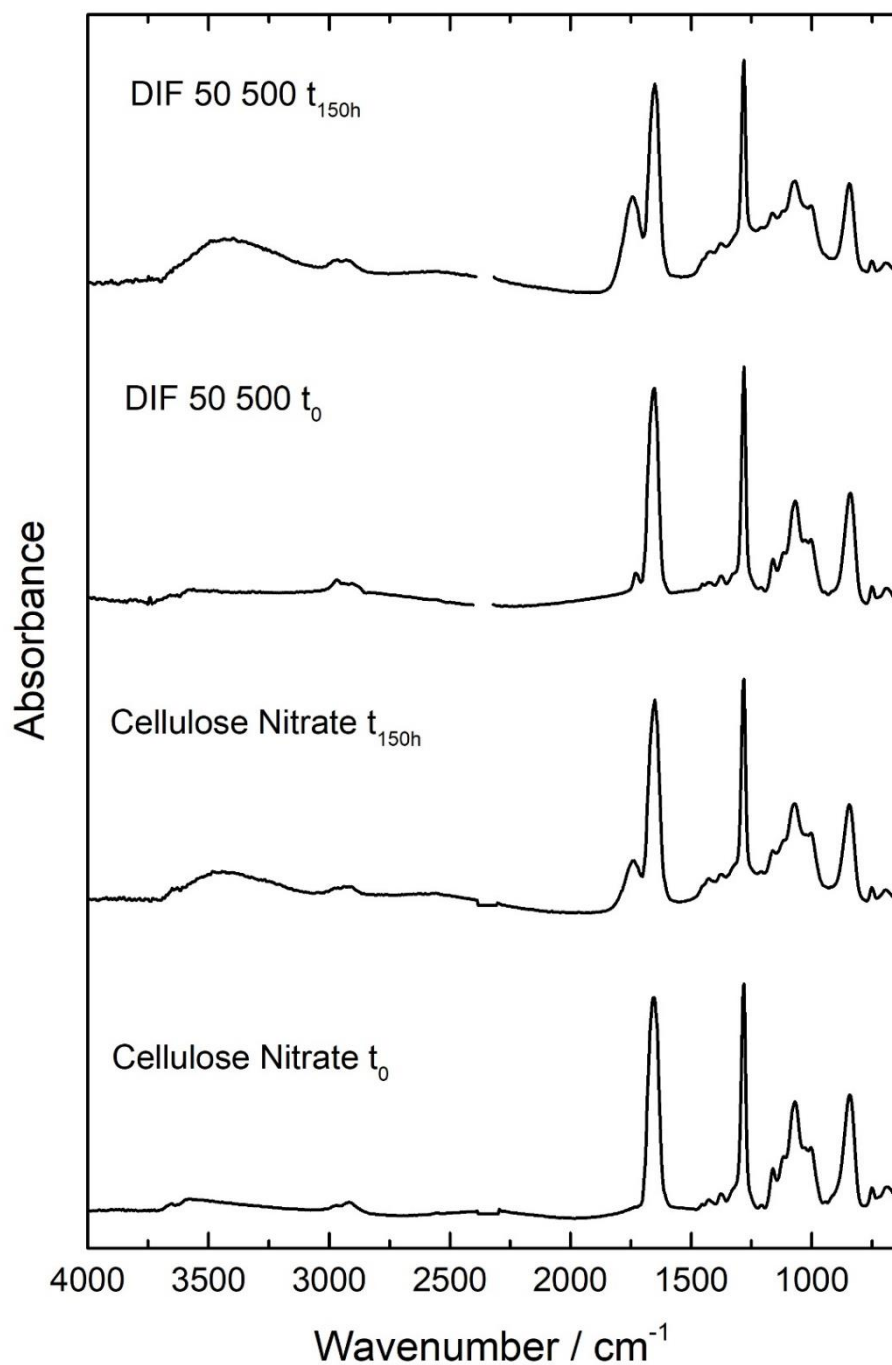


Figure A4.7. Infrared spectra of unaged and aged (150 hours, $\Phi_{\text{irr}} \geq 280\text{nm}$, 40°C) cellulose nitrate references and cinematographic film DIF 50 500 samples. Using Bussiere et al (2014) calibration curve for the quantification of camphor ($A_{1730}/A_{1655} = 0.013 \times \%\text{camphor}$, in a rough approximation without considering the degree of substitution), in DIF 50 500 we found 6% camphor w/w.

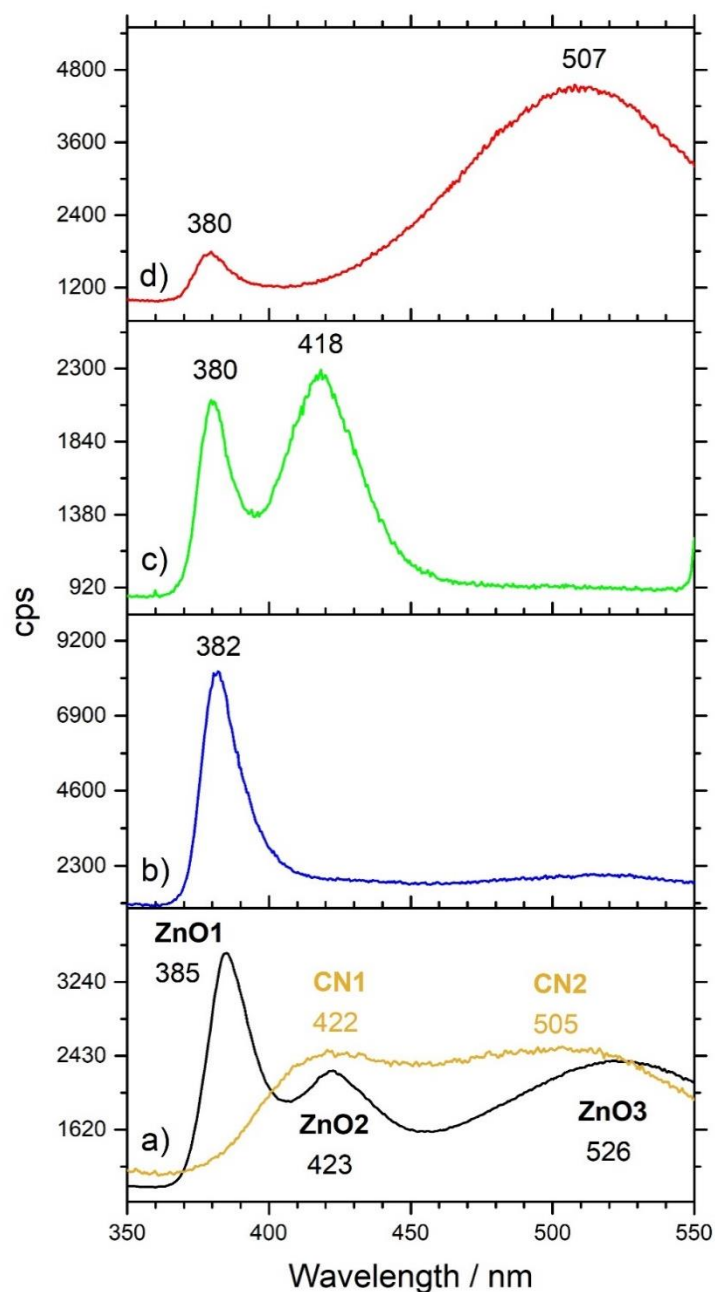


Figure A4.8. a) Emission spectra of zinc oxide from the American Flag Pin (black line) and of a 150h artificial aged cellulose nitrate reference sample (orange line). The ZnO1 band is the band edge emission of ZnO particles (380-385nm); the ZnO2 band/region is due to the ZnO crystal defect emissions between 400 and 450 nm; the ZnO3 broad band is the green emission from ZnO particles; the CN1 band (422nm) is the band that characterizes cellulose nitrate; the CN2 broad band (with max between 500-520 nm) is the band which intensity correlates with cellulose nitrate degradation. b) Emission spectra of a ZnO1 band with very high intensity obtained from the holy bible pin microsample. c) Emission spectra of a high intensity ZnO2 band in comparison to ZnO1, obtained from the 1899 calendar microsample analysis. d) Emission spectra of a ZnO3 band with very high relative intensity in comparison with ZnO1, obtained from the 1901 postcard analysis.

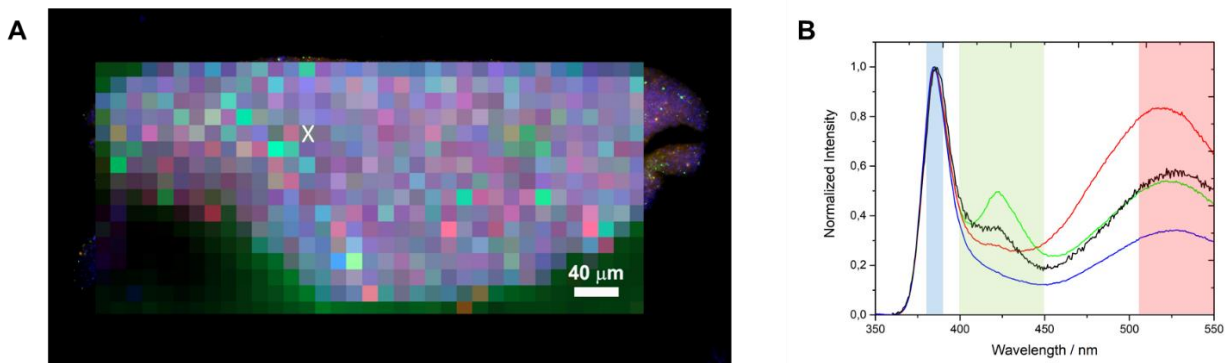


Figure A4.9. A) Raster scanning map by POLYPHEME ($15 \times 15 \mu\text{m}^2$, 5s, 2 accumulations, $\lambda_{\text{exc}} = 290 \text{ nm}$) of the American flag celluloid advertisement pin. Three spectral regions were used to map the emission spatial distribution, shown in B). Colors were designated as follows: blue for the band edge emission at 385 nm, green for the spectral region between 400-450 nm; red for the region between 510-550 nm. B) Average spectra, calculated from the selection of 10 spectra from A), were used as reference component spectra (loadings) to quantify the emission contributions of these spectral regions for each pixel in a direct classical least squares (DCLS) model. For more details, please see text. As an example of the output given by the model for one pixel, the emission spectrum of the marked pixel (X) in map A) is shown (black spectrum). For this spectrum, the model gave a match of 42.8% for the green loading, 28.9% for the blue loading and 28,5% for the red loading.

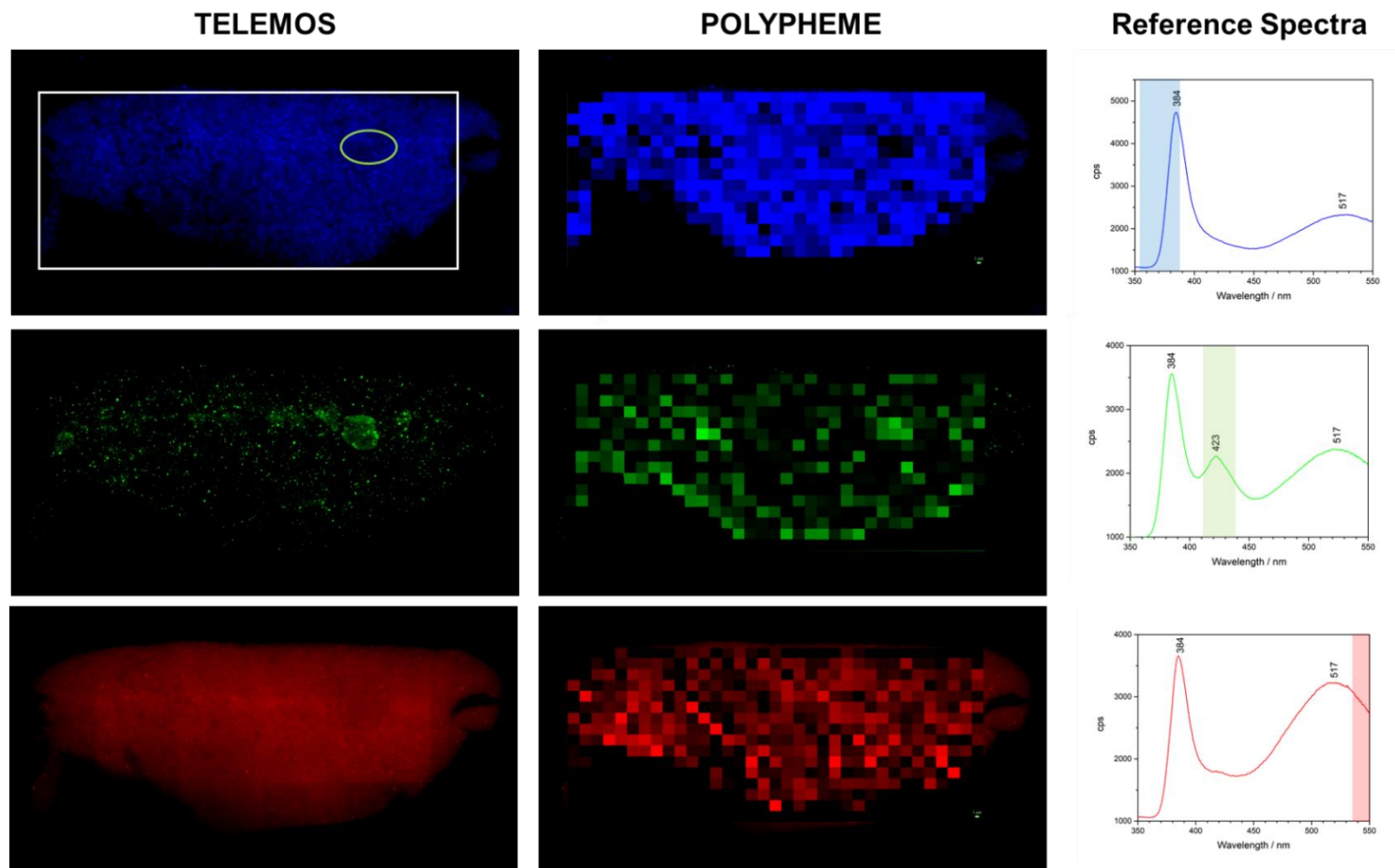






Figure A4.10. TELEMOS, full-field luminescence imaging of the American flag celluloid advertisement pin ($\lambda_{exc} = 290$ nm, 40x objective). Emission bandpass filters used: 352-388 nm (blue); 412-438 nm (green); 535-607 nm (red). The white-square marks indicate the POLYPHEME map area; POLYPHEME, emission distribution profiles for each reference component spectra used in the direct classical least squares (DCLS) modeling of the spectral array. For more details, please see text. It is interesting to observe that the area marked by the green ellipse on the TELEMOS mapping correlates with the POLYPHEME which shows a higher score of the green loading in comparison to blue loading; *Reference component spectra* used in the model, each one obtained for the average of 10 selected POLYPHEME emission spectra. The brighter the pixel on the distribution profile, the higher the correlation with the reference component spectra. The spectral regions viewed using TELEMOS full-field luminescence imaging setup are highlighted, with colors corresponding to the bandpass filters used.

Table A4.1. μ Raman main results for the celluloid object micro samples analysed. The degree of substitution (DS) was calculated with μ FTIR using the calibration curve described in Nunes et al. (2020).

Object	Date	FTIR DS	Type of sample	μ Raman main results
Postcard				
	Possibly from 1901	2.06	micro-sample embedded in polyester resin	Cellulose nitrate: 856, 1286, 1650, 2932 and 2970 cm^{-1} Camphor: 654 and 1730 cm^{-1} Zinc stearate: 1065, 1131, 1297, 1441, 1458, 2851 and 2884 cm^{-1} . Massicot and litharge (PbO): 89, 108, 125 and 141 cm^{-1}
American flag Pin				
	N.A.	2.01	micro-sample embedded in polyester resin	Cellulose nitrate: 864, 1286, 1652, 2932 and 2970 cm^{-1} Camphor: 650 and 1730 cm^{-1} Zinc Oxide (ZnO): 330 and 475 cm^{-1} Cerussite (PbCO₃): 1054 cm^{-1} Zinc stearate: 1062, 1094, 1127, 1296 and 1445 cm^{-1}
Holy Bible Pin				
	N.A.	2.00	Micro-sample embedded in polyester resin	Anatase (TiO₂): 257, 547, 583, 808, 1093 cm^{-1} Azurite: 141, 394, 512, 637 cm^{-1}
Calendar				
	1899	1.88	Micro-sample embedded in polyester resin	Cellulose nitrate: 862, 1284, 1653 cm^{-1} Camphor: 650 and 1733 cm^{-1} Zinc Oxide (ZnO): 475 cm^{-1} Lead chromate (PbCrO₄): 145, 321, 341, 379, 824, 837 and 846 cm^{-1}

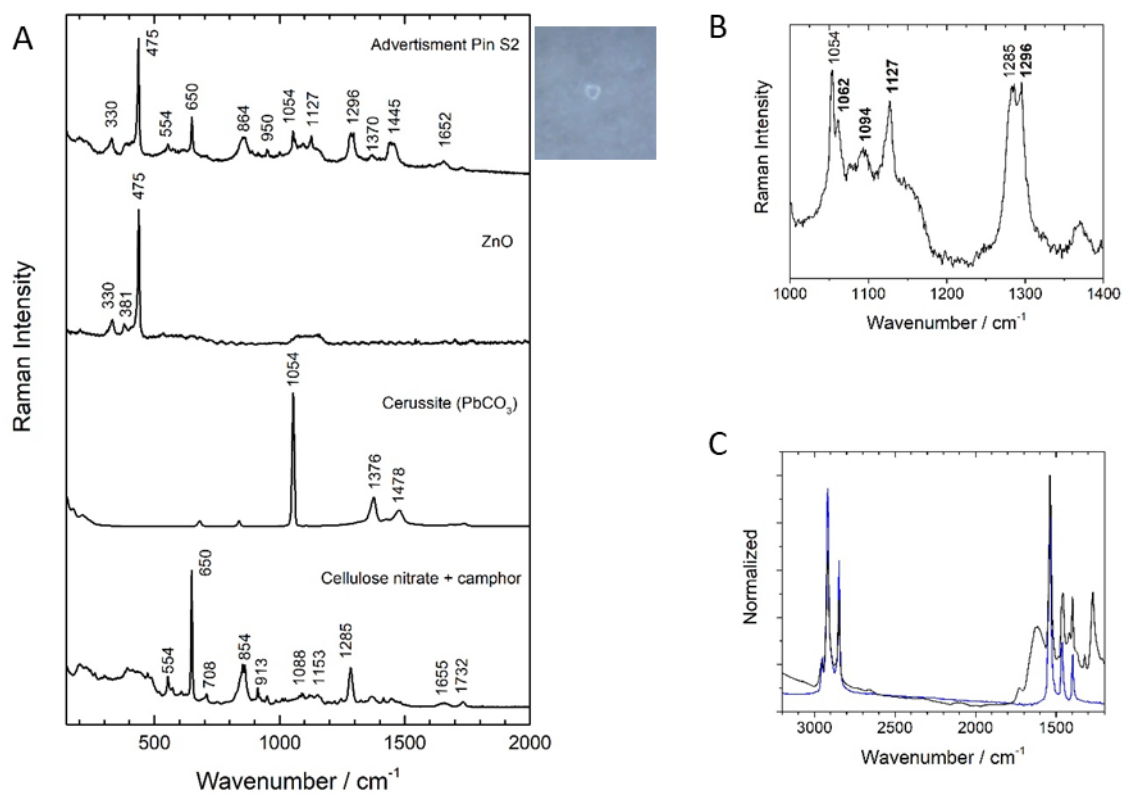


Figure A4.11. A) Raman spectra of a whitish particle in the American flag pin sample (633 nm laser) and references of zinc oxide, cerussite (PbCO_3) and celluloid (cellulose nitrate and camphor). B) Raman spectrum in the spectral region between 1000 and 1400 cm^{-1} . Peaks attributed to zinc stearate are emphasized in bold. C) FTIR-ATR spectra of the American flag pin (black) and of a zinc stearate reference (blue)

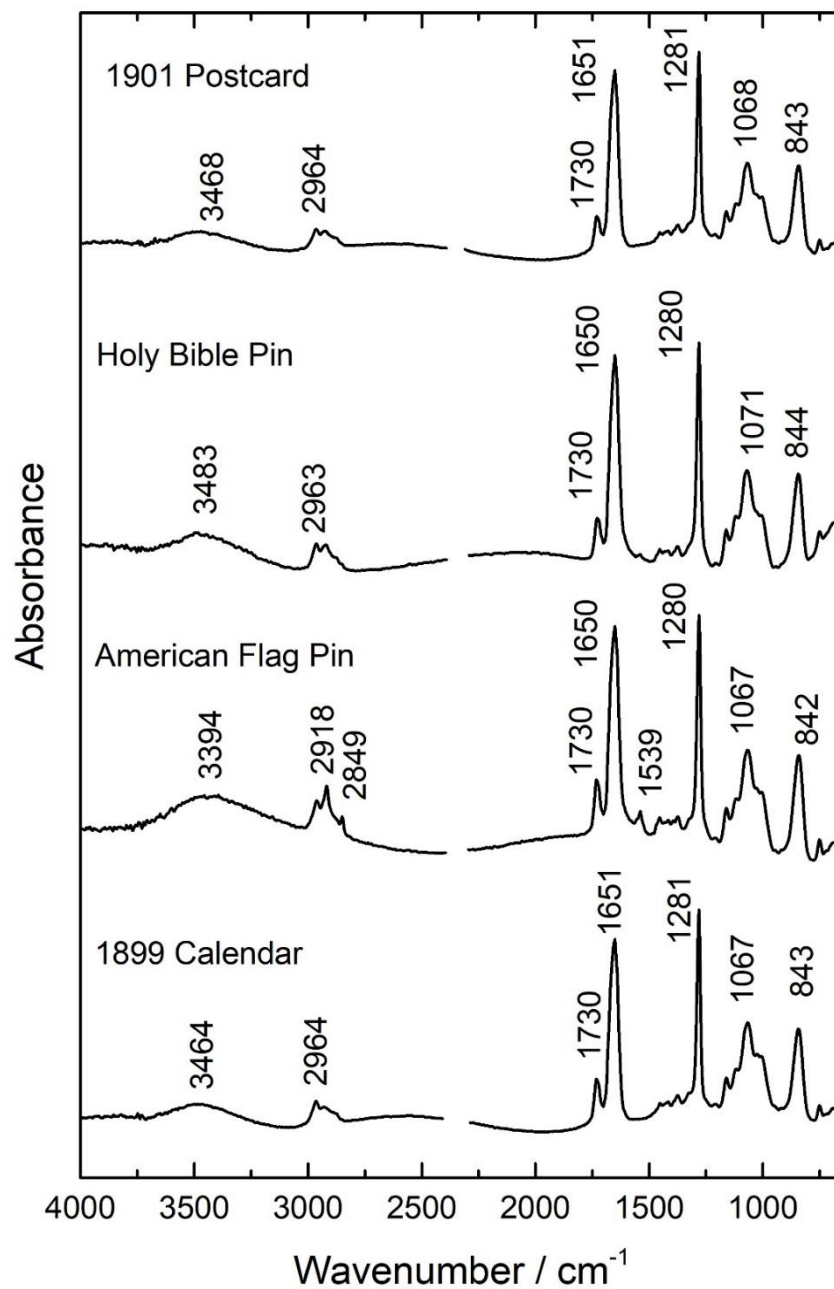


Figure A4.12. Infrared spectra of Perlov's celluloid objects analysed. Bands at 2918, 2849 and 1539 cm^{-1} observed in the American flag pin are due to zinc stearate. Using Bussiere et al (2014) calibration curve for the quantification of camphor ($A_{1730}/A_{1655} = 0.013 \times \% \text{camphor}$, in a rough approximation without considering the degree of substitution), in the calendar we found 18% w/w camphor, in the American flag pin 20%, in the holy bible pin 16% and in the 1901 postcard 15%.

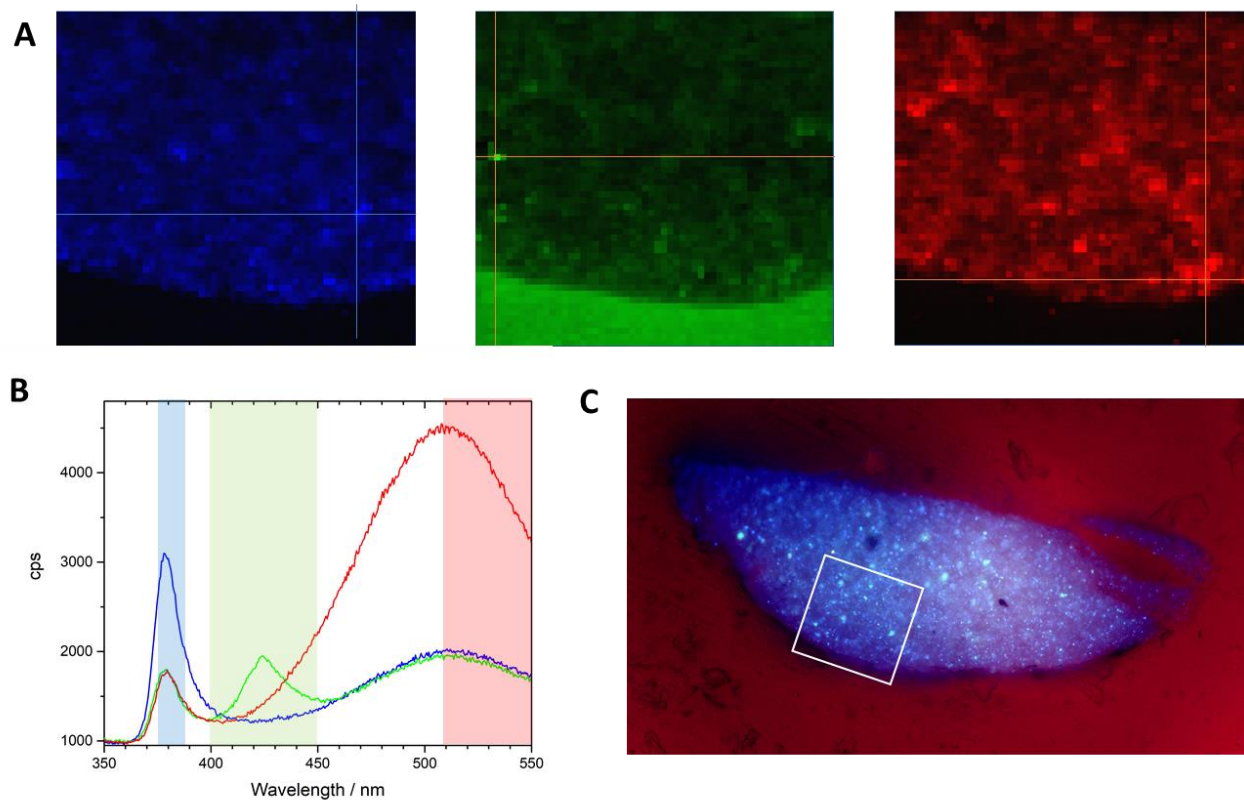


Figure A4.13. A) POLYPHEME raster scan mapping of the 1901 postcard ($3 \times 3 \mu\text{m}^2$, 5s, 2 accumulation, $\lambda_{\text{exc}} = 290 \text{ nm}$). Colors are associated to the following spectral regions: blue for the band edge emission at 385 nm, green for the spectral region between 400-450 nm; red for the region between 510-550 nm (these regions are highlighted in B). B) Emission spectra of the pixels marked with a cross in the maps showed in A). C) 1901 postcard sample spatially registered false-colour RGB image of the emission at excitations of 365 (blue), 385 (green) and 405 nm (red) with emission bandpass filter 514 nm (30 nm FWHM) The white rectangle marks the POLYPHEME map area.

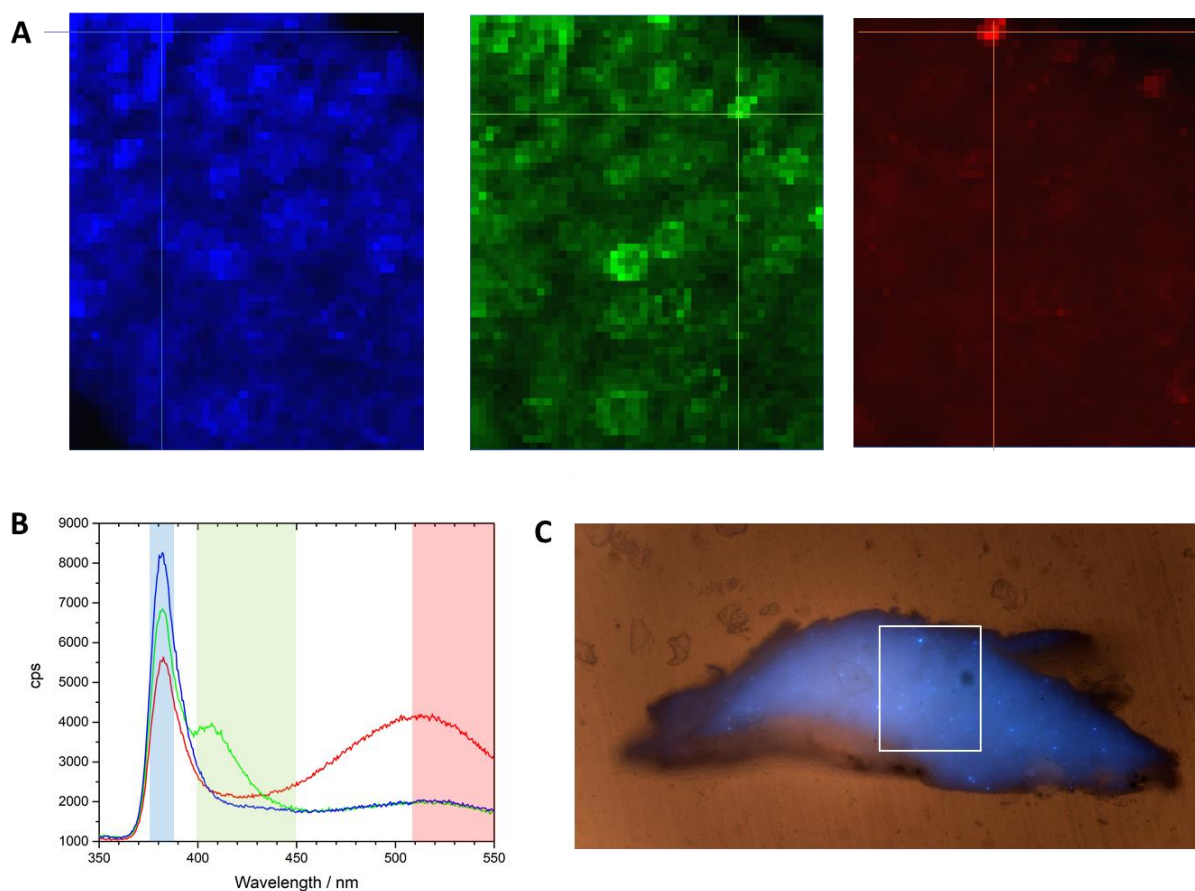


Figure A4.14. A) POLYPHEME raster scan mapping of the holy bible pin ($2 \times 2 \mu\text{m}^2$, 10s, 1 accumulation, $\lambda_{\text{exc}} = 290 \text{ nm}$). Colors are associated to the following spectral regions: blue for the band edge emission at 385 nm, green for the spectral region between 400-450 nm; red for the region between 510-550 nm (these regions are highlighted in B). B) Emission spectra of the pixels marked with a cross in the maps showed in A). C) Holy bible pin sample spatially registered false-colour RGB image of the emission at excitations of 365 (blue), 385 (green) and 405 nm (red) with emission bandpass filter 514 nm (30 nm FWHM) The white rectangle marks the POLYPHEME map area.

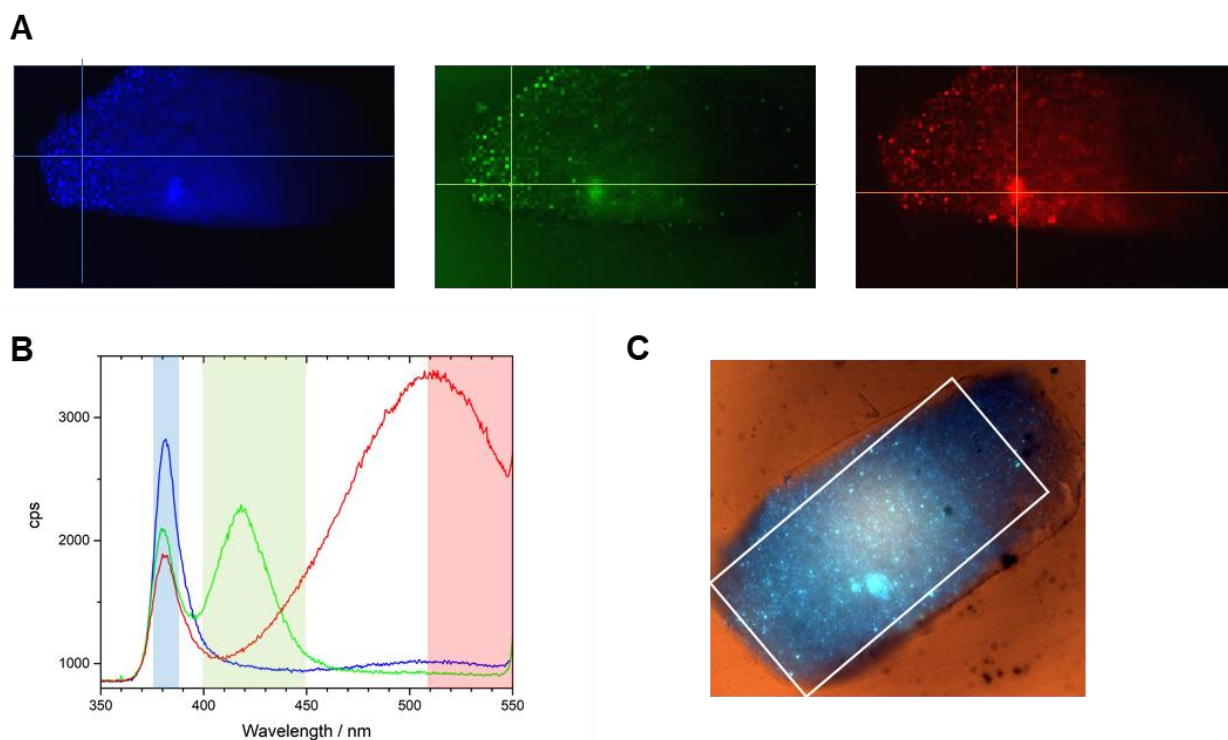


Figure A4.15. A) POLYPHEME raster scan mapping of the 1899 calendar ($6 \times 6 \mu\text{m}^2$, 2s, 2 accumulations, $\lambda_{\text{exc}} = 290 \text{ nm}$). Colors are associated to the following spectral regions: blue for the band edge emission at 385 nm, green for the spectral region between 400-450 nm; red for the region between 510-550 nm (these regions are highlighted in B). B) Emission spectra of the pixels marked with a cross in the maps showed in A). C) 1899 calendar sample spatially registered false-colour RGB image of the emission at excitations of 365 (blue), 385 (green) and 405 nm (red) with emission bandpass filter 514 nm (30 nm FWHM) The white rectangle marks the POLYPHEME map area.

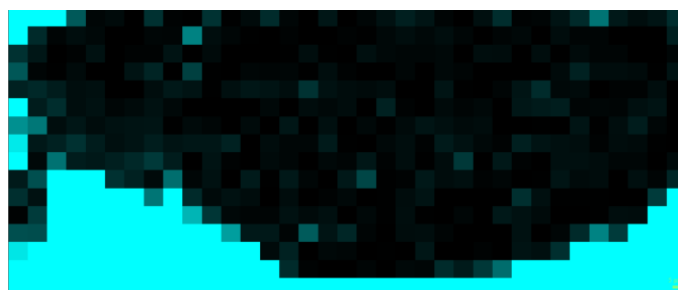


Figure A4.16. Error map of the DCLS modelling performed to the map of the American flag pin sample. Regions of high error (bright intensity) indicate a bad fit. Essentially, this map shows the resin surrounding the sample, which does not fit well with the reference component spectra used.

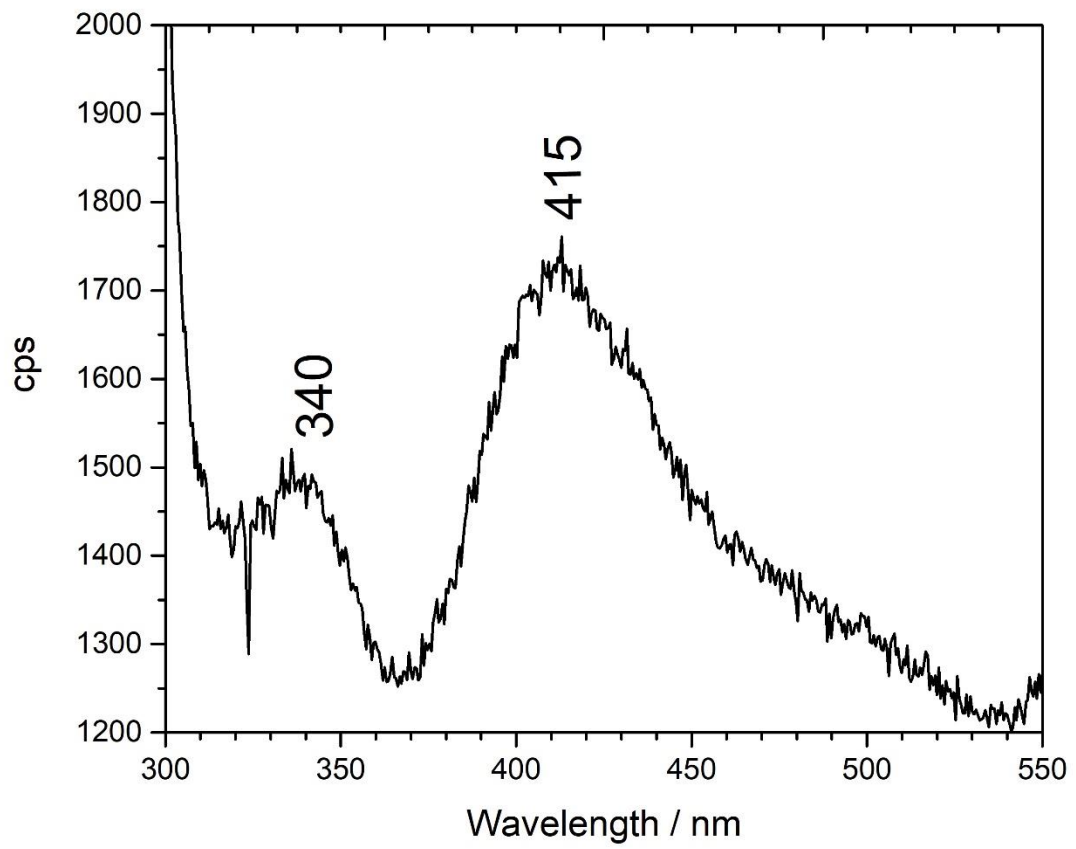


Figure A4.17. Emission spectrum of the polyester resin used for embedding the celluloid micro samples.

ZABRUR LOURO MENDONÇA NEVES

CELLULOSE NITRATE OBJECTS IN COLLECTIONS:
HISTORY OF SCIENCE AND TECHNOLOGY HAND IN HAND
WITH CONSERVATION OF CULTURAL HERITAGE

2023

ARTUR LOURO MENDONÇA NEVES

CELLULOSE NITRATE OBJECTS IN COLLECTIONS:
HISTORY OF SCIENCE AND TECHNOLOGY HAND IN HAND
WITH CONSERVATION OF CULTURAL HERITAGE

